SPATIAL SUITABILITY ANALYSIS FOR SITE SELECTION OF VINEYARDS USING BIOPHYSICAL MODELS AND COMPUTATIONAL INTELLIGENCE

By

GOLNAZ BADR

A dissertation submitted in partial fulfillment of
the requirements for the degree of

DOCTOR OF PHILOSOPHY

WASHINGTON STATE UNIVERSITY
Department of Biological Systems Engineering

MAY 2016

To the Faculty of Washington State University:

The members of the Committee appointed to examine the dissertation of GOLNAZ BADR find it satisfactory and recommend that it be accepted.

Gerrit Hoogenboom, Ph.D., Co-Chair

Claudio Stockle, Ph.D., Co-Chair

Joan Davenport, Ph.D.

Michelle Moyer, Ph.D.

Richard Rupp, Ph.D.

Markus Keller, Ph.D.

ACKNOWLEDGEMENTS

First and foremost, I am extremely grateful to my primary advisor, Professor Gerrit Hoogenboom for all his support and leadership. His constructive comments and feedback significantly enhanced the quality of this work. Under his supervision, I have learned about and gained experience with scientific topics which I was previously unfamiliar with. I am also indebted to all of my committee members for becoming part of the team. It was an honor to work with and learn from all of them. I am grateful to Professor Markus Keller for his constructive comments and recommendations during the research process. I am also indebted to Professor Joan Davenport for her help in understanding the underlying assumptions used in her research and for providing insight into many challenging questions. I am so appreciative of her and the NW Center for Small Fruits Research for providing partial funding for this project. I am especially grateful to Dr. Michelle Moyer for her constant feedback and support on several aspects of the work; having her expert opinion on the theoretical aspects of this project contributed substantially to the improvement of our work. Dr. Richard Rupp provided so much support on the technical aspects, especially when it came to gaining access to software license updates and refining the methodology. I am extremely thankful to Professor Claudio Stockle for agreeing to join the committee and be part of the team as a co-chair. I am also grateful to the faculty and staff of the Biological Systems Engineering department at WSU. I also want to thank Ms. Joan Hagedorn and Ms. Joanna M. Dreger for all their support. I am thankful to the V & E program at WSU for their assistance and for awarding scholarships to me. I am also thankful to Ms. Deborah L. Schewenson for her support. I am grateful to Ms. Jennifer Smithyman at Ste. Michelle Wine Estates for providing the aerial NDVI images. I am indebted to the International

Business Machines Corporation for awarding me their Ph.D. fellowship. I am indebted to the physical analytics group, which provided excellent mentorship to me at the IBM T.J. Watson Research Center. I am particularly thankful to Dr. Hendrik Hamann, Dr. Levente Klein, Dr. Marcus Frietag, Dr. Xiaoyan Liu, and Dr. Conrad Albrecht for all of the helpful discussions during my internship. To all the faculty and staff who are affiliated with the WSU Irrigated Agriculture Research and Extension Center, I am thankful for all the wonderful moments we have shared. I am specifically thankful to Ms. Frances Bardessono for always being so helpful. Mr. Guy Reisenauer, thank you for all the technical support, your help has been tremendous. To my AgWeatherNet family, thank you for all your support through the years. I am especially grateful to Mr. Sean Hill for providing the required weather datasets; and to Ms. Bonnie Copeland and Ms. Waylan Funk for helping us remain on-schedule and organized. To my other colleagues, Dr. Melba Salazar, Mr. Bernardo Chavez, Dr. Vakhtang Shelia, Dr. Nona Rurua, Dr. Mohammad Bannayan, and Dr. Tesfamichael Ghidey: thank you all for your kindness and support. I am also deeply grateful to my other fellow graduate students, especially Jonny, Tracy, and Zhen for all the good memories, laughter during lunch breaks, and their friendship. I would also like to acknowledge my friends across the globe, particularly those in Pullman and Tri-Cities; thank you all so much for always being there for me. Also, I am very grateful to my friends Delasa, Pouya, and Nasrin. To my late friend Ms. Dina Radjabalipour who lost her battle with cancer last April: Dina, I learned so much from you; you will always be my heroine who bravely fought until the last moment.

To my late grandmother Ms. Parvindokht and uncle Mr. Mahmoud, to whom I never had the chance to say goodbye to: I promise I will always cherish the wonderful memories. I am thankful for all my aunts, uncles, and cousins; I am especially grateful to my uncle Dr. Hamid R. Badr and his wife Ms. Parvin for all their support and kindness.

To my parents, whom I miss so dearly, I am unable to find the words to express my love and appreciation for you and all that you have done for me. Thank you for being so selfless as to let your only daughter follow her dream, despite the fact that she would be living so far away from you. Thank you for establishing the love of science in me as a little girl, and for always being a source of encouragement and support for me. Thanks for your unconditional love and for always being by my side when it came time to make challenging decisions. To my dad, Baba Saeed, thank you for providing me with a world of opportunity when I was growing up. I can never repay what you have done for me, but I want to express my deep gratitude for your love and devotion. To my kind and lovely mother, Maman Melii, you have always been by my side, like a great friend, and I can never thank you enough for your immense love. You have laughed with my laughter, cried with my sadness, supported me, encouraged me, and advised me whenever I needed it most. To my baby brother, Mr. Amirhossein, I cannot believe you are a grown man! In my mind I still see you as the little boy with shining eyes who always asked such clever questions. Thanks for all the great memories and laughter, and for your support and encouragement through the years.

Last but not least, to the love of my life, my better half, my best friend, and my husband, Dr. Mohammad Abouali, whom I appreciate most. Mohammad, you have touched my heart in so many ways and you are the reason I keep on going. Thank you for being such a strong supporter of everything I do, and for all your love, patience, admiration, advice, and motivation. I love you and I cannot wait to begin the next chapter of our life together.

SPATIAL SUITABILITY ANALYSIS FOR SITE SELECTION OF VINEYARDS USING BIOPHYSICAL MODELS AND COMPUTATIONAL INTELLIGENCE

Abstract

by Golnaz Badr, Ph.D.
Washington State University
May 2016

Co-Chairs: Gerrit Hoogenboom and Claudio Stockle

The goal of our study was to develop a comprehensive land-assessment system for grapevine (*Vitis vinifera* L.) suitability analysis with the ability to spatially incorporate biophysical information from the Pacific Northwest (PNW) region of the United States. The potential for using satellite remote-sensing products for estimating the key phenological metrics of several vineyards located in the Columbia Valley of Washington was first evaluated. Remote sensing products such as Land Surface Temperature (LST) and the Normalized Difference Vegetation Index (NDVI) were also used to estimate the near surface air temperature of the region, which has complex terrain. Our results indicated discrepancies in the bias distribution due to the type of landcover present. During the following phase of our study, daily weather data were obtained from the Gridded Surface Meteorological data-set from the University of Idaho (UI GSM) for a 30-year period (1983-2012). This weather dataset were utilized to compute

several bio-climatic indices that were used in turn for characterizing weather dynamics of the American Viticultural Areas (AVA) located within the PNW. Previously established bio-climatic indices were also modified to improve the capture of the underlying weather phenomena of the region, and were then used for the development of the weather component of our land-assessment system. For the edaphic and topographic components of the system, soil data were obtained from the gSSURGO dataset and topographical component data were obtained from the National Elevation Dataset (NED). The potential for grape production in a region can be restricted by many parameters; therefore, land-cover and water rights information were also incorporated into our system. Fuzzy logic rules were used to transform the input parameters in to a common scale and to calculate the vineyard potential for the study area. Finally, our developed land-assessment system was evaluated with a comparison of the vineyard potential of established vineyards. The results of our study has proven that our system can be used as an accurate method to help decision makers, growers, and researchers gain a better understanding of the underlying biophysical parameters that contribute to the potential of various areas of the PNW for wine grape production.

TABLE OF CONTENTS

Page

LIST OF TABLES

LIST OF FIGURES

Dedication

This dissertation is dedicated to my family and

my husband for their unconditional love and constant support.

"Remember that the best relationship is one in which your love for each other exceeds your need for each other."

Dalai Lama (2004)

CHAPTER ONE

INTRODUCTION

Background

The assessment of land potential for crop production requires a comprehensive technical analysis addressing all relevant biophysical, socio-economic, management, and regulation issues and their potential interactions. Hence, successful land assessment systems should have the ability to improve agricultural development within a region, as well as optimize resource allocation and economic expansion. Traditionally, land assessment has been conducted using empirical studies and the on-site evaluation of a region, including detailed lab analysis for chosen environmental factors. Although these procedures are accurate measures of quantifying the potential of a specific land parcel for agricultural production, evaluation of larger regions requires extensive time and financial investment. Further, combining the input data within a land assessment system, handling input data from large-scale studies, and additional analysis can hinder the development of such a progressive land assessment system. In order to counteract these limitations, computer technologies such as the Geographic Information System (GIS) have been employed in conducting land assessments (Pereira and Duckstein, 1993; Bojorquez-Tapia et al., 2001; Joerin et al., 2001; Hoolber et al., 2003; Phua and Minowa, 2005; Liu et al., 2007; Tapa and Murayama, 2008; Mendas and Delali, 2012; Kang et al., 2013; Saha and Eckelman, 2015). A GIS can analyze and conduct numerous procedures on spatial data and their attributes, and also has the powerful visualization capabilities and dynamic mapping system features to make it an ideal tool for land assessment of larger regions.

Grape (*Vitis vinifera* L.) is regarded as a unique crop because both crop quality and quantity are critical to its economic success and the life span of the vineyards are also contributing to the economic investments and return. Therefore, successful land assessment for grape production relies on optimization of both quality and yield quantity. The key environmental factors affecting the growth and development of grapes are edaphic, topographic, and climatic. Complex interactions between these factors determine the ultimate suitability or unsuitability of a region for a specific grape cultivar. These three factors are spatially contiguous across a landscape, and can vary both in space and time; therefore, land assessment for the detection of the most suitable sites for grape production also requires knowledge of the historical records of these environmental factors. In addition, the spatial resolution of the input data should capture the underlying dynamics of a region.

These three environmental factors should be set as the core and initial boundaries required for development of a land assessment system for grape production. A softer boundary set around the initial assessment could then be used to determine the potential impact of variables such as land cover type, availability of water and water rights, pest and disease distribution, and specific management strategies. A third, broader boundary could then be used to provide information on market demand, land ownership, the sustainability and reputation of vineyard practices within a region, socio-economic factors, and local governmental rules and regulations (Figure 1.1.).

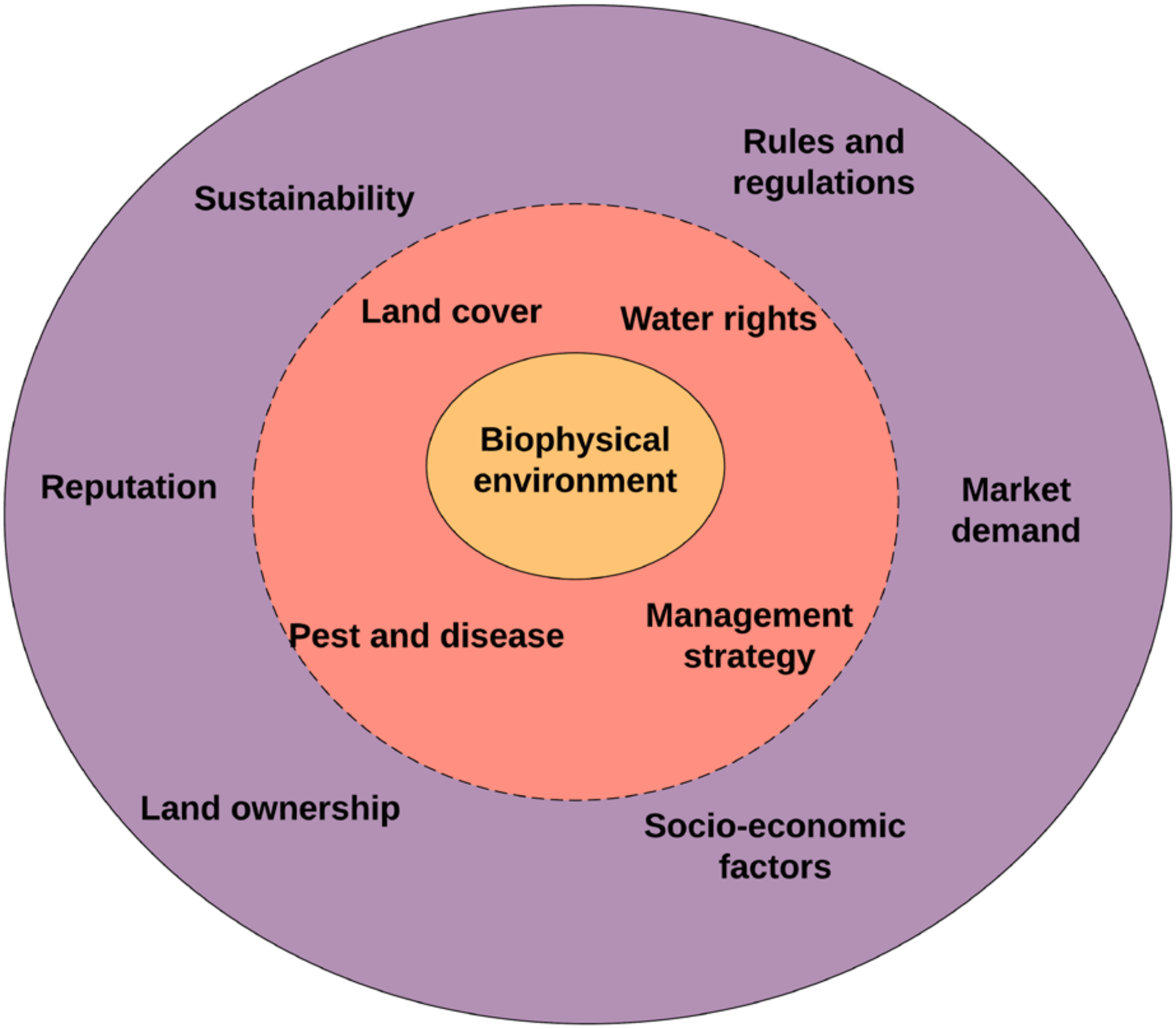

Figure 1. 1. The three main information boundaries required for the development of a land assessment system for wine grape.

The climatic, edaphic, and topographic factors involved each include additional sub-factors that can influence the growth and development of grapes. The climatic sub-factors include air temperature, precipitation, solar radiation, and to a lesser degree wind speed and direction. Air temperature influences many plant processes, including canopy temperature (Keller, 2010), which subsequently affects metabolic pathways such as photosynthesis and respiration (Kriedemann, 1968; Hendrickson et al., 2004; Geiger and Servaites, 1991; Keller, 2010). Temperature also impacts the duration and effectiveness of both flowering and fruit set (Jackson, 2008). Canopy temperature determines the evaporative potential of each plant and drives its demand for water (Keller, 2010). Solar radiation effects photosynthesis and carbohydrate synthesis in grapes (Jackson, 2008), while wind speed can have both a beneficial and detrimental impact on grapes. For example, strong winds can damage grapes (Keller, 2010; Jackson, 2008; Jones and Hellman, 2003; Jackson and Spurling, 1988), while a moderate wind speed promotes evaporative cooling and helps avoid excessive humidity buildout within the canopy (Keller, 2010; Jones and Hellman, 2003; Gladstones, 1992). Precipitation not only influences the availability of water, but also impacts the relative humidity of the air; hence, excessive moisture within the grape canopy, coupled with a specific range of air temperatures, can lead to a disease outbreak, especially those diseases that favor a high humidity (Keller, 2010; Moyer et al., 2010; Jackson, 2008).

Topographic sub-factors that can impact grape growth and development include slope, aspect, which is defined as the direction of the slope, and elevation. Topographic factors have the ability to modify the macro-climates of a region, and are important factors to be considered within grape land assessment systems. Elevation has a noticeable impact on air temperature, as the dry adiabatic lapse rate causes a drop of 1°C in air temperature for every 100 m increase in elevation. Slope controls air movement down hills as cooler, denser air sinks to the bottom of valleys and poses a greater frost risk to vineyards located in flatlands (Gladstones, 1992; Jones and Hellman, 2003; Jackson, 2008; Yau et al., 2013). Steep slopes substantially increasing a vineyard's expenses due to higher investments in transportation, terracing, and irrigation system design; there is also a risk of machinery roll over. Slope direction (i.e., aspect) also plays an important role in the amount of solar radiation intercepted by the canopy, as well as the corresponding heat accumulation (Gladstones, 1992; Jackson 2008; Keller 2010; Yau et al., 2013).

Edaphic (soil) factors that have a prominent influence on grape growth and development include soil pH, texture, drainage, depth to restrictive layer, and organic matter in soil. Soil pH controls the availability of nutrients for grape roots (Jones et al., 2004; Jackson 2008; Meinert and Curtin, 2005; Yau et al., 2013). Soil drainage controls the amount of water available for grape roots, and can significantly impact grape shoot and canopy vigor (Jones et al., 2004; Gladstones, 1992; Jackson, 2008; Yau et al., 2013). Well-drained soils are preferred by grapes as their roots favor less water; soil texture influences several physical and chemical attributes, including water percolation and water retention through the soil (Jackson 2008). Soil organic matter impacts both its water holding capacity and the availability of nutrients, due to mineralization (Gladstones, 1992; Jackson, 2008). Soil temperature also impacts grape plant, particularly their root activity (Gladstones, 1992). Potential grape production sites typically encompass the aforementioned environmental factors within their optimal range; however, it is uncommon for all factors to be simultaneously within the optimal range for any site. To resolve this issue, a proper management strategy must be developed which will successfully alter each limiting factor to the extent that the site will have the ability to provide a positive economic return despite initial investments made for soil amendment and other corrections. Such decisions require an extensive knowledge of all the pertinent environmental factors and also access to the historical weather data of a given region; thus requiring the development of a technological system with the ability to store and analyze a large volumes of spatio-temporal data to address the complex interactions (Figure 1.2.). Development of such a system would assist growers, decision-makers, and scientists interested in evaluating the potential of a specific land parcel for establishment of a new vineyard.

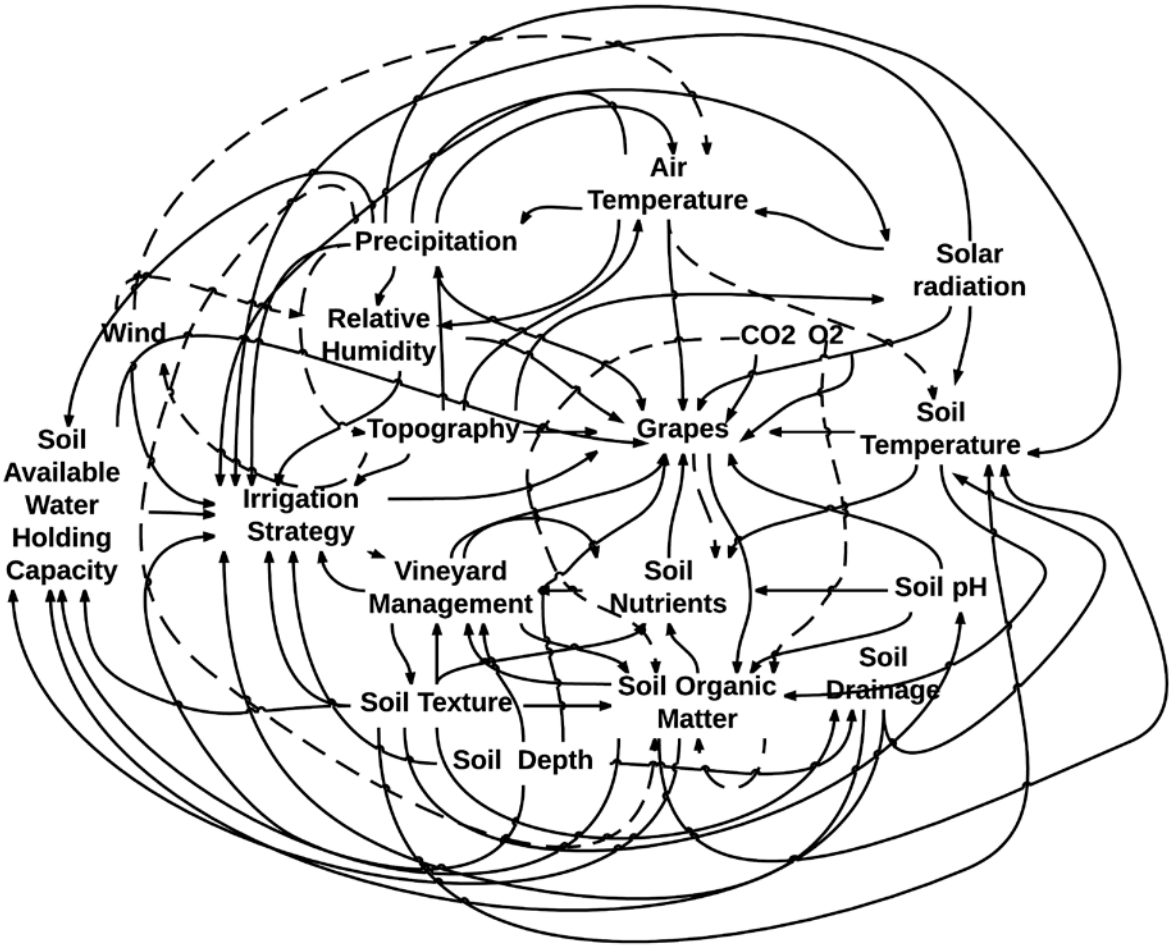

Figure 1. 2. Casual Loop Diagram depicting the interaction among various biophysical factors vital for grape growth and development.

The approach generally applied for vineyard land assessment has been discussed in detail in previous studies by Dry and Smart (1988), Gladstones (1992), Jackson (2008), and Sanga-Ngoie et al. (2010). Additional international studies have focused on specific regions including Canada (Sayed, 1992); Australia (Taylor and McBratney, 2001); Spain (Boufidou, 2011); Nepal (Acharya and Yang, 2015); and Romania (Irimia et al., 2014). Studies focused on grape regions of the United States (U.S.) include: New York (Shaulis and Dethier, 1970); Virginia (Wolf, 1997); Oregon (Jones and Hellman, 2003); Illinois (Kurtural et al., 2006); Kentucky (Kurtural, 2007); Texas (Takow, 2008); eastern Washington (Wolfe, 1999);Walla Walla, Washington (Meinert and Busacca, 2000; Sorensen, 2014); Washington and the Pacific Northwest (Yau, 2011; Yau et al., 2013; Yau et al., 2014).

Foss et al. (2010) applied Boolean logic to determine the viticultural potential of southeast England; however, their approach was unable to differentiate between marginally suitable sites and optimum sites. Another approach for assessing potential vineyard locations utilized a GIS to define the climatic differences of Australia's wine regions (Hall and Jones, 2010). Bowen et al. (2005) used vineyards located in the Okanogan and Similkameen Valleys of British Columbia, Canada to develop a GIS system for determining the relationship between site conditions, management practices, vineyard performance and winemaker's performance. They detected significant suitability differences by comparing the regional patterns of planted cultivars with the medals awarded to individual vineyards and found that loamy soils found in the region are best suited to produce quality wine grapes in British Columbia's Okanagan and Similkameen Valleys.

In the United States, the first online site selection maps were developed by Magarey et al. (1998) for New York State. For eastern California a GIS was used to analyze the *terroir* of vineyard locations (Watkins, 1997) with statistically significant differences in physical characteristics (slope, aspect, soil depth, and water-holding capacity) between vineyard and non-vineyard land use. Jones et al. (2004) and Kurtural et al. (2006) presented a similar spatial suitability analysis for Oregon and Illinois, respectively. Both utilized numerous layers of information, including slope, aspect, elevation, growing degree days (GDD), frost free days (FFD), drainage, soil, and land use to create their suitability indices.

For the Pacific Northwest (PNW) region of the U.S., most site selection studies have been conducted by Jones et al. (2004; 2006; 2010), and were mainly focused on site suitability analysis and evaluation of management practices in Oregon's Umpqua and Rouge Valleys (Jones et al., 2004 and 2006, respectively) and the North Olympic Peninsula of Western Washington (Jones and Duff, 2007). Yau et al. (2011; 2013; 2014) also used GIS to present the environmental features critical for vineyard site suitability analysis in the Pacific Northwest. They compared general characteristics such as elevation, slope, FFD, GDD, Precipitation, and drainage of the existing AVAs in the region; they also conducted principle component analysis, and concluded that most AVAs in the PNW region were affected by the interaction of GDD, FFD, elevation, and precipitation, and recommended that delineation and petitioning of new AVAs should rely more heavily on GIS and spatial datasets. They also highlighted the fact that a spatial comprehensive description of the features of each AVA would increase understanding of the unifying characteristics of the region.

Our study was based on the fact that environmental factors are spatially continuous across natural landscapes; hence, we proposed avoiding the classification of environmental factors into discrete classes, and instead employed fuzzy logic theory (Zadeh, 1975; McBratney and Odeh, 1997; Joss et al., 2008). Fuzzy logic allows the users to specify the likelihood that a value is a member of a set. Using a numeric scale, fuzzy logic assigns 1 to represent full membership and 0 to represent non-membership. We theorized that this would enable us to transform the datasets into a uniform scale and develop a potential vineyard system based on the rules of fuzzy logic. Improving the spatial and temporal resolution of the input datasets is also important; therefore, we focused in this study on the improvement of the input data for all significant climatic factors. Since the area of interest is prone to frost risk due to its geographical location in the PNW, we computed a Cold Damage index based on the Cold Hardiness model of Ferguson et al. (2011; 2014). In addition, wind speed index and water rights were coupled with our developed land assessment systems to provide an auxiliary source of information for users to gain more knowledge of the physical environment of proposed sites. If the core of the systems is well developed and evaluated (Figure 1.1.), other and softer data sources could potentially be added later in the land assessment process.

Goal and Research Questions

The overall goal of this research was of our research was the development of a land assessment system that would enable researchers, extension and education specialists, and stakeholders to understand the impact of environmental factors on wine grape performance.

Specific objectives included:

- Evaluation of available options for the selection of input data for development of a land assessment system.
- Use of bio-climatic indices to improve the classification of vinicultural production areas in the Pacific Northwest.
- Employ a state-of-the art methodology for use in the development of a land assessment system for determining potential vineyard locations.
- Develop a land assessment system based on high-resolution spatial and temporal biophysical data for the Pacific Northwest.

To achieve these specific objectives, several key steps were defined, each step serving as an essential stepping-stone to the next in the development of our land assessment system (Figure 1.3.). Hence, the land assessment system was strongly dependent on the successful completion of the initial steps, as the outputs from the initial steps were required to successfully calculate the vineyard potential of a particular site.

I

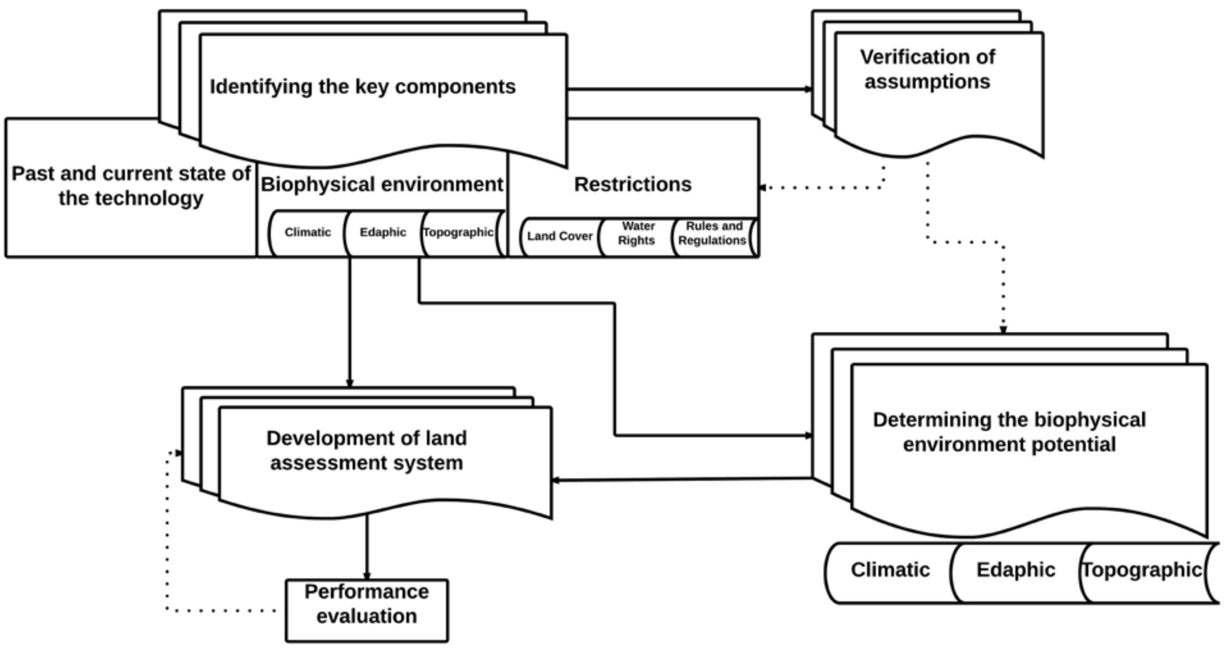

Figure 1. 3. Research overview and major steps.

Thesis outline and overview of study approaches

The following four chapters detail the steps taken to achieve our research specific objectives. Chapter Two explores the utilization of remote sensing technology, particularly Vegetation Indices (VIs) and their dynamics, for estimation of the key phenological stages of the grapevines commonly grown in state of Washington. Chapter Three investigates the use of satellite remote sensing products such as Land Surface Temperature (LST) when coupled with VIs to estimate the near-surface air temperature of regions featuring a complex terrain, with limited access to weather station data. Chapter Four focuses on the calculation of several bio-climatic indices for the state of Washington and parts of Oregon; these bio-climatic indices were computed based on 30 years of daily weather data and the scores were reported for each AVA in the region of study. A spatial wind index, a dynamic minimum temperature index, and a cold damage index were also developed to more accurately address the risk factors associated with the low air temperatures experienced by various regions. Chapter Five discusses development of a comprehensive land assessment system via assimilation of selected bio-climatic indices and edaphic and topographic information; our system utilizes fuzzy logic rules for determining the vineyard potential scores; the evaluation of the land assessment system is also discussed. Chapter Six provides a synthesis and final remarks on the topic and also discusses future implications and potential advancements of our study.

References

Acharya, T.D. and Yang, I.T. (2015). Vineyard suitability analysis of Nepal. International Journal of Environmental Sciences 6 (1) , 13-19.

Boufidou, E. (2011). Towards understanding the DOQ Priorat terroirs: A multivariate GIS analysis (Master thesis). TU Delft, Delft University of Technology. Available online at http://repository.tudelft.nl/view/ir/uuid:70b9c0da-be31-426e-8694-c082a5e36280/

Bojorquez-Tapia, L.A., Diaz-Mondragon, S., and Ezcurra, E. (2001). GIS-based approach for participatory decision making and land suitability assessment. Int. J. Geogr. Inf. Sci. 15 (2), 129–151.

Bowen, P.A., Bogdanoff, C.P., Estergaard, B.F., Marsh, S.G., Usher, K.B., Smith, C.A.S., and Frank. G. (2005). Geology and wine 10: Use of geographic information technology to assess viticulture performance in the Okanagan and Similkameen Valleys, British Columbia. Geoscience Canada, 32, 161–176.

Dry, P.R. and Smart, R.E. (1988). Vineyard site selection: in Coombe, B.G. and Dry, P.R.(eds.), Viticulture; Winetitles, Adelaide, Australia.

Ferguson, J. C., Tarara, J. M., Mills, L. J., Grove, G. G., and Keller, M. (2011). Dynamic thermal time model of cold hardiness for dormant grapevine buds. Annals of Botany, 107(3), 389–396.

Ferguson, J. C., Moyer, M. M., Mills, L. J., Hoogenboom, G., and Keller, M. (2014). Modeling Dormant Bud Cold Hardiness and Budbreak in 23 Vitis Genotypes Reveals Variation by Region of Origin. American Journal of Enology and Viticulture, ajev.2013.13098. http://doi.org/10.5344/ajev.2013.13098

Foss, C., Morris, D., Burnside, N., and Ravenscroft, N. (2010). Champagne comes to England: assessing the potential of GIS in the identification of prime vineyard sites in south east England. Findings in Built and Rural Environments, RICS, London.

Geiger, D. R., and Servaites, J. C. (1991). 5 - Carbon Allocation and Response to Stress A2 - Pell, Harold A. MooneyWilliam E. WinnerEva J. In Response of Plants to Multiple Stresses (pp. 103–127). San Diego: Academic Press.

Gladstones, J. (1992). Viticulture and Environment: Winetitles, Adelaide, Australia. 310 p.

Hall, A. and Jones, G.V. (2010). Spatial analysis of climate in winegrape-growing regions in Australia. Australian Journal of Grape and Wine Research, 16, 389–404.

Hendrickson, L., Ball, M. C., Wood, J. T., Chow, W. S., and Furbank, R. T. (2004). Low temperature effects on photosynthesis and growth of grapevine. Plant, Cell and Environment, 27(7), 795–809.

Hoobler, B. M., Vance, G. F., Hamerlinck, J. D., Munn, L. C., and Hayward, J. A. (2003). Applications of land evaluation and site assessment (LESA) and a geographic information system (GIS) in East Park County, Wyoming. Journal of Soil and Water Conservation, 58(2), 105–112.

Irimia, L., Patriche, C. V., and Quenol, H. (2014). Analysis of viticultural potential and deliniation of homogeneous viticultural zones in a temperate climate region of Romania. J Int Sci Vigne Vin, 48(3), 145-167.

Jackson, R.S. (2008). Wine Science Principles and Applications (3rd ed.). Burlington: Elsevier Science.

Jackson, D.I., and Spurling, M.B. (1988). Climate and viticulture in Australia: in Coombe, B.G. and Dry, P.R.(eds.), Viticulture; Winetitles, Adelaide, Australia.

Joerin, F., Theriault, M., and Musy, A. (2001). Using GIS and outranking multicriteria analysis for land-use suitability assessment. Int. J. Geogr. Inf. Sci. 15 (2), 153–174.

Jones, G.V. and Hellman, E. (2003). Site Assessment: in Hellman, E. (ed.), Oregon Viticulture: 5th Edition, Oregon State University Press, Corvallis, Oregon, p 44-50.

Jones, G. V., Snead, N., and Nelson, P. (2004). Geology and Wine 8. Modeling Viticultural Landscapes: A GIS Analysis of the Terroir Potential in the Umpqua Valley of Oregon. Geoscience Canada, 31(4).

Jones, G.V., Duff, A.A., and Myers, J.M. (2006). Modeling Viticultural Landscapes: a GIS Analysis of the Viticultural Potential in the Rogue Valley of Oregon. Proc. of the VIth Terroir Congress., Bordeaux and Montpellier, France.

Jones, G.V. and Duff, A.A. (2007). The climate and landscape potential for wine production in the North Olympic Peninsula region of Washington. Olympic Cellars, Port Angeles, WA.

Jones, G.V, Duff, A.A., Hall, A., and Myers, J. (2010). Spatial analysis of climate in winegrape growing regions in the western United States. American Journal of Enology and Viticulture, 61, 313–326.

Joss, B. N., Hall, R. J., Sidders, D. M., and Keddy, T. J. (2008). Fuzzy-logic modeling of land suitability for hybrid poplar across the Prairie Provinces of Canada. Environmental Monitoring and Assessment, 141(1-3), 79–96.

Kang, S., Post, W., Wang, D., Nichols, J., Bandaru, V., and West, T. (2013). Hierarchical marginal land assessment for land use planning. Land Use Policy, 30(1), 106–113.

Keller, M. (2010). The Science of Grapevines: Anatomy and Physiology. Academic Press/Elsevier.

Kriedemann, P.E. (1968). Photosynthesis in vine leaves as a function of light intensity, temperature, and leaf age. Vitis, 7, 213–220.

Kurtural, S.K., Dami, I.E. and Taylor, B.H. (2006). Utilizing GIS technologies in selection of suitable vineyard sites. International Journal of Fruit Science 6, 87–107.

Kurtural, S.K. (2007). Vineyard Site Selection. University of Kentucky Cooperative Extension Service.

Liu, Y., Lv, X., Qin, X., Guo, H., Yu, Y., Wang, J., and Mao, G. (2007). An integrated GIS-based analysis system for land-use management of lake areas in urban fringe. Landscape and Urban Planning, 82(4), 233–246.

Magarey, R., Seem, R. C. and DeGloria, S. D. (1998). Prediction of vineyard site suitability. Grape Research News 9: 1–2.

McBratney, A. B., and Odeh, O. A. (1997). Application of fuzzy sets in soil science: Fuzzy logic, fuzzy measurements and fuzzy decisions. Geoderma, 77, 85–113.

Meinert, L. D., and Busacca, A. J. (2000). Geology and Wine 3. Terroirs of the Walla Walla Valley appellation, southeastern Washington State, USA. Geoscience Canada, 27(4).

Meinert, L., and Curtin, T. (2005). Terroir of the Finger Lakes of New York. In: Bettison-Varga L, et al.., editors. 18th Keck Symposium. The Colorado College, Colorado Springs. Keck Geology Consortium, pp. 34–40.

Mendas, A., and Delali, A. (2012). Integration of MultiCriteria Decision Analysis in GIS to develop land suitability for agriculture: Application to durum wheat cultivation in the region of Mleta in Algeria. Computers and Electronics in Agriculture, 83, 117–126.

Moyer, M. M., Gadoury, D. M., Magarey, P. A., Seem, R. C., and Wilcox, W. F. (2010). Development of an Advisory System for Grapevine Powdery Mildew in Eastern North America: A Reassessment of Epidemic Progress. Plant Health Progress.

Pereira, J., and Duckstein, L. (1993). A Multiple criteria decision-making approach to GIS-based land suitability evaluation. Int. J. Geogr. Inf. Syst. 7, 407–424.

Phua, M.H., and Minowa, M. (2005). A GIS-based multi-criteria decision making approach to forest conservation planning at a landscape scale: a case study in the Kinabalu Area, Sabah, Malaysia. Landsc. Urban Plann. 71 (2–4), 207–222.

Saha, M., and Eckelman, M. J. (2015). Geospatial assessment of potential bioenergy crop production on urban marginal land. Applied Energy, 159, 540–547.

Sanga-Ngoie, K., Kumara, K. J. C. and Kobayashi, S. (2010). Potential Grape - Growing Sites in the Tropics: Exploration and Zoning using a GIS Multi-Criteria Evaluation Approach. In proceedings of Asian Association on Remote Sensing. PP. 6.

Sayed, H.A. (1992). Vineyard site suitability in Ontario: Ontario Grape and Wine Adjustment Program, OMAFRA and Agriculture Canada Publication N.10.92, Ministry of Agriculture and Food, Agriculture Canada.

Shaulis, N. and Dethier, B. (1970). New York site selection for wine grapes: New York State Horticultural Society, Proceedings, v. 115, p. 288-294.

Thapa, R. B., and Murayama, Y. (2008). Land evaluation for peri-urban agriculture using analytical hierarchical process and geographic information system techniques: A case study of Hanoi. Land Use Policy, 25(2), 225–239.

Taylor, J. A., and McBratney, A. B. (2001). Environmental management of a viticultural irrigation district. A "top-down bottom-up" model. In Proceedings 1st National Conference on Geospatial Information and Agriculture, Sydney (Causal Productions: Sydney) pp (pp. 609-619).

Watkins, R. L. (1997). Vineyard site suitability in Eastern California. GeoJournal, 43(3), 229–239.

Wolf, T.K. (1997). Site Selection for Commercial Vineyards: Virginia Agricultural Experiment Station, Winchester, Virginia, Publication no. 463–016.

Wolfe, W. (1999). Site Selection in Eastern Washington: Optimizing Site and Variety Choices. In: Growing Grapes in Eastern Washington. Good Fruit Grower.

Yau, I.H., and Washington State University. Dept. of Crop and Soil Sciences. (2011). Developing a grape site selection GIS for the Inland Pacific Northwest. Retrieved February 18, 2013, from http://www.dissertations.wsu.edu/Thesis/Fall2011/i_yau_092211.pdf

Yau, I.H., Davenport, J.R., and Rupp, R.A. (2013). Characterizing Inland Pacific Northwest American Viticultural Areas with Geospatial Data. Plos One, 8(4), 1–11.

Yau, I.H., Davenport, J. R., and Moyer, M. M. (2014). Developing a Wine Grape Site Evaluation Decision Support System for the Inland Pacific Northwestern United States. HortTechnology, 24(1), 88–98.

Zadeh, L., Fu, K., Tanaka, K., and Shimura, M. (Eds.) (1975). Fuzzy sets and their applications to cognitive and decision processes. New York: Academic.

CHAPTER TWO

ESTIMATING GROWING SEASON LENGTH USING VEGETATION INDICES BASED ON REMOTE SENSING: A CASE STUDY FOR VINEYARDS IN WASHINGTON[1]

Abstract

Knowledge of the phenological events which effect grapevines is essential for successful vineyard management. Conventional ground-observed phenological measurements are limited in scope, mainly due to their narrow spatial coverage; however, satellite data provides access to global spatial coverage, potentially providing high temporal resolution. The goal of our study was to use remote sensing to evaluate the efficacy of Vegetation Indices for estimating the length of the growing season for grapes grown in Central Washington. Several phenological metrics for vineyards located in the Columbia Valley region were derived from the satellite time series provided by the Moderate Resolution Imaging Spectroradiometer (MODIS), using the normalized difference vegetation index (NDVI). Our methodology included exponential smoothing and a moving average to compute both the onset of greenness and the end of greenness. The MODIS NDVI values were evaluated using aerial NDVI images for the same vineyard for August 2011. The average bias was -0.08, the average root mean squared error (RMSE) was 0.16, and the coefficient of determination (R^2) was 0.5(p-value 0.06). The results revealed an average growing season duration of 216 days for grapevines grown in this region over a period of five years. The average starting date of the growing season coincided with April

---

[1] Published as: Badr, G., Hoogenboom, G., Davenport, J., and Smithyman, J. (2015). Estimating Growing Season Length Using Vegetation Indices Based on Remote Sensing: A Case Study for Vineyards in Washington State. (2015). *Transactions of the ASABE*, 551–564. © 2015 by the American Society of Agricultural and Biological Engineers; reprinted with permission.

2nd, and the computed end of the growing season was November 4th. The highest NDVI value was 0.55 and coincided with July 12th. On average, the lowest NDVI value was 0.3, with an average range of 0.25. Our preliminary results showed that MODIS NDVI can be used to monitor vineyard vegetation dynamics in the Columbia Valley, and also has the potential to be applied to other grape-growing regions in the U.S.A. and even internationally.

Introduction

Vegetation phenology is the study of the life cycle of crops; the inter-annual variability of a crop's life cycle can be investigated using vegetation phenology (Cunha et al., 2010). Optimum grapevine production requires a distinct fusion of weather, soil, topography, and vineyard management. To monitor performance of grapevines within a region, growers obtain the phenological observations for their individual vineyards (Chuine et al., 2004; Cunha et al., 2010). Good vineyard management requires access to grapevine phenological data in order to make decisions based on the status of the specific vines (Cunha et al., 2010). Combining phenological data with local climate data enables assessment of the potential response of grape varieties in new regions, and this combination can also be used to index potential climate change (Chuine et al., 2004; Jones and Davis, 2000; Cunha et al., 2010).

There are two primary approaches for conducting phenological measurements: ground-based observation of the phenology of the individual grapevines and satellite-based observation of the phenology. Both methods have advantages and disadvantages: ground-based observation of phenology benefits from a high temporal resolution and detailed information regarding species and cultivar dynamics. However, the spatial resolution of ground-based observations can be limited (Ricotta and Avena, 2000; Schwartz et al., 2002; White et al., 2005; Studer et al., 2007). Satellite-based observation of phenology can potentially provide higher spatial resolution, making it a suitable complementary observation method (Studer et al., 2007). There are currently a large number of satellite datasets available in the public domain with extensive global coverage (Hall et al., 2002; Dobrowski et al., 2003; Johnson et al., 2003).

Remote sensing and NDVI metrics

Polar-orbiting environmental satellites provide daily coverage of the Earth. The Moderate Resolution Imaging Spectroradiometer (MODIS) is one of the NASA-designed instruments onboard the Terra satellite. Terra uses five sensors to observe the atmosphere, land surface, oceans, snow and ice, and energy budget (Terra, 2014). The Earth's bio-geochemical and energy systems are monitored by these sensors. The MODIS sensor is categorized as multispectral with a total of 36 spectral bands, and has a spatial resolution that ranges from 250 m to 1 km. These spectral bands are particularly effective for the monitoring of terrestrial vegetation systems (Barnes et al., 1998; Justice et al., 2002). For a complete review of the MODIS and its products, see Justice et al. (2002); Guenther et al. (2002); and Morisette et al. (2002).

The normalized difference vegetation index (NDVI) is the ratio of the difference between the reflectance in the red and near-infrared regions of the spectrum to the summation of these two values. Rouse et al. (1974), and is defined by NDVI as follows:

$$NDVI = \frac{\rho_{nir} - \rho_{red}}{\rho_{nir} + \rho_{red}} \qquad (2.1.)$$

where ρ_{nir} represents the reflectance at the near-infrared region of the spectrum (0.7 – 1.1 µm) and ρ_{red} denotes the reflectance at the red wavelengths (0.6 – 0.7 µm).

NDVI is often used in environmental studies because it has the ability to exploit the spectral properties of green leaves (Goward et al., 1985; Tucker et al., 1991; Petorrelli et al., 2005; Dougherty, 2012; Pettorelli, 2013). Various algorithms have been used to derive parameters related to vegetation phenology and production from NDVI time series' (reviewed in

Petorrelli et al., 2005; Atkinson et al., 2012; Jamali et al., 2015). Petorrelli et al., (2005) specifically referred to the stepwise logistic regression to represent the inter-annual dynamics of NDVI, and also as a means to obtain key transition dates such as the onset of greenness. The primary advantage of using logistic regression is that it treats each pixel separately and also takes into consideration the multi-modal vegetation profiles within a specific region (Petorrelli et al., 2005). In addition, this algorithm can successfully manage the false high values that can cause sudden increases in daily NDVI values (Petorrelli et al., 2005). Fischer (1994) developed a semi-empirical function to model the NDVI profile using a logistic function with five parameters to describe the annual time profile of NDVI, as crops with similar phenology behave like homogenous canopies. He reported two of these parameters as the slopes of the ascending and descending inflection points, respectively. Two additional parameters were set as the dates that the ascending and descending inflection points were observed, and the final parameter was related to the asymptotic value of the NDVI. Reed et al. (1994) derived 12 metrics related to key phenological stages taken from the NDVI time series of various land cover types found throughout the U.S., such as coniferous and deciduous forests, grasslands, and winter wheat. The chosen metrics included onset of greenness, time of peak NDVI, maximum NDVI, rate of green-up, rate of senescence, and integrated NDVI; a strong correlation was found between the satellite-derived metrics and the predicted phenological characteristics. Reed et al. (1994) categorized the NDVI metrics into three groups: 1) temporal metrics focused on the timing of an event; 2) NDVI-based metrics that report the value of the NDVI when specific phenological events occur; and 3) derived metrics computed from each NDVI time series. However, they also emphasized that these metrics may not necessarily correspond to conventional ground-based phenological events. Zhang et al. (2003) determined vegetation phenology based on MODIS data; their results were consistent with the vegetation dynamics of the chosen study area, and their MODIS-based estimates of phenology (green-up onset, maturity onset, and dormancy onset) depicted a strong spatio-temporal pattern based on the type of land cover present. No ground-based measurements were used to evaluate these MODIS-based estimates; therefore, the group recommended that future research also utilize ground-based data.

Several studies have focused on the application of NDVI obtained from satellite remote sensing to viticulture (Hall et al., 2011; Johnson et al., 2012). These studies have mainly concentrated on vineyard vigor mapping (Montero et al., 1999; Johnson et al., 2003; Johnson et al., 2012), canopy density estimation (Dobrowski et al., 2002; Johnson et al., 2012), high-resolution vineyard mapping (Hall et al., 2003; Johnson et al., 2012), cover crop estimation (Trout et al., 2008; Johnson et al., 2012), and pruning weight calculation (Stamatiadis et al., 2006; Johnson et al., 2012). Low spatial resolution NDVI imagery has proven more effective than LAI for mapping the spatial variability of minimally pruned, unconfined vineyards (Hall et al., 2008); Hall et al. (2002) derived grapevine canopy density and area from high spatial resolution aerial images. In another study, Hall et al. (2011) evaluated inter-seasonal changes to determine the correlation between canopy size, grape composition, and final yield. Lamb et al. (2004) reported a relationship between the physical properties of the grapevine canopy derived from remotely-sensed data and the measurement of grape phenolics and color for *Vitis vinifera* ‘Cabernet Sauvignon’. Their study was conducted over two growing seasons in vineyards located in the Coonawarra region of Southern Australia. The quantification of grape color (mg anthocyanins/gram berry weight) and total phenolics (280 nm absorbance units per gram berry weight) were conducted using the procedures described by Iland et al. (2000). The relationship between the remotely-sensed data and the berry properties varied with grapevine phenology, with the highest correlation observed at veraison. However, to date, few studies have focused on the application of satellite-based NDVI to estimate the vegetation phenology of grapevines, and none have been conducted in the Pacific Northwest. Cunha et al. (2010) successfully predicted the flowering date of grapevines, with an average deviation of three days, for an eight-year period (1999-2007) based on ten-day image composites of VEGETATION. They reported a significant correlation between the observations of full canopy dates based on satellite data and the occurrence of veraison observed under field conditions. No previous studies have focused on deriving grapevine phenological metrics from MODIS-based vegetation indices; the goal of our study was to determine the applicability of MODIS NDVI for the prediction of growing season length in grapes produced in the Pacific Northwest.

Materials and Methods

Study area

This study was conducted in the Columbia Valley of the State of Washington, United States (Figure 2.1.). Fourteen vineyards were used, all between the latitudes of 47.13° N and 46.2° N, and the longitudes of 120.2° W and 119.6° W (Table 2.1.).

Table 2. 1. The representative coordinates, average elevations, and major soil type of the test vineyards.

Vineyard ID	Coordinates: Longitude	Latitude	Elevation(m)	Soil type	Coresponding AgWeatherNet station
1	-119.96	47.12	416	Loam	George West
2	-119.92	46.90	374	Silt loam	Royal city west
3	-119.91	46.85	213	Silt loam	Royal city west
4	-119.89	46.75	262	Silt loam	Desert Aire
5	-119.64	46.75	235	Sand	Mattawa
6	-119.83	46.65	179	Silty clay loam	Mattawa
7	-119.82	46.54	423	Sandy loam	Mattawa
8	-120.20	46.44	416	Sandy loam	outlook
9	-119.83	46.26	289	Sandy loam	WSU Hamilton
10	-119.68	46.30	334	Fine sandy loam	Roza
11	-119.45	46.30	270	Loam	Benton City
12	-119.46	46.28	213	Loam	Benton City
13	-119.43	46.28	270	Fine sandy loam	Benton City
14	-119.79	46.75	276	Fine sandy loam	Mattawa

The varieties included were ‘Cabernet Sauvignon’, ‘White Riesling’, ‘Merlot’, ‘Syrah’, ‘Cabernet Franc’, ‘Malbec’, ‘Pinot Gris’, and ‘Petit Verdot’. The vineyards were located in Benton, Grant, and Yakima counties (Figure 2.1.). The majority of land in these three counties is covered by shrublands, pasture, corn (*Zea mays*), hops (*Humulus lupulus*), alfalfa (*Medicago sativa*), apples (*Malus domestica*), dry beans (*Phaseolus vulgaris*), and spring wheat (*Triticum aestivum*) (USDA-NASS, 2014). In this region, the dominant soil type is a silt loam, with the elevation ranging from 160 m to 460 m. The climate is characterized as continental, with an average annual temperature of 11.3°C, and a total annual precipitation of 12.6 mm

(AgWeatherNet, 2015). Vineyard block areas ranged from 20 ha to 200 ha, with the majority being fewer than 50 ha.

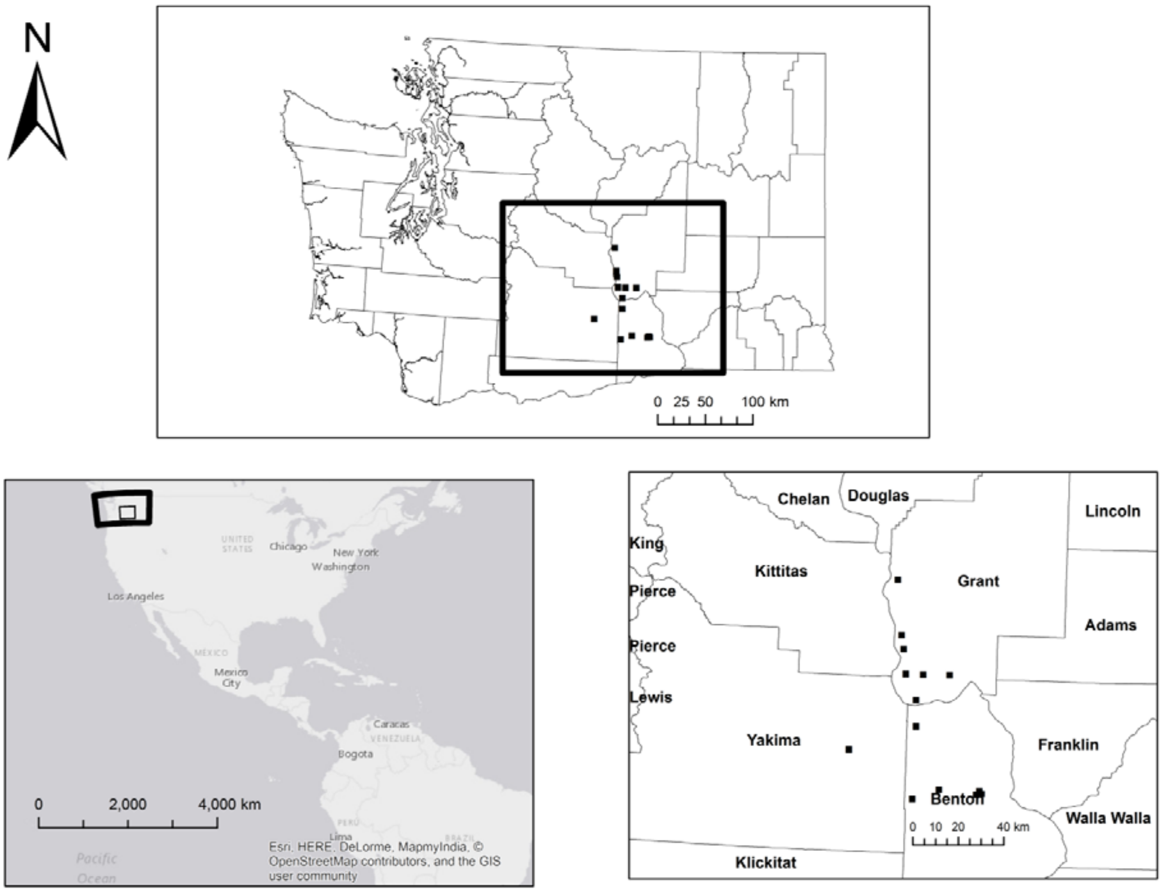

Figure 2. 1. Study area and locations of the selected vineyards in the State of Washington and its counties (all within the Grant, Benton, and Yakima counties).

NDVI

MODIS data were downloaded from the NASA Land Processes Distributed Active Archive Center (NASA, 2015); to better understand the grapevine dynamics, more than one year of MODIS products were retrieved (2009-2013). The downloaded data included 16-day composites of MODIS NDVI, and 23 composite images (featuring a spatial resolution of 1 km) were available for each year of the study period (Figure 2.2.). In this study, the NDVI composites were used because the changes in the vegetation status on a daily basis were not significant and the atmospheric effects could be eliminated by compositing.

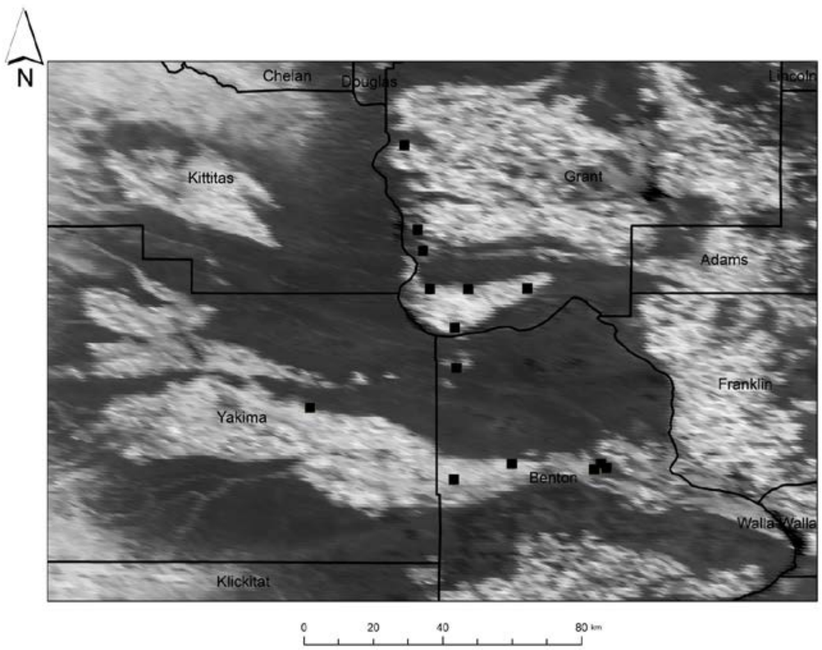

Figure 2.2. Example of a MODIS NDVI composite of the study area (August 13, 2009). The vineyard locations (black squares) and their corresponding counties are superimposed over the image.

Aerial images were acquired during 4-hour periods commencing at approximately solar noon throughout August 2011, using a camera sensor Canon D5 MK II with a pixel size of 0.5 meters; the images were also georeferenced (PCS_NAD1983_Washington_South). The aerial images were provided by the Ste. Michelle Wine Estates for several vineyards, and were only available for August of 2011. The images were converted to NDVI by the providing company, and the VISAT 4.10.3 (BEAM, 2013) was used to check the statistics of the aerial NDVI images (Table 2.2.).

Table 2.2. Descriptive statistics of the raw values of NDVI obtained from the aerial images, the NDVI from the aerial images after the vineyards were geometrically selected, and the NDVI from the aerial images after removing pixels below the NDVI threshold of 0.15.

	Raw NDVI Aerial Images						Geometrically Selected						Filtered					
Vineyard	Min.	Max.	Mean	SD	CV	Median	Min.	Max.	Mean	SD	CV	Median	Min.	Max.	Mean	SD	CV	Median
1	0	1.16	0.28	0.23	0.01	0.26	0	1.01	0.36	0.20	0.01	0.37	0.15	1.01	0.43	0.16	0.00	0.43
2	0	0.97	0.36	0.27	0.01	0.37	0	0.97	0.31	0.13	0.00	0.31	0.15	0.97	0.33	0.12	0.00	0.31
3	0	0.93	0.12	0.13	0.01	0.08	0	0.86	0.17	0.13	0.01	0.14	0.15	0.82	0.28	0.10	0.00	0.26
4	0	1.19	0.21	0.22	0.01	0.14	0	0.91	0.26	0.17	0.01	0.23	0.15	1.19	0.41	0.18	0.00	0.39
5	0	0.97	0.23	0.22	0.01	0.14	0	0.99	0.32	0.21	0.01	0.33	0.15	0.97	0.38	0.18	0.00	0.39
6	0	1.05	0.28	0.24	0.01	0.19	0	1.05	0.32	0.24	0.01	0.32	0.15	0.77	0.34	0.11	0.00	0.35
7	0	0.85	0.20	0.20	0.01	0.14	0	0.77	0.19	0.15	0.01	0.14	0.15	0.81	0.36	0.13	0.00	0.36
8	0	0.83	0.14	0.14	0.01	0.10	0	0.70	0.21	0.12	0.01	0.18	0.15	0.68	0.27	0.09	0.00	0.25
9	0	1.11	0.29	0.21	0.01	0.30	0	1.04	0.37	0.16	0.00	0.38	0.15	1.04	0.51	0.15	0.00	0.51
10	0	1.23	0.29	0.26	0.01	0.19	0	1.19	0.53	0.17	0.00	0.53	0.15	1.14	0.54	0.14	0.00	0.53
11	0	1.02	0.14	0.20	0.01	0.02	0	1.02	0.31	0.20	0.01	0.29	0.15	1.02	0.40	0.16	0.00	0.39
12	0	0.91	0.08	0.13	0.02	0.07	0	0.69	0.23	0.15	0.01	0.18	0.15	0.69	0.33	0.12	0.00	0.34
13	0	1.14	0.11	0.13	0.01	0.06	0	1.14	0.11	0.13	0.01	0.06	0.15	0.79	0.37	0.13	0.00	0.38
14	0	0.89	0.11	0.16	0.02	0.00	0	0.71	0.08	0.13	0.02	0.00	0.15	0.89	0.33	0.13	0.00	0.32
Average	0	1	0.20	0.20	0.01	0.15	0	0.93	0.27	0.16	0.01	0.25	0.15	0.91	0.38	0.14	0.00	0.37

The positional accuracy of the aerial images was verified using Google Earth (Google Earth, 2013), and the latitudinal and longitudinal coordinates at the top left corner and bottom right corner of the aerial images were obtained using VISAT (BEAM, 2013). Since the aerial images represent the vineyard locations, the obtained coordinates were used to define a frame for extracting the NDVI values from the MODIS NDVI composites (Figure 2.3.).

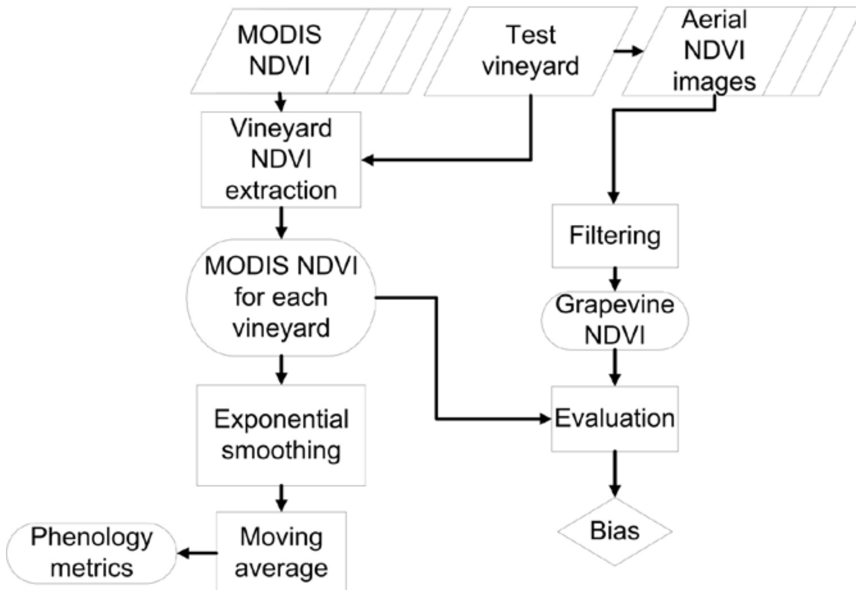

Figure 2. 3. The overall methodology used in this study.

Evaluation

The aerial images were filtered by omitting all NDVI values below 0.15 using the VISAT 4.10.3 (BEAM, 2013) band math tool (Table 2.2.), which reduced any noise introduced via the inter-row spaces of the vineyards. This particular threshold value was selected because the median for the NDVI obtained from the aerial images was 0.15 (Table 2.2.); additionally, inspection of the images showed that the NDVI corresponding to the inter-row spaces was less than 0.15. During the next phase, the vineyards were geometrically selected using the polygon drawing tool in VISAT 4.10.33 (BEAM, 2013). This polygon was then used as a mask to minimize any effect of other unwanted vegetation, such as annual crop fields and orchards, within the field of view of the camera on the NDVI values derived from the image (Figure 2.4.).

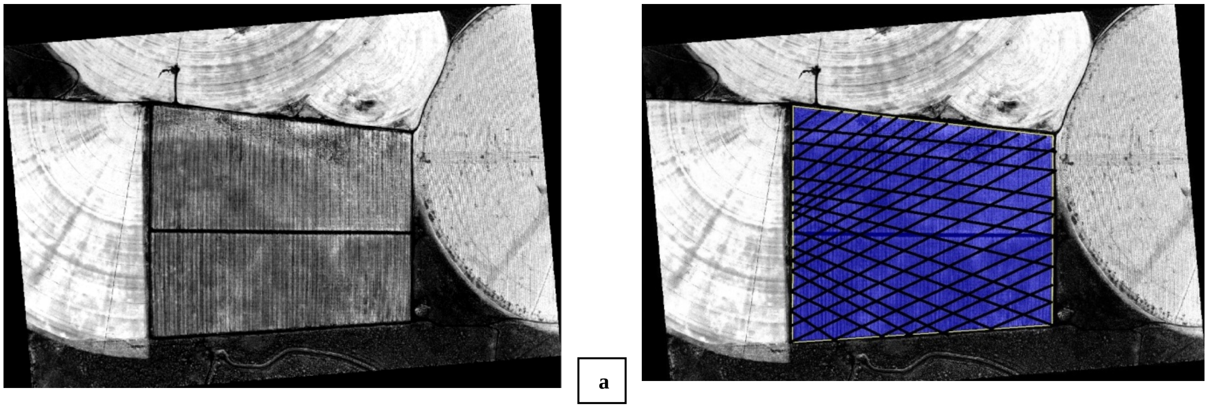

a b

Figure 2. 4. Example of geometric selection of the vineyards in the NDVI image, based on aerial images acquired in August of 2011: (a) original image; (b) geometrically-selected vineyard (in blue).

The VISAT pin manager tool (BEAM, 2013) was employed to extract the MODIS NDVI values using the coordinate values of the vineyards. For each vineyard, the MODIS NDVI values were narrowed to a single value because the spatial size of the vineyard blocks was small and the blocks were covered by individual MODIS pixels (Table 2.1.). The NDVI values obtained from the aerial images of the individual blocks were averages; using standard statistical methods, we compared the NDVI values based on the aerial images to the MODIS NDVI values. The primary purpose of this evaluation phase was to note any potential differences between the MODIS NDVI and the NDVI obtained from sources with much finer spatial resolutions (e.g. aerial images).

Grapevine phenological metrics

The vineyards' MODIS NDVI values for a period of five years were extracted using the VISAT pin manager tool (BEAM, 2013). In each of these five-year periods, a total of 115 MODIS NDVI values were available for each vineyard. We used the MODIS NDVI values extracted for each vineyard block to obtain the grapevine phenological metrics (Table 2.3.).

Table 2. 3. NDVI metrics and their phenological interpretation (adapted from Reed et al., 1994).

NDVI metric	Phenological interpretation
Temporal NDVI metric	
Time of onset of greenness	Beginning of growing season in grapevines
Time of end of greenness	Termination of growing season in grapevines
Duration of greenness	Duration of active photosynthesis in grapevines
Time of maximum NDVI	Time of maximum greenness, which coincides with veraision in grapevines (Cunha et al., 2010)
NDVI value metric	
Value of the onset of greenness	NDVI of grapevines at start of growing season
Value of the end of greenness	NDVI of grapevines at end of growing season
Value of maximum NDVI	Maximum NDVI of grapevines
Range of NDVI	Range of NDVI in grapevines
Derived metrics	
Time integrated NDVI	Net primary production of grapevines
Rate of green up	Pace of acceleration of photosynthesis in grapevines
Rate of senescence	Pace of deacclaration of photosynthesis in grapevines

The MODIS NDVI data showed extensive variability within a range of 0.65. The variability was due to issues such as cloud-contaminated pixels, ozone and water vapor absorption, solar illumination, instrument degradation, and insufficient calibration (Reed et al., 1994; Studer et al., 2007; Cunha et al., 2010). To counteract this variability, we smoothed the MODIS NDVI data using an approach similar to that employed by Reed et al. (1994); Studer et al. (2007); and Cunha et al. (2010). We utilized the exponential smoothing option from the Excel data analysis tool-box (Microsoft, 2010), with a damping factor of 0.75 (Figure 2.5.; Figure 2.6.).

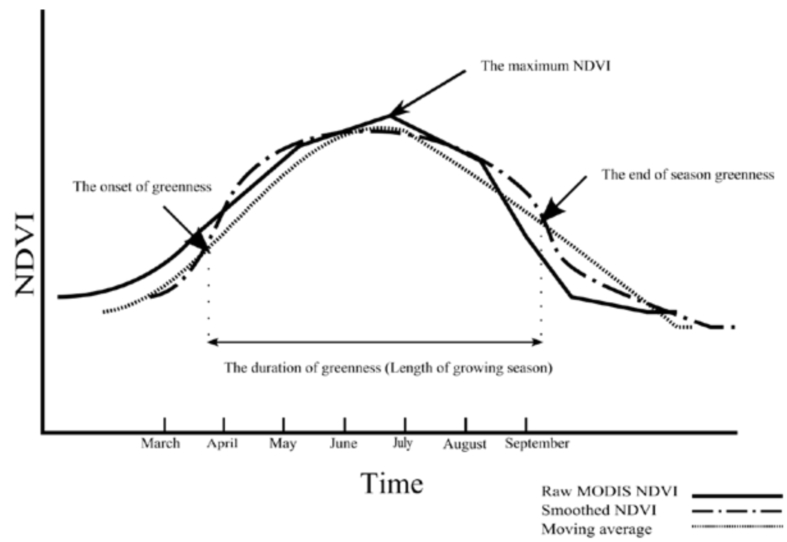

Figure 2.5. Schematic profile of the NDVI for a single growing season. The use of smoothed and moving average methods to detect the length of the growing season is also depicted.

We calculated a moving average of the MODIS NDVI data using the data analysis toolbox of Excel (Microsoft, 2010) so that we could obtain respective NDVI metrics from the MODIS NDVI data. The moving average was calculated using an equation based on autoregressive moving average (ARMA) models (Hoff, 1983; Granger, 1989). The autoregressive moving average model has been employed in the previous phenological studies (Reed et al., 1994; Studer et al., 2007; Cunha et al., 2010). The calculation of the moving average was based on the following equation:

$$Y_t = (X_t + X_{t-1} + X_{t-2} + \cdots + X_{t-(w-1)})/w \qquad (2.1.)$$

where Y_t is the computed moving average for time *t*, X_t is the smoothed NDVI value for time *t*, and *w* is the time interval employed to derive the moving average. The time interval was set to eight cycles of NDVI composites (Reed et al., 1994), and a time lag was introduced to the smoothed MODIS NDVI values. This was done because the moving average calculates the mean value from the last eight available MODI NDVI composites, forming "backward looking" filters over the MODIS NDVI values. The values obtained from the moving average were then compared against the NDVI time series in order to detect any departure from the established trend as a result of smoothing.

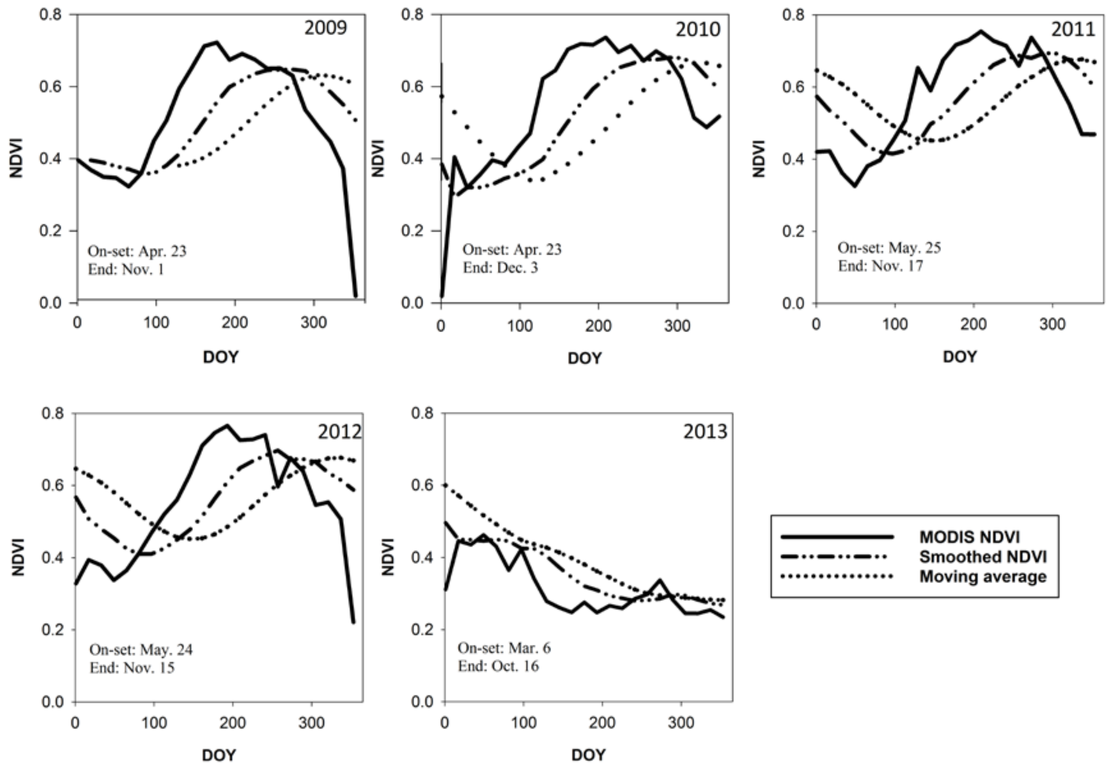

Figure 2.6. Original, smoothed, and moving average NDVI time series for test vineyard #10 over the study period (2009-2013). Onset of greenness (onset) and end of greenness (End) has also been reported for each year. The correlation between the raw MODIS NDVI and the smoothed NDVI was 0.7, and the correlation between the smoothed NDVI and the moving average was 0.76.

The onset of season greenness was defined as the beginning of the growing season in grapevines; thus, the period when the smoothed MODIS NDVI values either became greater than the moving average or showed the least amount of difference from the moving average values was considered the onset of greenness (Figure 2.5.). End of season greenness was defined as the termination of the growing season in grapevines. End of greenness was identified as the period when the smoothed MODIS NDVI values either became smaller than the moving average or showed the least amount of difference from the moving average values. Duration of greenness was defined as the number of days between the onset of greenness and the end of greenness. The maximum NDVI value was not susceptible to cloud contamination or any other source of bias (Reed et al., 1994), thus enabling us to derive the time and value of the maximum NDVI from the original NDVI values. The NDVI range was computed by subtracting the value of the lowest NDVI from that of the maximum NDVI. The green-up rate was the rate increase in the NDVI during the growing season, and was obtained via calculation of the slope of the relationship between the maximum NDVI value and the onset of greenness. The rate of senescence was the rate decrease in the NDVI, which was derived from the slope of the relationship between the NDVI value for the end of greenness and the maximum NDVI value. The smoothed NDVI values between the onset of greenness and the end of greenness were used to obtain the time-integrated NDVI value. The time-integrated NDVI value was computed using the following equation (Yang et al., 1998):

$$TI\ NDVI = \sum_{i}^{n} NDVI_i \qquad (2.3.)$$

where i is the i^{th} 16-day composite data, ranging from the onset of greenness (l) to the end of greenness (n).

Growing Degree Days (GDD)

The heat unit accumulation or growing degree days (GDD) value for each vineyard was calculated for each year of the study. The growing degree day calculation was based on the following equation, with a base temperature (T_{base}) of 10 °C (Winkler et al., 1974; Jones et al., 2010).

$$GDD = \left(\frac{T_{min} + T_{max}}{2}\right) - T_{base} \qquad (2.4.)$$

where T_{min} is the minimum air temperature value for a single day, and T_{max} is the maximum air temperature value for a single day. T_{base} is the base temperature at which the grapevine resumes its activity, and below which temperature there is no significant biological activity (i.e., no heat units accumulate when the average temperature is below that of the base temperature).

The weather data were obtained from AgWeatherNet (AgWeatherNet, 2015), a network of automated weather stations located in the State of Washington and managed by Washington State University. The AgWeatherNet weather stations located nearest each vineyard were used to obtain the daily air temperature data for the study period. We assumed two different growing seasons to accumulate GDD values: 1) a fixed growing season between April 1st and October 31st; and 2) a growing season based on the time of onset of greenness and the time of end of greenness derived from the MODIS NDVI. The GDD values based on the two different growing seasons were then compared using standard statistical methods.

Results and Discussion

Evaluation

The MODIS NDVI values were evaluated against the NDVI values derived from the vineyard aerial images acquired in August 2011 (Table 2.4.). The results indicated a coefficient of determination (R^2) of 0.5 (*p-value* 0.06), a RMSE value of 0.16, and an average bias of -0.08. The MODIS NDVI values were greater than the aerial image values for most of the vineyards, but not for all (e.g. vineyards 10, 11, and 13). The highest absolute bias value was obtained for vineyard 14, while the lowest absolute bias value was obtained for vineyards 3, 5, and 12. This difference in values can largely be attributed to the coarser spatial resolution of MODIS compared to that of the aerial images, since the incoming electromagnetic signal reaching the

MODIS sensor is comprised of a mixture of the spectral signatures of different land cover types within the pixel of interest.

Table 2. 4. NDVI values derived from the aerial images and MODIS and the corresponding bias.

Vineyard ID	*Predicted (Aerial images)*	*Predicted(MODIS)*	*Bias*
1	0.43	0.69	-0.27
2	0.33	0.40	-0.07
3	0.28	0.28	-0.01
4	0.41	0.71	-0.30
5	0.43	0.44	-0.01
6	0.34	0.30	0.04
7	0.36	0.39	-0.02
8	0.28	0.35	-0.07
9	0.43	0.70	-0.27
10	0.57	0.52	0.04
11	0.38	0.25	0.13
12	0.33	0.34	-0.01
13	0.29	0.26	0.03
14	0.31	0.65	-0.34
Average	0.37	0.45	-0.08
SD	0.08	0.17	0.15
RMSE			0.16

The land cover surrounding each vineyard was obtained from the National Agricultural Statistics Service (NASS) crop land data layer (CDL) for 2011 (USDA-NASS, 2014). In the case of vineyard 10 (the vineyard with the highest positive bias), there was open water adjacent to the vineyard. The NDVI value for open water is very low and can even be negative (Glenn et al., 2008); therefore, this value integrates with the extracted MODIS value for a particular pixel, resulting in a lower NDVI value compared with that of the NDVI obtained from the aerial image. The lowest absolute bias was observed in the pixels that were surrounded by other vineyards and/or pasture/hay land cover. The highest absolute bias was observed in vineyard 14, which was surrounded by shrublands. Vineyard 14 was established only a year prior to the image acquisition, therefore, the grapevine canopy was not fully developed and so the signal from the soil was dominant, resulting in a higher difference between the aerial image NDVI and that of the MODIS NDVI for that particular pixel.

Growing Degree Days (GDD)

The heat unit accumulations obtained for the individual vineyards were based on a period of the growing season between the onset of greenness and the end of greenness, and were computed using MODIS NDVI. Additionally, a GDD based on standard growing season duration (April 1st - October 31st) was also derived for each vineyard (Table 2.5.; Figure 2.7.).

Table 2. 5. GDD values computed for a fixed growing season (April-October) and the growing season derived from the MODIS NDVI.

	2009		2010		2011		2012		2013		Fixed 2009-2013		NDVI 2009-2013	
Vineyard	Fixed	NDVI	Fixed	NDVI	Fixed	NDVI	Fixed	NDVI	Fixed	NDVI	Avg.	SD	Avg.	SD
1	1661	1690	1386	1327	1388	1349	1615	1598	1759	1746	1562	168	1542	194
2	1712	1678	1453	1416	1354	978	1591	1486	1691	1707	1560	154	1453	293
3	1712	1706	1453	1160	1354	1334	1591	1423	1691	1707	1560	154	1466	239
4	1951	1886	1736	1627	1735	1574	1888	1868	2062	2096	1874	141	1810	212
5	1718	1713	1503	1474	1486	1457	1652	1635	1789	1807	1630	133	1617	151
6	1718	1635	1503	1352	1486	1390	1652	1584	1789	1807	1630	133	1554	187
7	1718	1650	1503	1383	1486	1332	1652	1488	1789	1807	1630	133	1532	196
8	1704	1753	1442	1496	1411	1461	1659	1659	1763	1785	1596	159	1631	147
9	1546	1592	1363	1345	1356	1302	1553	1200	1648	1659	1493	129	1420	197
10	1480	1496	1292	1290	1219	1205	1417	1287	1489	1506	1379	119	1357	136
11	1673	1772	1525	1537	1506	1385	1665	1458	1768	1798	1627	110	1590	186
12	1673	1593	1525	1613	1506	1571	1665	1625	1768	1791	1627	110	1639	88
13	1673	1772	1525	1539	1506	1576	1665	1625	1768	1798	1627	110	1662	117
14	1718	1715	1503	1419	1486	1457	1652	1661	1789	1807	1630	133	1612	168

The variability in the calculated GDD values is a result of the difference in length of the fixed growing season (213 days) versus that of the growing season obtained from the MODIS NDVI, which varied as a result of the heterogeneity of the MODIS NDVI pixel containing the vineyard. To accurately capture their dynamics, vineyards should be monitored using spatial, temporal, and spectral remotely-sensed data at higher resolutions. We obtained higher standard deviation values for the GDD from the MODIS NDVI-derived growing seasons for each vineyard, except vineyards 8 and 12. The total accumulated GDD value for a fixed growing season was greater for most of the vineyards, except for vineyards 8, 12, and 13; this higher

GDD value was directly related to the growing season length. The average bias of the accumulated GDD for the April-October growing season and that of the MODIS NDVI-derived growing season was 39.

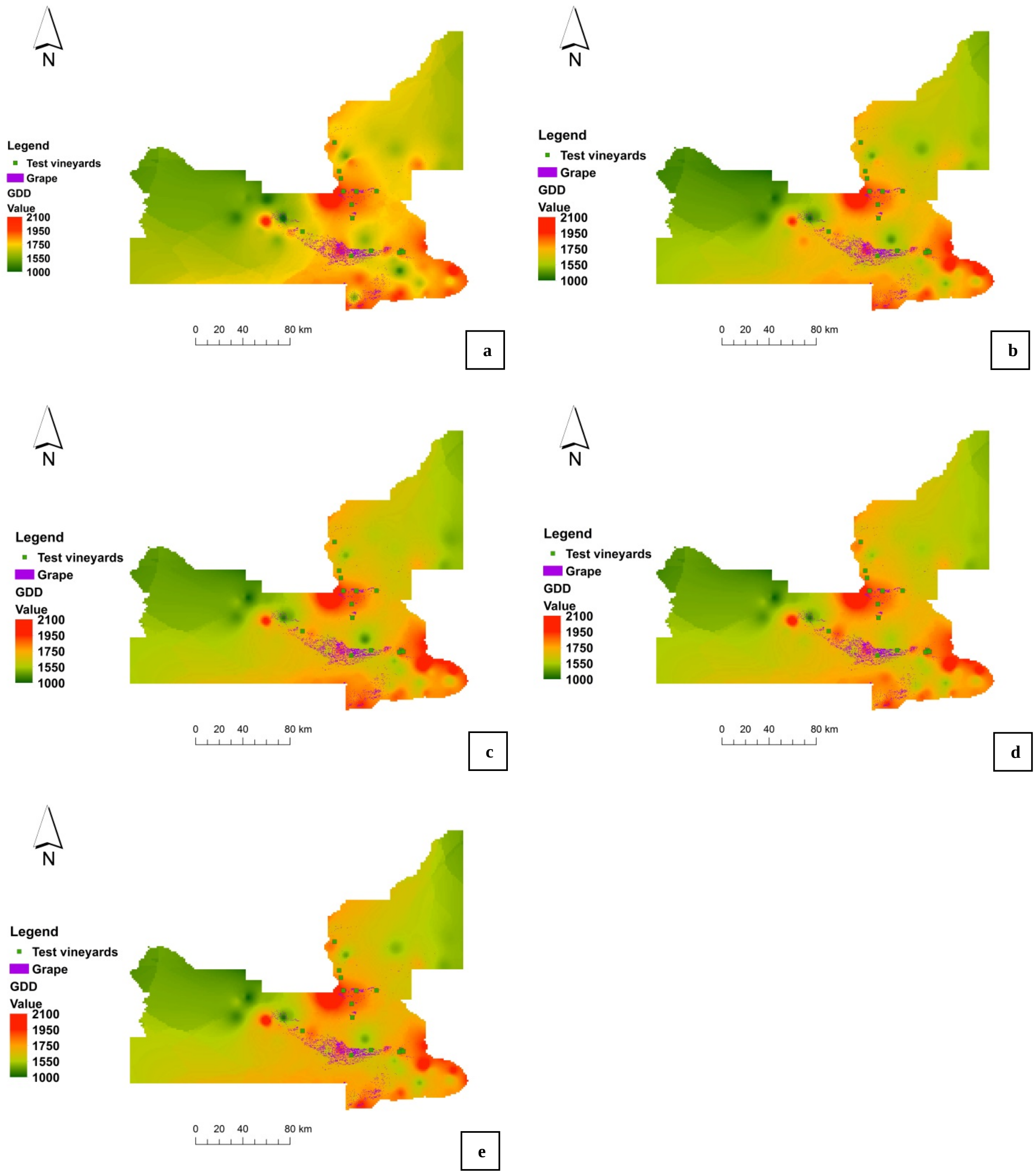

Figure 2.7. Interpolated accumulated growing degree days with a base of 10 °C (GDD) of a fixed growing season (April 1st - October 31st) in (a) 2009, (b) 2010, (c) 2011, (d) 2012, and (e) 2013.

Phenological metrics

The results indicated an average growing season length of 216 days for the test vineyards during the study period (2009-2013) (Table 2.6.). A fixed growing season between April 1st and October 31st has 213 days, while the growing season we obtained was 3 days longer. The estimated growing season length determined in our study was within 15% of the growing season length (190 days for Central Washington) reported by Gladstones (1992) and Howell (2001). Taking into account the coarse spatial resolution of the images and the fact that the MODIS NDVI images are actually a composite of 16-day values, we found our estimate within 15% of the known value for growing season length promising.

Table 2.6. The overall phenological metrics for all the test vineyards.

NDVI metric	Year				
Temporal NDVI metric	2009	2010	2011	2012	2013
Time of onset of greenness (DOY)	79	93	116	118	54
Time of end of greenness (DOY)	311	310	310	309	302
Duration of greenness	233	214	193	193	248
Time of maximum NDVI (DOY)	167	182	177	263	182
NDVI value metric					
Value of the onset of greenness	0.29	0.31	0.33	0.28	0.38
Value of the end of greenness	0.40	0.43	0.44	0.42	0.37
Value of maximum NDVI	0.50	0.56	0.57	0.55	0.56
Range of NDVI	0.22	0.23	0.23	0.25	0.32
Derived metrics					
Time-integrated NDVI	5.59	5.62	5.28	5.01	7.22
Rate of green-up (NDVI/day)	0.003	0.004	0.003	0.003	0.001
Rate of senescence(NDVI/day)	0.002	0.004	0.003	0.005	0.002

The average onset of greenness, i.e. the starting date of the growing season, was around April 2, while April 1 is commonly considered as the first day of the growing season, especially for the calculation of GDDs. The time for the onset of greenness, on average, was March 20 for

2009, April 3 for 2010, April 26 for 2011, April 28 for 2012, and February 23 for 2013 (Figure 2.8.). Keller et al. (2010) reported an average bud break date around April 26 for this region. Therefore, the 2011 and 2012 results were close to the value reported by Keller et al. (2010). Spring temperatures also control the onset of greenness. Among the reported years, 2013 was the warmest with an average air temperature of 11.4° C, and the onset of greenness was early and started on February 23. The coldest year among the five years was 2011, with an average air temperature of 10. 6° C and the onset of greenness was April 26. Investigation showed that bud break had not started by late April. The average annual air temperature was calculated for the month leading to onset of greenness, and the values were 6.3° C for March 2009 , 13° C for April 2010, 10.6° C for April 2011, 14.1° C for April 2012, and 6° C for February 2013, with an overall average of 10 ° C for five years.

Average air temperature of at least 6° C seems to have been required for grapevine bud break (AgWeatherNet data); the onset of greenness was indicated by the leaf appearance phase. Previous studies reported a base temperature of 4° C for bud break and a base temperature of 7° C for leaf appearance (Moncur et al., 1989). However, these base temperatures are highly variable with regard to grape cultivars. We expected that the onset of greenness would commence during the month in which air temperature values become equal to or greater than 6 °C. However, the results did not confirm this as the overall average temperature for the month leading to the onset of greenness was 10 ° C for the five year period of the study. This average temperature is higher than the previously reported air temperature required for the bud break of the grapes but agrees well with Winkler’s threshold. The difference might be due to the annual variation in the air temperature and the differences among the grape cultivars.

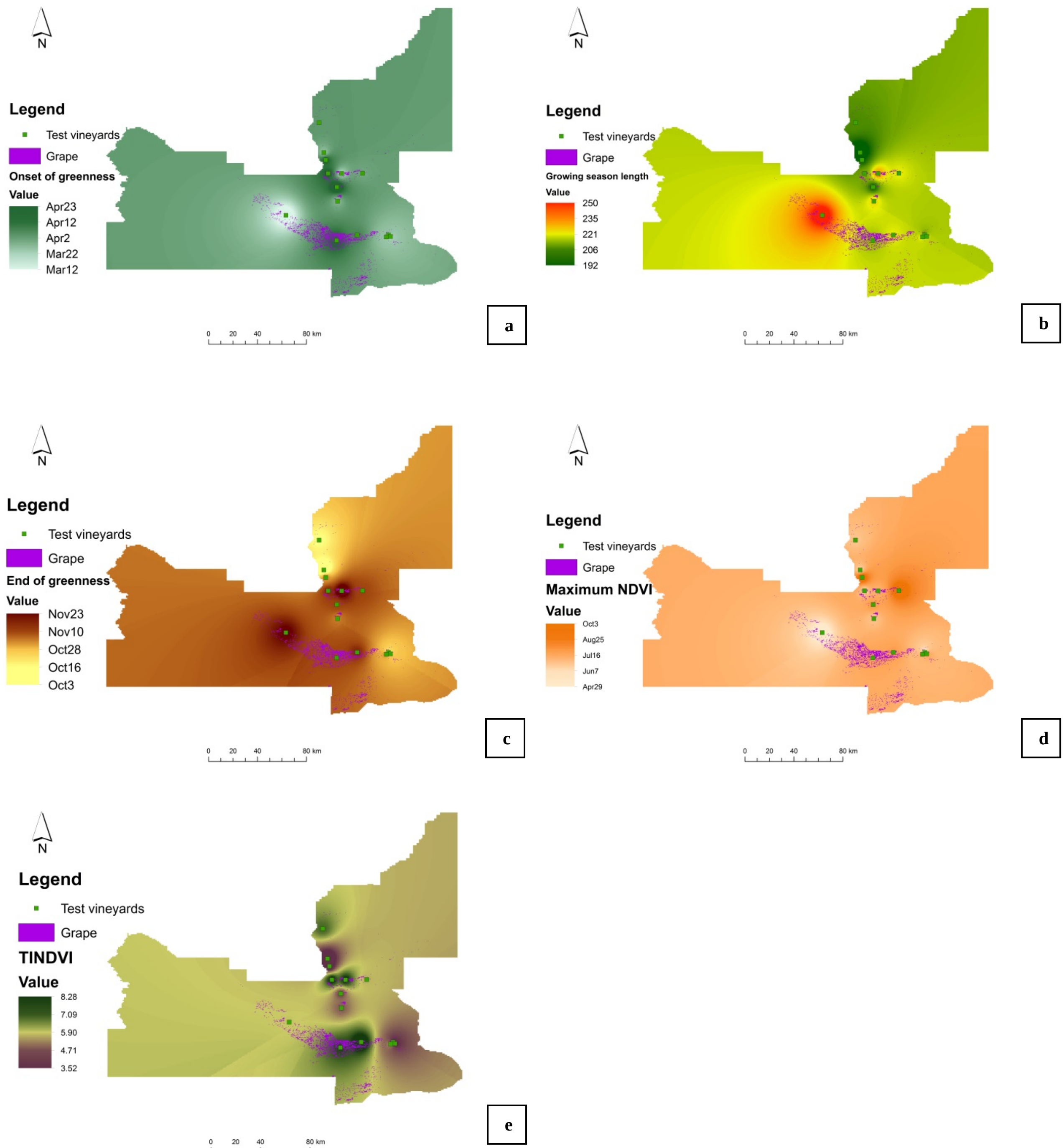

Figure 2.8. Spatial distribution of the main phenological metrics based on the MODIS NDVI (2009-2013): (a) date of onset of greenness; (b) duration of growing season (days); (c) date of the end of greenness; (d) date of maximum NDVI; and (e) TINDVI (similar to NDVI but without units).

The results indicated that the average time of the end of greenness was November 4th. The end of the growing season is set to be the end of October to permit comparisons across regions; therefore, there was a difference of four days between the MODIS NDVI-predicted dates for the end of the growing season. The end of greenness was November 7th in 2009, November 6th in 2010 and 2011, November 4th in 2012, and October 29th in 2013. The end of the growing season is traditionally regarded as the date of first frost, whereas the end of greenness is primarily due to the natural senescence of green vegetation.

The average date of maximum NDVI value was July 12th (Table 2.6.), which is close to the veraison date determined by Cunha et al. (2010). However, the veraison date is highly variable, due to factors such as variety and accumulated GDD. Veraison is typically reported to occur between 5 and 12 weeks after bud break, depending on the grape variety (Jackson, 2008); leading to the high variability of veraison, which may not be evident from the data if only the highest values of the NDVI were focused on. The time of maximum NDVI was June 16th in 2009, July 1st in 2010 and 2013, June 26th in 2011, and September 19th in 2012. The average dates of maximum NDVI, onset of ripening, growing season length, start of growing season, and end of growing season are highly dependent on the climate conditions in a given region. Our calculated average value of NDVI at the onset of greenness was 0.32, the average value of the NDVI at the end of greenness was 0.41, and the average maximum value of the NDVI was 0.55, while the average range in NDVI was 0.25. The onset of greenness reported in previous studies was 0.36 and the end-of-greenness NDVI value was 0.32 (Cunha et al., 2010).

The highest time-integrated value of NDVI was 7.22 for a growing season of 248 days (2013), while the lowest time-integrated value was 5.01 for a growing season of 193 days (2012; Table 2.6.). The average time-integrated value of NDVI was 5.74 for a growing season of 216 days. Time-integrated NDVI is a strong indicator of the net primary production of grapevines during a growing season, as time-integrated NDVI is directly related to growing season length: the longer the growing season, the higher the time-integrated NDVI. It has also been proven that NDVI is related to both vine size (Dobrowski et al., 2002) and fraction cover (Carlson and Ripley, 1997); both characteristics are related to planting density within a given vineyard (Johnson, 2003). The average green-up and senescence rates were both 0.0035 per day.

The variation in results is partially a result of the influence of the adjacent land cover types over the NDVI values. Soil moisture status, pruning system, and cover crop type can also influence spectral properties of vineyards (Cunha et al., 2010; Zhang et al., 2003). In addition, weather variability is a proven source of variation within NDVI values (Cunha et al., 2010; Studer et al., 2007; Ricotta and Avena, 2000; White et al., 2005).

Future Work

NDVI is strongly tied to the leaf area index (LAI) (Johnson et al., 2001; Johnson et al., 2003; Dobrowski et al., 2002; Johnson, 2003); thus, NDVI can be transformed into LAI via regression analysis (Johnson, 2003). LAI is a good representative of canopy density, and canopy density has a proven connection to fruit ripening rate (Winkler, 1958), infestation and disease (Wildman et al., 1983; English et al., 1989; Johnson et al., 2012), water status (Smart and Coombe, 1983; Johnson et al., 2012), yield (Clingeleffer and Sommer, 1995; Baldy et al., 1996; Johnson et al., 2012), and fruit characteristics and wine quality (Smart, 1985; Jackson and Lombard, 1993; Mabrouk and Sinoquet, 1998; Johnson et al., 2012). Therefore, future research should incorporate the LAI into its phenological analysis.

Based on our results, further studies should focus on locations surrounded by a more homogenous landcover; preferably grapevines or pasture. Vineyards should be established in a given location for more than three years in order to accurately capture the grapevine spectral signature. Further, as the spatial resolution of the remote sensing products is also influential on the accurate estimation of phenology metrics, there is potential for future studies to utilize our methoology, but using finer-resolution remote sensing products.

Conclusions

Utilizing MODIS NDVI data, our study produced several phenological metrics for grapevines grown in the Columbia Valley of Washington State. MODIS NDVI satellite images have proven viable tools for determining length of growing season, onset of greenness, end of greenness, and time of maximum NDVI, especially when there is a lack of access to historical phenological data for a region. A growing season of 216 days was obtained, based on the MODIS NDVI for the chosen study area; with an average onset of April 2nd, and an average end to the growing season of November 4th.

The evaluation of the MODIS NDVI via the NDVI derived from aerial images revealed that the MODIS NDVI had an average overestimation of 0.08; however, this bias does not influence temporal NDVI metrics (Table 2.3.; Table 2.6.). Therefore, metrics such as the time of onset of greenness, the time of end of greenness, the time of maximum NDVI, and the duration of greenness are not affected by the slight overestimation of the MODIS NDVI. However, the metrics that take into account the quantity of NDVI, including derived metrics and NDVI value metrics (Table 2.3.; Table 2.6.), do inherit the average 0.08 overestimation over the actual NDVI of each grape canopy.

The methods used in our study were able to accurately estimate the relevant phenology metrics; still, we recommend that future studies acquire observed phenology metrics comprising several years of data in order to make even more accurate estimates. Additionally, we recommend that remote-sensing methods be combined with the use of ground-based phenological studies. Also, because the number of test vineyards in this study was limited, we suggest that future studies focus on more homogenous regions with larger numbers of assigned test vineyards.

References

AgWeatherNet (AWN). (2015). Daily Temperature. Retrieved from http://weather.wsu.edu. Accessed Feb. 6, 2015.

Atkinson, P. M., Jeganathan, C., Dash, J., and Atzberger, C. (2012). Inter-comparison of four models for smoothing satellite sensor time-series data to estimate vegetation phenology. Remote Sensing of Environment, 123, 400–417.

Baldy, R., DeBenedictis, J., Johnson, L., Weber, E., Baldy, M., Osborn, B., and Burleigh, J. (1996). Leaf color and vine size are related to yield in a phylloxera-infested vineyard. VITIS-GEILWEILERHOF, 35, 201-206.

Barnes, W.L., Pagano, T.S., and Salomonson, V.V. (1998). Prelaunch characteristics of the Moderate Resolution Imaging Spectroradiometer (MODIS) on EOS-AM1. Geoscience and Remote Sensing, IEEE Transaction, 36, 1088 –1100.

BEAM. (2013). Earth Observation and Toolbox and Development Platform. V4.10.2. European Space Agency.

Carlson, T.N., and Ripley, D.A. (1997). On the relation between NDVI, fractional vegetation cover, and leaf area index. Remote Sensing of Environment, 62, 241–252.

Chuine, I., Yiou, P., Viovy, N., Seguin, B., Daux, V., and Laudurie, E. L. (2004). Historical phenology: grape ripening as a past climate indicator. Nature, 432, 289–290.

Clingeleffer, P.R., and Sommer, K.J. (1995). Vine development and vigour control. In: Canopy Management Ed. P.F. Hayes (Australian Society of Viticulture and Oenology: Adelaide) 7–17.

Cunha, M., Marcal, A. R. S., and Rodrigues, A. (2010). A comparative study of satellite and ground-based vineyard phenology. In Symposium of the European Association of Remote Sensing Laboratories (pp. 68-77). I. Manakos, and C. Kalaitzidis, eds. Chania, Greece: EARSel.

Dobrowski, S.Z., Ustin, S. L., and Wolpert, J. A. (2002). Remote estimation of vine canopy density in vertically shoot positioned vineyards: Determining optimal vegetation indices. Australian Journal of Grape and Wine Research, 8, 117–125.

Dobrowski, S.Z., Ustin, S. L., and Wolpert, J. A. (2003). Grapevine dormant pruning weight prediction using remotely sensed data. Australian Journal of Grape and Wine Research, 9, 177–182.

Dougherty, P. H. (2012). The Geography of Wine: Regions, Terroir and Techniques. Springer.
English, J.T., Thomas, C.S., Marois, J.J., and Gubler, W.D. (1989). Microclimates of grapevine canopies associated with leaf removal and control of Botrytis bunch rot. Phytopathology, 79, 395–401.

Fischer, A. (1994). A model for the seasonal variations of vegetation indices in coarse resolution data and its inversion to extract crop parameters. Remote Sensing of Environment, 48, 220–230.

Gladstones, J.S. (1992). Viticulture and Environment. Adelaide, Australia: Wine Titles, Hyde Park Press.

Glenn, E.P., Huete, A.R., Nagler, P.L., and Nelson, S.G. (2008). Relationship between remotely-sensed vegetation indices, canopy attributes and plant physiological processes: What vegetation indices can and cannot tell us about the landscape. Sensors, 8(4), 2136–2160.

Google Earth. (2013). V. 7.1.2.2041.Mountainview, CA:Google,Inc.

Goward, S.N., Tucker, C.J. and Dye, D.G. (1985). North American vegetation patterns observed with the NOAA-7 Advanced Very High Resolution Radiometer. Vegetation, 64, 3–14.

Granger, C.W.J. (1989). Forecasting in Business and Economics, 2nd ed. Boston, MA: Academic Press, Inc.

Guenther, B., Xiong, X., Salomonson, V., Barnes, W., and Young. J. (2002). On-orbit performance of the Earth observing system Moderate Resolution Imaging Spectroradiometer; First year of data. Remote Sensing of Environment, 83, 16–30.

Hall, A., Lamb, D.W., Holzapfel, B. and Louis, J. (2002). Optical remote sensing applications in viticulture - a review. Australian Journal of Grape and Wine Research, 8, 36–47.

Hall, A., Louis, J., and Lamb, D. (2003). Characterising and mapping vineyard canopy using high-spatial-resolution aerial multispectral images. Computers and Geosciences, 29(7), 813–822.

Hall, A., Louis, J. p., and Lamb, D. W. (2008). Low-resolution remotely sensed images of winegrape vineyards map spatial variability in planimetric canopy area instead of leaf area index. Australian Journal of Grape and Wine Research, 14, 9–17.

Hall, A., Lamb, D. W., Holzapfel, B. P., and Louis, J. P. (2011). Within-season temporal variation in correlations between vineyard canopy and winegrape composition and yield. Precision Agriculture, 12(1), 103–117.

Hoff, J.C. (1983). A Practical Guide to Box-Jenkins Forecasting. Belmont: CA: Lifetime Learning Publications.

Howell, G.S. (2001). Sustainable grape productivity and the growth-yield relationship: a review. American Journal of Enology and Viticulture, 52, 165–174.

Iland, P., Ewart, A., Sitters, J., Markides, A., and Bruer, N. (2000). Techniques for chemical analysis and quality monitoring during winemaking. Campbelltown, SA: Patrick Iland Promotions.

Jackson, R. S. (2008). Wine Science Principles and Applications, 3rd ed. Burlington, MA: Elsevier Science.

Jackson, D.I., Lombard, P.B. (1993). Environmental and management practices affecting grape composition and wine quality: a review. Am. J. Enol. Viticulture, 44, 409–430.

Jamali, S., Jönsson, P., Eklundh, L., Ardö, J., and Seaquist, J. (2015). Detecting changes in vegetation trends using time series segmentation. Remote Sensing of Environment, 156, 182–195.

Johnson, L. F. (2003). Temporal stability of an NDVI-LAI relationship in a Napa Valley vineyard. Australian Journal of Grape and Wine Research, 9(2), 96–101.

Johnson, L.F., Roczen, D.E., and Youkhana, S.K. (2001). Vineyard canopy density mapping with IKONOS satellite imagery. In Proc, 3rd International. Conference on Geospatial Information in Agriculture and Forestry, Denver, Colorado.

Johnson, L.F., Roczen, D. E., Youkhana, S. K., Nemani, R. R. and Bosch, D. F. (2003). Mapping vineyard leaf area with multispectral satellite imagery. Computers and Electronics in Agriculture, 38, 33–44.

Johnson, L. F., Nemani, R., Hornbuckle, J., Bastiaanssen, W., Thoreson, B., Tisseyre, B., and Pierce, L. (2012). Remote Sensing for Viticultural Research and Production. In P. H. Dougherty (Ed.),The Geography of Wine (pp. 209–226). Springer Netherlands.

Jones, G. V., and Davis, R. E. (2000). Using a synoptic climatological approach to understand climate–viticulture relationships. International Journal of Climatology, 20, 813–837.

Jones, G.V., Duff, A.A., Hall, A. and Myers, J. (2010). Spatial analysis of climate in wine grape growing regions in the western United States. American Journal of Enology and Viticulture, 61, 313–326.

Justice, C., Townshend, J. R., Vermote, E., Masuoka,E., Wolfe, R. , Saleous, N., Roy, D. P. and Morisette, J. T. (2002). An overview of MODIS land data processing and product status. Remote Sensing of Environment, 83, 3–15.

Keller, M., Tarara, J.M., and Mills, L. J. (2010). Spring temperatures alter reproductive development in grapevines. Australian Journal of Grape and Wine Research, 16, 445–454.

Lamb, D.W., Weedon, M.W., and Bramley, R. G. V. (2004). Using remote sensing to predict grape phenolics and colour at harvest in a Cabernet Sauvignon vineyard: Timing observations against vine phenology and optimizing image resolution. Australian Journal of Grape and Wine Research, 10, 46–54.

Mabrouk, H., and Sinoquet, H. (1998). Indices of light microclimate and canopy structure of grapevines determined by 3D digitising and image analysis, and their relationship to grape quality. Australian Journal of Grape and Wine Research, 4(1), 2–13.

Moncur, M.W., Rattigan, K., Mackenzie, D.H., and Intyre, G.N.M. (1989). Base temperatures for budbreak and leaf appearance of Grapevines. American Journal of Enology and Viticulture, 40(1), 21–26.

Montero, F. J., Meliá, J., Brasa, A., Segarra, D., Cuesta, A., and Lanjeri, S. (1999). Assessment of vine development according to available water resources by using remote sensing in la mancha, spain. Agricultural Water Management, 40(2-3), 363-375.

Morisette, J. T., Privette, J. L. and Justice, C.O. (2002). A framework for the validation of MODIS Land products. Remote Sensing of Environment, 83, 77–96.

Microsoft. (2010). Microsoft Excel [computer software]. Redmond, Washington: Microsoft.

NASA Land Processes Distributed Active Archive Center (LP DAAC). (2015). MODIS13A2 satellite product. USGS/Earth Resources Observation and Science (EROS) Center, Sioux Falls, South Dakota. Retrieved from https://lpdaac.usgs.gov/. Accessed Feb. 9, 2015.

Pettorelli, N., Vik, J. O., Mysterud, A., Gaillard, J.M., Tucker, C.J. and Sternest, N. C. (2005). Using the satellite-derived NDVI to assess ecological responses to environmental change. Trends in Ecology and Evolution, 20, 503–510.

Pettorelli, N. (2013). The Normalized Difference Vegetation Index. Oxford University Press.
Reed, B.C., Brown, J.F., VanderZee, D., Loveland, T.R., Merchant, J.W. and Ohlen, D.O. (1994). Measuring phenological variability from satellite imagery. Journal of Vegetation Science, 5(5), 703–714.

Ricotta, C., and Avena, G.C. (2000). The remote sensing approach in broad-scale phenological studies. Applied Vegetation Science, 3, 117–122.

Rouse, J.W., Haas, R.H., Schell, J. A., and Deering, D.W. (1974). Monitoring vegetation system in the Great Plains with ERTS. In Proc of the Third Earth Resources Technology Satellite-1 Symposium, Greenbelt, MD: NASA SP-351.

Schwartz, M.D., Reed, B. C., and White, M. A. (2002). Assessing satellite-derived start-of-season (SOS) measures in the conterminous USA. International Journal of Climatology, 22, 1793 –1805.

Smart, R.E. (1985). Principles of grapevine canopy microclimate manipulation with implications for yield and quality. Am. J. Enol. Viticulture, 36, 230–239.

Smart, R.E., and Coombe, B.G. (1983). Water relations of grapevines, in: T. Kozlowski (Ed.), Water Deficits and Plant Growth, 2Academic Press, New York, 137–196.

Stamatiadis, S., Taskos, D., Tsadilas, C., Christofides, C., Tsadila, E., and Schepers, J. S. (2006). Relation of Ground-Sensor Canopy Reflectance to Biomass Production and Grape Color in Two Merlot Vineyards. American Journal of Enology and Viticulture, 57(4), 415–422.

Studer, S., Stöckli, R., Appenzeller, C., and Vidale, P. L. (2007). A comparative study of satellite and ground-based phenology. International Journal of Biometeorology, 51, 405–414.

Terra satellite. (2014). Retrieved from http://terra.nasa.gov/. Accessed May 28, 2014.

Trout, T. J., Johnson, L. F., and Gartung, J. (2008). Remote Sensing of Canopy Cover in Horticultural Crops. HortScience, 43(2), 333–337.

Tucker, C. J., Newcomb, W. W., Los, S. O., and Prince, S. D. (1991). Mean and inter-year variation of growing-season normalized difference vegetation index for the Sahel 1981-1989. International Journal of Remote Sensing, 12(6), 1133–1135.

USDA National Agricultural Statistics Service Cropland Data Layer (USDA-NASS). (2014). Published crop-specific data layer. Retrieved from http://nassgeodata.gmu.edu/CropScape/ USDA-NASS, Washington, DC.

White, M. A., Hoffman, F., and Hargrove, W. W. (2005). A global framework for monitoring phenologcal responses to climate change. Geophysical Research Letters, 32, 4

Wildman, W., Nagaoka, R., Lider, L. (1983). Monitoring spread of grape phylloxera by color infrared aerial photography and ground investigation. Am. J. Enol. Viticulture, 34, 83–94.

Winkler, A. J. (1958). The relation of leaf area and climate to vineperformance and grape quality. American J. Enol. Viticulture, 9(1), 10-23.

Winkler, A.J., Cook, J.A., Kliewer, W.M., and Lider, L.A. (1974). General Viticulture. 4th ed. Berkeley, CA: University of California Press.

Yang, L., Wylie, B. K., Tieszen, L.L. and Reed, B.C. (1998). An analysis of relationships among climate forcing and time-integrated NDVI of grasslands over the U.S. northern and central Great Plains. Remote Sensing of Environment, 65, 25–37.

Zhang, X., Friedl, M.A., Schaaf, C.B., Strahler, A.H., Hodges, J.C. F., Gao, F., Reed, B.C., and Huete, A. (2003). Monitoring vegetation phenology using MODIS. Remote Sensing of Environment, 84, 471–475.

CHAPTER THREE

IMPACT OF LAND-COVER TYPE ON THE ESTIMATED NEAR-SURFACE AIR TEMPERATURE DERIVED FROM MODIS PRODUCTS[2]

Abstract

Precise estimation of near-surface air temperature (T_a) is essential for the study of terrestrial ecosystems. However, it is not always a simple task to obtain the T_a for regions with high elevations, as there are a limited number of weather stations, especially in remote locations. Therefore, the T_a should be estimated using techniques that do not solely rely on weather station data. The goal of our study was to use satellite remote sensing products to estimate T_a for an area featuring complex terrain, as well as analyze the impact of land cover type on the accuracy of the estimated T_a. The normalized difference vegetation index (NDVI) and land surface temperature (LST) were obtained from the MODerate resolution Imaging Spectroradiometer (MODIS) satellite imagery obtained for the Yakima Valley, in the state of Washington. The estimated T_a was then evaluated against the T_a obtained from the North American Land Data Assimilation System (NLDAS). The coefficient of determination (R^2), average bias, and root mean square error (RMSE) for the estimated T_a and the NLDAS T_a were calculated. The lowest R^2 was associated with grapes (R^2= 0.22), while the highest R^2 was associated with fallow cropland (R^2=0.9). The lowest mean bias was associated with evergreen forest (2.43°C), and the highest average bias with woody wetlands (6.68°C). Our study re-confirmed that, to obtain more accurate estimates of T_a using remote sensing products, knowledge of the chosen study area's land cover and its properties are required.

Introduction

[2] Submitted to the Remote Sensing journal.

Near-surface air temperature (T_a) is an important parameter affecting terrestrial ecosystems. T_a has many applications in various fields, including ecology, agriculture, hydrology, climate variability, and climate change (Vancutsem et al., 2010; WMO, 2008). T_a affects plant species distribution (Hoch and Korner, 2005; Randin et al., 2013), and soil-plant-water system dynamics can also be impacted by T_a (Chartzoulakis and Psarra, 2005; Zavala, 2004). T_a is a critical component of hydrological and evapotranspiration models (Allen et al., 1998; Carlson et al., 1995; Purkey et al., 2007; Yates et al., 2005). T_a also influences phenology, as well as photosynthesis and respiration rates; thus, plant growth and net primary production are also influenced by T_a (Bustos and Meza, 2015).

Traditionally, air temperature is recorded by weather stations, with a thermometer typically installed 2 m above the soil surface. Weather stations are usually distributed heterogeneously within a region (Abatzoglou, 2011; Lu et al., 2009; Jabot et al., 2012; Minder et al., 2010; Marquinez et al., 2003; Vancutsem et al., 2010); thus, a weather station may not represent its surrounding environment very accurately (Pielke et al., 2007; Jiménez et al., 2010; Menne and Williams Jr., 2009). In addition, surface properties that vary both in space and time control the spatiotemporal patterns of air temperature (Prihodko and Goward, 1997); as a result, each weather station is only capable of representing a very small region, especially those located within complex terrain.

Regions containing areas of complex terrain with high elevations usually have limited accessibility; thus, the number of weather stations in those regions are even smaller. The limited number of weather stations at high elevations thereby hinders the accurate estimation of the spatial variation of T_a. T_a records can be spatially interpolated and/or extrapolated to create a spatial weather dataset; however, the accuracy of the interpolated spatial dataset can prove unsatisfactory, as T_a is influenced by local parameters such as elevation, sun exposure, topography, and proximity to bodies of water (Marquinez et al., 2003; Flores P. and Lillo S., 2010; Van De Kerchove et al., 2013; Marques da Silva et al., 2015).

It has been shown that the spatial and temporal resolutions of the T_a measurements play an important role in our understanding of global weather dynamics (Willmott and Robeson, 1991; Madden et al., 1993; Karl et al., 1994; Robeson, 1995). To fill in the gap of the measured T_a caused by scattered and unevenly distributed weather stations, satellite data can be incorporated as an ancillary source. Satellite remote sensing provides spatially contiguous data that are consistently available on a regular basis (Seguin, 1991); however, this is not always true of meteorological measurements (Prihodko and Goward, 1997). The spatial and temporal resolution of weather data has been improved by the advent of satellites (Vancutsem et al., 2010; Running et al., 2004); and previous studies have shown that T_a can be estimated from satellite data (Vancutsem et al., 2010; Dash, 2002; Norman and Becker, 1995; Prihodko and Goward, 1997; Prince et al., 1998; Lin et al., 2012). Prior studies have also utilized thermal remote sensing to derive near-surface air temperatures (Chokmani and Viau, 2006; Jang et al., 2004).

There is a need for accurate weather information at the regional and even the continental level, to ensure the necessary weather parameters are accessible at both fine spatial and temporal resolutions. These datasets are required inputs for environmental, agricultural, and economical models. In regions with limited access to ground-based meteorological observations, spatial weather data can be partially derived from satellite-based remote sensing data as a means of compensating for the lack of observations. The aim of our study was the estimation of the T_a in an area comprising complex terrain, using satellite remote sensing and vegetation indices. An additional objective was the determination of the impact of land cover type on both estimated and observed T_a.

Methods

Study Area

The study area was located in the Yakima Valley of the state of Washington, the United States, within a latitudinal range of 47°19′20″N to 45°32′23″N and a longitudinal range of 121°20′21″W to 119°2′59.99″W. This area includes complex terrain, with the Cascade Mountains to the west, the Wenatchee Mountains to the north, Rattlesnake Mountain and the Rattle Snake Hills to the east, and the Horse Heaven Hills to the south. The area is approximately 15,900 km^2 (Figure 3.1.) with elevations ranging from 50 m to 1,970 m.

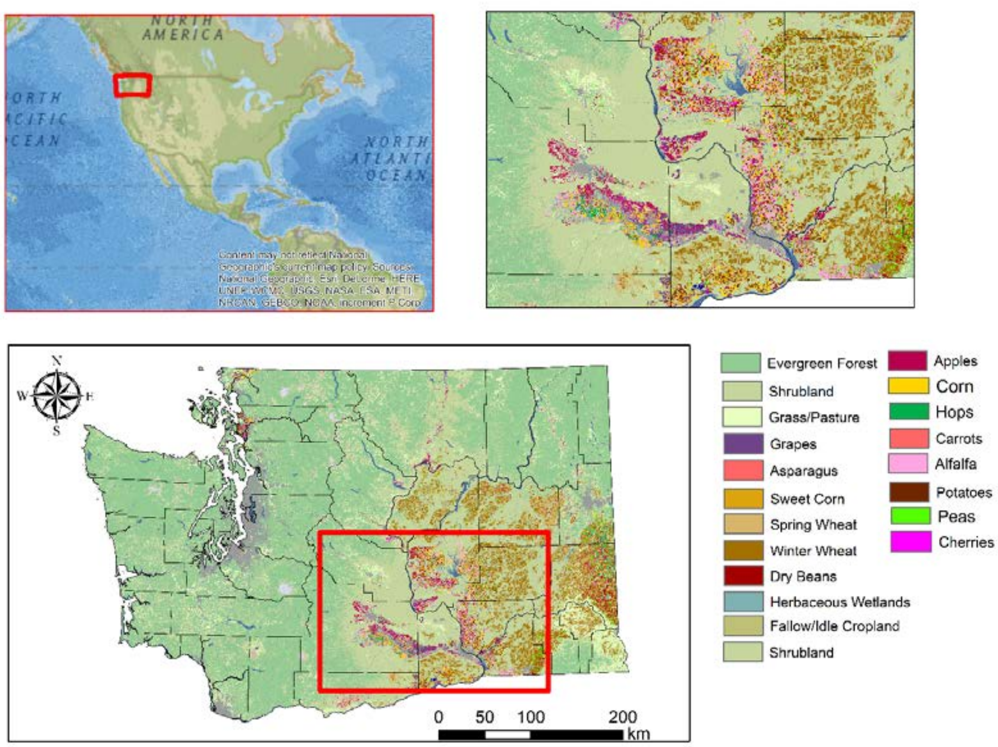

Figure 3. 1. Study area (Yakima Valley, Washington, USA).

The Yakima Valley is famous for the diversity of its agricultural production. As an agricultural and crop production region, knowledge of the dynamics of T_a patterns, especially during the growing season, can help growers and decision-makers apply best management practices such as frost controls or the irrigation managemnet at the most opportune times. In cases where risks such as frequent frost events are associated with extreme values of T_a, appropriate measures can be taken to minimize any potential damage to crops or livestock. The dominant land cover in the study area is shrubland, evergreen forest, pasture, and intensive specialty-crop production, including apples *(Malus domestica*), cherries (*Prunus avium*), grapes (*Vitis spp.*), and hops (*Humulus lupulus*) (Table 3.1.).

Table 3.1. The major land covers present in the study area extracted fromland cover map 2010 (within a grid super-imposed on the Yakima Valley, Washington, U.S.A).

Land Cover	**Area (%)**	**Area (km^2)**
Shrubland	41.61	94.42
Evergreen Forest	23.24	52.75
Grass/Pasture	10.72	24.33
Alfalfa	2.93	6.64
Winter Wheat	2.43	5.50
Fallow/Idle Cropland	2.29	5.20
Maize	2.18	4.94
Developed/Open Space	1.67	3.79
Developed/Low Intensity	1.64	3.72
Open Water	1.50	3.39
Grapes	1.16	2.62
Apples	1.09	2.48
Potatoes	1.00	2.26
Other Hay/Non Alfalfa	0.97	2.21
Spring Wheat	0.96	2.17
Woody Wetlands	0.54	1.22
Cherries	0.53	1.21
Herbaceous Wetlands	0.53	1.19
Developed/Med Intensity	0.51	1.16
Sweet Corn	0.40	0.91
Dry Beans	0.36	0.83
Peas	0.29	0.65
Barren	0.27	0.61
Onions	0.19	0.43
Hops	0.19	0.42
Pears	0.13	0.30
Sod/Grass Seed	0.12	0.26
Developed/High Intensity	0.08	0.18
Herbs	0.08	0.18
Asparagus	0.07	0.16
Carrots	0.06	0.14

Moderate Resolution Imaging Spectroradiometer (MODIS)

The Moderate Resolution Imaging Spectroradiometer (MODIS) instrument onboard the NASA Terra satellite (NASA 2012) has a spatial resolution ranging from 250 m to 1 km. For any location in the northern hemisphere, the Terra satellite overpass is approximately 10 am local time. The spectral bands (36 bands) of this instrument enable accurate monitoring of the global terrestrial ecosystems as they were chosen because of the spectral properties of the major physiological phenomena of plants (Barnes et al., 1998; Justice et al., 2002). Detailed background information on MODIS products can be found in Justice et al. (2002); Guenther et al. (2002); and Morisette et al. (2000). MODIS products are available for free download, including derived products such as vegetation indices (NASA, 2012).

MODIS images were used for this study due to their high temporal resolution (daily), and were obtained from the NASA (Land Processes Distributed Active Archive Center) website (NASA, 2012). We used the 2010 images that spatially covered the study area; daily Land Surface Temperature (LST) images were also available for 2010, comprising a total of 365 values. However, there was variation in the number of pixels that contained useful information as a result of clouds affecting the available data by the satellite sensor.

The NDVI images were condensed into 16-days image composites based on the assumption that daily changes in the NDVI are not significant. The 16-day composites of the NDVI were available twice per month throughout 2010. The 16-day NDVI composite images were initially mosaicked because the Yakima Valley is covered with more than one MODIS tile; they were then re-projected using the MODIS Reprojection Tool (MRT) (NASA, 2012). The Yakima Valley region was covered by the images at a grid size of 0.01 arc degree.

The Normalized Difference Vegetation Index (NDVI)

The Normalized Difference Vegetation Index (NDVI) is the most commonly used vegetation index in environmental studies (Goward et al., 1985; Tucker et al., 1986; Fung et al., 1987; Nemani and Running, 1989; Tucker et al., 1991; Pettorelli et al., 2005; Chen et al., 2004; Son et al., 2012; Badr and Hoogenboom, 2013; Badr et al., 2015). Previous studies have shown the potential uses of NDVI in the study of vegetation dynamics (Townshend and Justice, 1986; Verhoef et al., 1996; Running, 1990; Myneni et al., 1995; Pettorelli, 2013; Badr and Hoogenboom, 2013; Badr et al., 2015). The effect of weather on biomass and phenology has been assessed using NDVI (Nemani et al., 2003; Roerick et al., 2003; Zhou et al., 2003; Zhao and Schwartz, 2003; Wang et al., 2003; Pettorelli et al., 2005; Pettorelli, 2013).

Rouse et al. (1974) defined NDVI as follows (Equation 3.1.):

$$NDVI = \frac{\rho_{nir} - \rho_{red}}{\rho_{nir} + \rho_{red}} \qquad (3.1.)$$

where ρ_{nir} represents the reflectance at the near infrared region of the spectrum (0.7 –1.1 μm) and ρ_{red} denotes the reflectance at the red wavelengths (0.6–0.7 μm).

A near-linear relationship between the NDVI and an intercepted fraction of photosynthetically-active radiation has been reported (Asrar et al., 1984; Sellers, 1985). The NDVI is highly correlated with photosynthetic capacity, net primary production, Leaf Area Index (LAI), carbon assimilation, and evapotranspiration (Myneni et al., 1995; Buermann et al., 2002; Hicke et al., 2002; Wang et al., 2005; Pettorelli, 2013). It is also a reliable means of measuring photosynthetically-active biomass (Tucker and Sellers, 1986; Los, 1998; Turner et al., 1999; Hill and Donald, 2003), and is also capable of estimating vegetation quantity and greenness (Walsh et al., 1997; Walsh et al., 2001; Pettorelli, 2013).

Land Surface Temperature (LST)

The LST product from MODIS is considered a measurement of the surface or "skin" temperature of the outer layer of the Earth (Wan et al., 2004a, b; Sims et al., 2008; Hashimoto et al., 2008), and can therefore represent the surface temperature of anything scanned by satellite sensor, including a swimming pool or the top of a grape canopy. Given a particular microclimate, T_a and LST can essentially simulate the effect of a plant canopy. Thus, if the LST is known for a specific plant canopy although the T_a is unmeasured, the LST can be used as an estimator of the T_a for that particular plant canopy. A dense canopy has the ability to cancel out any signal attempting to reach the sensor from the soil; therefore, the T_a for such a dense canopy must be estimated from the LST (Sims et al., 2008; Yan et al., 2011; Petropoulos et al., 2009). The correlation between T_a and LST is potentially a useful tool for the estimation of T_a, especially in areas where geographical features limit accessibility (Colombi et al., 2007).

Air Temperature

Several studies have used LST for estimating T_a (Zakšek and Schroedter-Homscheidt, 2009; Mostovoy et al., 2006; Zhang et al., 2011; Colombi et al., 2007); however, we chose to focus on approaches that utilized temperature-vegetation indices (Saravanapavan and Dye, 1995; Prihodko and Goward, 1997; Czajkowski et al., 2000; Wloczyk et al., 2011). The temperature-vegetation index (TVX method), also referred to as the contextual method, relies on red, near-infra-red, and thermal bands to map air temperature. This approach assumes the quantity of the vegetation expressed by the NDVI is linearly correlated with the LST (Zakšek and Schroedter-Homscheidt, 2009).

The temperature at the top of a canopy is assumed to be the same as that within a thick vegetation canopy for which the LAI tends to be infinite. When an area is mainly covered with vegetation, the radiation emitted by the soil cannot reach the satellite sensor and can thus be ignored. Hence, the temperature recorded by the sensor can then become associated with the temperature of the canopy cover (Jackson et al., 1988). A dense plant canopy characterized by a high NDVI value is so structured that it leads to maximum heat diffusion (Gates, 1968; Geiger et al., 1995); causing the non-stressed canopy cover to have a tendency of reaching thermal equilibrium with the adjacent air. Prior studies have shown that the LST of pixels within dense covers of vegetation are a reliable approximation of the surrounding air temperature (Bustos and Meza, 2015).

The NDVI has been used for estimating T_a because it is known that land cover type and soil conditions influence the heat exchange between land-surface and near-surface atmosphere (Nemani and Running, 1989; Goward et al., 1994; Prince and Goward, 1995). It has been indicated that the air temperature is induced to be below canopy temperature due to a small canopy heat flux (Stisen et al., 2007). This canopy heat flux is inversely related to the LAI, and directly related to lowest leaf stomatal resistance (Monteith, 1973); however, this sensible heat flux will be negligible when the LAI tends to the infinite (Allen et al., 2006; Noilhan and Planton, 1989).

Carlson et al. (1995) derived T_a directly from an NDVI-T_s scatter plot using the assumption that the T_a can be approximated via the surface temperature of an infinitely thick vegetation cover. The study assumed that a high NDVI value is representative of a dense canopy. Colombi et al. (2007) used correlation analysis and equation generalization for spatial distribution to define the relationship between the LST and the T_a. Blum et al. (2013) reported that MODIS thermal images estimated the canopy temperature of an olive grove more accurately than that provided by the interpolated data from weather stations. Bustos and Meza (2015) used the LST provided by MODIS to estimate the maximum and minimum temperatures of the Maipo Basin in Chile. Only pixels with high NDVI scores were used, in order to ensure that the surface and T_a of the pixels were similar. Bustos and Meza (2015) evaluated the LST of the selected pixels using the observed T_a from local meteorological stations, and reported no significant differences in the estimated and observed T_a, except in urban areas. They ascribed the observed differences in the urban areas to being a result of heat island phenomenon.

In our study, a regression relationship was established between the LST and the NDVI (both products of MODIS), and the slope (*b*) and intercept (*a*) from the regression equation were then obtained (Equation 3.2.) (Wang et al., 2001; Sun and Kafatos, 2007; Price, 1990; Carlson et al., 1995).

$$LST = a(NDVI) + b \qquad (3.2.)$$

Subsequently, the LST was used to estimate the T_a, based on the assumption that the LST of a dense canopy is close to the T_a of that canopy (Prihodko and Goward, 1997; Riddering and Queen, 2006). Prihodko and Goward (1997) measured leaf reflectance and transmittance for various species of vegetation, deriving an $NDVI_{max}$ of 0.86 using the radiative transfer model. In our study the $NDVI_{max}$ of vegetation with a dense canopy was assumed to be 0.86, based on the previous studies (Prihodko and Goward, 1997; Riddering and Queen, 2006; Hong et al., 2009; Lakshmi et al., 2011). In the next phase (Equation 3), the LST was calculated as a function of $NDVI_{max}$, with the slope (*b*) and intercept (*a*) having already been obtained in the previous set of regressions (Figure 3.2.).

$$LST = a(NDVI_{\max}) + b \approx T_a \qquad (3.3.)$$

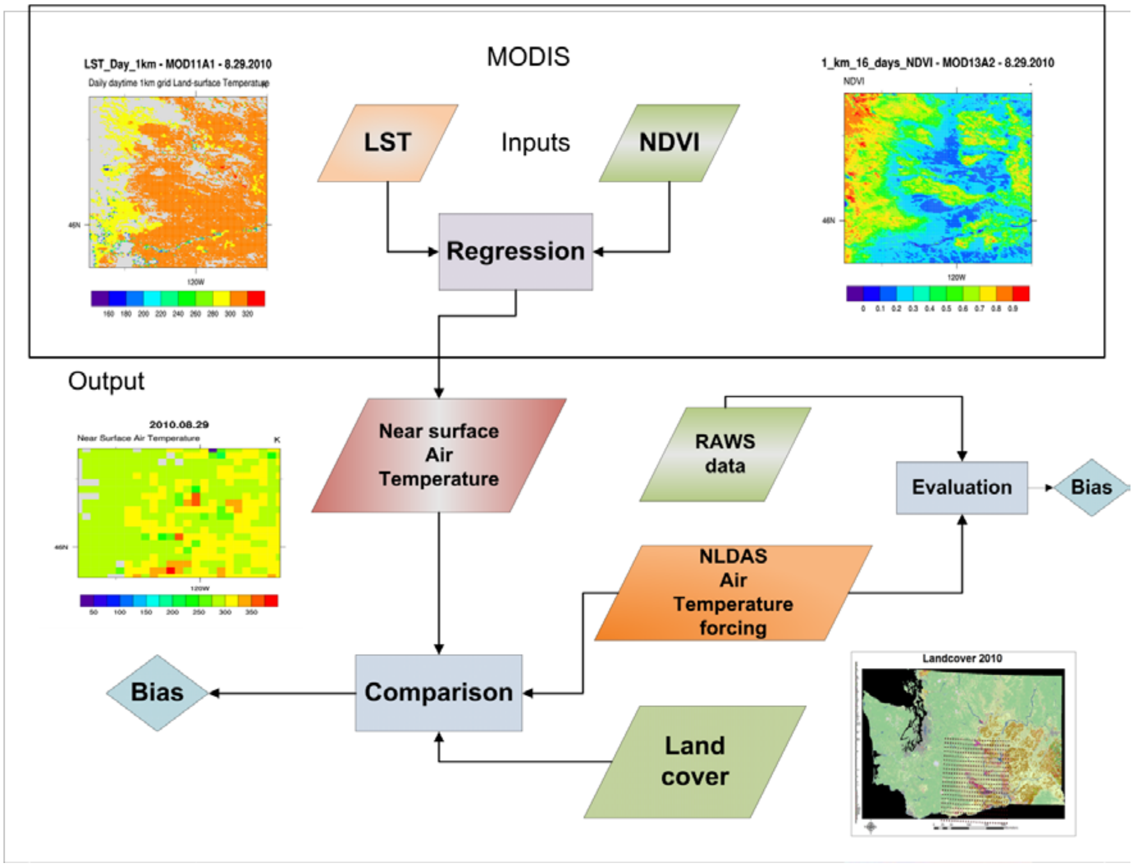

Figure 3. 2. Flowchart summarizing the methodology used in this study.

North American Land Data Assimilation System (NLDAS)

In this study the North American Land Data Assimilation System (NLDAS) was used to evaluate the estimated T_a, as it results in the creation of continuous spatial surfaces for the estimated T_a. By adopting the NLDAS dataset as the evaluation dataset, there was no longer a need to employ spatial interpolation techniques, as the NLDAS data is spatially continuous. This allowed us to avoid any added bias that could potentially be introduced via interpolation techniques.

The NLDAS was initially developed as a real-time retrospective data assimilation system for providing land surface states in land-ocean-atmosphere models (Mitchell et al., 2004; Xia et al., 2012). NLDAS includes four land surface models (LSMs): Noah (Ek et al., 2003), Mosaic (Koster and Suarez, 1996), Sacramento Soil Moisture Accounting (SAC-SMA) (Burnash et al., 1973; Burnash, 1995), and Variable Infiltration Capacity (VIC) (Liang et al., 1994). It has a spatial resolution of 1/8 ° grid over the continental United States, and a temporal resolution of one hour. The NLDAS has been evaluated using the measurement of energy fluxes, surface meteorology, soil moisture and temperature, mountain snowpack from surface stations, daily stream flow observations, satellite-derived land surface temperature (LST), and snow cover (Mitchell et al., 2004; Luo et al., 2003; Cosgrove et al., 2003).

The initial assessment of the NLDAS

The T_a from the NLDAS dataset was initially assessed by comparing it to the observed T_a obtained from Remote Automated Weather Stations (RAWS) (Table 3.2.). RAWS stations are distributed throughout the U.S. and monitor the weather continuously (RAWS, 2015). A total of eight RAWS stations located in the Yakima Valley were selected, and T_a observations were obtained for the period of study, depending on the number of days data was available for 2010. The total number of available observations was variable for each station during 2010, adding to a total number of 668 observations. The time of all observations was approximately 10 am local time, based on the overpass time of the MODIS satellite. The T_a from NLDAS was compared with the RAWS T_a and the coefficient of determination (R^2) determined for each location. The average bias (the average difference between the observed and estimated T_a), Root Mean Squared Error (RMSE), and Mean Absolute Bias (ME) were also calculated.

Land cover data

Information regarding the type of vegetation cover in the study area was requisite since our method was based on the NDVI, although some studies have used LST to indirectly relate land cover to T_a (Karnieli et al., 2010; Cheng et al., 2008; Mostovoy et al., 2008). The land cover type was obtained from the 2010 Cropland Data Layer (CDL) (Table 3.2.). The CDL is a raster, geo-referenced, crop-specific land cover data layer with a 30m spatial resolution based on moderate-resolution satellite imagery (Landsat 5, Landsat 7 and Indian Remote Sensing Advanced Wide Field Sensor images) with extensive agricultural ground trothing. It is produced annually for the continental U.S.A. (Figure 3.1.) (Boryan et al., 2011; Boryan et al., 2012; Han et al., 2012).

Table 3.2. The Remote Automated Weather Stations (RAWS) located within Yakima Valley, Washington, USA, that were used for evaluation of North American Land Data Assimilation System (NLDAS) temperature data.

Station Name	Latitude (N)	Longitude (W)	Elevation (m)	Major land-cover	County	Closest city
Signal Peak	46° 13' 37"	121° 08' 15"	1540	Developed (Low Intensity)	Yakima	White Swan
Sawmill Flats	46° 58' 07"	121° 04' 07"	1067	Evergreen Forest	Kittitas	Cliffdell
Sedge Ridge	46° 29' 42"	121° 00' 48"	1311	Evergreen Forest	Yakima	Ahtanum
Tepee Creek	46° 09' 47"	121° 01' 56"	908	Evergreen Forest	Yakima	Glenwood
Buck Creek	46° 03' 24"	121° 32' 19"	820	Grass/Pasture	Skamania	Trout lake
YTC-RC	46° 40' 31"	120° 20' 50"	613	Shrubland	Yakima	Selah
Highbridge	46° 04' 52"	120° 32' 37"	642	Shrubland	Yakima	White Swan
Mill Creek	46° 15' 45"	120° 51' 44"	860	Shrubland	Yakima	White Swan

Results and Discussion

Initial assessment of the NLDAS

The T_a recorded at 10 am daily by RAWS stations across the Yakima Valley were compared with the T_a obtained from the NLDAS (also recorded at 10 am daily). The average T_a (T_{avg}) for the days the RAWS stations were available during 2010 was 16.8°C, while the average

NLDAS T_{avg} during 2010 was 15.8 °C (Table 3.4.). This resulted in an average bias of -1.0 °C and an RMSE of 2.8°C for 2010 (Table 3.5.). The minimum and maximum T_a for both RAWS and NLDAS were also obtained and their differences determined. In 2010, the total number of available records for each RAWS station was variable; therefore, we only used the days during 2010 for which the RAWS data actually existed (Table 3.3.).

Table 3.3. The average elevation, total sample size (availability of MODIS products), total number of sampling locations (points or grids, left corner), and total number of days in 2010 (MODIS products used) for each land cover type in Yakima Valley, Washington.

Land cover type	**Average elevation (m)**	**Sample size (# locations* # days)**	**Number of sample locations**	**Number of available days MODIS products were available during 2010**
Shrubland	726	9106	195	47
Evergreen forest	564	4475	98	46
Spring wheat	458	147	30	5
Pasture/grass*	696	1070	22	49
Alfalafa	346	853	16	53
Maize	317	815	15	54
Pasture/hay	665	724	14	52
Grassland /herbaceous*	875	443	11	40
Winter wheat	571	400	8	50
Fallow/Idle Cropland	633	324	7	46
Developed low intensity	1051	212	5	42
Developed open space	829	216	5	43
Open water	451	243	5	49
Cherries	701	203	4	51
Herbaceous wetlands	1158	90	3	30
Peas	956	80	2	40
Potatoes	929	89	2	45
Developed medium intensity	1087	84	2	42
Dry beans	870	131	2	66
Woody wetlands	1404	52	2	26
Grapes	382	85	2	43
Asparagus	1396	23	1	23
Carrots	951	20	1	20
Apples	392	53	1	53
Sweet corn	342	54	1	54
Hops	1130	38	1	38
Pears	539	54	1	54
Average	756.26	743.85	16.89	44
Total		20084	456	1159

** Pasture/grass land-cover refers to areas covered with grasses, legumes, or grass-legume mixtures planted for livestock grazing or the production of seed (USGS, 2015).*
**Grasslands/herbaceous refers to* areas dominated by upland grasses and forbs. In rare cases, herbaceous cover is less than 25 percent, but exceeds the combined cover of the woody species present. These areas are not subject to intensive management; but are often utilized for grazing (USGS, 2015).

The mean R^2 between the T_a obtained from the RAWS stations and the T_a acquired from the NLDAS was 0.91, with a range from of 0.84 to 0.97 (Table 3.5.). These results confirmed that the NLDAS provides a robust performance compared to the observed meteorological records, and can therefore be used as a substitute for weather station records in our study area. However, it should be noted that it does contain a small amount of noise that is not present in the observed data.

Table 3.4. T_{avg} from the Remote Automated Weather Stations (RAWS) and the North American Land Data Assimilation System (NLDAS) for the period that the data was available, their difference (Dif= NLDAS-RAWS), the T_{max} and T_{min} for the RAWS and NLDAS data, and their respective difference (bias). The number of observations used from each station is also reported.

Stations	T_{avg} (°C)			T_{max} (°C)			T_{min} (°C)			# observations
	RAWS	NLDAS	Dif	RAWS	NLDAS	Dif	RAWS	NLDAS	Dif	
Sawmill Flat	19.1	16.0	-3.1	30.6	24.7	-5.9	5.6	7.6	2.0	79
YTC-RC	23.1	21.4	-1.8	32.8	30.3	-2.5	10.6	8.8	-1.8	70
Highbridge	18.8	15.8	-3.1	32.2	28.9	-3.3	0.6	1.0	0.4	104
Sedge Ridge	12.5	11.7	-0.8	25.0	23.9	-1.1	-3.3	-2.9	0.4	104
Mill creek	17.5	18.3	0.8	31.1	30.6	-0.5	1.7	4.5	2.8	104
Tepee creek	14.7	14.0	-0.7	28.3	26.3	-2.0	0.6	-0.7	-1.3	104
Signal peak	12.2	13.3	1.2	24.4	25.3	0.9	-4.4	-1.3	3.2	103
Average	16.8	15.8	-1.1	29.2	27.1	-2.1	1.6	2.4	0.8	95

Previous studies have evaluated NLDAS data by comparing it with weather station observations, and have reported a bias of -0.5°C, RMSE of 2.3°C, and an R^2 of 0.98 (Luo et al., 2003). The slight differences observed in the bias, RMSE, and R^2 noted in the results of this and previous studies is attributable to several facts, including the number of stations, and the total number of observations (668 total observations in this study vs. 12,861 observations in Luo et al., 2003), as could the complexity of the terrain used in our study compared with that of the Luo et al. (2003). This study was conducted in Plevna, Kansas, a relatively flat area, especially when compared with the Yakima Valley. Based on these results, and because of the fact that the NLDAS data provides a continuous surface, we utilized it for the evaluation of the estimated T_a.

Table 3.5. Comparison between the NLDAS T_a and the Observed T_a using RAWS (R^2, Mean Absolute Bias, and RMSE).

RAWS Station	R^2	Mean Absolute Bias (°C)	RMSE(°C)	# observations
Sawmill Flat	0.89	-3.1	3.6	79
YTC-RC	0.93	-1.8	2.4	70
Highbridge	0.96	-3.1	3.5	104
Sedge Ridge	0.97	-0.8	1.6	104
Mill Creek	0.86	0.8	3.1	104
Tepee Creek	0.84	-0.7	3.2	104
Signal Peak	0.92	1.2	2.5	103
Average	0.91	-1.1	2.8	95

Land cover and estimated T_a

The estimated T_a based on the MODIS LST was compared with the T_a obtained from the NLDAS for the land-cover types that are present in the study area. The average estimated T_a based on MODIS LST was 23.7 °C for 2010 and the average T_a from the NLDAS was 19.4°C for 2010 (Figure 3.3.). The average bias between the estimated and the observed T_a was 4.3 ± 1.4 °C. The R^2 between the estimated T_a based on MODIS LST and the NLDAS T_a had a range of 0.2 to 0.96, with an average R^2 of 0.63 (Table 3.6.).

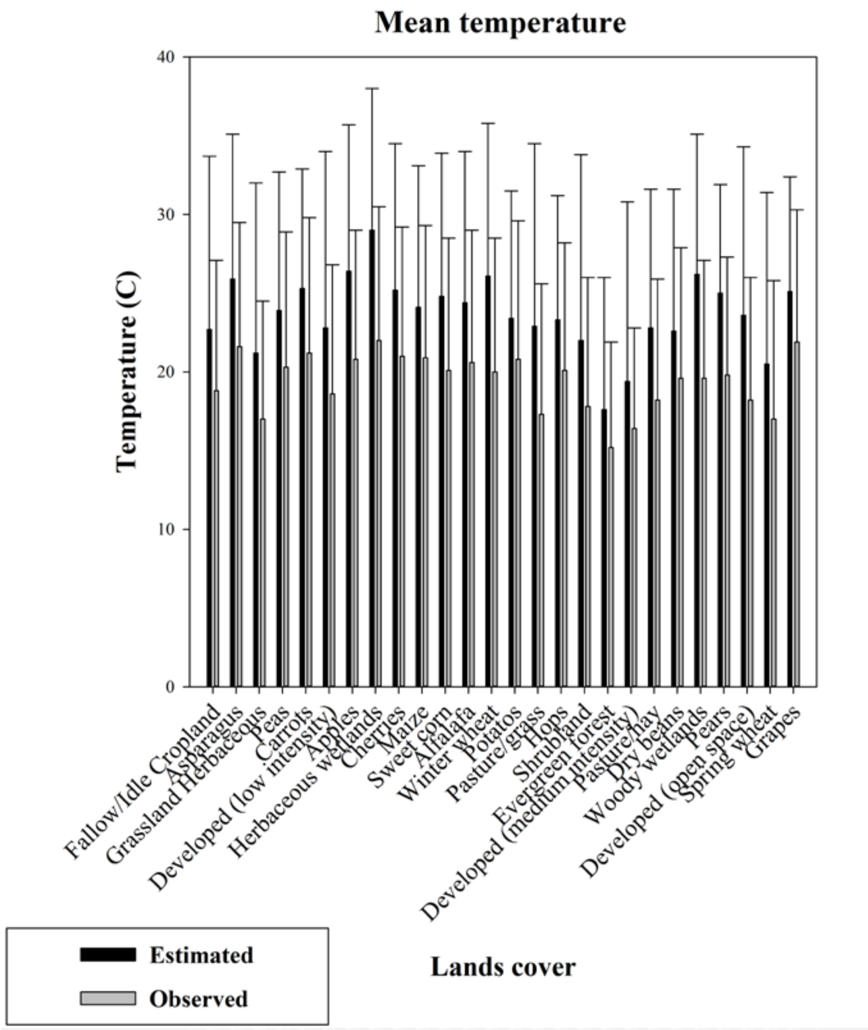

Figure 3.3. Comparison of the 2010 estimated and observed mean temperatures of the dominant land covers in our study area.

The variability within the R^2 values is explained by the heterogeneity of the land cover types. Stisen et al. (2007) reported an average R^2 of 0.64 using the Spinning Enhanced Visible and Infrared Imager (SEVIRI), which is a part of the sensors of the geostationary Meteosat Second Generation (MSG) satellite. The calculated R^2 between the estimated T_a based on MODIS LST and the NLDAS T_a is in agreement with the average R^2 reported by Stisen et al. (2007). Zhang et al. (2011) reported a minimum R^2 of 0.57 for the correlation between the LST and T_a. Although we converted the MODIS LST to T_a by employing the MODIS NDVI values we acquired during this study, the calculated R^2 between the estimated T_a based on the MODIS NDVI and the NLDAS T_a was close to the value reported by Zhang et al. (2011).

The land cover type had a significant impact on the estimated T_a (*p-value* = 0.0019). Initially, the T_a was estimated by combining the MODIS LST with the MODIS NDVI; however, because land cover type has a direct impact on NDVI, we anticipated a substantial impact of the land cover type on the results. Shen and Leptoukh (2011) also reported the strong influence of land cover type on the relationship between the T_a and LST when the T_a is at its highest daily value.

Table 3.6. Accuracy measures for study areas' land cover types (based on the comparison between the estimated T_a and the T_a obtained by NLDAS).

Land-cover type	Average R^2	Error margin	Mean Absolute Bias (°C)	Error margin	Absolute Bias (%)	Average Bias (°C)	Error margin	Average Bias (%)	RMSE(°C)

Fallow/Idle Cropland	0.90	±0.05	6.34	±5.97	1.96	3.88	±7.78	1.20	9.4
Asparagus	0.85	±0.00	4.90	±3.69	21.30	4.23	±4.45	18.39	6.1
Grassland Herbaceous	0.83	±0.07	5.59	±6.22	1.26	4.14	±8.09	0.93	9.4
Peas	0.81	±0.01	5.23	±5.23	6.54	3.58	±6.37	4.48	5.6
Carrots	0.80	±0.00	4.65	±3.63	23.25	4.08	±4.26	20.40	5.9
Developed (low intensity)	0.76	±0.10	6.21	±5.90	2.93	4.25	±7.28	2.00	7.9
Apples	0.74	±0.00	6.53	±4.27	12.32	5.65	±5.40	10.66	7.8
Herbaceous wetlands	0.73	±0.10	7.05	±5.37	7.83	4.67	±5.41	5.19	6.0
Cherries	0.72	±0.12	6.00	±5.88	2.96	4.18	±7.64	2.06	6.2
Maize	0.71	±0.20	6.17	±5.95	0.76	3.17	±7.76	0.39	5.8
Sweet corn	0.70	±0.00	5.07	±3.70	9.39	4.77	±4.07	8.83	6.3
Alfaalfa	0.68	±0.24	5.88	±5.95	0.69	3.85	±7.73	0.45	6.9
Winter wheat	0.67	±0.15	6.37	±5.98	1.59	6.16	±7.79	1.54	8.7
Potatoes	0.67	±0.19	6.24	±6.35	7.01	2.55	±8.39	2.87	4.6
Pasture/grass	0.66	±0.24	5.98	±5.94	0.56	5.63	±7.69	0.53	10.4
Hops	0.65	±0.00	4.77	±3.77	12.55	3.17	±5.21	8.34	6.1
Shrubland	0.61	±0.25	5.99	±5.99	0.07	4.20	±7.76	0.05	10.2
Evergreen forest	0.58	±0.24	6.09	±5.93	0.14	2.43	±7.70	0.05	5.7
Developed (medium intensity)	0.57	±0.26	6.55	±6.03	7.80	3.03	±7.73	3.61	11.4
Pasture/hay	0.56	±0.19	6.37	±6.30	0.88	4.51	±8.21	0.62	6.8
Dry beans	0.55	±0.10	6.43	±6.42	4.91	3.01	±8.38	2.30	6.0
Woody wetlands	0.51	±0.25	7.29	±7.03	14.02	6.68	±9.15	12.85	8.8
Pears	0.45	±0.00	5.63	±3.98	10.43	5.20	±4.53	9.63	6.9
Developed (open space)	0.40	±0.29	5.90	±5.94	2.73	5.42	±7.71	2.51	7.9
Spring wheat	0.34	±0.30	6.39	±6.12	4.35	3.53	±7.86	2.40	9.0
Grapes	0.22	±0.24	6.66	±6.44	7.84	3.21	±8.37	3.78	6.1
Average	0.64	±0.14	6.01	±5.54	6.39	4.29	±7.03	4.85	7.4

Impact of radiative factors on the estimated T_a

The radiative behavior of the various land cover types also influenced variation amongst the estimated T_a. The variety of available vegetation types in the study area, their pigments, as well as their reflection coefficients (albedo) should also be taken into account when discussing estimated air temperature (Gates, 1980; Monteith and Unsworth, 2013). The reflection coefficient was reported to be 22% for maize (*Zea mays* L.) (Monteith and Unsworth, 2013), and the results of our study indicated that when the estimated T_a was compared to the observed T_a, the average bias was 3.17°C with an RMSE of 5.8°C (Table 3.6.). For wheat (*Triticum aestivum* L.), the reflection coefficient was reported as 26% (Monteith and Unsworth, 2013), and the results of our study indicated an average bias of 3.53°C with an RMSE of 9°C when the estimated T_a was compared with the observed T_a. The slightly higher bias and RMSE for the wheat land cover can be partially attributed to its higher surface albedo, which causes it to reflect the incoming radiation from the sun to a higher degree than the maize. This causes its surface to heat at a slower pace compared to the air temperature surrounding it, leading to a higher degree of discrepancy between the estimated and observed T_a. It should also be noted that, at the end of season and during senescence, plant browning also affects the reflection coefficient of plants compared to bare soil (Sacks and Kucharik, 2011), and can therefore impact the net radiation of the land cover as well as the heat flux, which in turn can cause the near-surface air temperature to be cooler or warmer than the surface, depending on the season. However, this is not the only factor contributing to these differences, and it is recommended that future studies use MODIS albedo products (Schaaf et al., 2011; Schaaf et al., 2002; Wang et al., 2012; Lucht et al., 2000; Wanner et al., 1997), along with similar methods, to address the impacts of vegetation type on the estimated T_a.

Impact of aerodynamic factors on the estimated T_a

Leaf orientation and canopy architecture also affect the relationship between air and surface temperatures (Wloczyk et al., 2011). Geiger et al. (1995) reported that the upright growing habit of plants forces the enclosed air to act as insulation, causing the air temperature and canopy (surface) temperature to be similar. Use of NDVI to estimate the T_a makes the results sensitive to the density of the plant canopy; however, small, scattered, and open canopies found in grasslands and peas had a higher R^2 compared to the denser canopies of evergreen forests (Table 3.6.; Figure 3.4.).

R^2=0.71
n=815

R^2=0.58
n=4475

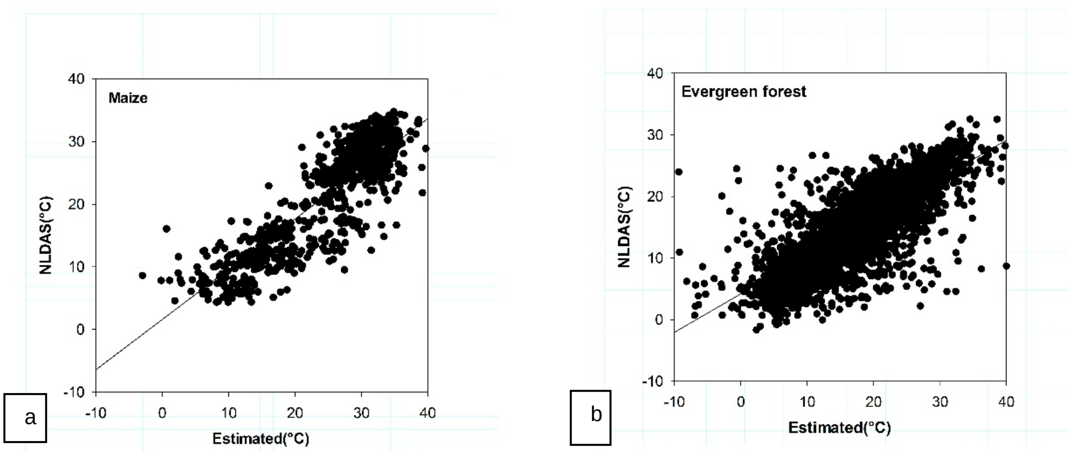

R^2=0.66
n=724

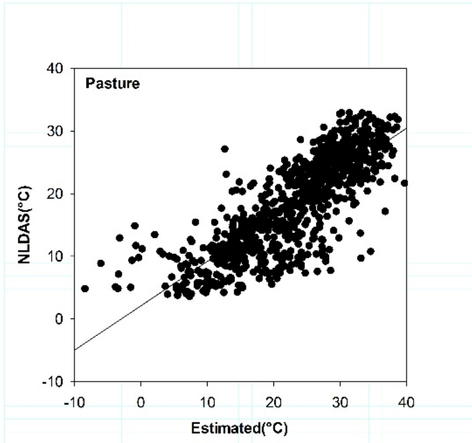

c

R^2=0.67
n=400

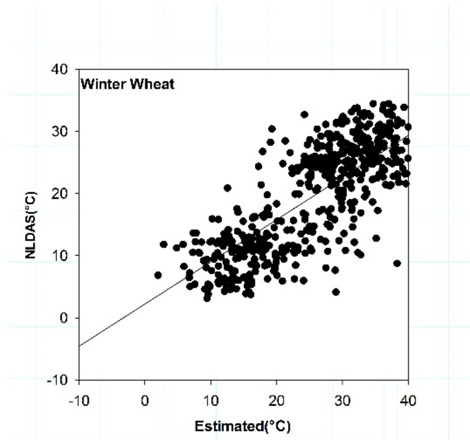

d

R^2=0.68
n= 853

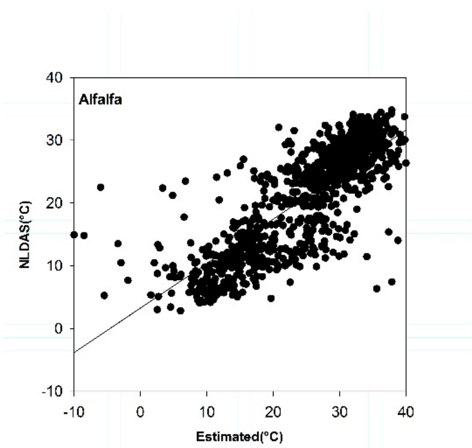

e

R^2=0.55
n= 131

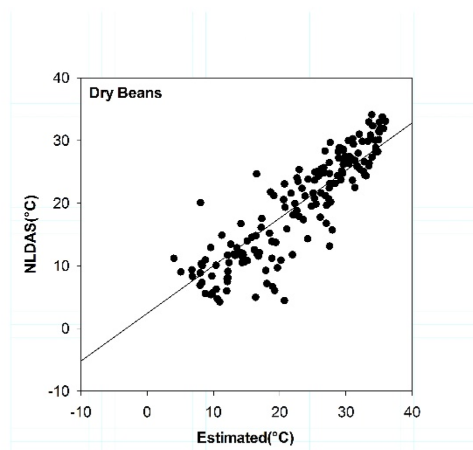

f

R^2=0.72
n=203

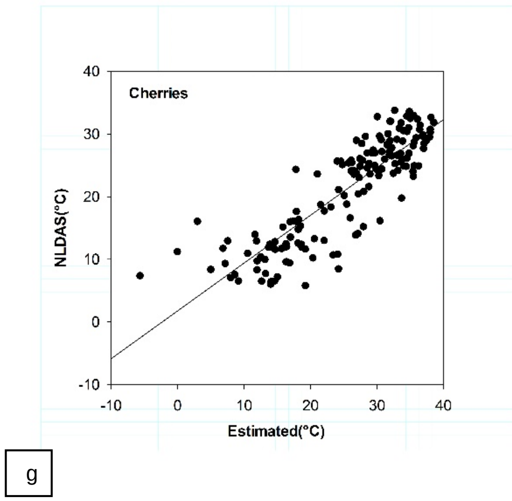

R^2=0.22
n=65

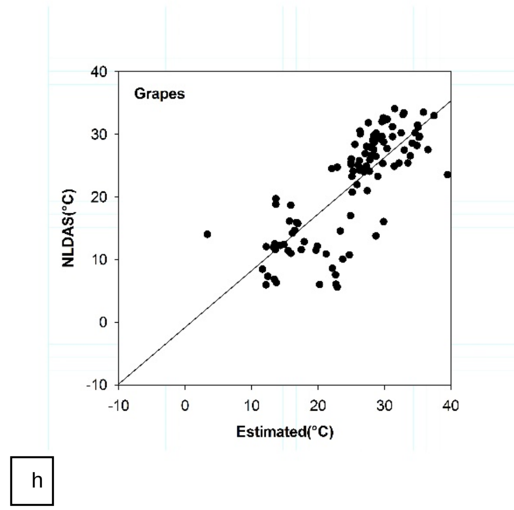

R^2=0.45
n= 54

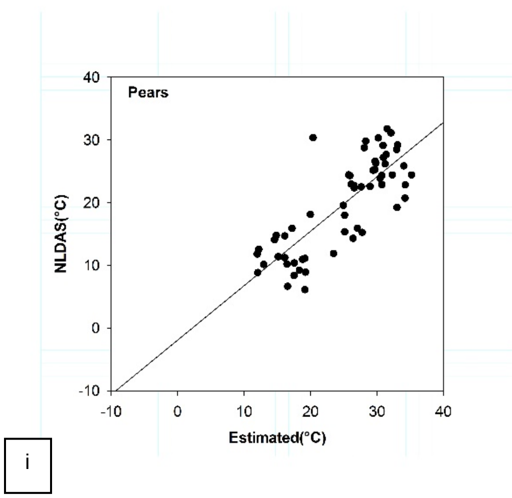

R^2=0.61
n=9106

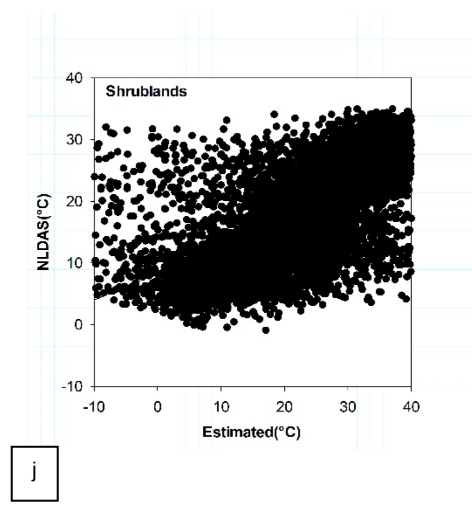

Figure 3. 4. The correlation between estimated T_a and T_a from the NLDAS for major land cover types: Maize (a); Evergreen forest (b); Pasture (c); Winter wheat (d); Alfalfa (e); Dry beans (f); Cherries (g); Grapes (h); Pears (i); Shrublands (j).

We divided the major land cover types into two primary groups: woody plants and herbaceous plants. The average R^2 for woody plants was 0.55 and the average R^2 for herbaceous plants was 0.68. The average R^2 for “Developed” land was 0.58, while the average R^2 “Fallow” land cover was 0.9. The percent absolute bias and percent average bias were also computed (Table 3.6.), and the results indicated that the percent absolute bias is 6.8°C for woody plants, 6.9°C for herbaceous plants, 4.5°C for developed land cover, and 2°C for fallow land cover. The percent average bias was also computed for these four groups, and the results indicated that the percent average bias for woody land cover was 5.6, for herbaceous land cover it was 5.2, for developed land it was 2.7, and for fallow land it was 1.2. The results also showed that fallow land had the lowest bias and the highest coefficient of determination when compared with other land cover types. Therefore, the results imply that the assumptions made in this paper are able to more accurately capture regions with sparse vegetation, such as fallow land, and may need modification and/or adjustment in order to capture the temperature of regions with vegetation covers that have different structures and properties. By dividing the major vegetation land covers into two groups and excluding fallow and developed land, the average bias for woody vegetation was 4.5°C, whereas the average bias for herbaceous vegetation was 4.1°C.

Impact of water relations on the estimated T_a

The highest bias was observed for woody wetlands (6.7°C). This high bias is closely related to the ecosystem of wetlands, especially specific properties of their soil and the availability of surface water. Wetlands are saturated with water and their vegetation type is mainly composed of aquatic plants; these differences may be contributing to a higher bias. The average bias was 4.2°C for all the land cover of this type in our study area.

.

An average difference of 4.2°C between the LST and the observed air temperature was reported by Bustos and Meza (2015). They attributed the over-estimation of the results to a decrease in canopy vapor flow as a result of the simultaneous occurrence of high temperatures and low soil-moisture conditions. This implies a decrease in the gas exchange rate of the stomata, creating a high vapor pressure deficit (Ehrler et al., 1978; Jackson et al., 1981; Duffkova, 2006), and decreasing vapor flow at the canopy level (Vitale et al., 2007). Eventually, the rate of carbon assimilation decreases and the surface temperature increases (Bustos and Meza, 2015). Plants and canopies under water stress tend to close their stomata; consequently, the leaf temperature increases as some of the cooling power of transpiration is lost (Zavala, 2004; Vitale et al., 2007; Bustos and Meza, 2015).

Previous studies revealed that the uncertainty associated with NDVI measurements from AVHRR images can lead to air temperature errors of 4°C (Prihodko and Goward, 1997), as well as the bias associated with the observed air temperature (Czajkowski et al., 1997). Thus, part of the bias in the results of our study may have been caused by the same sources. The fact that growers control the canopy water status as well as the canopy temperature via irrigation might be a contributing factor in the reduced bias that occurs during summer in the Yakima Valley region. In winter and early spring there is usually no canopy cover for most crops, so the LST is mainly influenced by soil and other permanent land covers.

Impact of turbulent heat flux on the estimated T_a

The various heating and cooling properties of the different types of land cover have an impact on the LST (Sohrabinia et al., 2012); our results showed that permanent evergreen vegetation, such as evergreen forest, had the lowest bias (2.4°C) (Table 3.6.), followed by potato

(*Solanum tubersum* L.) fields with a bias of 2.5°C (Table 3.6.). The low bias of evergreen forest confirms the previous results on smaller canopy heat flux when the LAI tends to the infinite (Allen et al., 2006; Noilhan and Planton, 1989). The differences in impact of the vegetation in the distribution of bias within our applied methods can be explained to some extent by variability in the emissivity of each type of land cover. Chemical composition, water content, structure, and surface roughness also influence emissivity (Snyder et al., 1998; Weng et al., 2004). Vegetation emissivity is largely controlled by the plant species, its growth stage, and its areal density (Snyder et al., 1998; Weng et al., 2004). The average emissivity for different land cover types can also influence their heating and cooling properties. For instance, maize has an emissivity of 0.963 (Wittich, 1997), and the results of our study indicated that the average bias was 3.17°C and the average RMSE was 5.8°C (Table 3.6.) when the estimated T_a was compared to the observed T_a. However, for a land cover type with higher emissivity, such as spring wheat (Wittich, 1997) (ε=0.984), the average bias was 3.58°C and the RMSE was 9°C. Therefore, higher emissivity leads to higher RMSE, which can be partially explained by the higher emissivity of the land cover, which then leads to higher surface temperature, which may have a greater difference with the air temperature at the same location. Since the emissivity of all land cover types in this the Yakima Valley unknown, it should be acknowledged that, based on previous studies (Dash et al., 2002) a lack of knowledge about emissivity can introduce a bias ranging from 0.2 to 1.4 K during mid-latitude summers, and 0.8 to1.4 in winter conditions. In our study, the bias had a slight difference across all seasons: 4.1°C from June 1st - to September 30th, 4.5°C from January 1st - to May 31st and October 1st - December 31st. As a result, we recommend that future studies use additional MODIS products to resolve this issue, such as the MODIS BRDF (Schaaf et al., 2011; Schaaf et al., 2002; Wang et al., 2012; Lucht et al., 2000; Wanner et al., 1997) coupled with the estimated outputs. This will improve our understanding of the discrepancies between the observed LST and T_a for various land cover types.

Deviation of leaf temperature from air temperature has been attributed to several factors including the variation found in convective heat loss (Miller, 1972; Smith, 1978; Helliker and Richter, 2008). It has been reported that the low thermal capacity of plant leaves can lead to a difference of up to 15°C between surface and air temperature (Geiger et al., 1995). Other factors, including herbicide uptake, pests, and disease can also create differences between surface and air temperature (Chaerle et al., 2009). For several subalpine species such as the *Abies*, *Pinus*, and *Picea*, leaf temperature is reported to be 5-9°C higher than air temperature (Smith and Carter, 1988; Helliker and Richter, 2008). The difference between leaf and air temperature in a dense mixed forest versus a less dense mixed forest is reportedly 4-5°C and 0.3-2.7°C, respectively (Leuzinger and Korner, 2007; Helliker and Richter, 2008). The canopy temperature is higher than the air temperature from the morning hours until the early afternoon in the case of apples (Meng et al., 2007), cherries (Buyukcangaz et al., 2007), and grapes (a difference of 9°C) (Frühauf and Jagoutz, 2003). We obtained an average bias of 5.6°C for apples, 4.2°C for cherries, 5.2°C for pears, and 3.2°C for grapes. The lower bias for grapes in the Yakima Valley can be attributed to the irrigation strategies of the growers which reduces the stress in plants and decreases the differnces between canopy temperature and air temperature. However, additional information on leaf angle, stomatal opening, and roughness parameters is needed to better understand the actual underlying factors creating these discrepancies among the estimated values of each type of land cover.

Impact of other environmental factors on T_a

The main factor contributing to the estimation of T_a based on remote sensing data is radiation. However, there are also environmental factors involved, including relative humidity (RH), wind speed, and proximity to bodies of water. While some of these factors are interconnected, the variability in the results can partially be described by the effect of these environmental factors. Since water bodies only cover one percent of the Yakima Valley, any variability in the estimated T_a and the T_a obtained from NLDAS was not influenced by closeness to water bodies.

However, wind speed and RH definitely contributed to the difference between the estimated T_a from MODIS LST and the T_a obtained from NLDAS, as the wind speed for our study area during 2010 was, on average, 8.3 km/h, and the relative humidity averaged 57% (RAWS, 2015). Although we acknowledge the impact of RH and wind speed on these discrepancies, a detailed discussion of this phenomena is beyond the objectives of this paper. Previous studies have reported an accuracy of ±1.2°C when RH and wind speed were considered in conjunction with remote sensing data (Konda et al., 1996). A separate study reported that the wind speed influenced both the canopy and soil temperature by 2°C (Goward et al., 2002).

A positive bias was associated with the start of the growing season in April, as well as the end of the growing season in October. The primary cause of this positive bias are the low values of NDVI present at the beginning and end of the growing season. As a result, T_a estimates tend to show greater values compared to the T_a obtained from NLDAS, particularly at the beginning and end of the growing season.

In our study, the highest R^2 obtained was for the fallow/idle cropland, whereas the lowest R^2 was for grapes and spring wheat (Table 3.6.); while the alfalfa had both a high and low R^2.

The variability in the R^2 for the alfalfa can be attributed to the fact that this type of crop is heavily managed, and frequent cutting during the growing season leads to this variation in its NDVI. In addition, environmental factors such as water and energy fluxes have also proven influential in the estimated T_a over the alfalfa, as a result of modification of the green leaf area and its corresponding transpiration via agricultural management.

Further comparison of the estimated T_a and the observed T_a

The RMSE for our study area was obtained by comparing the estimated and the observed T_a, resulting in a temperature of 7.4°C when averaged across all land covers (Table 3.6.). In our study we found the highest RMSE in the urban (medium intensity) land cover, followed by shrubland and pasture, while the lowest RMSE was obtained for potatoes (Table 3.6.). Colombi et al. (2007) reported an RMSE of 1.9°C for comparison of the MODIS LST and the T_a for the alpine areas. An RMSE of 3.6°C was reported when the MODIS LST for pixels with high NDVI values was compared to the T_a (Bustos and Meza, 2015). Wloczyk et al. (2011) estimated the air temperature provided by Landsat 7ETM+ data, and reported an average RMSE of 3°C for a study area in the north-eastern part of Germany. Prince et al. (1998) used Advanced Very High-Resolution Radiometer (AVHRR) satellite data to estimate air temperature, and found an RMSE of 3.9°C for a variety of land cover types, including boreal forest (Kansas, U.S.), tropical bush savannah (Niger, West-Africa), tall-grass prairie (Saskatchewan and Manitoba, Canada), and intensive agriculture production on the mountain prairies (south-central U.S.). However, the RMSE for the location with intensive agriculture was 4.8°C, while another study reported an RMSE of 2.5°C for a homogenous location covered with annual grasses near Darham, Senegal, West Africa, using MSG SEVIRI data to estimate the air temperature (Stisen et al., 2007). The

RMSE obtained by our research was higher than that acquired in previous studies; however, we did not omit the outliers for the statistical analysis in our study. Further, we used all pixels within the study area for our work, whereas previous studies only used the pixels with high NDVI values. The highest NDVI value for setting up the relationship between the LST and the T_a also varied, depending on the studies and sensors used. Wloczyk et al. (2011) used a maximum NDVI of 0.95; which factor might also contribute to the higher RMSE found in the results of our study. Topographic variability within the study area might also be influential on the bias and RMSE via changes in wind and solar radiation (Nieto et al., 2011). In addition, bidirectional effects that define how lights will be reflected from the canopy should also be taken into account in order to obtain more accurate estimates (Nieto et al., 2011).

The implementation of the methods similar to what we used in this study for a particular region should be based on the availability of other sources of spatial T_a data for that region. When there is a lack of observed T_a data with a high temporal resolution, the method used in this study can be used to estimate T_a or improve the missing observations in a big dataset. However, the impact of the land-cover type and other physical processes should be considered when estimating T_a. This can be done by selection of a relatively homogenous area with a land-cover such as evergreen forest.

In a region with similar topography and weather as the Yakima Valley, fallow cropland, grassland (herbaceous), woody and herbaceous wetland, and maize and potato fields, should have the most reliable estimated T_a when this method applied. Future studies that focus on the use of remote sensing data for estimating T_a should take in to account the effect of other environmental factors such as wind speed, relative humidity, and closeness to water bodies on the associated bias between the estimated and observed T_a.

Conclusions

A vegetation-temperature index method was applied to estimate the air temperature for regions located in Yakima Valley, Washington. The estimated air temperature can be used for applications in many different disciplines. However, since the accuracy of the air temperature estimates, on average, was 4.3°C, it is not accurate enough to be used as a substitute for ground measurements of air temperature. For future studies, it is recommended that the $NDVI_{max}$ should be adjusted to accommodate the diversity in the landcover types and therefore, improve the air temperature estimates. The large RMSE score implies that there is a high noise that can be attributed to the spatial resolution of the vegetation indices, the uncertainties associated with the NLDAS data and inaccuracies of the satellite data.

References

Abatzoglou, J. T. (2011). Development of gridded surface meteorological data for ecological applications and modelling. International Journal of Climatology, 33,121–131.

Allen, R.G., Pereira, L. S., Raes, D., and Smith, M. (1998). Crop evapotranspiration-Guidelines for computing crop water requirements. FAO Irrigation and drainage paper 56. FAO, Rome, 300, 9, D05109.

Allen, R.G., Pruitt W.O., Wright, J.L., Howell, T.A., Ventura, F., Snyder, R., Itenfisu, D.. Steduto, P., Berengena, J., Yrisarry, J.B., Smith, M., Pereira, L.S., Raes, D., Perrier, A., Alves, I., Walter, I., Elliott, R. (2006). A recommendation on standardized surface resistance for hourly calculation of reference ETo by the FAO56 Penman-Monteith method Agricultural Water Management, 81, 1–22.

Asrar, G., Fuchs, M., Kanemasu, E. T., and Hatfield, J. L. (1984). Estimating absorbed photosynthetic radiation and leaf area index from spectral reflectance in wheat. Agronomy Journal, 76, 300-306.

Badr, G., and Hoogenboom, G. (2013). Estimating the growing season length using remotely sensed based vegetation indices: a case study for Washington State vineyards. 2013 American Society of Agricultural and Biological Engineers International Meeting.

Badr, G., Hoogenboom, G., Davenport, J., and Smithyman, J. (2015). Estimating growing season length using vegetation indices based on remote sensing: A case study for vineyards in Washington. Transactions of the ASABE, 58, 3, 551-564.

Barnes, W.L., Pagano, T.S., and Salomonson, V.V. (1998). Prelaunch Characteristics of the Moderate Resolution Imaging Spectroradiometer (MODIS) on EOS-AM1. IEEE Transactions on Geoscience and Remote Sensing, 36, 1088 –1100.

Blum, M., Lensky, I. M., and Nestel, D. (2013). Estimation of olive grove canopy temperature from MODIS thermal imagery is more accurate than interpolation from meteorological stations. Agricultural and Forest Meteorology, 176, 90–93.

Boryan, C., Yang, Z., Mueller, R., and Craig, M. (2011). Monitoring US Agriculture: The US Department of Agriculture, National Agricultural Statistics Service Cropland Data Layer Program. Geocarto International, 26, 341–358.

Boryan, C., Yang, Z., and Di, L. (2012). Deriving 2011 cultivated land cover data sets using USDA National Agricultural Statistics Service historic Cropland Data Layers. Geoscience and Remote Sensing Symposium (IGARSS), IEEE International, Munich, Germany, 6297 – 6300.

Buermann, W., Wang, Y. J., Dong, J. R., Zhou, L., Zeng, X., Dickinson, R. E., Potter, C. S., and Myneni, R. B. (2002). Analysis of a multiyear global vegetation leaf area index data set. Journal of Geophysical Research Atmospheres, 107D, 4646.

Burnash, R. J. C. (1995). The NWS river forecast system catchment modeling. Computer Models of Watershed Hydrology, V. P. Singh Ed., Water Resour. Publ., Littleton, Colo., 311– 366.

Burnash, R. J. C., Ferral, R. L., and McGuire R. A. (1973). A generalized streamflow simulation system: Conceptual models for digital computer, Technical Report, Joint Federal and State River Forecast Center, U.S. National Weather Service and California Department of Water Resources, Sacramento, CA, 204 pp.

Bustos, E., and Meza, F. J. (2015). A method to estimate maximum and minimum air temperature using MODIS surface temperature and vegetation data: application to the Maipo Basin, Chile. Theoretical and Applied Climatology, 120, 211–226.

Buyukcangaz, H.. Koksal, E. S., and Yazgan, S. (2007). Diurnal variation of remotely sensed ET and some indices on sweet cherry trees in subhumid climate conditions. Pakistan Journal of Biological Sciences, 10, 9, 1380–1389.

Carlson, T. N., Capehart, W. J., and Gillies, R. R. (1995). A new look at the simplified method for remote sensing of daily evapotranspiration. Remote Sensing of Environment, 54,161–167.

Chaerle, L., Lenk, S., Leinonen, I., Jones, H. G., Van der Straeten, D., and Buschmann, C. (2009). Multi-sensor plant imaging: towards the development of a stress-catalogue. Biotechnology Journal, 4, 1152–1167.

Chartzoulakis, K., and Psarras, G. (2005). Global change effects on crop photosynthesis and production in Mediterranean: the case of Crete, Greece. Agriculture, Ecosystems and Environment, 106, 147–157.

Chen, J., Jönsson, P., Tamura, M., Gu, Z., Matsushita, B., and Eklundh, L. (2004). A simple method for reconstructing a high-quality NDVI time-series data set based on the Savitzky–Golay filter. Remote Sensing of Environment, 91, 332–344.

Cheng, K., Su, Y., Kuo, F., Hung, W., and Chiang, J. (2008). Assessing the effect of land cover changes on air temperature using remote sensing images-A pilot study in northern Taiwan. Landscape and Urban Planning, 86, 297–29.

Chokmani, K. and Viau, A.A. (2006). Estimation of the air temperature and the vapour quantity in atmospheric water with the help of the AVHRR data of the NOAA. Canadian Journal of Remote Sensing, 32, 1–14.

Colombi, A., Michele, C. De, Pepe, M., and Rampini, A. (2007). Estimation of daily mean air temperature from MODIS LST in Alpine areas. New Developments and Challenges in Remote Sensing, Z. Bochenek, Ed., 563–573.

Cosgrove, B. A., Lohmann, D., Mitchell, K. E., Houser, P. R., Wood, E. F., Schaake, J. C., Robock, A., Marshall, C., Sheffield, J., Duan, Q., Luo, L., Higgins, R.W., Pinker, R.T.,. Tarpley, J. D., and Meng, J. (2003). Real-time and retrospective forcing in the North American Land Data Assimilation System (NLDAS) project. Journal of Geophysical Research, 108, 8842.

Czajkowski, K. P., Mulhern, T., Goward, S.N., Cihlar, J., Dubayah, R.O., Prince, S.D. (1997). Biospheric environmental monitoring at BOREAS with AVHRR observations. Journal of Geophysical Research, [Atmospheres], 102, 29,651–29,662.

Dash, P., Göttsche, F. M., Olesen, F. M., and Fischer H. (2002a). Land surface temperature and emissivity estimation from passive sensor data: Theory and practice – current trends. International Journal of Remote Sensing, 23, 2563–2594.

Duffkova, R. (2006). Difference in canopy and air temperature as an indicator of grassland water stress. Soil Water Research, 1,127–138.

Ek, M. B., Mitchell, K. E., Lin, Y., Rodgers, E., Grunman, P., Koren, V., Gayno, G., and Tarpley, J. D. (2003). Implementation of Noah land surface model advances in the National Centers for Environmental Prediction operational mesoscale Eta model. Journal of Geophysical Research, 108, D22, 885.

Ehrler, W.L., Idso, S.B., Jackson, R.D., Reginato, R.J. (1978). Wheat canopy temperature: relation to plant water potential. Agronomy Journal, 70, 251-256.

Flores P., F., and Lillo S., M. (2010). Simple air temperature estimation method from MODIS satellite images on a regional scale. Chilean Journal of Agricultural Research, 70, 436–445.
Frühauf, C., and Jagoutz, H. (2003). Untersuchung zum Verhalten der Temperatur oberhalbund innerhalb eines Rebbestandes in Abhängigkeit von den herrschenden Strahlungsbedingungen. Tharandter Klimaprotokolle, 5. BIOMET-Tagung Mensch-Pflanze-Atmosphäre, C. Bernhofer and V. Goldberg, Eds., 9, 109–111.

Fung, I. Y., Tucker, C. J., and Prentice, K. C. (1987). Application of advanced very high resolution radiometer vegetation index to study atmosphere-biosphere exchange of CO2. Journal of Geophysical Research, 92, 2999–3015.

Gates, D. M. (1968). Transpiration and leaf temperature. Annual Reviews of Plant Physiology, 19, 211–238.

Geiger, R., Aron, R. H, and Todhunter, P. (1995). The Climate near the ground. Friedr. Vieweg and Sohn Verlagsges. mbH, braunschweig, Wiesbaden, 528 pp.

Goward, S. N., Tucker, C. J., and Dye, D. G. (1985). North American vegetation patterns observed with the NOAA-7 advanced very high resolution radiometer. Vegetation, 64, 3 –14.

Goward, S.N., Waring, R. H., Dye, D. G., and Yang, J. (1994). Ecological remote sensing at otter: satellite macroscale observations. Ecological Application, 4, 322–343.

Goward, S.N., Xue, Y., and Czajkowski, K. P. (2002). Evaluating land surface moisture conditions from the remotely sensed temperature/vegetation index measurements: An exploration with the simplified simple biosphere model. Remote Sensing of Environment, 79, 2–3, 225–242.

Guenther, B., Xiong, X., Salomonson, V., Barnes, W., and Young, J. (2002). On-orbit performance of the Earth Observing System Moderate Resolution Imaging Spectroradiometer; first year of data. Remote Sensing of Environment, 83, 16–30.

Han, W., Yang, Z., Di, L., and Mueller, R. (2012). CropScape: A Web service based application for exploring and disseminating US conterminous geospatial cropland data products for decision support. Computers and Electronics in Agriculture, 84, 111–123.

Hashimoto, H., Dungan, J. L., White, M. A., Yang, F., Michaelis, A. R., Running, S. W., and Nemani, R. R. (2008). Satellite-based estimation of surface vapor pressure deficits using MODIS land surface temperature data. Remote Sensing of Environment, 112, 142 –155.

Helliker, B. R., and Richter, S. L. (2008). Subtropical to boreal convergence of tree-leaf temperatures. Nature, 454, 7203, 511–514.
Hicke, J. A., Asner, G. P., Randerson, J.T., et al. (2002). Trends in North American net primary productivity derived from satellite observations, 1982-1998. Global Biogeochemical Cycles, 16, 1018–1032.

Hill, M. J., and Donald, G. E. (2003). Estimating spatio-temporal patterns of agricultural productivity in fragmented landscapes using AVHRR NDVI time series. Remote Sensing of Environment, 84, 367–384.

Hong, S., Lakshmi, V., Small, E. E., Chen, F., Tewari, M., and Manning, K. W. (2009). Effects of vegetation and soil moisture on the simulated land surface processes from the coupled WRF/Noah model. Journal of Geophysical Research: Atmospheres, 114, 1–13.

Hoch, G. and Körner, C. (2005). Growth, demography and carbon relations of Polylepis trees at the world's highest treeline. Functional Ecology, 19, 941–951.

Jabot, E., Zin, L., Lebel, T., Gautheron, A., and Obled, C. (2012). Spatial interpolation of sub-daily air temperatures for snow and hydrologic applications in mesoscale Alpine catchments. Hydrological Processes, 26, 2618–2630.

Jackson, R. D., Kustas, W. P., and Choudhury, B. J. (1988). A reexamination of the crop water stress index. Irrigation Science, 9, 309–317.

Jang, D., Viau, A.A., and Anctil, F. (2004). Neural network estimation of air temperatures from AVHRR data. International Journal of Remote Sensing, 25, 4541–4554.

Jiménez, P.A., González-Rouco, J. F., Navarro, J., Montávez, J. P., and García-Bustamante, E. (2010). Quality Assurance of Surface Wind Observations from Automated Weather Stations. Journal of Atmospheric and Oceanic Technology, 27, 1101–1122.

Justice, C., Townshend, J. R., Vermote, E., Masuoka, E., Wolfe, R., Saleous, N., Roy, D., et al. (2002). An overview of MODIS Land data processing and product status. Remote Sensing of Environment, 83, 3–15.

Karl, T. R., Knight, R. W., and Christy, J. R. (1994). Global and Hemispheric Temperature Trends: Uncertainties Related to Inadequate Spatial Sampling. Climate, 7, 1144–1163.

Karnieli, A., Agam, N., Pinker, R. T., Anderson, M., Imhoff, M. L., Gutman, G. G., Panov, N., Goldberg, A. (2010). Use of NDVI and land surface temperature for drought assessment: merits and limitations. Journal of Climate, 23, 618–633.

Konda, M., Imasato, N., and Shibata, A. (1996). A new method to determine near-sea surface air temperature by using satellite data. Journal of Geophysical Research: Oceans, 101, C6, 14349–14360.

Koster, R., and Suarez, M. (1996). Energy and water balance calculations in the Mosaic LSM, NASA Tech. Memo., NASA TM-104606, 9, 60 pp.

Lakshmi, V., Hong, S., Small, E. E., and Chen, F. (2011). The influence of the land surface on hydrometeorology and ecology: new advances from modeling and satellite remote sensing. Hydrology Research, 42, 95–112.

Leuzinger, S. and Korner, C. (2007). Tree species diversity affects canopy leaf temperatures in a mature temperate forest. Agriculture and Forest Meteorology, 146, 29–37.

Liang, X., Lettenmaier, D. P., Wood, E. F., and Burges S. J. (1994). A simple hydrologically based model of land surface water and energy fluxes for GCMs. Journal of Geophysical Research, 99, D7, 14,415–14,428.

Lin, S., Moore, N. J., Messina, J. P., DeVisser, M. H., and Wu, J. (2012). Evaluation of estimating daily maximum and minimum air temperature with MODIS data in east Africa. International Journal of Applied Earth Observation and Geoinformation, 18, 128–140.

Los, S.N. (1998). Estimation of the ratio of sensor degradation between NOAA AVHRR channels 1 and 2 from monthly NDVI composites. IEEE Transactions on Geoscience and Remote Sensing, 36, 206–213.

Lu, X., Chow, K. C., Yao, T., Fung, J. C. H., and Lau, A. K. H. (2009). Seasonal variation of the land-sea breeze circulation in the Pearl River Delta region. Journal of Geophysical Research: Atmospheres, 114, 1–14.

Lucht, W., Schaaf, C.B., and Strahler, A.H. (2000). An algorithm for the retrieval of albedo from space using semi empirical BRDF models. IEEE Transactions on Geoscience and Remote Sensing, 38, 977–998.

Luo, L., Robock, A., Mitchell, K. E., Houser P. R., Wood, E. F., Schaake, J. C., Lohmann, D., et al. (2003). Validation of the North American Land Data Assimilation System (NLDAS) retrospective forcing over the southern Great Plains. Journal of Geophysical Research, 108, 1–10.

Marquínez, J., Lastra, J., and García, P. (2003). Estimation models for precipitation in mountainous regions: The use of GIS and multivariate analysis. Journal of Hydrology, 270, 1–11.

Marques da Silva, J. R., Damásio, C. V., Sousa, A. M. O., Bugalho, L., Pessanha, L., and Quaresma, P. (2015). Agriculture pest and disease risk maps considering MSG satellite data and land surface temperature. International Journal of Applied Earth Observation and Geoinformation, 38, 40–50.

Meng, P., Zhang, J.S., Gao, J., Wang, H.S., and Ren, Q. F. (2007). Variation of apple tree canopy-air temperature difference and its relations to environment factors. The Journal of Applied Ecology, 18, 9, 2030–2034.

Menne, M. J., and Williams, Jr. C. N. (2009). Homogenization of Temperature Series via Pairwise Comparisons. Journal of Climate, 22, 1700–1717.

Minder, J. R., Mote, P. W., and Lundquist, J. D. (2010). Surface temperature lapse rates over complex terrain: Lessons from the Cascade Mountains. Journal of Geophysical Research: Atmospheres, 115, 1–13.

Miller, P. C. (1972). Bioclimate, leaf temperature, and primary production in red mangrove canopies in south Florida. Ecology, 53, 22–45.

Mitchell, K. E., Lohmann, D., Houser, P. R., Wood, E. F., Schaake, J. C., Robock, A., Cosgrove, B. A., et al., (2004). The multi-institution North American Land Data Assimilation System (NLDAS): Utilizing multiple GCIP products and partners in a continental distributed hydrological modeling system. Journal of Geophysical Research: Atmospheres, 109, 1–23.

Monteith, J. L. (1973). Principles of environmental physics. London: Edward Arnold

Monteith, J., and Unsworth, M. (2013). Principles of Environmental Physics: Plants, Animals, and the Atmosphere. Academic Press.

Morisette, J. T., Privette, J. L., and Justice, C. O. (2002). A framework for the validation of MODIS Land products. Remote Sensing of Environment, 83, 77–96.

Mostovoy, G.V., King, R. L., Reddy, K. R., Kakani, V. G., Filippova, M. G. (2006). Statistical estimation of daily maximum and minimum air temperatures from MODIS LST data over the state of Mississippi. GIScience and Remote Sensing, 43, 1, 78–110.

Mostovoy, G.V., Anantharaj, V., King, R. L., and Filippova, M. G. (2008). Interpretation of the relationship between skin temperature and vegetation fraction: Effect of subpixel soil temperature variability. International Journal of Remote Sensing, 29, 2819–2831.

Myneni, R.B., Hall, F. G., Sellers, P. J., and Marshak, A. L. (1995). The interpretation of spectral vegetation indexes. IEEE Transactions on Geoscience and Remote Sensing, 33, 481–486.

NASA Land Processes Distributed Active Archive Center (LP DAAC). (2012). MODIS A2. USGS/Earth Resources Observation and Science (EROS) Center, Sioux Falls, South Dakota.

Nemani, R.R. and Running, S. W. (1989). Estimation of resistance to evapotranspiration from NDVI and thermal-IR AVHRR data. Journal of Climate and Applied Meteorology, 28, 276–294.

Nemani, R., and Running, S. W. (1996). Implementation of a hierarchical global vegetation classification in ecosystem function models. Journal of Vegetation Science, 7, 337–346.

Nieto, H., Sandholt, I., Aguado, I., Chuvieco, E., and Stisen, S. (2011). Air temperature estimation with MSG-SEVIRI data: Calibration and validation of the TVX algorithm for the Iberian Peninsula. Remote Sensing of Environment, 115, 1,107–116.

Noilhan, J., Planton, S. (1989). A simple parameterization of land surface processes for meteorological models. Monthly Weather Review, 117, 536–549.

Norman, J.M., and Becker, F. (1995). Terminology in thermal infrared remote sensing of natural surfaces. Agricultural and Forest Meteorology, 77,153–166.

Pettorelli, N., Vik, J. O., Mysterud, A., Gaillard, J. M., Tucker, C. J., and Stenseth, N. C. (2005). Using the satellite-derived NDVI to assess ecological responses to environmental change. Trends in Ecology and Evolution, 20, 503–510.

Pettorelli, N. (2013). The Normalized Difference Vegetation Index. Oxford University Press.

Petropoulos, G., Carlson, T. N., Wooster, M. J., and Islam, S. (2009). A review of Ts/VI remote sensing based methods for the retrieval of land surface energy fluxes and soil surface moisture. Progress in Physical Geography, 33, 224–250.

Pielke, R., Nielsen-Gammon, J., Davey, C., Angel, J., Bliss, O., Doesken, N., Cai, M., Fall, S., Niyogi, D., Gallo, K., Hale, R., Hubbard, K. G., Lin, X. M., Li, H., and Raman, S. (2007). Documentation of uncertainties and biases associated with surface temperature measurement sites for climate change assessment. Bulletin of the American Meteorological Society, 88, 913–928.

Price, J. C. (1990). Using spatial context in satellite data to infer regional scale evapotranspiration, IEEE Transactions on Geoscience Remote Sensing, 28, 940– 948.

Prihodko, L., and Goward, S. N. (1997). Estimation of Air Temperature Sensed Surface Observations from Remotely. Remote Sensing of Environment, 60, 335–346.

Prince, S.D., Goetz, S. J., Dubayah, R. O., Czajkowski, K. P., and Thawley, M. (1998). Inference of surface and air temperature, atmospheric perceptible water and vapor pressure deficit using Advanced Very High-Resolution Radiometer satellite observations: comparison with field observations. Journal of Hydrology, 212-213, 230-249.

Prince, S.D. and Goward, S. N. (1995). Global primary production: a remote sensing approach. Journal of Biogeography, 22, 2829–2849.

Purkey, D. R., Joyce, B., Vicuna, S., Hanemann, M. W., Dale, L. L., Yates, D., and Dracup, J. A. (2007). Robust analysis of future climate change impacts on water for agriculture and other sectors: a case study in the Sacramento Valley. Climate Change, 87,109–122.

Randin, C. F., Paulsen, J., Vitasse, Y., Kollas, C., Wohlgemuth, T., Zimmermann, N. E., and Körner,C. (2013). Do the Elevational Limits of Deciduous Tree Species Match Their Thermal Latitudinal Limits? Global Ecology and Biogeography, 22, 8, 913–23.

RAWS (Remote Automated Weather Stations). (2010). Daily Temperature. Western Regional Climate Center. [Last visit September 09, 2015. Available online at http://www.raws.dri.edu/.]

Riddering, J. P., and L. P. Queen, 2006: Estimating near-surface air temperature with NOAA AVHRR. Canadian Journal of Remote Sensing, 32, 33–34.

Robeson, S. M. (1995). Resampling of network-induced variability in estimates of terrestrial air temperature change. Climate Change, 29, 213-229.

Roerick, G.J., Meneti, M., Soepboer, W., and Su, Z. (2003). Assessment if climate impact on vegetation dynamics by using remote sensing. Physical Chemistry of the Earth, 28, 103-109.

Rouse, J.W., Haas, R. H., Schell, J. A., and Deering, D. W. (1974). Monitoring vegetation system in the Great Plains with ERTS. Proceedings, 3rd Earth Resources Technology Satellite-1 Symposium, Greenbelt, USA, NASA SP-351.

Running, S.W. (1990). Estimating primary productivity by combining remote sensing with ecosystem simulation. Remote Sensing of Biosphere Functioning, R.J. Hobbs and H. A. Mooney, Eds., Springer, 65–86.

Sacks, W. J., and Kucharik C. J. (2011). Crop management and phenology trends in the U.S. Corn Belt: Impacts on yields, evapotranspiration and energy balance. Agricultural and Forest Meteorology, 151(7), 882–894.

Saravanapavan, T., and Dye, D. G. (1995). Satellite Estimation of Environmental Variables by the Contextual Analysis Method: Validation in a Seasonal Tropical Environment. Global Engineering Laboratory Institute of Industrial Science University of Tokyo, Japan.

Schaaf, C., Gao, F., Strahler, A. H., Lucht, W., Li, X., Tsang, T., Strugnell, N. C., Zhang, X., Jin, Y., Muller, J. P., Lewis, P., Barnsley, M., Hobson, P., Disney, M., Roberts, G., Dunderdale, M., Doll, C., d'Entremont, R., Hu, B., Liang, S., Privette, J. L., and Roy, D. P. (2002). First operational BRDF, albedo and nadir reflectance products from MODIS. Remote Sensing of Environment, 83, 135–148.

Schaaf, C. L. B., Liu, J., Gao, F., and Strahler, A. H. (2011). MODIS albedo and reflectance anisotropy products from aqua and terra. In B. Ramachandran, C. Justice, and M. Abrams (Eds.), Land remote sensing and global environmental change: NASA's earth observing system and the science of ASTER and MODIS. Remote Sensing and Digital Image Processing Series, 11, Springer (873 pp.).

Seguin, B. (1991). Use of surface temperature in agrometeorology. Applications Of Remote Sensing to Agrometeorology, F. Toselli, Ed., Kluwer Academic Press, Boston, 221- 240.

Sellers, P. J. (1985). Canopy reflectance, photosynthesis and transpiration. International Journal of Remote Sensing, 6, 1335-1372.

Shen, S., and Leptoukh, G. G. (2011). Estimation of surface air temperature over central and eastern Eurasia from MODIS land surface temperature. Environmental Research Letters, 6, 4, 045206.

Sims, D. A., Rahman, A. F., Cordova, V. D., El-Masri, B. Z., Baldocchi, D. D., Bolstad, P. V., Flanagan, L. B., et al. (2008). A new model of gross primary productivity for North American ecosystems based solely on the enhanced vegetation index and land surface temperature from MODIS. Remote Sensing of Environment, 112, 1633–1646.

Smith, W. K. (1978). Temperatures of desert plants—another perspective on adaptability of leaf size. Science, 201, 614–616.

Smith, W. K. and Carter, G. A. (1988). Shoot structural effects on needle temperatures and photosynthesis in conifers. American Journal of Botany, 75, 496–500.

Snyder, W. C., Wan, Z., Zhang, Y., Feng, Y.Z. (1998). Classification-based emissivity for land surface temperature measurement from space. International Journal of Remote Sensing, 19, 2753–2774.

Sohrabinia, M., Rack, W., and Zawar-Reza, P. (2012). Analysis of MODIS LST Compared with WRF Model and in situ Data over the Waimakariri River Basin, Canterbury, New Zealand. Remote Sensing, 4, 11, 3501–3527.

Son, N. T., Chen, C. F., Chen C. R., Chang, L. Y., and Minh, V. Q. (2012). Monitoring agricultural drought in the Lower Mekong Basin using MODIS NDVI and land surface temperature data. International Journal of Applied Earth Observation and Geoinformation, 18, 417–427.

Sun, D., and Kafatos, M. (2007). Note on the NDVI-LST relationship and the use of temperature-related drought indices over North America. Geophysical Research Letters, 34, 1–4.

Stisen, S., Sandholt, I., Nørgaard, A., Fensholt, R. and Eklundh, L. (2007). Estimation of Diurnal Air Temperature Using MSG SEVIRI Data in West Africa. Remote Sensing of Environment, 110, 262–274.

Townshend, J. R. G., and Justice, C.O. (1986). Analysis of the dynamics of African vegetation using the normalized difference vegetation index. International Journal of Remote Sensing, 8, 8, 1189–1207.

Tucker, C. J., Fung, I. Y., Keeling, C. D. and Gammon, R. H. (1986). Relationship between atmospheric CO_2 variations and a satellite-derived vegetation index. Nature, 319, 195–199.

Tucker, C. J., and Sellers, P. J. (1986). Satellite remote sensing of primary production. International Journal of Remote Sensing, 7, 1395–1416.

Turner, D.P., Cohen, W. B., Kennedy, R. E., Fassnach, K. S., and Briggs, J. M. (1999). Relationships between leaf area index and Landsat TM spectral vegetation indices across three temperate zone sites. Remote Sensing of Environment, 70, 52–68.

USGS (United States Geological survey), cited 2015: NLCD 92 Land Cover Class Definitions (Last visit May 3rd, 2015; available online http://landcover.usgs.gov/classes.php#herb)

Vancutsem, C., Ceccato, P., Dinku, T., and Connor, S. J. (2010). Evaluation of MODIS land surface temperature data to estimate air temperature in different ecosystems over Africa. Remote Sensing of Environment, 114, 449–465.

Van De Kerchove, R., Lhermitte, S., Veraverbeke, S., and Goossens, R. (2013). Spatio-temporal variability in remotely sensed land surface temperature, and its relationship with physiographic variables in the Russian Altay Mountains. International Journal of Applied Earth Observation and Geoinformation, 20, 4–19.

Verhoef, W., Menenti, M., and Azzali, S. (1996). A colour composite of NOAA-AVHRR-NDVI based on time series analysis (1981–1992). International Journal of Remote Sensing, 17, 2, 231–235.

Vitale, M., S. Anselmi, E. Salvatori, F. Manes, 2007: New approaches to study the relationship between stomatal conductance and environmental factors under Mediterranean climatic conditions. Atmospheric Environment, 41, 5385–5397.

Walsh, S. J., Moody, A., Allen, T. R., and Brown, D. G. (1997). Scale dependence of NDVI and its relationship to mountainous terrain. Scale in Remote Sensing and GIS. D. A. Quattrochi, and M. F. Goodchild, Eds., Boca Raton, FL: Lewis Publishers, 27– 55.

Walsh, S. J., Crawford, T. W., Welsh, W. F., and Crews-meyer, K. A. (2001). A multiscale analysis of LULC and NDVI variation in Nang Rong district, Northeast Thailand. Agriculture, Ecosystems and Environment, 85, 47–64.

Wan, Z., Zhang, Y., Zhang, Q., and Li, Z. L. (2004a). Quality assessment and validation of the MODIS global land surface temperature. International Journal of Remote Sensing, 25, 261–274.

Wan, Z., Wang, P., and Li, X. (2004b). Using MODIS Land Surface Temperature and Normalized Difference Vegetation Index products for monitoring drought in the southern Great Plains, USA. International Journal of Remote Sensing, 25, 61–72.

Wang, P.X., Li, X. W., Gong, J., and Song, C. (2001). Vegetation temperature condition index and its application for drought monitoring. Proceedings IEEE International, Geoscience and Remote Sensing Symposium (IGARSS) Sydney, Australia, 141 –143.

Wang, Z., Schaaf, C.B., Chopping, M. J., Strahler, A.H., Wang, J., Román, M. O., Rocha, A.A., Woodcock, C.E., and Shuai, Y. (2012). Evaluation of Moderate-resolution Imaging Spectroradiometer (MODIS) snow albedo product (MCD43A) over tundra. Remote Sensing of Environment, 117, 264–280.

Wanner, W., Li, X., and Strahler, A.H. (1995). On the derivation of kernels for kerneldriven models of bidirectional reflectance. Journal of Geophysical Research, 100, 21077–21090.

Weng, Q., Lu, D., and Schubring, J. (2004). Estimation of land surface temperature–vegetation abundance relationship for urban heat island studies. Remote Sensing of Environment, 89(4), 467–483.

Willmott, C.J., and Robeson, S. M. (1991). Influence of spatially variable instrument networks on climatic averages. Geophysical Research Letters, 18, 2249-225.

Wittich, K.P. (1997). Some simple relationships between land-surface emissivity, greenness and the plant cover fraction for use in satellite remote sensing. International Journal of Biometeorology, 41(2), 58–64.

WMO (World Meteorological Organization). (2008). Guide to Meteorological Instruments and Methods of Observations. WMO-No.8, Geneva, Switzerland.

Wloczyk, C., Borg, E., Richter, R., and Miegel, K. (2011). Estimation of instantaneous air temperature above vegetation and soil surfaces from Landsat 7 ETM+ data in northern Germany. International Journal of Remote Sensing, 32, 24, 9119–9136.

Xia, Y., Mitchell, K., Ek, M., Cosgrove, B., Sheffield, J., Luo, L., Alonge, C., Wei, H., Meng, J., Livneh, B., Duan, Q, Lohmann, D. (2012). Continental-scale water and energy flux analysis and validation for North American Land Data Assimilation System project phase 2 (NLDAS-2): 2. Validation of model-simulated streamflow. Journal of Geophysical Research: Atmospheres, 117,D3, D03110.

Yan, J., Chen, L., Li, H., Gao, Y., and Tao, J. (2011). Application of the land surface temperature from MODIS in the estimation of gross primary productivity for a subtropical pinus plantation in southern China. International Conference on Remote Sensing, Environment and Transportation Engineering (RSETE), 115–118.

Yates, D., Sieber, J., Purkey, D., and Huber-Lee, A. (2005). WEAP21—a demand, priority, and preference-driven water planning model. Water International, 30,487–500.

Zakšek, K., and Schroedter-Homscheidt, M. (2009). Parameterization of Air Temperature in High Temporal and Spatial Resolution from a Combination of the SEVIRI and MODIS Instruments. ISPRS Journal of Photogrammetry and Remote Sensing, 64, 414–421.

Zavala, M. (2004). Integration of drought tolerance mechanisms in Mediterranean sclerophylls: a functional interpretation of leaf gas exchange simulators. Ecological Modelling, 176, 211–226.

Zhang, W., Huang, Y., Yu, Y., and Sun, W. (2011). Estimation of daily mean air temperature from MODISLST in alpine areas. International Journal of Remote Sensing, 32, 1–26.

Zhao, T.T., and Schwartz, M. D. (2003). Examining the onset of spring in Wisconsin. Climate Research, 24, 59–70.

Zhou, L., Kaufmann, R. K., Tian, Y., Myneni, R. B., and Tucker, C. J. (2003). Relation between inter annual variations in satellite measures of northern forest greenness and climate between 1982 and 1999. Journal of Geophysical Research, 108, D1, ACL 3-1–ACL 3-16, 16.

CHAPTER FOUR

SPATIO-TEMPORAL ANALYSIS OF SEVERAL BIOCLIMATIC INDICES FOR VITICULTURAL ZONING

Abstract

The growth and development of grapevines (*Vitis vinifera* L.) is highly dependent on the weather dynamics of a region. The quality and quantity of the grapes produced is controlled by the weather conditions during each growing season as well as the previous season; subsequently, a vineyard's economic profitability is also affected by weather dynamics. In this study, several bio-climatic indices were computed using 30 years (1983-2012) of daily weather data obtained from the gridded surface meteorological dataset at the University of Idaho (UI GSM). The bio-climatic indices were extracted for each of the American Viticultural Areas (AVA) located in the State of Washington and parts of Oregon. Descriptive statistics were computed for the bio-climatic indices of each separate AVA, and the statistics were then compared based on their bio-climatic indices. Several new indices were developed, based on modifications made on previous indices and models. The Dynamic Minimum Temperature Index (DyMin. Temp.) was developed via a series of modifications made to the previously established Minimum Temperature Index. The Cold Damage Index (CDI) was developed based on the Cold Hardiness Model, and a new Wind Speed Index (WSI) was also introduced. Puget Sound has many distinct features not present in other eastern Washington AVAs: in terms of growing season temperature, Puget Sound, Columbia Gorge, and Naches Heights were categorized as cool climate maturity groupings, and the remaining AVAs were categorized as intermediate maturity groupings. The average for frost free days ranged from 146 to 230; the mean growing degree days (GDD) ranged from 948 to 1662; the mean biologically effective degree days (BEDD) ranged from 318 to

1590; the mean Huglin Index (HI) ranged from 1452 to 2425; the mean length of growing season (LGS) ranged from 164 to 189 days; and the average growing season suitability (GSS) ranged from 82% to 92%. Once obtained, the bio-climatic indices were then used to categorize the AVAs; these relative categories have the ability to assess the climate potential of specific AVAs for optimal grape production. They can improve our understanding of a region's climate, potentially enabling us to match the best cultivars to a region based on its specific climate dynamics.

Introduction

Climate plays the predominant role in grapevine (*Vitis spp.*) growth and development (van Leeuwen et al., 2004; Santos et al., 2011, Fraga et al., 2013); specific environmental conditions determine grapevine physiology and development (Magalhães, 2008; Jackson 2008; Santos et al., 2012b; Toth and Vegvari, 2016). A strong correlation has been reported between grape yield and climate traits, such as monthly mean temperature and precipitation totals during the growing season for a specific region (Makra et al., 2009; Santos et al., 2012a). Jones et al. (2004) described the impact of climate as the most profound factor in determining the ability of a region to produce quality grapes. The macro-climate requirements for vines require that the lowest temperature in winter does not fall below -15°C to -20°C, and that there be a minimum of 1000 growing degree days with a base of 10°C available for the grapes (Van Leeuwen and Seguin, 2006; Keller, 2010; White, 2015). The meso-climate is mainly determined by the topography of a region (Van Leeuwen and Seguin, 2006; Keller, 2010; White, 2015), while the micro-climate is primarily decided by local soil and canopy management, and is focused on the fruit zone (Van Leeuwen and Seguin, 2006; Keller, 2010; White, 2015).

Bio-climatic indices

Several indices have been developed based on the heat load (daily accumulated temperatures above a threshold of 10°C for a fixed period) and temperature requirements of grapevines. Growing season suitability (GSS) (Malheiro et al., 2010; Santos et al., 2012b) is the fraction of days from April to September with daily mean air temperatures above 10°C. The length of growing season (LGS) (Jackson, 2008) is the number of days with mean temperatures above 10°C for a growing season ranging from April 1st to October 31st. The Cool night Index (CI) (Tonietto and Carbonneau, 2004) takes into account the minimum temperature during grape maturation, and is the average minimum air temperature in September.

The Frost Free Days index (FFD) (Magarey et al., 1998) is used to determine growing season length; it is the period between the last frost (temperatures below 0°C) in spring and the first frost in fall. Temperatures below −17°C are commonly considered the lethal lower temperature limit for grapes; defined as the minimum temperature index (Min. Temp.) (Hidalgo, 2002), it is a vital constraint of growing grapevines. However, cold acclimation is a physiological process that happens over a period of time, so using a single temperature threshold to represent it may not be effective in capturing grapevine behavior in response to low temperatures. In reality, lethal low temperatures are dynamic, and vary based on the cold hardiness status of each grapevine. Grapevine cold hardiness is likewise a dynamic phenomenon that responds to seasonal changes in air temperature (Ferguson et al., 2011). Cold hardiness starts with the acclimation at the end of the growing season (fall), which coincides with a decrease in the air temperature. During the winter, when temperatures are low and stable, cold hardiness remains steady. De-acclimation begins when the temperature rises at the end of winter/early spring (Ferguson et al., 2011). The injuries caused by frost and freezes on grapes are well-documented (Fennell, 2004; Goffinet, 2001; Wample et al., 2001; Davenport et al., 2008); however, there are differences among cultivars in terms of their cold hardiness (Clark et al., 1996; Fennell, 2004; Wolfe, 2001; Mills et al., 2006; Davenport, 2008; Ferguson et al., 2011; Ferguson et al., 2014). Cultural practices such as crop load except for the regions where the plants can not complete their development before the start of frost and plant nutrient status have no significant effect on the cold hardiness of grapes (Davenport, 2008). The temperature at which 50% of the organ or sample tissue is injured due to freeze is called LT_{50} (Ferguson et al., 2011); the prediction of cold hardiness is based primarily on the measured LT_{50} of the dormant buds of multiple grape cultivars (Ferguson et al., 2011).

The impact of high wind speeds on grapevine growth and yield is well-documented (Takahashi et al., 1976; Freeman et al., 1982; Hamilton, 1988; Jackson, 2008; Keller, 2010), but no comprehensive index has been developed using wind speed as a supplemental tool for viticultural zoning. Previous studies have indicated that strong winds can cause physical damage to grapevines (Hamilton, 1988); wind speed impacts evapotranspiration due to its impact on stomatal resistance (Dry et al., 1990; Campbell-Clause, 1998; Tarara et al., 2005; Keller, 2010) and boundary layer thickness (Keller, 2010). Jackson (2008) discussed the impact of wind velocity on the heating of grape berries, canopy water deficiency, irrigation systems, soil erosion, disease dispersion, physical damage to vines, shoot length, leaf size, stomatal density, number of clusters per vine, ripening, and the solubility of solids. The impact of wind is increased by the number of wind perturbations (Keller, 2010; Tarara et al., 2005; Williams et al., 1994); Gladstones (1992) reported two types of damage resulting from strong winds: 1) injury caused by strong winds in spring and early summer that mainly affects young and tender growth; and 2) injury caused by hot, dry winds in summer that damages the vines, and leads to imperfect ripening and the collapse of berries.

The Winkler index (WI) (Winkler et al., 1974; Jones et al., 2010), more commonly recognized as growing degree days (GDD) are the degree day units accumulated during the growing season with a base temperature of 10°C. This required heat load (GDD) is a function of grapevine variety; therefore, the reported minimum value and optimal range of the GDD can vary. In our sudy GDD was computed based on a fixed growing season from April to October in order to enable further comparisions with other grape producing regions. The Huglin Index (HI) (Huglin, 1978) combines the air temperature during the active period of vegetative growth with a coefficient of day length that varies according to the latitude (Appendix A). It provides valuable information on the local heat summations by considering the average and maximum temperatures and weighting the accumulated temperatures to the daytime period. Huglin and Schneider (1998) classified grape varieties based on HI. Growing Season Temperature (GST) (Jones, 2005a) is the average temperature of the growing season from April to October. Biologically effective degree days (BEDD or E°) (Gladstones, 1992) account for heat accumulations that are defined by upper and lower temperature thresholds (between 10 °C to 19 °C); BEDD formulation also adjusts the heat accumulation for diurnal range adjustments (Appendix A). Gladstones (1992) applied BEDD to define corresponding maturity groupings of various grape cultivars (Table 4.1.).

Table 4. 1. Wine grape maturity groupings and corresponding BEDD to ripeness (Gladstones, 1992).

	Red	White or Rose
Group 1 1050 day°	-	Madeline, Madeline-sylvaner
Group 2 1100 day°	Blue Portuguese	Chasselas, Muller-Thurgau, Siegerrebe, Bacchus, Pinot Gris, Muscat Ottonel, Red Veltliner, Pinot Noir, Meunier
Group 3 1150 day°	Pinot Noir, Meunier, Gamay, Dolcetto, Bastardo, Tinta Carvalha, Tinta Amarella	Traminer, Sylvaner, Scheurebe, Elbling, Morio-Muskat, Kerner, Green Veltliner, Chardonnay, Aligote, Melon, Sauvignon, Blanc, Frontignac, Pedro ximenes, Verdelho, Sultana
Group 4 **1200 day°**	Malbec, Durif, Zinfandel, Schiava (=Trollinger), Temranillo, Tinta Maderia, Pinotage	Semillon, Muscadelle, Riesling, Welschriesling, Furmint, Leanyka, Harslevelu, Sercial, Malvasia Bianica, Carbernet Franc
Group 5 1250 day°	Merlot, Carbernet Franc, Shiraz, Cinsaut, Barbera, Sangiovese, Touriga	Chenin Blanc, Folle Blanche, Crouchen, Rousanne, Masanne, Viognier, Taminga, Carbernet Sauvignon
Group 6 1300 day°	Cabernet sauvignon, Ruby Cabernet, Mondeuse, Tannat, Kadarka, Corvina, Nebbiolo, Ramisco, Alvarelhao, Mourisco Tinto, Valdiguie	Colombard, Palomino, Dona Branca, Rabigato, Grenache
Group 7 1350 day°	Aramon, Petit Verdot, Mataro, Carignan, Grenache, Freisa, Negrara, Grignolino, Souzao, Graciano, Monastrell	Muscat Gordo Blanco, Trebiano, Montils
Group 8 1400 day°	Tarrango, Terret Noir	Clairette, Grenache Blanc, Doradillo, Biancone

The Huglin Index (HI) and biologically effective degree days (BEDD) use a coefficient (k) to represent the changes in day length imposed by latitude (Appendix A). The increase in day length during the growing season occurs in concurrence with an increase in latitude. A clear definition of k is absent; however, Huglin (1978) categorized k based on the latitudes between 40° and 50° to five classes where k had a range of 1.02 to 1.06. The k for latitudes lower or equal to 40° was reported to be 1 (Huglin, 1978; Tonietto and Carbonneau, 2004; KNMI, 2013). Mean thermal amplitude (MTA) (Mullins et al., 1992; Ramos et al., 2008) is the difference between the minimum and maximum temperature in September, and is associated with grape quality and composition (Montes et al., 2012). However, it should be noted that it should be adjusted based on phenology rather than calender. The latitude temperature index (LTI) (Jackson and Cherry, 1988) is the result of multiplying the mean temperature of the warmest month by (60 minus the latitude).

The Growing Season Precipitation index (GSP) (Blanco-Ward et al., 2007) provides the general suitability used in climate zoning for viticulture that accumulates precipitation during the growing season (Appendix A). However, the GSP is only relevant for regions where grapes are normally not irrigated. The hydrothermic index (HyI) (Branas, 1974) combines the effect of air humidity and temperature using precipitation as a surrogate during the growing season, to assess the risk of grapevine exposure to certain diseases such as downy mildew. The Dryness Index (DI) (Riou et al., 1994; Tonietto and Carbonneau, 2004) indicates the presence of drought conditions and the intensity of a drought. This index takes into account the evaporative demands of the vines, bare soil evaporation, and precipitation. The DI also provides an indication of potential soil water availability and the level of regional dryness. The determination of DI can be challenging due to a lack of proper data on the irrigation and evapotranspiration of a region, as well as difficulties in modeling them. Both HyI and DI are measures that capture moisture surplus and deficiencies, and both have been used in viticulture zoning studies (Blanco-Ward et al., 2007).

The composite index (CompI) (Malheiro et al., 2010; Santos et al., 2012b) combines the HI, DI, minimum temperature, and HyI. Malheiro et al. (2010) reported the CompI as the ratio of years which simultaneously verify that HI $\geq$ 1400°C, DI $\geq$ -100 mm, HyI $\leq$ 5100°Cmm and Min. Temp. Always > -17°C. CompI has a range between 0 and 1, and is binomial and dimensionless. It depicts the fraction of "optimal years" for growing grapevines in a selected region within a selected timeframe (Malheiro et al., 2010). Santos et al. (2012b) modified this index in order to capture the actual distribution of the viticultureal regions in Europe. They claimed that the HyI was too restrictive and resulted in unrealistic CompI values for some of the more well-established viticultural regions in Europe. Santos et al. (2012b) eliminated HyI from the CompI calculations and defined the modified CompI as the ratio of the years which simultaneously verify HI ≥ 1200°C, DI ≥ -100 mm and Min. Temp. > -17°C. In our study, the majority of bio-climatic indices discussed in this section were computed for a period of 30 years, except the DI (Appendix A). Since CompI requires DI as one of its inputs, this index was not computed either.

Bio-climatic zoning of grape-growing regions

Climatic zones outside the U.S.

Several studies have investigated the use of bio-climatic indices to classify potential grapevine growing regions. Jackson and Cherry (1988) calculated and compared 14 bio-climatic indices for 78 locations in Europe, North America, Australia, and New Zealand to determine the most useful index among those proposed for the classification of grape-growing regions. They reported LTI and HI to be the best indices for differentiation of grape-growing regions, based on the information provided on the heat requirements of different cultivars. Their climate dataset was obtained via weather stations; thus, their temporal and spatial resolutions were not optimal. Tonietto and Carbonneau (2004) undertook a climatic classification that combined HI, CI, and DI, and found that HI and CI are able to describe most of the variability within the climatic zones of grape-producing regions around the world. However, they used World Meteorological Organization (WMO) stations that were located near each grape-producing region; therefore, their weather dataset was based on the point measurements provided by the weather stations and did not spatially cover the study area. Jones et al. (2009) also determined the climatic indices for grape-growing regions worldwide; they used several bio-climatic indices, including HI, CI, DI, BEDD, and GST. They Utilized WorldClim (WorldClim, 2009) 1km resolution for the period from 1950-2000, and the temporal resolution of the data was obtained monthly. Jones et al. (2009) recommended use of climate grids with a finer spatial resolution and recent weather data to update bio-climatic indices. With an improved climate structure, the variability and change of suitability can be monitored more accurately and efficiently (Jones et al., 2009). Santos et al. (2012b) provided a macro-climate and classification analysis for grape-growing regions in Europe. They used the E-OBS gridded daily temperature and precipitation dataset of a period of 59 years (1950-2009) for the European continent, and calculated the GSS, GSP, Min. Temp., CI, WI, HI, DI, HyI, and CompI in order to determine any potential trends in the individual indices. They identified significant trends in WI and HI, and using a canonical correlation analysis, demonstrated that the observed inter-annual variability of the HI was strongly controlled by large-scale atmospheric circulations during the growing season. Santos et al. (2012b) also analyzed the inter-annual variability and long-term trends in the bio-climatic indices, and updated the bio-climatic indices using high-resolution datasets for Europe.

Hall and Jones (2010) calculated GST, GDD, HI, and BEDD for Australian wine grape growing regions from 1971-2000 and they found that the knowledge of climate dynamics helps to better undrestand the cultivar suitability within each region. Anderson et al. (2012) used daily historical data from weather stations (1971-2000) to calculate bio-climatic indices such as GST, WI, HI, and BEDD, and then interpolated the indices to a spatial grid with a 500 m resolution. They found that elevation plays an important role in determining the climate suitability of a particular region for grape production. They argued that GST and WI functionally capture the same information, and that HI is most capable of representing the actual structure of suitable regions for grape production in New Zealand. However, they suggested the need for within-region assessment of potentially suitable areas in future studies. Montes et al. (2012) used CI, DI, HI, and MTA for a multi-criteria climate classification of seven Chilean viticultural valleys represented by 54 different weather stations. They reported that the CI index did not accurately represent climate variation in Chile and had a lack of discriminating capacity. Montes et al. (2012) found a similar spatial trend for MTA and HI, and concluded that MTA was a suitable index for characterizing the thermal regime in Chile. Conceição and Tonietto (2005) evaluated the climate potential of three regions in Brazil by calculating the HI, CI, and DI using average historical meteorological data obtained from weather stations in those areas.

Climatic zones in the U.S.

The most suitable climatic zones for viticulture in California were first classified and formulated by Amerine and Winkler (1944) and Winkler et al. (1974). It was later updated for the western U.S. by Jones et al. (2010) using the PRISM (Parameter Elevation Relationships on Independent Slopes Model) (Daly et al., 2008) for the period from 1971 to 2000, using a spatial resolution of 15 arc-seconds (400 m) and a monthly temporal resolution. They calculated four bio-climatic indices: GDD, HI, BEDD, and GST; in addition, Jones et al. (2010) emphasized the importance of updating the long-term wather data for the calculation of bio-climatic indices and recommended further research on this issue. Yau (2011) computed GDD, LTI, and FFD using the PRISM monthly dataset for the PNW region. Yau et al. (2013) used principle component analysis (PCA) to determine the dominant factors influencing the AVAs in the PNW region, and found that the combination of elevation, GDD, FFD and precipitation were the most important. One Yau et al. (2013) conclusions was that the climate component of AVAs is the most difficult to obtain and analyze, implying that any research capable of providing an improved climate component would enable the advancement of characterization of AVAs in the PNW region.

The goal of our study was to determine the critical bio-climatic indices for the AVAs located in the State of Washington and parts of Oregon, and to evaluate the performance of new indices based on the cold hardiness dynamics of grapes, minimum temperature, and wind speed thresholds.

Materials and Methods

American Viticultural Areas (AVAs)

Officially recognized appellations that allow vintners and consumers to attribute wine characteristics to the specific geographic origin of its grapes are called American Viticultural Areas (AVAs) (Yau et al., 2013; TTB, 2015). AVAs are acknowledged by the Alcohol and Tobacco Tax and Trade Bureau (TTB), and it is the U.S. Department of the Treasury that allows vintners to describe the origin of their wine to consumers (TTB, 2015). AVAs also impact the price of the grapes and the wines produced from these grapes for the various appellations (Yau et al., 2013). A total of 14 AVAs have been established in the State of Washington, eastern and north-central Oregon (Table 4.2.; Figure 4.1.); the Columbia Valley is the largest, covering an area of 4,597,090 ha. Yakima Valley was the first AVA to be federally recognized in Washington in 1983 (WSW, 2015). The most recent AVA to be federally recognized was Oregon’s Rocks District of Milton-Freewater in 2015, which is enclosed by the Walla Walla AVA.

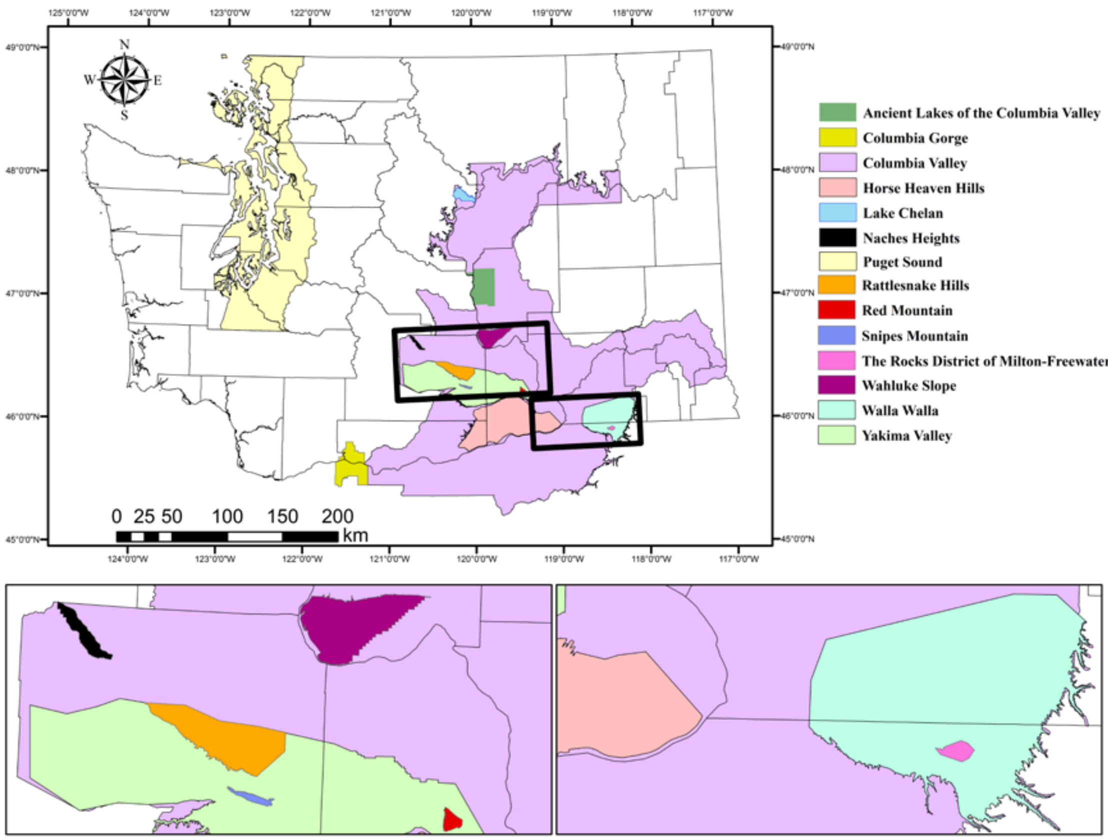

Figure 4.1. Geographic locations of the Washington-Oregon American Viticultural Areas (AVAs).

Several of the AVAs are shared among Washington, eastern and north-central Oregon (Figure 4.1.). The study area was, therefore, expanded to include parts of Oregon in order to calculate the bio-climatic indices for all the shared AVAs. The latitude ranged from 45.25° N to 49° N and the longitude ranged from 116.8° W to 124.78° W. The total area under grape cultivation in Washington was 27,186 ha based on the USDA published statistics for 2012 and it is expanding annually (USDA-NASS, 2015).

Table 4.2. List of American Viticultural Areas (AVAs) located in the State of Washington and/or Oregon and some of their properties.

AVA	State(s)	Area (ha)	Elevation (m) Min.	Max.	Mean	AVA Recognition Year
Columbia Valley	Washington-Oregon	4,597,090	20	1442	451	1984
Puget Sound	Washington	1,179,606	0	1046	109	1995
Yakima Valley	Washington	289,775	128	1099	339	1983
Horse Heaven Hills	Washington	233160	81	671	321	2005
Walla Walla	Washington-Oregon	129059	122	696	315	1984
Ancient Lakes of the Columbia Valley	Washington	68607	173	583	377	2012
Columbia Gorge	Washington-Oregon	48431	23	840	377	2004
Wahluke slope	Washington	32631	122	504	251	2005
Rattle Snake Hills	Washington	29934	258	922	434	2006
Lake Chelan	Washington	13291	278	1152	445	2009
Naches Heights	Washington	5315	359	647	543	2012
Red Mountain	Washington	1837	167	429	228	2001
Snipes Mountain	Washington	1585	224	399	280	2009
The Rocks District of Milton-Freewater	Oregon	1483	241	307	278	2015

Weather Data

We used weather data obtained from the University of Idaho's Gridded Surface Meteorological Data (UI GSM, 2015). The UI GSM (Abatzoglou, 2011) employs the spatial attributes of the Parameter-elevation Regression on Independent Slopes Model (PRISM, Daly et al., 2008), with temporal attributes of regional-scale reanalysis and daily gauge-based precipitation from the North American Land Data Assimilation System Phase 2 (NLDAS-2; Mitchell et al., 2004). The dataset has a spatial resolution of 4 km for the contiguous United States and a daily temporal resolution. The UI GSM is evaluated by (Abatzoglou, 2011) comparing the dataset with the observed data recorded by the weather station networks such as RAWS (RAWS, 2011), AgriMet (AgriMet, 2011), AgWeatherNet (AgWeatherNet, 2011) and USHCN-2 (USHCN, 2011).

The daily minimum and maximum air temperatures of the dataset have a reported median error of 1.7°C to 2.3°C, and the median correlations of the daily maximum and minimum air temperatures is reported to be 0.94 – 0.95 and 0.87 – 0.90, respectively (Abatzoglou, 2011). For the wind speed, a median correlation of 0.54 and 0.68 was reported during the cold season (Oct-Apr) and a correlation of 0.52 and 0.62 for the warm season (May-Sept), revealing an overestimation ranging from 5% to 30% (Abatzoglou, 2011).Still, the dataset has great potential for landscape-scale modeling in areas where there is a limited amount of comprehensive, long-term, daily historical weather data (Abatzoglou, 2011).

In our study, the bio-climatic indices were calculated using several variables obtained from the UI GSM, which covered a period of 30 years (1983-2012). The variables included precipitation, temperature, and wind velocity at 10 m above ground. The initial resolution was 4 km, and was downscaled to a spatial resolution of 482 m using a bi-linear interpolation algorithm (MATLAB 2014a); the indices were developed for the period between 1983 and 2012 (MATLAB, 2014a). For our study, the day length/latitude coefficient (k) required for obtaining HI and BEDD was calculated by applying a linear interpolation to the previously reported k for each region (this interpolation modified k based on linear changes in latitude). The k was linearly increased from 1.03 to 1.06 by changing the latitude from 44° to 50°.

The bio-climatic indices for each AVA were extracted using ArcGIS v.10 (ESRI, 2015) based on the AVA boundaries. All the shapefiles, except for the Rocks District of Milton-Freewater, were obtained courtesy of the Davenport Lab, Washington State University Irrigated Agriculture and Research and Extension Center, Prosser, WA, U.S.A. The computed bio-climatic indices were statistically compared among AVAs to detect significant differences at the 95% confidence level. The statistical analysis was conducted to compare the mean values using the analysis of variance (ANOVA) test with SAS v.9.4. (SAS, 2015). It should be noted that the AVAs differed in area and number of pixels, and were also not independent, as Columbia Valley encompasses most of the AVAs located in Eastern Washington (Figure 4.1.). However, use of statistical techniques can assist with further categorizing these AVAs and obtain more profound insight into how each AVA compares with the others.

Cold Damage Index (CDI)

The cold hardiness ($H_{c,i}$) for day *i* is computed based on the cold hardiness of the previous day ($H_{c,i-1}$) plus the changes in the cold hardiness (ΔH_c) over the course of a single day (Equation 4.1.). The cold hardiness was computed for a hypothetical cultivar to ensure that the most sensitive cultivars have been taken in to account.

$$H_{c,i} = H_{c,i-1} + \Delta H_c \qquad (4.1.)$$

The changes in cold hardiness (ΔH_c) were computed as follows:

$$\Delta H_c = (DD_c \times k_a \times c_{log,a}) + (DD_h \times k_d \times c_{log,d}) \qquad (4.2.)$$

Where k_a is the constant for acclimation rate, k_d is the constant for de-acclimation rate, $c_{log,a}$ is the dimensionless logistic component for acclimation, $c_{log,d}$ is the de-acclimation logistic component, DD_c represents the chilling degree days, and DD_h the heating degree days (Ferguson et al., 2011; Ferguson et al., 2014). The initial cold hardiness ($H_{c,initial}$) was modified to -3 °C, which is the reported hardiness of green tissue (Fennell, 2004).

The Cold Damage Index (CDI) was developed to evaluate the minimum daily temperature in a specific location with respect to the predicted LT_{50} for that location. The index utilizes a predicted LT_{50} to count the number of events that occur when the daily minimum temperature falls below the LT_{50} threshold. Hence, the CDI compares the minimum daily temperature with the predicted LT_{50} for a given day. If the minimum temperature falls below the threshold, it is counted as one event. Consequently, the number of events can be counted for each month, and the total number of incidents per year can then be summed up to calculate the annual CDI. Depending on the availability of long-term weather data, CDI can be computed for several years. It is also possible to sum up the CDI for periods of 5, 10, 20, and 30 years, and then discuss the probability of the occurrence of critical low temperatures in a region based on the results. In fact, CDI could be computed for 30 years, and then used to calculate the CDI for 100 years.

Dynamic Minimum Temperature Index (DyMin.Temp.)

The Dynamic Minimum Temperature index (DyMin.Temp.) was created as a modification of the Min.Temp. (Appendix A). By comparing the daily minimum temperatures with the dynamic low threshold for each month, grapevines' various levels of sensitivity to low temperatures (during both the growing season and winter) can be monitored for each location. The DyMin.Temp. compares daily low air temperatures with the assigned threshold for a particular month (T_t); consequently, it returns the number of events (days) that the temperature fell below a certain threshold during a particular month. The total number of incidents occurring in a single month ranges from 0 ("no events") to n = the number of days in a particular month; ultimately, leading to determination of the total number of incidents occurring within a specific month. Depending on the availability of a given region's long-term weather data, the total number of events recorded for each month must then be averaged for each year of the study. The (DyMin.Temp.) was ultimately obtained by summing up the average number of events that occurred within each individual month for a specific12-month period (Equation 4.3.).

$$T_{Dynamic\ min} = \sum_{m=Jan}^{Dec} \bar{e}_m \qquad (4.3.)$$

where $T_{Dynamic\ min}$ is the dynamic minimum temperature and $\bar{e}_m$ is the average number of events in the month denoted by m (Equation 4.4.).

$$\bar{e}_m = \frac{1}{n}\sum_{1983}^{2012} e_{T,y,m} \qquad (4.4.)$$

Where n is the number of years and $e_{T,y,m}$ is the number of events occurring within a specified year and month, as denoted by *y* and *m*, respectively (Equation 4.5.).

$$e_{T,y,m} = \sum_{d=1}^{eom\,(y,m)} cond_T(T_{min,y,m,d}, T_{th,m}) \qquad (4.5)$$

where *eom(y,m)*(end of month) returns the number of days in a given month and year, represented by *m* and *y*, $T_{min,y,m,d}$ is the minimum temperature for a specific day, $T_{th,m}$ is the temperature threshold for a chosen month (the thresholds were as follows: Jan and Dec= -10 °C; Oct, Nov, and Feb = -5 °C, Mar = -3 °C, and Apr-Sept = 0 °C) , and $cond_T\,(T_{min,y,m,d}, T_{th,m})$ is defined as follows (Equation 4.6.):

$$cond_T\left(T_{min,y,m,d}, T_{th,m}\right) = \begin{cases} 1 & T_{min,y,m,d} < T_{th,m} \\ 0 & otherwise \end{cases} \qquad (4.6.)$$

Wind Speed Index (WSI)

Wind speed index (WSI) was developed to help address the impact of wind speed on viticultural zoning. The WSI initially takes into account the 10 m daily average wind velocity ($\bar{U}_{y,m,d}$); WSI essentially uses the same procedure as described for the Dynamic Minimum Temperature, but uses $e_{T,y,m}$ instead of $e_{w,y,m}$(Equation 4.7.).

$$e_{T,y,m} = \sum_{d=1}^{eom\,(y,m)} cond_w(\bar{U}\mathbf{y}, \mathbf{m}, \mathbf{d}, U_{th}) \qquad (4.7.)$$

where $\bar{U}_{y,m,d}$ is the average wind velocity for the specified day, U_{th} is the wind velocity threshold, and the $cond_w\,(\bar{U}\mathbf{y}, \mathbf{m}, \mathbf{d}, U_{th})$ is obtained as follows (Equation 4.8.):

$$cond_w(\bar{U}y, m, d, U_{th}) = \begin{cases} 1 & \bar{U}y, m, d > U_{th} \\ 0 & otherwise \end{cases} \qquad (4.8.)$$

The $\bar{U}_{th}$ used in our study was 4 m/s (Freeman et al., 1982; Hamilton, 1989; Hunter and Bonnardot, 2011). Since the daily wind velocities obtained from the UI GSM were based on 10 m wind speeds, the logarithmic wind profile conversion equation was used to convert the threshold to a 2 m wind velocity (Allen et al., 1998).

Precipitation

Spatio-temporal analysis of the precipitation used in our study was divided into two groups: 1) refers to precipitation during the growing season (Growing Season Precipitation (GSP)) (Blanco-Ward et al., 2007); and 2) Out of Growing Season Precipitation (OutGSP). The motivation for dividing precipitation into two different groups was to obtain a better understanding of local water availability prior to the start of a new growing season. This knowledge can help decision-makers, extension specialists, and growers gain more insight into the need for irrigation of grapes in specific regions. For each AVA, the total precipitation was calculated and the percentage of precipitation was also obtained. Out of growing season precipitation is a particularly useful index as it can potentially indicate the amount of water available for filling the soil profile prior to the start of a new growing season.

Results and Discussion

Bio-climatic indices

Growing Degree Days (GDD)

The calculated Growing Degree Days (GDD) indicated that Puget Sound had the lowest accumulated thermal units (948°C GDD), while Wahluke Slope had the highest GDD (1662°C GDD). The multiple comparisons of GDDs among AVAs indicated that there was no significant difference in the GDD with a 95% confidence level between Wahluke Slope and The Rocks

District of Milton-Freewater. There were also no substantial differences noted between Red Mountain and Snipes Mountain, or Horse Heaven Hills and Walla Walla with a 95% confidence level (Table 4.3.; Appendix B). The results show that the AVAs used in our study were primarily categorized (Jackson, 2008) based on their GDD in the region I (≤1390) and region II (1391-1670). Jones et al. (2010) also reported that most of the regions in Washington are categorized as region I, and the Columbia Valley (Oregon) is categorized as region II (Figure 4.2.). The higher the heat unit accumulation in a region, the greater the ability to ripen grapes, especially cultivars that mature late in the growing season (Wolfe, 1999). Our results also confirm previous reports on New Zealand (Anderson et al., 2012) and the western U.S. (Jones et al., 2010).

Table 4. 3. Mean GDD calculated for each AVA in this study (1983-2012).

AVA	Mean GDD	Region[a]
Puget Sound	948	I
Columbia Gorge	1089	I
Naches Heights	1189	I
Lake Chelan	1329	I
Rattle Snake Hills	1386	I
Columbia Valley	1414	II
Yakima Valley	1488	II
Ancient Lakes	1525	II
Walla Walla	1566	II
Horse Heaven Hills	1566	II
Red Mountain	1622	II
Snipes Mountain	1624	II
The Rocks District of Milton-Freewater	1649	II
Wahluke Slope	1662	II

[a] The classification only pertains to this index.

Biologically Effective Degree Days (BEDD)

Biologically Effective Degree Days (BEDD) were also computed for each AVA. Puget Sound had the lowest BEDD (318 °C BEDD), while the highest BEDD was obtained for Snipes Mountain (1590°C BEDD) (Table 4.4.; Appendix B). Jones et al. (2010) recommended a classification of grape-growing regions based on BEDD, and suggested that if BEDD is below 1000 then the region is too cold for grapes; however, five AVAs within our study area have BEDDs lower than 1000, including: Puget Sound, Lake Chelan, Columbia Gorge, The Rocks District of Milton-Freewater, and Ancient Lakes of the Columbia Valley. The rest of the classes start at 1000 BEDD, with a range of 200 BEDD for each class (Table 4.4.). Gladstones (1992) reported the wine grape maturity groupings and their corresponding BEDD to ripeness for making dry or semi-sweet table wines (Table 4.1.). Among our chosen AVAs, only Snipes Mountain matches Group 8, for which cultivars such as 'Tarrango', 'Terret Noir', 'Clairette', 'Grenache Blanc', 'Doradillo', 'Biancone' are recommended (Figure 4.2.; Table 4.4.).

Table 4. 4. The average BEDD calculated for several AVAs in Washington and Oregon.

AVA	BEDD	Classification[a]	Maturity Group (Gladstones 1992)
Puget Sound	318	Too cold	-
Lake Chelan	838	Too cold	-
Columbia Gorge	941	Too cold	-
The Rocks District of Milton-Freewater	969	Too cold	-
Ancient Lakes of the Columbia Valley	976	Too cold	-
Columbia Valley	1086	1	Group 1
Walla Walla	1108	1	Group 2
Wahluke Slope	1129	1	Group 2
Horse Heaven Hills	1160	1	Group 3
Red Mountain	1208	2	Group 4
Naches Heights	1221	2	Group 4
Rattle Snake Hills	1286	2	Group5
Yakima Valley	1339	2	Group 6
Snipes Mountain	1590	3	Group 8

[a] The classification only pertains to this index (based on Jones et al., 2010)

Huglin Index (HI)

The calculated Huglin Index (HI) calculated for our study indicated that, among the chosen AVAs, Puget Sound has the lowest HI (1452) and Snipes Mountain the highest HI (2425) (Table 4.5.). The different values of HI found indicate that there is a significant difference at the 95% confidence interval for some AVAs; however, no such differences were observed for the following pairs: Ancient Lakes of the Columbia Valley and Yakima Valley, Horse Heaven Hills and Walla Walla, Columbia Valley and Rattle Snake Hills (Appendix A). We next categorized the AVAs based on their HI (Jones et al., 2010) (Table 4.5.), the accepted classification stating that HI values below 1200 are too cold for grapes. The classes start at 1200, each comprising 300 units. The first class of HI (1200-1500) is termed "very cool" the second is "cool" (1500-1800), the third is "temperate" (1800-2100), the fourth is "warm temperate" (2100-2400), and the fifth is "warm" (2400-2700). Our results indicated that the majority of AVAs in the study area are located in a "warm temperate" region (class 4), based on their HI (Figure 4.2.).

Table 4. 5. The calculated HI for AVAs in Washington and Oregon.

AVA	HI	Classification[a]
Puget Sound	1452	Very cool
Columbia Gorge	1740	Cool
Naches Heights	1931	Temperate
Lake Chelan	2019	Temperate
Columbia Valley	2124	Warm temperate
Rattle Snake Hills	2138	Warm temperate
Yakima Valley	2248	Warm temperate
Ancient Lakes of the Columbia Valley	2248	Warm temperate
Walla Walla	2274	Warm temperate
Horse Heaven Hills	2289	Warm temperate
The Rocks District of Milton-Freewater	2332	Warm temperate
Red Mountain	2362	Warm temperate
Wahluke Slope	2397	Warm temperate
Snipes Mountain	2425	Warm

[a] The classification only pertains to this index.

Growing Season Temperature (GST)

The GST for all the AVAs was greater than 13.7°C: Puget Sound had the lowest GST (13.7°C) and the Rocks District of Milton-Freewater had the highest GST (16.9°C) (Table 4.6.; Appendix B). Comparison of the mean GST for each AVA revealed that there is a substantial difference in GST among the AVAs, except for Red Mountain and Snipes Mountain, the Rocks District of Milton-Freewater, and Wahluke Slope, which have only slight differences at the 95% confidence level.

Table 4.6. Mean GST calculated for each AVA from 1983-2012, and some examples of the possible grape cultivar matches for each climate maturity grouping.

AVA	Mean GST	Climate Maturity grouping	Example of recommended grape cultivars
Puget Sound	13.7	Cool(1)	Riesling, Muller-Thurgau, Pinot Gris, Gewurztraminer, Pinot Noir, Chardonnay, Sauvignon Blanc
Columbia Gorge	14.0	Cool (1)	
Naches Heights	14.4	Cool (1)	
Lake Chelan	15.1	Intermediate(2)	Riesling,Pinot Gris, Gewurztraminer, Pinot Noir, Chardonnay,Sauvignon Blanc,Semillon, Cabernet Franc, Tempranillo, Merlot, Malbec,Syrah, Viognier, Dolcetto, Cabernet Sauvignon
Rattle Snake Hills	15.5	Intermediate (2)	
Columbia Valley	15.6	Intermediate (2)	
Yakima Valley	16.0	Intermediate (2)	
Ancient Lakes of the Columbia Valley	16.2	Intermediate (2)	
Horse Heaven Hills	16.4	Intermediate (2)	
Walla Walla	16.5	Intermediate (2)	
Red Mountain	16.7	Intermediate (2)	
Snipes Mountain	16.7	Intermediate (2)	
Wahluke Slope	16.9	Intermediate (2)	
The Rocks District of Milton-Freewater	16.9	Intermediate (2)	

Additional classifications have been made based on the average GST as a means of determining grape maturity groupings and cultivars (Jones, 2007; Jones et al., 2010; Yau, 2011). These groupings begin to form average GSTs at 13°C and end at 24°C. There are four major maturity groups within this range: 1) the cool climate maturity group ranges from 13°C to 15°C; 2) the intermediate climate maturity group ranges from 15°C to 17°C; 3) the warm climate maturity group ranges from 17°C to 19°C; and 4) the hot climate maturity group ranges from 19°C to 24°C. Based on the GST calculated for each AVA in our study, they can be categorized as belonging in either climate maturity group one or climate maturity group two (Figure 4.2.; Table 4.6.). There are also several cultivars associated with these climate maturity groupings (Jones, 2007; Yau, 2011); use of the GST can help us to better distinguish the climate maturity groupings for AVAs, therefore enabling us to provide better cultivar recommendations for each specific climate maturity grouping (Figure 4.2.; Table 4.6.).

Latitude Temperature Index (LTI)

The Latitude Temperature Index (LTI) was computed for all the AVAs, and it was determined that Puget Sound had the lowest LTI (223.2) and the Rocks District of Milton-Freewater had the highest LTI (336.9) (Table 4.7.). Interestingly, because this index takes into account the latitude of each location, the LTI was significantly different (Figure 4.2.; Appendix B) for all of the AVAs except for Walla Walla and Horse Heaven Hills, due to the fact that they are located within nearly the same latitude range (45.6° N to 46.2° N).

Table 4.7. Calculated LTI for a period of 30 years for AVAs in Washington and parts of Oregon. Grouping based on AVA LTIs was also conducted, based on the grouping recommendations from Jackson and Cherry (1988).

AVA	LTI	LTI group	Example of cultivars
Puget Sound	223.2	B	Riesling, Pinot Noir and Chardonnay
Lake Chelan	269.3	B	
Naches Heights	281.3	C	Cabernet Sauvignon, Cabernet Franc, Merlot, Malbec, Sauvignon Blanc, and Semillion
Columbia Gorge	285.3	C	
Ancient Lakes	299.3	C	
Rattle Snake Hills	301.8	C	
Columbia Valley	304.4	C	
Yakima Valley	312.0	C	
Wahluke Slope	319.4	C	
Snipes Mountain	322.3	C	
Red Mountain	324.8	C	
Horse Heaven Hills	328.3	C	
Walla Walla	328.6	C	
The Rocks District of Milton-Freewater	336.9	C	

[a] LTI grouping does not correspond to groupings in other indices.

Yau (2011) also calculated the LTI for AVAs in our study area, and a comparison between the two sets of results shows that the AVA rankings were nearly the same for both studies. Although the LTIs calculated for our study were generally slightly higher than those reported by Yau (2011). Jackson and Cherry (1988) reported an LTI grouping based on the cultivars grown in each group; the four main groups are as follows: 1) group A with LTI < 196; 2) group B with an LTI ranging from 200 to 275; 3) group C with an LTI ranging from 275 to 370; and 4) group D with an LTI> 370. The results of our study have indicated that the majority of AVAs in Washington and Oregon are within group C, except for Puget Sound and Lake Chelan (Table 4.7.). Jackson and Cherry (1988) reported the favored cultivars for group B to be ‘Riesling’, ‘Pinot Noir’, and ‘Chardonnay’, and the favored cultivars for group C were reported to be ‘Cabernet Sauvignon’, ‘Cabernet Franc’, ‘Merlot’, ‘Malbec’, ‘Sauvignon Blanc’, and

‘Semillion’. This classification can thus be used as a tool for assisting in the selection of cultivars based on their LTI groupings.

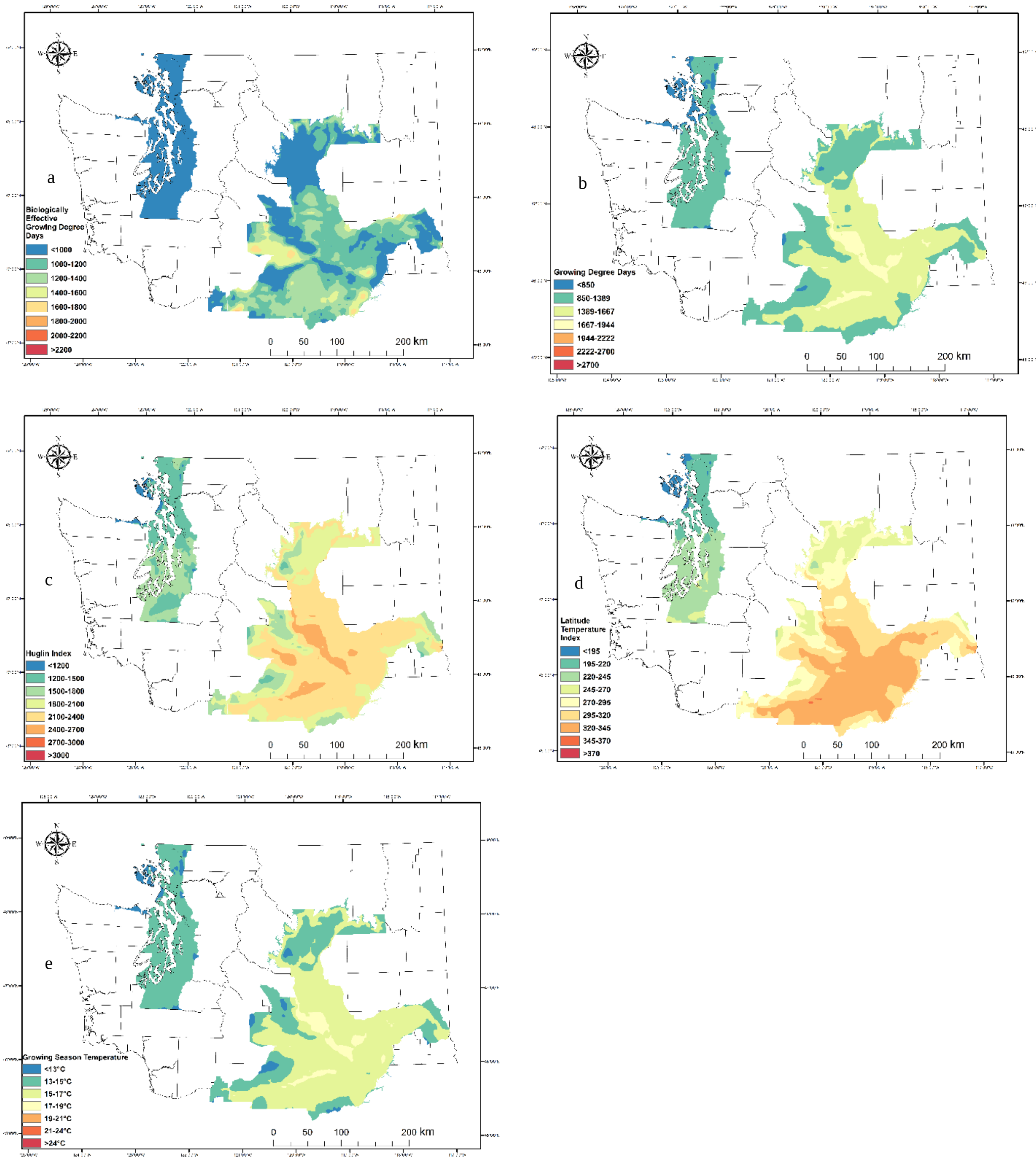

Figure 4.2. Key bio-climatic indices primarily dealing with thermal heat unit accumulation for AVAs located in the State of Washington and parts of Oregon. Class limits in legends are not directly comparable. Biologically Effective Growing Degree Days (a); Growing Degree Days (b); Huglin Index(c); Latitude Temperature Index (d); Growing Season Temperature (e).

Frost Free Days (FFD)

The calculation of Frost Free Days (FFD) for each AVA revealed that Naches Heights had the lowest number of FFD (146 days) and Puget Sound had the highest number of FFD (230 days). Red Mountain and Wahluke Slope did not show a significant difference in FFD at the 95% confidence level (Appendix B), implying that the average length of growing season in these regions is similar. This information can help decision-makers select cultivars that will complete their growing cycles prior to the first freeze in fall, and start their activity after the last frost in the spring for each specific AVA.

Previous studies have indicated that a region requires a minimum FFD of 180 days to be considered optimal for grape production (Becker, 1985; Prescott, 1965; Rosenberg et al., 1983; Jackson and Cherry, 1988; Yau et al., 2013). Among our selected AVAs, Wahluke Slope, Walla Walla, the Rocks District of Milton-Freewater, and Puget Sound all had FFD ≥ 180 days. Knowledge of the ranking of AVAs based on their FFD is important for the assignment of early or late cultivars in these regions. The remaining AVAs with an FFD < 180 days have already been established, and they are still able to produce marketable grapes; however, this may be due in part to amendments such as wind machines. Still, the reported optimal growing season length for regions with a proven record of sustainable grape production should be updated based on the risks that the growers are willing to take in a region that has a higher risk of damage due to low temperature (Figure 4.3.).

Growing Season Suitability (GSS)

Growing Season Suitability (GSS) was also calculated for the AVAs in our study: Columbia Gorge had the lowest GSS (0.82) and the Rocks District of Milton-Freewater had the highest GSS (0.92) (Figure 4.3.). All the AVAs had a GSS higher than 0.8 (Table 4.8.), indicating that for 80% of the period from April to September, the air temperature is higher than 10°C. Santos et al. (2012b) reported that, because temperatures above 10°C are required for grape growth and development, a GSS higher than 90% is required for a region to be considered best suited for grape production by satisfying the heat requirement of the plants. Although, the calculated GSS for half of the AVAs in our study was lower than 90%; still, because they have a GSS ranging from 80% to 90%, they are suitable for viticulture. However, they are best suited for areas in the higher latitudes, at slightly greater elevations, with growing seasons of fewer than 180 days, where the risk of frost is higher, and that show a manifest in their climate variability (Santos et al., 2012b; Malheiro et al., 2012). Regions with lower GSS (Table 4.8.) are similar to viticultural regions in Western Europe such as Burgundy, Champagne, and the Mosel and Rhine Valleys of Germany (Santos et al., 2012b; Malheiro et al., 2012).

Table 4. 8. The range of GSS calculated and averaged over a period of 30 years (1983-2012).

AVA	GSS	Preference based on GSS[a]
Columbia Gorge	0.82	Suitable
Naches Heights	0.83	Suitable
Lake Chelan	0.86	Suitable
Puget Sound	0.86	Suitable
Rattle Snake Hills	0.87	Suitable
Columbia Valley	0.87	Suitable
Yakima Valley	0.89	Suitable
Ancient Lakes of the Columbia Valley	0.90	Most suitable
Horse Heaven Hills	0.90	Most suitable
Walla Walla	0.91	Most suitable
Wahluke Slope	0.91	Most suitable
Snipes Mountain	0.92	Most suitable
Red Mountain	0.92	Most suitable
The Rocks District of Milton-Freewater	0.92	Most suitable

[a] The classification only pertains to this index.

Length of Growing Season (LGS)

The calculated length of growing season (LGS) had a range of 164-189 days. Naches Heights had the lowest LGS (164 days) and the Rocks District of Milton-Freewater had the highest LGS (189 days). Warmer regions located at lower elevations tend to have a higher LGS compared with colder regions at higher elevations (Figure 4.3.). However, since this index is essentially implying similar concepts to those of FFD, it might be better to evaluate AVAs by checking both indices simultaneously. By comparing the LGS and FFD for all the AVAs, it was determined that some had similar LGS and FFD (Table 4.9.), while others presented substantial differences. Two main conditions arise as a result: 1) FFD > LGS: in this case, the risk of frost is low and there is a long period between the last frost in spring and the first frost in fall. However, if the selected cultivars in regions with these types of conditions do not complete their growth and development cycle within the LGS, they cannot be guaranteed to mature properly and be of optimal quality. 2) FFD < LGS: in this case (the dominant case for the majority of AVAs in our study) (Table 4.9.), the risk of frost during the growing season is higher; because of this, it is better to adjust the LGS based on the FFD. In other words, in the case of condition two, the LGS should be adjusted in order to be equal to the FFD.

Table 4. 9. Calculated Length of Growing Season (LGS) for all the AVAs and their corresponding FFD. We recommend use of an adjusted LGS to compare the LGS and FFD, and report the index with a lower value

AVA	LGS	FFD	FFD < LGS	adjusted LGS
Naches Heights	164	146	Yes ➔report FFD	146
Columbia Gorge	165	164	Yes ➔report FFD	164
Lake Chelan	169	166	Yes ➔report FFD	166
Rattle Snake Hills	174	157	Yes ➔report FFD	157
Columbia Valley	175	168	Yes ➔report FFD	168
Puget Sound	176	230	No➔ report LGS	176
Ancient Lakes of the Columbia Valley	179	171	Yes ➔report FFD	171
Yakima Valley	179	164	Yes ➔report FFD	164
Horse Heaven Hills	183	178	Yes ➔report FFD	178
Walla Walla	184	189	No➔ report LGS	184
Wahluke Slope	185	180	Yes ➔report FFD	180
Snipes Mountain	186	166	Yes ➔report FFD	166
Red Mountain	186	179	Yes ➔report FFD	179
The Rocks District of Milton-Freewater	189	203	No➔ report LGS	189

All of the AVAs in our study match condition two, except for Puget Sound, Walla Walla, and the Rocks District of Milton-Freewater (Figure 4.3.). In regions with shorter growing seasons, grapes may be unable to complete their full growth cycles, and the chilling period may prove insufficient in Puget Sound AVA. This index can be integrated with other indices to more accurately match specific cultivars with regions that have shorter growing seasons; thereby providing useful information to assist decision-makers in cultivar selection.

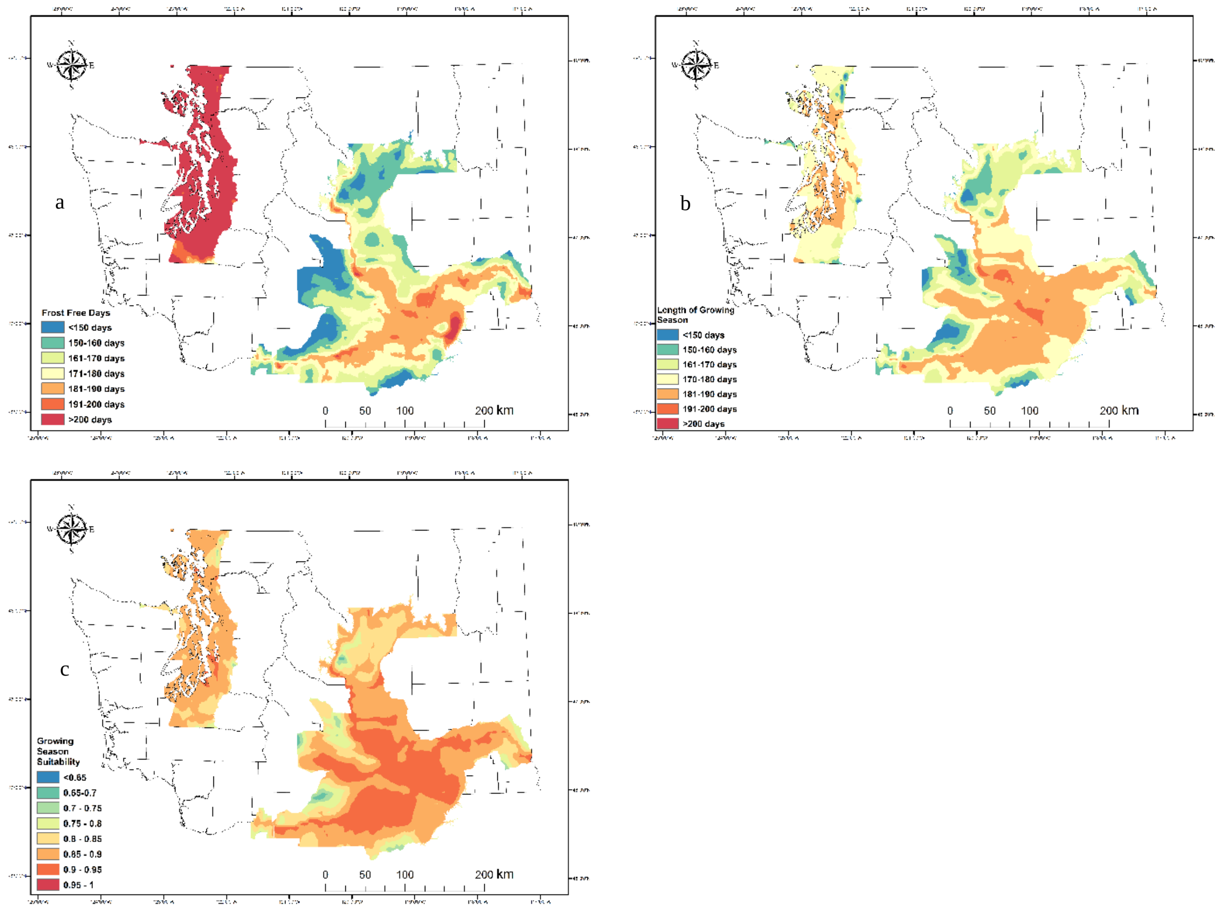

Figure 4. 3. Key bio-climatic indices focusing on the length of growing season for AVAs located in the state Washington and parts of Oregon. Class limits are not directly comparable. Frost Free Days (a); Length of Growing Season (b); Growing Season Suitability (c).

Cool Night Index (CI)

Our calculation of the cool night index (CI) indicated that Naches Heights had the lowest average CI (6.8°C) and the Rocks District of Milton-Freewater had the highest average CI (10.2°C). Comparison of the CI among all the AVAs revealed a significant difference among most of the AVAs at a 95% confidence level, except for the following AVA pairs: Ancient Lakes and Puget Sound, Horse Heaven Hills and Red Mountain, Columbia Valley and Snipes Mountain, and Yakima Valley and Lake Chelan (Appendix B; Figure 4.4.). Knowledge of regions with similar CIs can aid growers and decision-makers in the more accurate allocation of cultivars to specific regions, thus improving the quality of their produce. Based on the CI classifications discussed by Tonietto and Carbonneau (2004), all the AVAs in our study are categorized as CI+2 regions with a CI≤ 12°C. This category of viticultural climate is reported (Tonietto and Carbonneau, 2004) to have great potential for producing quality grapes when thermal heat units in the region are adequate. Lower CIs enforces lower rates of metabolism for aromatic materials and pigments during the night.

Mean Thermal Amplitude (MTA)

Mean Thermal Amplitude (MTA) calculations indicated that Puget Sound has the lowest MTA (11.4 °C) among all the AVAs and Snipes Mountain had the highest MTA (18.1 °C). Multiple comparisons of the MTA among the AVAs indicated that there is no significant difference in the MTAs of Columbia Gorge, Colombia Valley, Red Mountain, and Wahluke Slope at a 95% confidence level (Appendix B; Figure 4.4.). Ancient Lakes of the Columbia Valley, Horse Heaven Hills, and Walla Walla had no significant difference at 95% confidence level. Lake Chelan and The Rocks district of Milton-Freewater also had no significant difference at 95% confidence level. This index is reported to influence the quality of grapes, including grape composition, flavor, and aroma (Mullins et al., 1992; Ramos et al., 2008; Montes et al., 2012). Therefore, similar AVAs (based on their MTA), if managed by the same management and irrigation strategies, can potentially produce grapes with many similar qualitative traits. However, further assessments is required to evaluate fruit quality traits in AVAs with comparable bio-climatic ranges.

Dynamic Minimum Temperature (DyMin. Temp.)

The number of events that the minimum air temperature drops below a dynamic low temperature threshold were calculated for all the AVAs for a period of 30 years. Puget Sound was determined to have the lowest number of events (3) (Appendix B), with the highest number obtained for Naches Heights (45) (Figure 4.4.). Multiple comparisons of the DyMin. Temp. revealed significant differences between the AVAs (Appendix B), except in the case of the Ancient Lakes of the Columbia Valley and Rattlesnake Hills and Red Mountain and Columbia Gorge. The degree of damage caused by low temperatures depends on where individual plants are in their physiological and phenological stages (proving that temporal analysis of this index is as important as its spatial analysis.). In both the Naches Heights and Puget Sound AVAs, the temporal distribution of events was focused in the month of April, with no incidents occurring during the summer months (June, July, and August). The concentration of most of the events in April might be partiallydue to the assumptions made for the calculation of the index.

Our study is the first of its type to consider a dynamic minimum temperature rather than a fixed minimum temperature. Although this index is not sufficient to fully categorize grape-growing regions, it can be used in conjunction with other indices to better explore climate variability in viticultural regions. Future studies should evaluate the risks associated with viticulture in regions that suffer from frequent freezes, and evaluate each region based on its resilience, adaptability, and technological advancement.

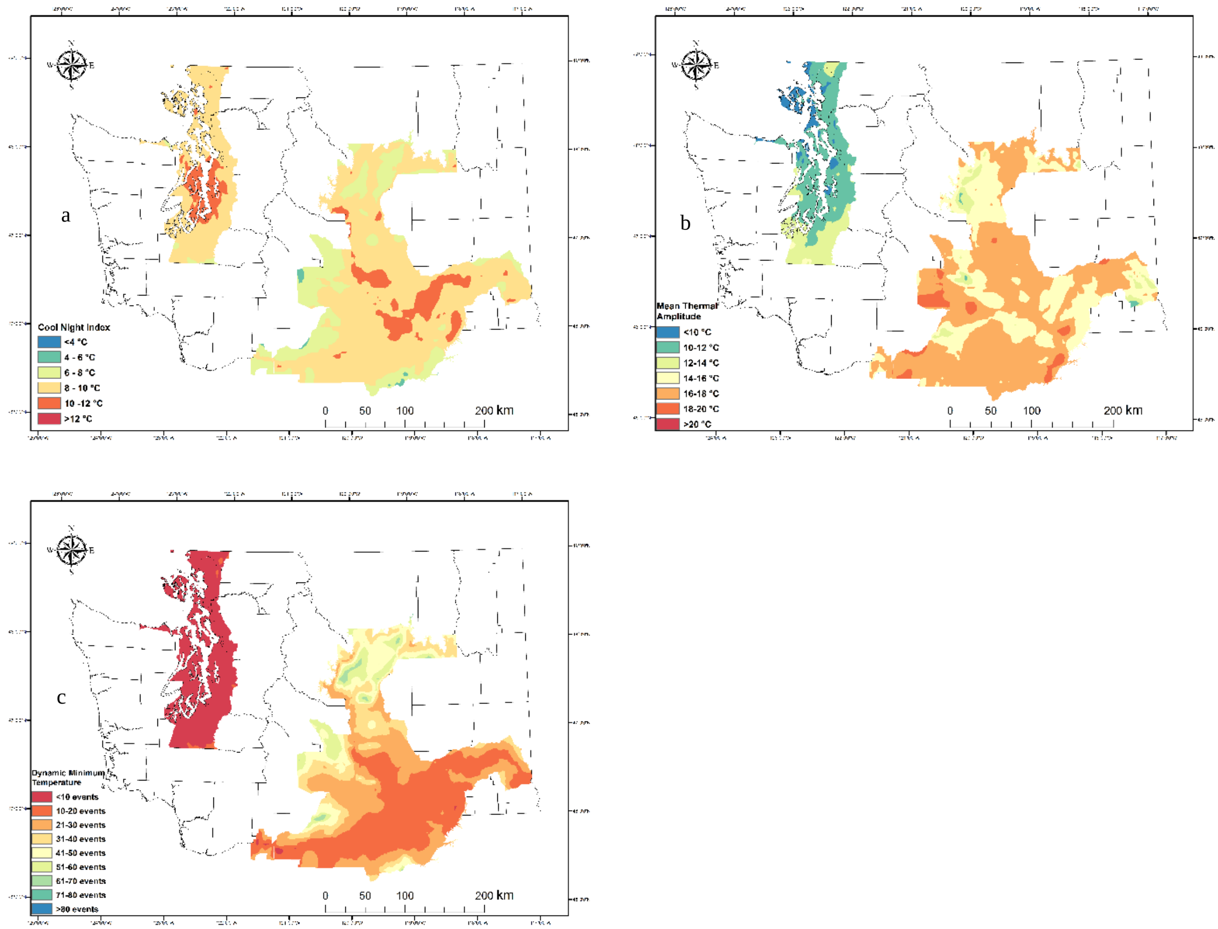

Figure 4. 4. Key bio-climatic indices used in calculation of minimum temperature for AVAs the AVAs located in the state of Washington and parts of Oregon. Class limits not directly comparable. Cool Night Index (a); Mean Thermal Amplitude (b); Dynamic Minimum Temperature(c).

Cold Damage Index (CDI)

Total number of events when the minimum temperature drops below a threshold (Bud LT_{50}) was calculated and the number were reported for 5, 10, 20, and 30 years and projected for 100 years (Table 4.10.). Puget Sound proved to have the lowest number of events (zero within five years and one for up to 30 years), while the highest number of events was found for Naches Heights (30, 47, 86, and 119 events for five, 10, 20, and 30 years, respectively) (Figure 4.5.). Our comparison of the CDI results indicated that there was a significant difference between the Puget Sound results versus those obtained for the remaining AVAs (Appendix B).

Table 4. 10. Number of incidents for each AVA that the minimum air temperature drops below a cold hardiness threshold (calculated for 5, 10, 20, and 30 years). The number of events for a century was calculated based on CDI for 30 years.

AVA	CDI 5 years	CDI 10 years	CDI 20 years	CDI 30 years	Century CDI
Puget Sound	0	1	1	1	5
Red Mountain	4	5	13	15	49
The Rocks District of Milton-Freewater	5	5	5	22	74
Wahluke Slope	6	7	13	18	59
Walla Walla	7	9	47	16	52
Snipes Mountain	7	12	25	33	112
Horse Heaven Hills	9	12	20	23	78
Yakima Valley	11	17	33	46	155
Ancient Lakes of the Columbia Valley	11	13	23	30	99
Lake Chelan	13	16	30	38	126
Columbia Gorge	13	23	43	56	187
Columbia Valley	14	20	36	48	161
Rattle Snake Hills	15	23	13	72	239
Naches Heights	30	47	86	119	397

The risk associated with CDI events in a given location depends on various factors, such as the duration of a cold spell, economic profitability of the vineyard, availability of affordable technologies, and the adaptation of the grower to the risks associated with potential crop loss. Discussing the limiting ranges of CDI events is beyond the scope of this paper and needs further investigation; hence, the results presented here should be used as a stepping-stone for future studies; this index can be an effective tool for the determination of regions with higher numbers of CDI events.

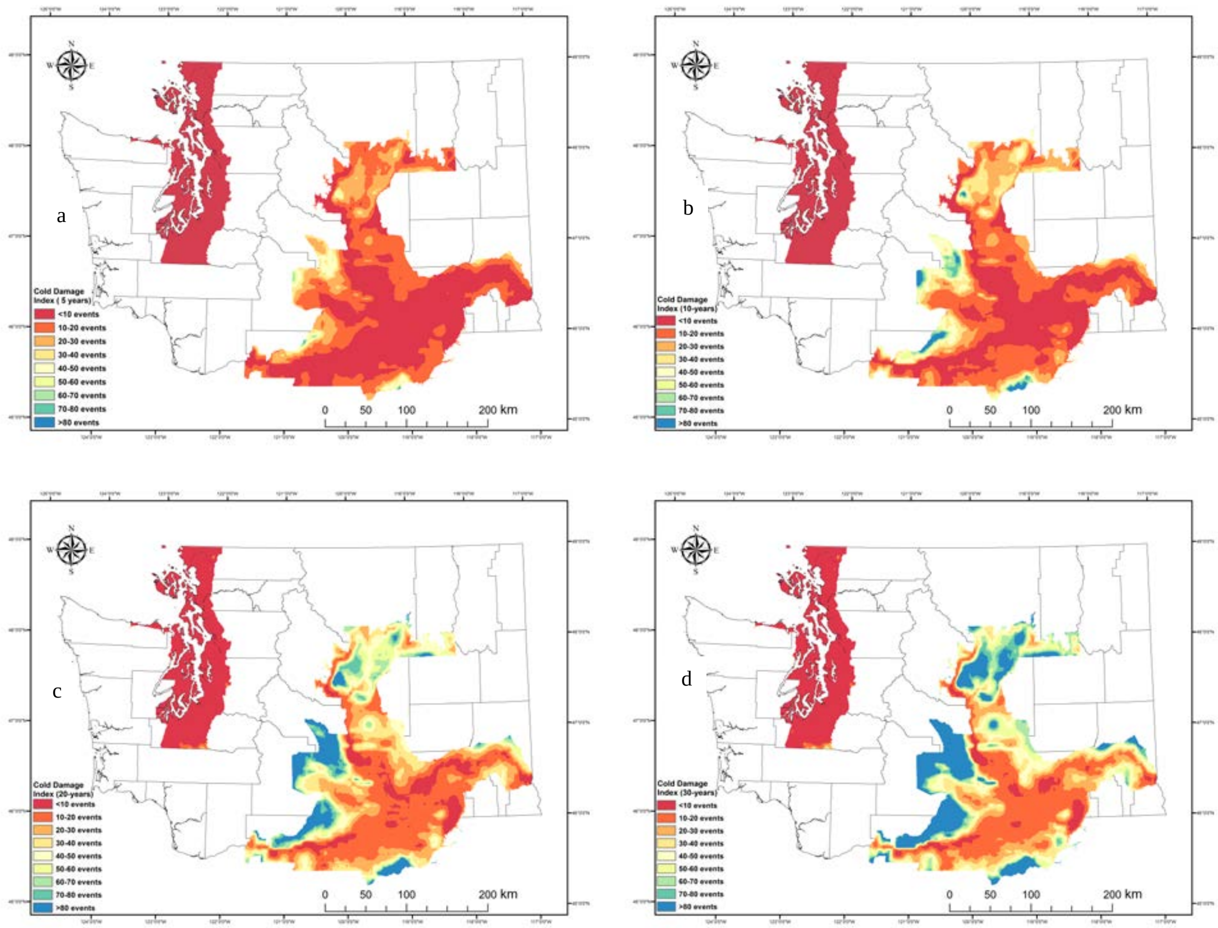

Figure 4. 5. Cold Damage Index for AVAs located in the state of Washington and parts of Oregon. Cold Damage Index for 5 years (a); Cold Damage Index for 10 years (b); Cold Damage Index for 20 years (c); Cold Damage Index for 30 years(d).

Precipitation

Our results indicated that, for the majority of AVAs, most precipitation falls during winter and early spring (~ 60%), except in the Columbia Gorge (~40%). This information can prove beneficial to decision-makers and growers in determining their options for supplemental irrigation. Gladstones (1992) reported an average GSP of 53 mm and 70 mm for Fresno and San Jose, California. When the calculated GSP for the AVAs in this current study was compared with the reported GSP values from Gladstones (1992), it was indicated that Snipes Mountain, Rattlesnake Hills, Wahluke Slope, Ancient Lakes, Red Mountain, Yakima Valley, and Horse

Heaven Hills are within the same range of GSP reported for these locations in California. However, the out of growing season precipitation (OutGSP) for these AVAs is lower than the values reported for Fresno (178 mm) and San Jose (300mm).

It is important to evaluate the potential of a region based on both the GSP and OutGSP in order to better understand the options for dryland viticulture versus irrigated viticulture. Furthermore, the amount of precipitation that finally reaches a grapevine's root zone is generally lower than the recorded precipitation, due to the partial interception of raindrops by the canopy and vineyard cover crops as well as evaporation at the surface. Therefore, the actual available water to the plants is even lower than the calculated values based only on precipitation; hence, when assessing the precipitation of various AVAs, two questions must first be answered: a) does the region needs supplementary irrigation? b) If the region does require supplementary irrigation, does the land have access to water and rights to use it?

Growing Season Precipitation (GSP)

Growing Season Precipitation (GSP) was computed for all the AVAs, proving that Snipes Mountain had the lowest GSP (52 mm) and Puget Sound had the highest GSP (332 mm). While the Puget Sound GSP showed a notable difference when compared with the other AVAs (Appendix B), Columbia Gorge and Walla Walla's GSPs also showed significant difference compared with the other AVAs at the 95% confidence level (Figure 4.6.; Appendix B). This index provides an accurate means of determining the general economic suitability of a region for viticulture (Santos et al., 2012b), especially in locations where irrigation is not an option. If a region has a GSP < 200 mm it is regarded as extremely dry, and if it has a GSP > 600 mm, it is regarded as excessively humid. All AVAs that were assessed in our study had a GSP lower than 200 mm, except for Columbia Gorge and Puget Sound (Figure 4.6.).

Out of Growing Season Precipitation (OutGSP)

Out of Growing Season Precipitation (OutGSP) provides further insight into the available water in a specific soil profile prior to the start of the growing season. Our results indicated that Wahluke Slope had the lowest OutGSP (73 mm) and Puget Sound had the highest OutGSP (415 mm) (Figure 4.6.; Table 4.11.). Statistical comparison of AVAs based on their OutGSP indicated a significant difference at a 95% confidence level (Appendix B). Preference is generally given to regions that receive the majority of their precipitation during winter, thus providing the plants in these regions with sufficient water already in the soil profile prior to the start of their growth in spring (Jackson, 2008).

Table 4. 11. Growing Season Precipitation (GSP) and Out of Growing Season Precipitation (OutGSP), and total precipitation for the AVAs and their respective percentage out of total precipitation.

AVA	GSP (mm)	OutGSP (mm)	Total precipitation (mm)	GSP %	OutGSP %
Snipes Mountain	52	78	130	40	60
Rattle Snake Hills	57	90	147	39	61
Wahluke Slope	58	73	132	44	56
Ancient Lakes of the Columbia Valley	59	78	137	43	57
Red Mountain	61	86	147	41	59
Yakima Valley	63	87	150	42	58
Horse Heaven Hills	65	96	160	40	60
Columbia Valley	81	120	201	40	60
Lake Chelan	83	108	191	44	56
Naches Heights	96	112	208	46	54
The Rocks District of Milton-Freewater	98	185	283	35	65
Walla Walla	112	197	309	36	64
Columbia Gorge	262	195	457	57	43
Puget Sound	332	415	747	44	56

Hydrothermic Index (HyI)

Among all the AVAs Wahluke Slope had the lowest HyI (833.9) and Puget Sound had the highest HyI (3144.6) (Appendix B). The multiple comparison indicated that Puget Sound and Columbia Gorge had a significant difference when compared to all the other AVAs and between themselves. HyI indicates the potential risk of downy mildew (Santos et al., 2012b) in a region as well as the water availability (Fraga et al., 2014) downy mildew is not a source of concern in Washington since the pathogen does not exist in this state.

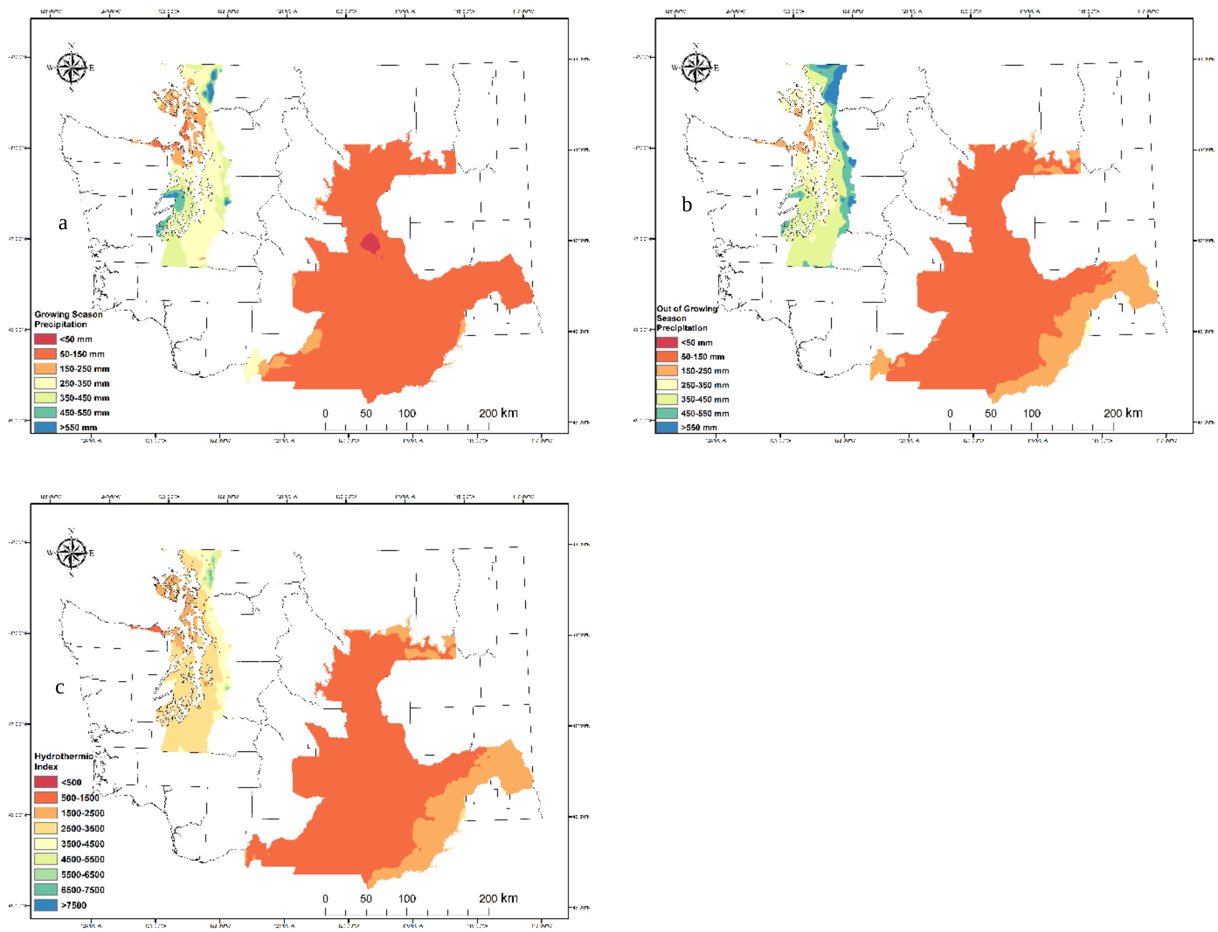

Figure 4. 6. Key bio-climatic indices focused on the precipitation of AVAs located in the state of Washington and parts of Oregon. Class limits are not directly comparable for Hydrothermic Index. Growing Season Precipitation (a); Out of Growing Season Precipitation (b); Hydrothermic Index (c).

Wind Speed Index (WSI)

The Wind Speed Index (WSI) was calculated for the AVAs located in our study area, with Red Mountain proving the least windy AVA (16 incidents) and Snipes Mountain the most windy AVA (56 incidents) (Appendix B). Our comparison of the WSI indicated that both Red Mountain and Snipes Mountain had significant differences at the 95% confidence level compared to the other AVAs. Wind speed is influenced by the complexity of topographic elements in a region as well as the variability in the thermal properties of different land cover types, leading to thermal gradient. This index cannot be used as a standalone tool for climate zoning; however, it can serve as a surrogate to help growers and decision-makers gain valuable knowledge about a site. In addition, it can help them make more effective decisions regarding management strategies such as installing a windbreak. Future studies can use this index to focus on locations that have higher WSI scores and conduct more detailed studies on the impact of wind speed on vines (physical damage, shoot growth, and photosynthesis disruption).

Meso-climate and Terrain Features

The similarities and differences between the AVAs based on their bio-climatic indices can be described by the factors that impact the meso-climate; specifically, the topographic features and complexity of the terrain in a region, including the elevation, slope, and aspect of the sites. The effect of elevation on minimum temperature was clearly captured for Naches Heights, as this AVA has the highest elevation of them all (543 m), and the lowest CI, lowest FFD, highest CDI, and highest Dy.Min.Temp were also reported for this AVA. Puget Sound had the lowest elevation among all the AVAs, as well as the highest CI, highest FFD, lowest CDI, and lowest Dy.Min.Temp.

Weather parameters such as relative humidity also indirectly impact the behavior of bio-climatic indices. Hence, for an index such as HyI, the value increases in wet regions such as Puget Sound, where the relative humidity is much higher compared to other regions located to the east of the Cascade Mountains. Consequently, future studies should relate the impact of relative humidity on the overall dynamics of bio-climatic indices on a local scale within each AVA. There is also a need for development of a management framework based on the current cultural practices that are implemented in AVAs with similar climate groupings.

Conclusions

This study categorized the AVAs located in the state of Washington and parts of Oregon based on the dynamics of bio-climatic indices evaluated for a 30-year period. Several new bio-climatic indices were introduced, including CDI, Dy.Min. Temp., and WSI. Future studies should focus on the development and improvement of bio-climatic indices based on recent advancements in sensor technology and the availability of finer resolution spatial and temporal data.

References

Abatzoglou, J. T. (2011). Development of gridded surface meteorological data for ecological applications and modelling. International Journal of Climatology, 33(1), 121–131.

AgriMet (Cooperative Agricultural Weather Data). (2011). (Last accessed on Feb 22, 2016 http://www.usbr.gov/pn/agrimet/wxdata.html).

AgWeatherNet. (2011). Daily weather data. Prosser, Washington: Washington State University, AgWeatherNet. (Last accessed on Feb 23, 2016 from http://weather.wsu.edu)

Allen, R. G., Pereira, L. S., Raes, D., and Smith, M. (1998). Crop evapotranspiration-Guidelines for computing crop water requirements-FAO Irrigation and drainage paper 56. FAO, Rome, 300(9).

Amerine, M.A., and Winkler, A.J. (1944) Composition and quality of musts and wines of California grapes, Hilgardia, 15(4), 493–675.

Anderson, J. D., Jones, G. V., Andrew, T., Hall, A., and Throught, C. T. (2012). Analysis of viticulture region climate structure and suitability in New Zealand. Journal International des Sciences de la Vigne et du Vin, 46(3), 149–145.

Becker, N. (1985). Site selection for viticulture in cooler climates using local climatic information. In: Proceedings of the International Symposium on Cool Climate Viticulture and Enology. Oregon State University Technical Publication 7628:20-34.

Blanco-Ward, D., Queijeiro, J. M. G., and Jones, G. V. (2007) Spatial climate variability and viticulture in the Miño River Valley of Spain. Vitis, 46, 63−70.

Branas, J. (1974). Viticulture. Imp. Dehan, Montpellier.

Branas, J., Bernon, G., and Levadoux, L. (1946). Eléments de viticulture générale. Imp Dehan, Montpellier.

Campbell-Clause, J.M. (1998). Stomatal response of grapevines to wind. Aust. J. Exp. Agric. 38, 77–82.

Clark, J. R., Wolf, T. K. and Warren, M. K. (1996). Thermal Analysis of Dormant Buds of Two Muscadine Grape Cultivars and of Vitis Labrusca L. `Mars'. HortScience 31(1), 79–81.

Conceição, M. A. F., and Tonietto, J. (2005). Climatic potential for wine grape production in the tropical north region of Minas Gerais State, Brazil. Revista Brasileira de Fruticultura, 27(3), 404–407.

Davenport, J.R., Keller, M., and Mills, L.D. (2008). How cold can you go? Frost and winter protection for grape. HortScience 43:1966-1969.

Daly, C., Halbleib, M., Smith, J.L., Gibson, W.P., Doggett, M.K., Taylor, G.H., Curtis, J., and Pasteris, P.A. (2008). Physiographically-sensitive mapping of temperature and precipitation across the conterminous United States. International Journal of Climatology, 28, 2031–2064.

Dry, P.R., Reed, S., and Potter, G. (1989). The effect of wind on the performance of cabernet franc grapevines. Acta Hort. (ISHS) 240:143-146.

ESRI.(2015). ArcGIS Desktop10.2. Redlands, CA: Environmental Systems Research Institute.

Fennell, A. (2004). Freezing Tolerance and Injury in Grapevines. Journal of Crop Improvement, 10(1-2), 201–235.

Ferguson, J. C., Tarara, J. M., Mills, L. J., Grove, G. G., and Keller, M. (2011). Dynamic thermal time model of cold hardiness for dormant grapevine buds. Annals of Botany, 107(3), 389–396.

Ferguson, J. C., Moyer, M. M., Mills, L. J., Hoogenboom, G., and Keller, M. (2014). Modeling Dormant Bud Cold Hardiness and Budbreak in 23 Vitis Genotypes Reveals Variation by Region of Origin. American Journal of Enology and Viticulture, 32pp.

Fraga, H., Malheiro, A. C., Moutinho-Pereira, J., and Santos, J. A. (2013). Future scenarios for viticultural zoning in Europe: ensemble projections and uncertainties. International Journal of Biometeorology, 1–17.

Fraga, H., Malheiro, A. C., Moutinho-Pereira, J., and Santos, J. A. (2014). Climate factors driving wine production in the Portuguese Minho region. Agricultural and Forest Meteorology, *185*, 26–36.

Freeman, B. M., Kliewer, W. M., and Stern, P. (1982). Influence of windbreaks and climatic region on diurnal fluctuation of leaf water potential, stomatal conductance, and leaf temperature of grapevines. Am. J. Enol. Vitic. 33:233-236.

Gladstones, J. (1992). Viticulture and Environment. Winetitles, Adelaide.

Hamilton, R. P. (1988). Wind effects on grape vines. In ‘Proceedings of the 2nd international symposium for cool climate viticulture and oenology’. January 1988, Auckland, New Zealand. (eds r. E. Smart, r. J. Thornton, s. B. Rodriques and j. E. Young.) pp. 65–8. (New Zealand society of viticulture and oenology; wine institute of New Zealand, Auckland.)

Hall, A., and Jones, G.V. (2010). Spatial analysis of climate in wine grape-growing regions in Australia. Australian Journal of Grape and Wine Research, 16, 389–404.

Hidalgo, L. (2002). Tratado de viticultura general. Ediciones Mundi-Prensa, Madrid.

Huglin, P. (1978). Nouveau mode d’e´valuation des possibilite´s he´liothermiques d’un milieu viticole, Comptes Rendus de l’Acade´mie d’Agriculture, 117–126.

Huglin, P., and Schneider, C. (1998). Biologie et écologie de la vigne. Paris, Lavoisier. 370p.

Hunter, J. J., and Bonnardot, V. (2011). Suitability of some climatic parameters for grapevine cultivation in South Africa, with focus on key physiological processes. S. Afr. J. Enol. Vitic, 32(1), 137-154.

Jackson, D.I., and Cherry, N.J. (1988). Prediction of a district’s grape-ripening capacity using a Latitude-Temperature Index (LTI), American Journal of Enology and Viticulture, 39(1), 19–28.

Jackson, R. S. (2008). Wine science principles and applications. 3rd ed. Academic Press, Burlington, MA.

Jones, G.V., Snead, N., and Nelson, P. (2004). Geology and wine 8 – modeling viticultural landscapes: A GIS analysis of the terroir potential in the Umpqua valley of Oregon. Geoscience Canada, 31, 167–178.

Jones, G.V., (2005). Climate change in the western United States grape growing regions. *Acta Horticulturae* (ISHS), 689:41-60.

Jones, G.V. (2007). Climate change: observations, projections and general implications for viticulture and wine production. *In* Climate and Viticultural Congress, Zaragoza, Spain. 10-14 Apr. 2007. OIV, Paris.

Jones, G.V., Moriondo, M., Bois, B., A. Hall, A., and Duff, A. (2009). Analysis of the spatial climate structure in viticulture regions worldwide. Le Bulletin de l'OIV, 82, 507–518.

Jones, G. V., Duff, A. A., Hall, A., and Myers, J. W. (2010). Spatial Analysis of Climate in Winegrape Growing Regions in the Western United States. American Journal of Enology and Viticulture, 61(3), 313–326.

Keller, M. (2010). The Science of Grapevines: Anatomy and Physiology. Academic Press/Elsevier.

MATLAB V2014a. (2014). The MathWorks, Inc., Natick, Massachusetts, United States. MATLAB and Simulink 2014a.

Magalhães, N. (2008). Tratado de viticultura: a videira, a vinha e o terroir. Chaves Ferreira Publicações, Lisboa.

Magarey, R., Seem, R. C. and DeGloria, S. D. (1998). Prediction of vineyard site suitability. Grape Research News 9: 1–2.

Makra, L., Vitanyi, B., Gal, A., Mika, J., Matyasovszky, I., and Hirsch, T. (2009). Wine quantity and quality variations in relation to climatic factors in the Tokaj (Hungary) Winegrowing Region. Am J Enol Vitic 60(3):312–32.

Malheiro, A.C., Santos, J.A., Fraga, H., and Pinto, J.G. (2010). Climate change scenarios applied to viticultural zoning in Europe. Clim Res 43:163-177.

Malheiro, A., Santos, J., Pinto, J., and Jones, G. (2012). European Viticulture Geography in a Changing Climate. Bulletin De L'oiv, 85(971-972), 973.

Mills, L.J., Ferguson, J. C., and Keller, M. (2006). Cold-hardiness evaluation of grapevine buds and cane tissues. Am. J. Enol. Vitic. 57:194-200.

Mitchell, K.E., Lohmann, D., Houser, P.R., Wood, E.F., Schaake, J.C., Robock, A., Cosgrove, B.A., Sheffield, J., Duan, Q., Luo, L., Higgins, R.W., Pinker, R.T., Tarpley, J.D., Lettenmaier, D.P., Marshall, C.H., Entin, J.K., Pan, M., Shi, W., Koren, V., Meng, J., Ramsay, B.H., and Bailey, A.A. (2004). The multi-institution North American Land Data Assimilation System (NLDAS): Utilizing multiple GCIP products and partners in a continental distributed hydrological modeling system. Journal of Geophysical Research 109, D07S90.

Montes, C., Perez-Quezada, J. F., Peña-Neira, A., and Tonietto, J. (2012). Climatic potential for viticulture in Central Chile. Australian Journal of Grape and Wine Research, 18(1), 20–28.

Mullins, M.G., Bouquet, A., and Williams, L.E. (1992). Biology of the grapevine. Cambridge University Press, Cambridge, New York.

Prescott, J. A. (1965). The climatology of the vine (*Vitis vinifera* L.). The cool limits of cultivation. Trans. Roy. Soc. S. Aust. 89:5-23.

Rosenburg, N. J., Blad, B. L., and Verma, S. B.(1983). Microclimate the Biological Environment. Wiley-lnter science Publishers, New York.

Ramos, M. C., Jones, G. V., and Martínez-Casasnovas, J. A. (2008). Structure and trends in climate parameters affecting wine grape production in northeast Spain. Climate Research, 38, 1–15.

RAWS (Remote Automatic Weather Stations). (2011). (Last accessed Feb. 22, 2016 http://raws.fam.nwcg.gov/)

Riou, C., Becker, N., Sotés Ruiz, V., Gomez-Miguel, V., and others. (1994). Le déterminisme climatique de la maturation du raisin: application au zonage de la teneur en sucre dans la communauté européenne. Office des Publications Officielles des Communautés Européennes, Luxembourg.

SAS software v9.4. (2015). SAS Institute, Cary, NC, USA.

Santos, J.A., Grätsch, S.D., Karremann, M.K., Jones, G.V., and Pinto, J.G. (2012a). Ensemble projections for wine production in the Douro Valley of Portugal. Clim. Chang.

Santos, J. A., Malheiro, A. C., Pinto, J. G., and Jones, G. V. (2012b). Macroclimate and viticultural zoning in Europe: observed trends and atmospheric forcing. Climate Research. 51: 89-103.

Takahashi, K., Kuranaka, M., Miyagawa, A., and Takeshita, O. (1976). The effect of wind on grapevine growth; windbreaks for vineyards. Bull. of Shimane Agric. Exp. Stn. 14:39-83

Tarara, J. M., Ferguson, J. C., Hoheisel, G.A., and Perez Peña, J. E. (2005). Asymmetrical canopy architecture due to prevailing wind direction and row orientation creates an imbalance in irradiance at the fruiting zone of grapevines. Agricultural and Forest Meteorology, 135(1–4), 144–155.

T.T.B. (2015). Alcohol and Tobacco Tax and Trade Bureau (TTB), U.S. department of treasury. RRD. (n.d.). TTB | Wine | American Viticultural Area (AVA) [Facts and Overview]. Retrieved March 6, 2015, from http://www.ttb.gov/wine/ava.shtml

Tonietto, J., and Carbonneau, A. (2004). A multicriteria climatic classification system for grape-growing regions worldwide. Agric Meteorol 124: 81−97.

Tóth, J. p., and Végvári, Z. (2016). Future of winegrape growing regions in Europe. *Australian* Journal of Grape and Wine Research, 22(1), 64–72.

UI GSM. (2015). The University of Idaho Gridded Surface Meteorological Dataset. http://metdata.northwestknowledge.net/. Visited February 20, 2015.

USDA National Agricultural Statistics Service (USDA-NASS). (2015). Retrieved from http://quickstats.nass.usda.gov, Washington, DC.

USHCN. (2011). United States Historical Climate Network (Last accessed, http://cdiac.ornl.gov/ftp/ushcn daily/, Feb 22, 2016).

Van Leeuwen C., Friant Ph., Choné X., Trégoat O., Koundouras S., and Dubourdieu D. (2004). The influence of climate, soil and cultivar on terroir. Am. J. Enol. Vitic., 55, 207-217.

Wample, R.L., Hartley, S. and Mills. L. (2001). Dynamics of grape-vine cold hardiness. InProceedings of the American Society forEnology and Viticulture 50thAnniversary Annual Meeting, June2000. J.M. Rantz (Ed.), pp. 81-93. ASEV, Davis, CA.

White, R. E. (2015). Understanding Vineyard Soils. Oxford University Press.

Williams, L. E., Dokoozlian, N. K., and Wample, R. (1994). Grape. In B. Schaffer and P. C. Andersen (Eds.), Handbook of Environmental Physiology of Fruit Crops. Vol. I. Temperate Crops (pp. 85–133). Boca Raton, FL: CRC Press.

Winkler, A.J., Cook, J.A., Kliewer, W.M., and Lider, L.A. (1974). General Viticulture. 4th ed. University of California Press, Berkeley.

Wolfe, W. (1999). Site Selection in Eastern Washington: Optimizing Site and variety Choices. In: Growing Grapes in Eastern Washington (Eds:J. Watson). Good Fruit Grower.101 pp.

Wolfe, W. (2001). Vine and vineyard management following low temperature injury, p. 101–110. In: Rantz, J.M. (ed.). Proc. ASEV 50th Anniversary Annual Meeting, Amer. Soc. Enology Viticulture, Davis, CA.

Worldclim. (2009). (Last accessed on Feb 23, 2016: http://www.worldclim.org/)

WSW. (Washington State Wines). (2015). Accessed [March, 9, 2015] http://www.washingtonwine.org/wine-101/regions/

Yau, I.H., and Washington State University. Dept. of Crop and Soil Sciences. (2011). Developing a grape site selection GIS for the Inland Pacific Northwest. Retrieved February 18, 2013, from http://www.dissertations.wsu.edu/Thesis/Fall2011/i_yau_092211.pdf

Yau, I.H., Davenport, J.R., and Rupp, R.A. (2013) Characterizing Inland Pacific Northwest American Viticultural Areas with Geospatial Data. PLoS ONE 8(4): e61

CHAPTER FIVE

SPATIAL SUITABILITY ASSESSMENT FOR SITE SELECTION OF VINEYARDS BASED ON FUZZY LOGIC

Abstract

Developing a sustainable agricultural production system that uses the full potential of land resources requires knowledge of the climate, soil, and topography of the area of interest. There is a great potential for wine grape (*Vitis vinefera* L.) production in the Pacific Northwest region of the U.S.; however, few studies have focused on the development of a comprehensive spatial suitability system. The main objective of our study was the development of a spatial suitability system to aid in the selection of suitable areas for grapevine cultivation. Several bio-climatic indices, such as Growing Degree Days (GDD), Frost Free Days (FFD), and the Huglin Index (HI) were calculated over a period of 30 years using daily weather data obtained from the University of Idaho's Gridded Surface Meteorological Dataset (UI GSM). The soil data was obtained from the gSSURGO dataset, and key properties such as soil depth, pH, and soil texture were extracted for the study area. The topographical data were obtained from the national elevation dataset. The data were then transformed using fuzzy logic, and soil, weather, and topographic suitability maps were subsequently developed. The final vineyard potential scores were obtained by combining the soil, weather, and topographic potential scores. The potential scores had a range from 0 to 1, where 0 pertained to non-suitable areas and 1 referred to optimal sites. The vineyard potential scores for vineyards currently established in the state of Washington were then evaluated, and the percent area in each vineyard potential class reported. Our spatial land assessment system was able to classify the study area into five main regions, based on their

vineyard potential. The evaluation results indicated that 97.3 % of the vineyards currently established in the study area have vineyard potential scores ranging from 0.80001 to 1, and the rest had potential scores of 0.60001 to 0.8. The results of our study can help decision-makers, growers, and others with conducting more precise land assessments for winegrape production.

Introduction

Many factors can directly or indirectly impact the growth and development of plants. Terrain attributes, soil properties, and the climate of a specific region are all regarded as permanent spatial factors (Spomer and Piest, 1982; Stone et al., 1985; Jones et al., 1989; Kravchenko and Bullock, 2000; McKinion et al., 2010b), while insects and other pests, diseases, and management practices are regarded as transient spatial factors (McKinion et al., 2010a, 2010b). The interaction of an ecosystem that includes climate, soil, and the genetics of grapevines (*Vitis* spp.) is the foundation for viticultural regions (Seguin, 1984), and the environmental factors involved in grapevine production are primarily soil and climate (Jones et al., 2004; van Leeuwen and Seguin, 2006; MacQueen and Meinert, 2006; Gladstones, 2011; Dougherty, 2012). However, the socioeconomic and historical aspects of a region also have the potential to contribute to the complex concept of viticultural regions (Deloire et al., 2008).

Weather is regarded as the most important factor in agricultural enterprises. Annual and seasonal weather and its variability determine crop suitability, productivity, and quality. High-quality, economically-sustainable crop production across the globe is a function of local climate and weather conditions (Rosenzweig and Hillel, 2008; Jones et al., 2010; Anderson et al., 2012). For grapevines, both yield and quality are impacted by local weather conditions (van Leeuwen et al., 2004; Santos et al., 2011; Santos et al., 2012b). Several soil characteristics are also important for establishment of a vineyard. Grapevines tolerates a wide range of soil conditions, but the two main areas of importance are moisture management and nutrient availability (Jones et al., 2004). Soil drainage (Jones et al., 2004; Gladstones, 1992) and the distance to any restrictive layer also impact grapevines performance. Unrestricted soil drainage to a depth of >2 to 3 m is recommended for most vineyards (Gladstones, 1992; Jackson, 2008). Ideal soil for a vineyard should be able to maintain plant available water even without constant irrigation (Gladstones, 1992; Malheiro et al., 2010). Soil pH enables grapevines access to certain micro- and macro-nutrients (Jones et al., 2004; Jackson, 2008). Grapevines benefit from an optimal soil pH ranging from 6.5-7.2 that ensures ion solubility (White, 2009; Dry and Coombe, 2004; Meinert and Curtin, 2005). Soil texture controls root growth, root respiration and oxygen availability to the roots, as well as soil water availability (Lanyon et al., 2004; Quezada et al., 2014).

The topography of a region is also an important factor, particularly the slope and aspect, and their relative impacts on grapevine performance. Sites with steep slopes hinder the practical use of machinery, and topography also affects cool air movement down slopes; therefore, moderate slopes (5%-15%) are regarded as optimum values (Jones et al., 2004). The direction of slope (aspect) is likewise highly influential on the performance of certain vineyards. In the Northern Hemisphere, southern facing slopes enable maximum solar insolation and heat accumulation, and are thus classified as optimum.

Suitability assessment

Suitability analysis focused on cropland assessment is necessary to determine the full potential of land resources for the development of a sustainable agricultural production (Nisar Ahmed et al., 2000). It is a function of crop requirements and the physical characteristics of a region, and is a process that helps to quantify the convergence of land characteristics with crop requirements (FAO, 1976). Land suitability evaluation for crops uses suitability ratings as a measure of land characteristics based on climate, terrain, and soil properties (FAO, 1976).

Structure of suitability classification

The Food and Agricultural Organization of the United Nations (FAO, 1976) has defined the framework structure for land suitability classification based on different categories, with land being classified based on its capacity for a given use. There are four main categories of land suitability with land suitability order the most generalized category; the order is further divided into suitable (S) or not-suitable (N) for the proposed use of the land. These land suitability orders are further divided into several classes indicating the degree of suitability within each order. For the "suitable" order, three main classes are recommended. A suitability order with three classes includes highly suitable (S1), moderately suitable (S2), and marginally suitable (S3) (Table 5.1.). The differences in the suitability classes are mainly related to the relationship between the benefits and the inputs. The "not-suitable" order is usually divided into two classes: currently not suitable (N1) and permanently not suitable (N2) (Table 5.1.). There are other classes, including not relevant (NR), which are rarely used and refer to areas that have not been assessed for the proposed land use.

Table 5.1. Major land suitability orders and classes adopted for our study based on FAO (1976).

Orders	Classes	Description
Suitable (S)	Highly suitable (S1)	No significant limitation for a given land use.
	Moderately suitable(S2)	Minor limitations for a given land use.
	Marginally suitable(S3)	Moderate limitations for a given land use.
Non- suitable(N)	Currently not suitable(N1)	Major limitations that cannot be corrected with current knowledge; costs for any changes not deemed acceptable.
	Permanently not suitable(N2)	Limitations are severe and the successful use of the land for a given use is not possible.

The classes can be further divided into subclasses; the aim of defining subclasses within a class is to indicate the limitations and any required improvements. The final and most detailed category of land suitability is "land suitability units," which indicate minor differences in management required for each subclass (FAO, 1976).

The fundamentals of vineyard land assessment have been discussed in detail by Dry and Smart (1988); Gladstones (1992); Jackson (2008); and Sanga-Ngoie et al. (2010). In the U.S., Magarey et al. (1998) published the first online site-selection maps for New York. Grape regions in Eastern California were analyzed by Watkins (1997) using GIS, in Oregon by Jones et al. (2004), and in Illinois by Kurtural et al. (2006). Most studies for site selection in the PNW have been conducted by Jones et al. (2004; 2006; 2010); while Yau et al., (2011; 2013; 2014) developed a GIS for the inland PNW, and analyzed key spatial biophysical parameters with focus on the soil properties of the region.

Fuzzy logic

Fuzzy logic was first introduced by Zadeh (1965) and has been used as a non-statistical method for geographical decision-making (Fisher, 1996; Tavana et al., 2016). Initial attempts to introduce fuzzy set theory into GIS applications were conducted by Robinson and Frank (1985). Fuzzy logic provides a smooth transition between non-members and members of a set, by avoiding the sharp boundaries between non-members and members. Fuzzy logic allows for continuous classifications of variables, along with proper handling of uncertainty, which yields more realistic outputs. For a fuzzy set *A*, the continuum of membership grades are represented by a class of events X={x}. This class of events is characterized by a fuzzy membership function $\mu_A(x)$; the membership function takes a real number in the interval of [0, 1] (Equation 5.1.) (Zadeh, 1965; Nisar Ahamed et al., 2000; Pan et al., 2011; Tavana et al., 2016).

$$\mu_A : A \rightarrow [0,1] \qquad (5.1.)$$

For a fuzzy set *A*, the characteristic function is often called a membership function and can be represented as follows (Equation 5.2.), where U is the universal set and takes on all values between 0 and 1.

$$A = \{x | x \in U \wedge \mu_A > 0\} \qquad (5.2.)$$

The assessment of land suitability for agricultural purposes has borrowed from fuzzy logic, which has been applied to single crop suitability assessment (Chang and Burrough, 1987; Van Ranst et al., 1996; Oberthur et al., 2000; Braimoh et al., 2004; Joss et al., 2008), as well as multiple crop suitability assessment (Sicat et al., 2005; Reshmidevi et al., 2009; Avellan et al., 2012; Zabel et al., 2014; Das and Sudhakar, 2014). For grapevines, few studies have been done on the application of fuzzy logic focusing on the relationship between vintage quality and other environmental variables (Grelier et al., 2007; Paoli et al., 2005; Tagarakis et al., 2014; Perrot et al., 2015). The fuzzy expert system has been applied for evaluation of the impact of agronomical practices and organic viticulture on the environment (Fragoulis et al., 2007); evaluation of the impact of micrometeorological conditions on pesticide applications (Gil et al., 2008), and delineation of management zones (Tagarakis et al., 2012; Urretavizcaya et al., 2014; Morari et al., 2009). Coulon-Leroy et al. (2012; 2013; 2014) developed a vine vigor model using a fuzzy set based on data related to soil, rootstock, and inter-row management strategies. However, to date, no single study has applied fuzzy logic to land assessment for evaluation of vineyard potential in a region.

In the PNW region of the U.S there is great potential for growing wine grapes, and the wine industry in that region is expanding vigorously. Out of this arises the need for a comprehensive land assessment system, which could help determine the potential of various regions for growing grapes, and could prove a useful tool for determining areas requiring further assessment. The objective of our study was the development of a land assessment system for aiding in the selection of potential grape-growing sites. Our study used fuzzy logic to combine various biophysical parameters and obtain vineyard potential scores for the chosen region.

Materials and Methods

Our land assessment system spatially covered Washington State, located in the PNW region of the U.S. Parts of central and north-eastern of Oregon were also included in the study area in order to better represent the American Viticultural Areas (AVAs) located in the region. The spatial datasets used in our study were obtained from various online public domain sources. The majority of data was downloaded from the United States Department of Agriculture (USDA) geo-spatial gateway website (GDG, 2015) for both Washington and Oregon.

A Digital Elevation Model (DEM) was obtained from the National Elevation Dataset (NED), provided by the U.S. Geological Survey (USGS). For this study, the NED DEM at a 10 m spatial resolution was obtained; other derivatives of elevation, such as slope and aspect, were also computed using the NED DEM dataset within the ArcGIS 10.2. Soil data was obtained from the gridded SSURGO (gSSURGO), which is a product of the National Cooperative Soil Survey (NCSS; Soil Survey Staff, 2015). The spatial resolution of soil data is 10 m (NRCS, 2015); several key soil parameters, including soil texture, soil pH, and depth to any restrictive layer were retrieved from the gSSURGO database. Weather data was obtained from the University of Idaho's Gridded Surface Meteorological Data (UI GSM, 2015); this weather dataset (Abatzoglou, 2011) was developed by employing Parameter-elevation Regressions on the Independent Slope Model (PRISM; Daly et al., 2008). Its spatial attributes and regional-scale reanalysis and daily gauge-based precipitation were obtained using the North American Land Data Assimilation System Phase 2 (NLDAS-2; Mitchell et al., 2004).

The Crop Data Layer (CDL) is a georeferenced, crop-specific land cover dataset that encompasses over 100 crop categories for the continental U.S. Several satellite remote-sensing products have been used for development of the CDL as of 2013 (Landsat 4/5/ 7 and Indian remote sensing advanced wide field sensor images, MODIS, DMC satellites, Deimos-1 and UK-DMC 2, and Landsat 8), and the data has a spatial resolution of 30 m. It was developed by running a supervised land cover classification over the satellite images; the CDL is produced once per year for the continental U.S. (Boryan et al., 2011; Boryan et al., 2012; Han et al., 2012).

The land cover data utilized in our study was mainly used for evaluation; for the first application a mask was developed based on land cover type (Kurtural et al., 2007) to classify the study area into two major classes a) restricted areas currently covered with a land cover such as forest or urban areas that make the conversion of the land parcel into a vineyard almost impossible; b) land covers that have the potential to be turned into a vineyard, such as fallow land or an orchard (Table 5.2.). For the second application, the land cover class corresponding to "grape" was selected and a data layer was developed that only included grape land cover. This data layer was then used for the determination of potential vineyard scores are already established in the study area.

Table 5.2. Initial land covers in the study area and their corresponding scores for the developed land cover mask.

Land-cover	Score	Land-cover	Score
Corn	1	Open water	0
Sweet corn	1	Perennial snow/ice	0
Mint	1	Developed	0
Barley	1	Forest	0
Wheat	1	Woody wetlands	0
Alfalfa	1	Herbaceous wetlands	0
Other hay	1		
Dry beans	1		
Potatoes	1		
Onions	1		
Lentils	1		
Peas	1		
Hops	1		
Fallow cropland	1		
Barren	1		
Cherries	1		
Peaches	1		
Apples	1		
Grapes	1		
Other tree fruits	1		
Shrubland	1		
Grass/pasture	1		

Since the land cover data had limited accuracy, a confidence layer was published along with the land cover data layer using the national cropland data layer (NASS, 2015). The confidence layer provides confidence scores as a percentage ranging from 0 for a low confidence in the accuracy, to 100 for a very high confidence in the accuracy, such that the classification is valid (Liua et al., 2004). The confidence layer together with the data layer only containing areas with grape land cover were used to omit any pixels with a low confidence score. Hence, only pixels that contained grape land cover and were associated with a confidence score of 100 were selected.

Statewide water rights data for Washington was obtained from the Department of Ecology and included spatial location of the surface water points of diversion available as a vector data model (ECY, 2015). The study area was then divided into two classes based on water rights, and a mask was developed to represent the two classes, which included regions with water rights and regions without water rights. For Oregon the water rights data was obtained from the Department of Water Resources website (WRD, 2015); this water rights mask was then coupled with the land cover mask to further restrict the available areas for potential vineyard development.

Data Transformation (Fuzzification)

The input datasets had various ranges and units, thus in order to bring the input data into a common scale the layers were transformed. The major classification functions used to transform the various input datasets included Gaussian function, exponential growth, and exponential decay. The Gaussian function has the following form:

$$f(x) = ae^{-\frac{(x-b)^2}{2c^2}} \qquad (5.3.)$$

where x is the input values, a is the upper bound of function, b is the position of the center of the peak and c is the width of the function curve (Figure 5.1.).

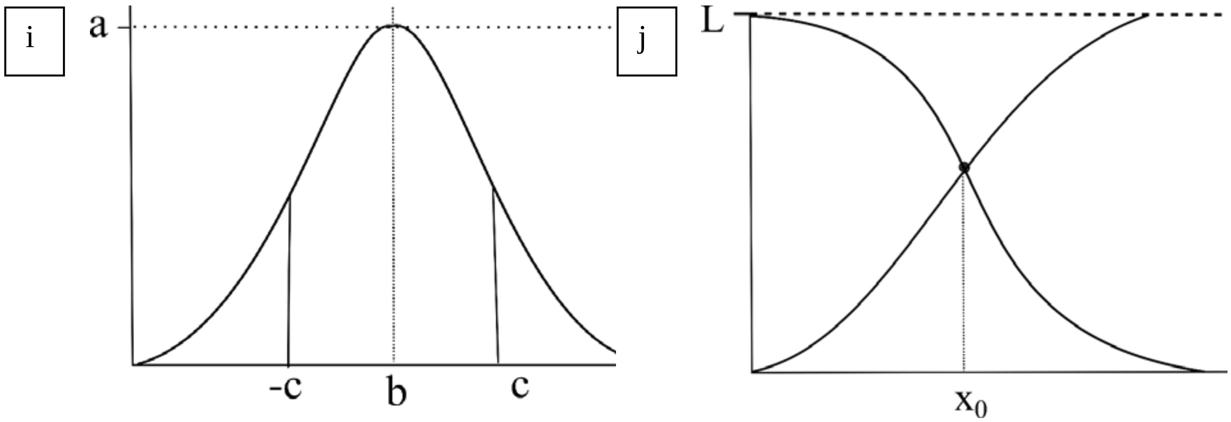

Figure 5.1. Schematic figure of a Gaussian function (where b is the position of the center of the peak and c is the width of the function curve) (i). The schematic figure depicting the logistic functions is located on the right, where x_0 is the x value of the mid-point (j).

The logistic function, which can either have a form of logistic growth or a logistic decay, generally has the following equation (Equation 5.4.):

$$f(x) = \frac{L}{1+e^{-k(x-x_0)}} \qquad (5.4.)$$

where e is the natural logarithm base; x_0 is the x value of the midpoint, L is the upper bound of the function, and k is the steepness of the function (Figure 5.1.).

The major input biophysical parameters were transformed using the Gaussian, logistic growth, and logistic decay functions discussed earlier. Later, a fuzzy overlay procedure was applied to combine input raster datasets together and obtain vineyard potential scores. Three key overlay methods employed in our study were fuzzy gamma, fuzzy sum, and fuzzy product. The overlay process using fuzzy gamma (Equation 5.5.) was developed based on the algebraic product of fuzzy sum and fuzzy product, but the fuzzy sum is raised to the power of γ and the fuzzy product is raised to the power of (1-γ) (ESRI, 2015).

$$\mu(x) = (FuzzySum)^{\gamma} * (FuzzyProduct)^{1-\gamma} \quad (5.5.)$$

The fuzzy sum overlay method adds the fuzzy scores of each input raster for each pixel; however, it does not use the algebraic method for adding the input layers (ESRI, 2015).

$$fuzzySumValue = 1 - product(1 - arg1, .., 1 - argn) \quad (5.6.)$$

The fuzzy product overlay method multiplies all input data layers for each individual pixel. The output of fuzzy product is usually smaller than all the inputs; when the number of input parameters is high the value of the output data layer can be quite small (ESRI, 2015).

$$fuzzyProductValue = product(arg1, \ldots, argn) \quad (5.7.)$$

The fuzzy gamma was mainly applied to develop topographic and weather potential scores, where γ was assumed to be 0.9 because it produces results thatare a combination of fuzzy sum and fuzzy product, and the fuzzy sum was applied to develop the soil potential scores. The main reason for applying the fuzzy sum to the overlay soil parameters is the wider margin of amendments that can be done to correct for minor departures in soil properties from the optimal ranges. The final vineyard potential was also computed using the fuzzy gamma method, with weather, topographic, and soil potential layers used to obtain the final vineyard potential scores.

Topographic fuzzification

The elevation data was initially transformed by a Gaussian function for elevations ranging from 0 m to 670 m (Table 5.3.), which was based on the classes suggested by Kurtural et al. (2007), where the highest-ranking elevations (259 m-393 m) were assigned as the peak of the function. The elevation suitability scores ranged from 0 to 1, where zero refers to least suitable areas based on their elevation and 1 refers to the locations with the most suitable areas regarding elevation.

Table 5.3. Elevation based on Kurtural et al. (2007), soil pH (White, 2009; Dry and Coombe, 2004), and soil texture rankings.

Elevation	
Elevation class (m)	**Class ranking**
>137	2
137-152	4
152-168	6
168-183	8
183-198	10
198-213	12
213-229	14
229-244	16
244-259	18
259-393	20
393-488	10
Soil pH	
pH	**Class ranking**
<=5, >=8.4	1
5.5-6.5, 8-8.3	2
6.5 - 8.0	3
Soil texture	
type	**Class ranking**
Sandy loam	4
Loam	4
Very fine sandy loam	4
Loam very fine sand	4
Coarse sandy loam	4
Silt loam	3
Loamy sand	3
Loamy fine sand	3
Loamy coarse sand	3
Silt	2.5
Silty clay loam	2
Silty clay	2
Clay loam	2
Sandy clay loam	2
Clay	1

The slope of each pixel was transformed based on a Gaussian function using class rankings of slopes developed by Jones et al. (2004). The function was applied to slopes ranging from 0-30 %, where the upper bound of function (Equation 5.3.) was defined at 10% slope because the 5-15% slope gets the highest preference based on previous studies (Jones et al., 2004). The aspect in each pixel was transformed based on class ranking reports obtained from Jones et al. (2004). A Gaussian function was used to transform the aspect to suitability scores ranging from 0 to 1, where the optimal aspect range (southern-facing slopes) was assigned as the upper bound of the Gaussian function (Equation 5.3.), and were assigned final scores of 1. The lowest suitability score refers to regions with northern-facing slopes; hence, these areas received final scores of 0.

Soil fuzzification

Several key soil parameters, such as available water holding capacity, soil drainage, soil organic matter, soil pH, depth to any restrictive layer, and soil texture, were obtained from the soil database (gSSURGO) for the study area. Among these parameters, soil pH, depth to any restrictive layer, and soil texture were selected for incorporation into the soil component of the system, and the rest of the dataset were used as auxiliary information for further analysis of the suitability of a specific land parcel. The soil pH for the study area was transformed by a Gaussian function that covered a range of 5 to 8.4, with optimum pH between 6.7 and 7.2 because this range make the micro and macro nutrients available to the roots (Table 5.3.).

The depth to any restrictive layer was transformed into a dataset ranging from 0 to 1, based on the classification reported by Yau et al. (2014) using a logistic growth function

(Equation 5.4.). This transformation required all regions with a shallow restrictive layer (<51 cm) be assigned a score of zero, because as the depth increases toward 1 m, the score also increases, and depths that are equal or greater than one meter are assigned a score of 1.

The soil texture classes for our study area were categorized into 5 major classes (Table 5.3.); these classes were then further transformed into a scale with a range from 0 to 1 using a logistic growth function. This transformation implied that, as the amount of clay in soil increases, the final score decreases due to its impact on the water retention and availability of water to the roots; hence, soils with sandy textures obtain higher scores than clayey or silty soils. This classification system is a useful tool for determining areas that may need extra soil amendment.

Weather fuzzification

Several bio-climatic indices were computed based on daily weather data provided by the UI GSM, which covered the 30-year period between 1983 and 2012. These included Growing Degree Days (GDD); the Huglin Index(HI); Biologically Effective Degree Days (BEDD); Frost Free Days (FFD); dynamic minimum temperature; Growing Season Temperature (GST); Length of Growing Season (LGS); Growing Season Suitability (GSS); Mean Thermal Amplitude (MTA); Latitude Temperature Index (LTI), the Hydrothermic Index (HyI), and the Cold Damage Index (CDI). The growing degree days or Winkler index (WI) (Winkler et al., 1974; Jones et al., 2010) takes into account the degree day units accumulated during the growing season with a base temperature of 10°C (Equation 5.8.). It is assumed that the growing season begins on April 1st and ends on October 31st (Winkler et al., 1974; Jones et al., 2010).

$$\sum_{Apr1}^{Oct31} \max[\left(\frac{[Tmax+Tmin]}{2}\right) - 10{,}0] \qquad (5.8.)$$

The GDD were then transformed into a scale ranging from 0 to 1, based on previous classifications reported by Jones et al. (2010). Jones et al. (2010) reported five main regions based on GDD values ranging from 850 to 2700, where values lower than 850 were considered too cold, and values higher than 2700 were considered too hot. For this study, the GDD range started at 850 and went up to the maximum range for the given region, which was 1389 GDD. For the transformation, a logistic growth function was used to convert the GDD scores into least favorable and optimal scores ranging from 0 to 1.

The Dynamic Minimum Temperature Index is a modification of the Minimum Temperature developed by Hidalgo (2002). The index was modified in order to account for the the dynamic nature of cold hardiness and frost risk as related to growing season and grapevine development. This index compared the daily minimum temperature against a threshold that varied from month-to-month, and reported the number of days that the minimum air temperature dropped below the threshold value. The dynamic minimum temperature scores where then transformed into a scale of 0 to 1 via use of a logistic decay function. The function assigns the highest score (1) to zero incidents and declines as the number of incidents increases to the lower threshold value of 60. This lower boundary of the function was set to a value of 60 based on the average highest dynamic minimum temperature value for the AVAs in our study area.

Frost Free Days represent the length of the growing season in terms of the number of days between the last frost in spring and the first frost in fall (Magarey et al., 1998). The FFD scores were transformed using a logistic growth function, with a score of zero set for FFD values of 150 days or less, based on previous reports by Yau et al. (2014); they gradually increased to a score of 1 for FFDs reaching 180 days or more.

The Huglin Index reflects heat accumulation during the growing season of a particular region (HI; Huglin, 1978), using a day-length coefficient to adjust the accumulated daily heat units based on the latitude (Equation 5.9.).

$$\sum_{Apr1}^{Sep30} max\left(\left[\frac{[Tmean-10]+[Tmax-10]}{2}\right],0\right)\times k \qquad (5.9.)$$

where k is the latitude/day length adjustment index, and 10 indicates the threshold temperature above which grapes are considered active. HI classes were previously established by Jones et al. (2010), and were used to fit a logistic growth function to the HI values in our study. The function assigns a score of zero to HI ≤ 1200 and then gradually increases the score to 1 when the HI reaches 2601.

Biologically effective degree days also deals with heat accumulation during the growing season (Gladstones, 1992), but also considers a diurnal range adjustment or a latitude/day-length adjustment, and basically eliminates heat accumulation above 19°C or below 10°C (Equation 5.10.)

$$\sum_{Apr1}^{Oct31} \min\left[\left(\max\left[\left(\frac{[Tmax+Tmin]}{2}\right)-10,0\right]\right),9\right]\times DTRadj\times k \qquad (5.10.)$$

$$\text{Where } DTR\ adj = \begin{cases} 0.25[DTR-13].[DTR]>13 \\ 0,10<[DTR]<13 \\ 0.25[DTR-10].[DTR]<10 \end{cases}$$

where k is an adjustment for latitude/day length, DTR is Diurnal Temperature Range, DTR_{adj} is the adjusted Diurnal Temperature Range based on different ranges of air temperature. The BEDD classes (Jones et al., 2010) were then transformed using a logistic growth function where any BEDD value of 1000 assigned a score of 0 and then the scores gradually increased to a score of 1 as BEDD reaches a value of 1883.

The Latitude Temperature Index (LTI) (Jackson and Cherry, 1988) is computed by multiplying the mean temperature of the warmest month by 60 - the latitude. This index was transformed using a logistic growth function that assigned a score of zero to LTI values of zero, with the scores gradually increasing to 1 when the LTI values reached 195.

The Growing Season Suitability index (GSS) (Malheiro et al., 2010; Santos et al., 2012b) reports the ratio of the number of days for which the daily temperature is higher than 10°C to the total number of days between April 1st and September 30th. Since this index reports a ratio and all our values were already between 0 and 1, no transformation was applied. The Growing Season Temperature (GST) (Jones, 2005a) reports the average daily temperature for a growing season of April to October. This index was transformed using a logistic growth function that would assign a score of 0 to GST values lower that 13°C (Jones et al., 2010) up to a score of 1 for GST values of 18°C.

The Length of Growing Season (LGS) (Jackson, 2008) is an index for counting the number of days when the mean daily air temperature from April to October is above 10°C. LGS values were transformed using a logistic growth function starting at 150 days for an index of 0, and gradually increasing to an index of 1 when the LGS reached 180 days.

The Hydrothermic Index (HyI) (Branas et al., 1974) is based on precipitation and air temperature, and calculates the relative risk of certain diseases such as downy mildew as well as water availability. This index was transformed to a range between 0 and 1 using a logistic decay function.

The Mean Thermal Amplitude (MTA) (Mullins et al., 1992; Ramos et al., 2008) is based on the difference between the daily maximum and minimum air temperatures during the month of September. For our study, the MTA was transformed into a scale ranging from 0 to 1 using a logistic growth function, for which MTA value of 5.7°C were assigned a score of 0, and gradually increased to a score of 1 when MTA values reached 20.8°C.

The grapevine cold damage index is based on modifications of the cold hardiness model developed by Ferguson et al. (2011). The cold damage index determines the number of times the daily minimum temperature drops below a predicted temperature at which 50% of buds are injured due to freeze (LT_{50}) (Ferguson et al., 2011; Ferguson et al., 2014). This index was transformed using a logistic decay function, and CDI values of 0 were assigned a score of 1, gradually decreasing to a score of 0 as the value of the CDI increased to a cut-off threshold of 40 events. This cut-off threshold was obtained using the average CDI over a period of 30 years for all the AVAs.

Fuzzy Logic Implementation and Vineyard Potential Scores

The application of fuzzy logic for spatial suitability analysis was utilized in several stages of our study. During the initial stage, the data layers were transformed into a layer with values ranging from 0 to 1. In the next stage the weather, topography, and soil potential scores were computed as the three main components for determining a vineyard's potential. To determine topographic potential, the slope, aspect, and elevation data layers were combined using fuzzy gamma (γ=0.9). The weather potential was determined by applying the fuzzy gamma function (Equation 5.5.) to various bio-climatic indices, and different combinations were defined based on 6 different scenarios (Table 5.4.). The scenarios were based on the recommendations from previous studies (Table 5.4) and also some hypothesis testing. Lastly, the soil potential was developed by applying the fuzzy sum function (Equation 5.6.) to the soil pH, soil depth, and soil texture data layers. During the final stage the vineyard potential scores were determined by combining the weather, soil, and topographic potential scores (a fuzzy gamma (γ=0.9) function was applied to combine these three scores).

Table 5. 4. Weather scenarios based on various bio-climatic indices.

Scenario	Bio-climatic indices*	Based on
1	GDD, HI, BEDD,GST	Jones et al., 2010
2	GDD, FFD	Yau et al., 2013
3	LTI, HI	Jackson and Cherry, 1988
4	HI, GDD, LTI, FFD, MTA	
5	GDD, FFD, GST, LTI, LGS, DyMin. Temp.	
6	BEDD, DyMin. Temp., CDI, FFD, GDD, GSS, GST, HI, HyI, LGS, LTI, MTA	

*Growing Degree Days (GDD); the Huglin Index (HI); Biologically Effective Degree Days (BEDD); Growing Season Temperature (GST); Frost Free Days (FFD); Latitude Temperature Index (LTI); Mean Thermal Amplitude (MTA); Length of Growing Season (LGS); Cold Damage Index (CDI); Dynamic Minimum Temperature (DyMin. Temp.); Growing Season Suitability (GSS); Hydrothermic Index (HyI).

For the interpretation of our results, the output layers were first re-classified into five main classes based on the FAO land evaluation system (FAO, 1976). This step, referred to as de-fuzzification, was applied in order to make the visualization of the fuzzy logic outputs more intuitive for users. The final output datasets for each scenario also featured five major classes, including S1, S2, S3, N1, and N2, and vineyard potential was organized within the five major classes, assuming an equal interval (Table 5.5.; Figure 5.2.).

Table 5. 5. Major classes for determining vineyard potential.

Suitability range	Class	Linguistic equivalent
0.8-1	S1	High potential
0.6-0.79999	S2	Moderate potential
0.4-0.59999	S3	Low potential
0.2-0.39999	N1	No potential
0-0.199999	N2	Not applicable

Evaluation

The evaluation of vineyard potential scores was conducted for both ideal locations and non-ideal locations. For ideal locations, evaluation included obtaining vineyard potential scores for established vineyards and determination of the percent area of each vineyard for each potential class. In addition, the locations of several premium grape-producing vineyards within Washington were obtained and their vineyard potential scores were used to evaluate the general performance of our land assessment system. These premium vineyards were located in eight different American Viticultural Areas (AVAs); and are considered premium due to a combination of several factors such as biophysical and quality traits; the average vineyard potential score for each premium vineyard was computed for every scenario. This method was also used to separate our study area into three main classes: a) areas with a vineyard potential score higher than the average potential score of the premium vineyards; b) areas with vineyard potential scores below the average potential score of premium vineyards; and c) areas with restricted application due to limitations imposed by land cover or water rights.

In this study, final vineyard potential scores were also assessed for locations that lacked certain criteria required to support a successful, sustainable vineyard. The evaluation of non-ideal sites was conducted by applying a conditional algorithm to several datasets and developing a final dataset that classified the study area into several regions. To develop the conditional restrictions, five layers were incorporated into the conditional statement, including elevation, slope, depth to any restrictive layer, FFD, and GDD (Table 5.6.). These layers were selected because their cut-off thresholds were regarded as critical to vineyard establishment. For example, slopes steeper than 30% severely limit vineyard development.

Table 5. 6. Summary of rules applied for evaluation of non-ideal sites.

Layers	Critical range
Elevation	> 1000 m
Slope	> 30 %
Frost Free Days (FFD)	< 150 days
Growing Degree Days (GDD)	< 875 GDD
Depth to any restrictive layer in soil	< 51 cm

Our main objective in evaluating non-ideal sites was to acknowledge that computed potential scores accurately represent reality and that our methodology had the ability to capture both high and low scores with high spatial accuracy. The method employed in all six scenarios and the percentage for each class range was reported accordingly.

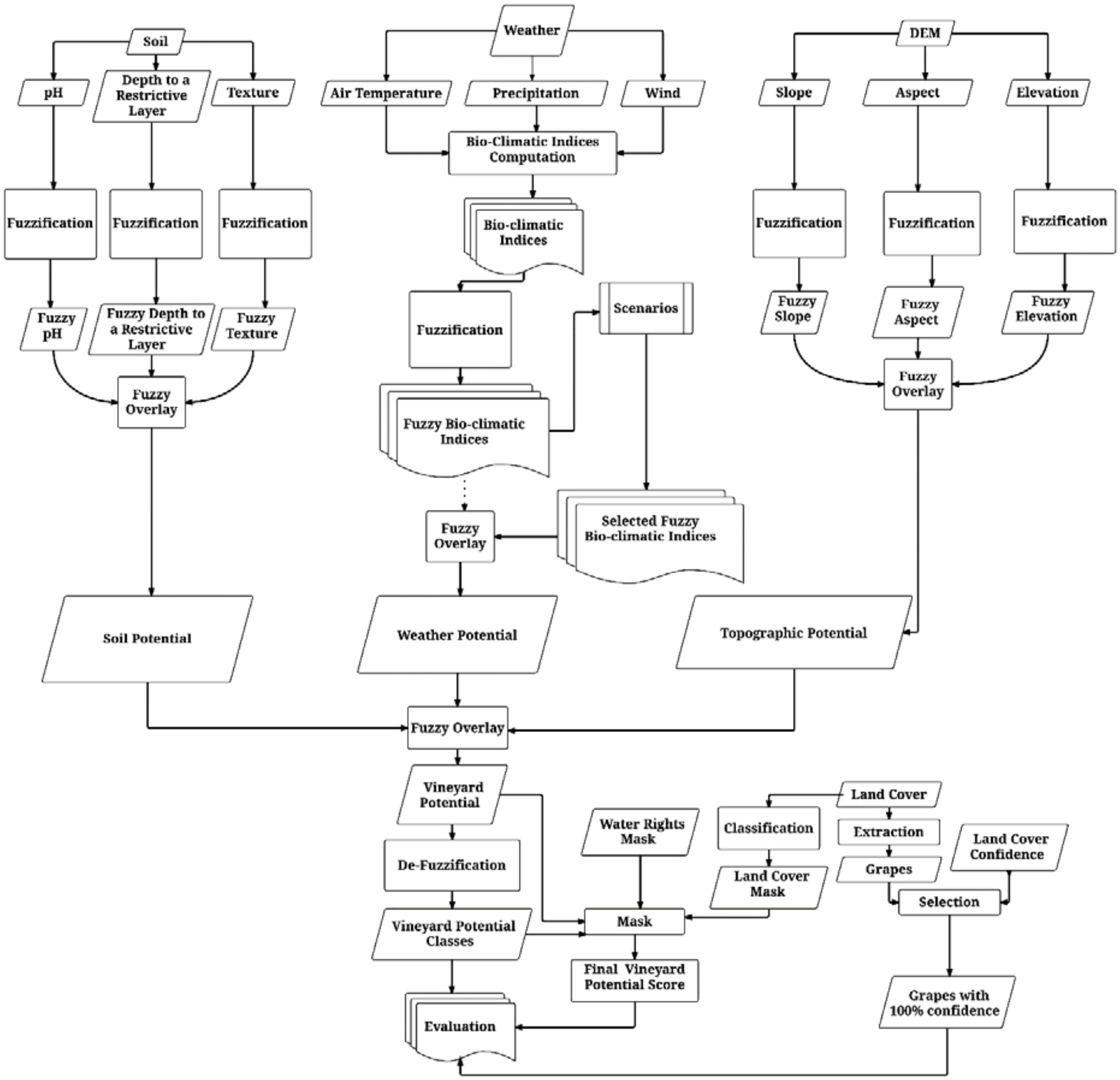

Figure 5. 2. Workflow of the overall study method.

Results and Discussion

Our vineyard potential scores were computed and reported for the study area using a fuzzy rule-based system. The potential scores ranged from 0 to 1; regions with a potential score of 0 represented the “not applicable” class (Table 5.7.), and a score of 1 meant that there was a great potential for grapevine growth and development in a particular location. The percentage for each class was then reported for each scenario.

When restrictive land cover or lack of water rights were not considered, scenario 6 (Table 5.4.) had the smallest area (20 %) in the “high potential” class, whereas scenario 2 (Table 5.4.) had the greatest area (34.3 %) in the “high potential” class. Since the difference between the scenarios is solely based on the difference in their weather components, it can be interpreted that relying only on GDD and FFD for the computation of the weather components might be contributing larger areas being categorized as “high potential” in scenario 2. However, in scenario 6, there are more bio-climatic indices contributing to the weather component, possibly resulting in a smaller percentage of the area being categorized as “high potential.” Scenario 6 not only had the smallest area of “high potential” land, but also had the greatest amount of land (26.8 %) categorized as “not applicable” (Table 5.7.).

Table 5. 7. Vineyard potential classes for all areas.

Scenario*	Not applicable (% area)	No potential (% area)	Low potential (% area)	Moderate potential (% area)	High potential (% area)
1	4.0	17.4	25.1	27.2	26.4
2	11.3	14.4	15.1	24.9	34.3
3	26.7	1.4	11.2	28.2	32.4
4	26.7	1.3	11.6	29.8	30.6
5	11.0	18.4	15.9	28.2	26.4
6	26.8	5.1	18.7	29.4	20.0
Average	17.8	9.7	16.2	28.0	28.4

*See Table 5.4. for a complete list of weather scenarios

The vineyard potential scores for established vineyards in our study area (a total of 40,185 ha) were obtained for each scenario, and the results revealed that 97.3 % of the vineyards were located in “high potential” regions, 2.7 % of the vineyards were located in “moderate potential” regions, and none were located in the “low potential” regions (Table 5.8.).

Table 5. 8. Vineyard potential classes for grape land cover based on CDL for all scenarios.

Scenario*	Moderate potential (% area)	High potential (% area)
1	3.9	96.1
2	2.7	97.3
3	2.6	97.4
4	3.0	96.9
5	3.7	96.3
6	0.0	100.0
Average	2.7	97.3

*See Table 5.4. for a complete list of weather scenarios

When restrictive land covers or lack of water rights was taken into consideration, our results indicated a total area of 78.5 % was masked (Table 5.9.; Figure 5.3.). On average, each of the scenarios had an area of 11.4 % with a vineyard potential score greater than 0.8, classifying them as “high potential.” Once again, scenario 6 again had the smallest area (9.3%) classified as “high potential,” but it also had the greatest area (7.2%) classified as “moderate potential,” adding up to an area of 16.5% with potential scores higher than 0.6, and also the greatest area (3.4%) classified as “low potential.” Scenario 3 (Table 5.4.) had the greatest area (13.5%) in the “high potential” class, but also had the smallest area (5.5%) with “moderate potential,” adding up to an area of 19% with a potential score higher than 0.6, and the smallest area (1.3 %) classified as “low potential.”

Table 5. 9. Vineyard potential classes post-exclusion of the restrictive areas (total study area is 19,070,000 ha).

Scenario*	Restricted (% area)	Not applicable (% area)	No potential (% area)	Low potential (% area)	Moderate potential (% area)	High potential (%area)
1	78.5	0.1	0.8	2.5	6.0	12.1
2	78.5	0.4	1.3	2.6	5.6	11.6
3	78.5	0.9	0.2	1.3	5.5	13.5
4	78.5	0.9	0.2	1.8	6.8	11.7
5	78.5	0.4	1.6	2.8	6.4	10.2
6	78.5	0.9	0.7	3.4	7.2	9.3
Average	78.5	0.6	0.8	2.4	6.2	11.4

*See Table 5.4. for a complete list of weather scenarios

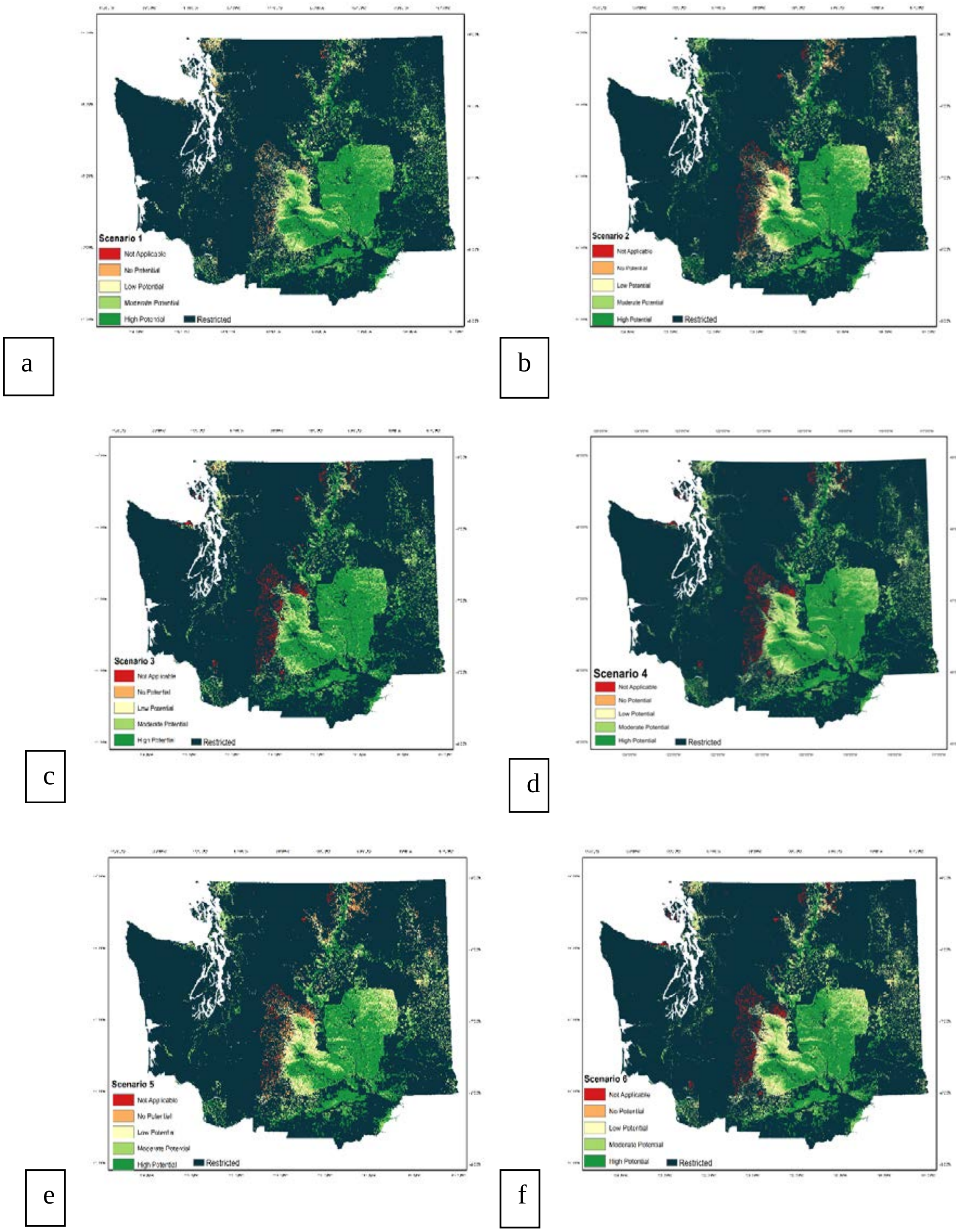

Figure 5. 3. Main vineyard potential classes for scenario 1(a); scenario 2(b); scenario 3(c); scenario 4(d); scenario 5(e); scenario 6(f). For a complete list of scenarios see Table 5.4.

Ground truthing for premium vineyards

The evaluation of established vineyards in our study area indicated that the majority are located in “high potential” regions; therefore, future potential vineyards should also be located in areas categorized as “high potential.” However, there is a substantial sub-class variation within vineyards categorized as “high potential,” since their classification scores ranged from 0.80001 to 1. Therefore, the calculation of vineyard potential for several vineyards regarded as “premium” is a good benchmark for determining the best locations for vineyard establishment (Figures 5.4. and 5.5.; Table 5.10).

Table 5. 10. The potential score of premium vineyards located in various American Viticultural Areas (AVAs).

		Scenarios*					
Vineyard ID	**American Viticultural Areas**	**1**	**2**	**3**	**4**	**5**	**6**
1	Columbia Gorge	0.86	0.87	0.87	0.87	0.86	0.84
2	Columbia Gorge	0.71	0.77	0.76	0.76	0.73	0.69
3	Columbia Valley	0.99	0.99	0.99	0.99	0.99	0.98
4	Columbia Valley	0.85	0.86	0.86	0.86	0.86	0.84
5	Horse Heaven Hills	0.96	0.96	0.96	0.96	0.96	0.95
6	Puget Sound	0.70	0.88	0.73	0.80	0.83	0.72
7	Red Mountain	0.82	0.84	0.84	0.83	0.83	0.81
8	Rocks District	0.82	0.85	0.85	0.84	0.85	0.81
9	Rocks District	0.85	0.86	0.86	0.86	0.86	0.85
10	Rocks District	0.89	0.91	0.91	0.90	0.91	0.89
11	Walla Walla	0.85	0.87	0.87	0.86	0.86	0.84
12	Walla Walla	0.94	0.95	0.95	0.95	0.95	0.93
13	Walla Walla	0.87	0.89	0.89	0.89	0.89	0.86
14	Walla Walla	0.87	0.88	0.88	0.88	0.88	0.86
15	Walla Walla	0.88	0.91	0.91	0.90	0.91	0.87
16	Walla Walla	0.83	0.85	0.85	0.85	0.85	0.81
17	Walla Walla	0.90	0.93	0.93	0.93	0.93	0.89
18	Walla Walla	0.92	0.94	0.94	0.94	0.93	0.91
19	Walla Walla	0.92	0.94	0.94	0.94	0.94	0.91
20	Walla Walla	0.95	0.97	0.97	0.97	0.97	0.94
21	Walla Walla	0.89	0.90	0.90	0.90	0.90	0.89
22	Yakima Valley	0.89	0.88	0.91	0.87	0.85	0.84
	Average	0.87	0.90	0.89	0.89	0.89	0.86
	SD	0.07	0.05	0.06	0.06	0.06	0.07

*See Table 5.4. for a complete list of weather scenarios

The average score for premium vineyards ranged from 0.86 to 0.9. This variability across the different regions can be attributed to various environmental factors and differences in management strategies that may be able to compensate for a lower suitability score. In addition, some of the assumptions and input data might include some associated uncertainty resulting in differences in vineyard potential scores. The premium vineyard scores were used as a threshold to further divide the “high potential” class (Table 5.11.); the premium grape growing regions, on average, covered 6.3% of the study area (Table 5.11.), with scenario 4 having the smallest premium area (5.1%). An average area of 15.1% meant that a score was below the premium threshold (Table 5.11.).

Table 5. 11. Vineyard potential classes based on premium vineyard potential scores.

Scenario	Restricted (% area)	Less Suitable (% area)	Suitable (% area)
1	78.5	13.5	8.0
2	78.5	16.0	5.5
3	78.5	13.9	7.5
4	78.5	15.5	5.9
5	78.5	16.4	5.1
6	78.5	15.4	6.0
Average	78.5	15.1	6.3

These categories help the potential users such as growers, decision makers, and researchers to gain a better understanding of the region and to define the premium grape growing regions and their associated land use characteristics. However, if a site is categorized as a moderate potential due to its environmental limitations, a complete onsite assessment should be conducted and soil and water samples should be obtained and analyzed prior to making a decision with respect to the suitability; this is even required for the sites with a “high potential” score. In addition, vineyard management practices such as installation of drainage, adding manure to the soil, and using heaters along with wind machines can to a limited degree offset some of the environmental factors such as soil poor drainage, low soil organic matter,and the risk of frost that can potentially limit vineyard establishment.

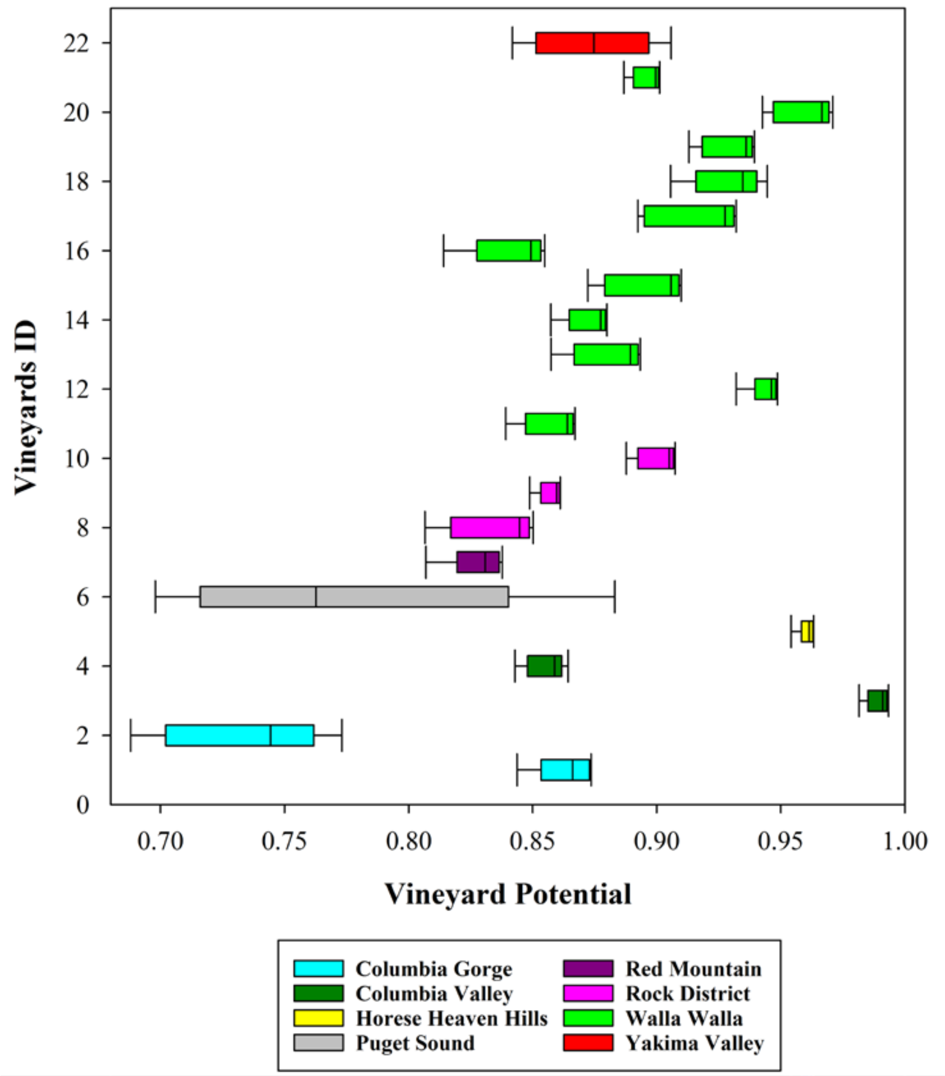

Figure 5. 4. The range of potential scores across all scenarios for each individual premium vineyard (See Table 5.10. for the list of vineyards).

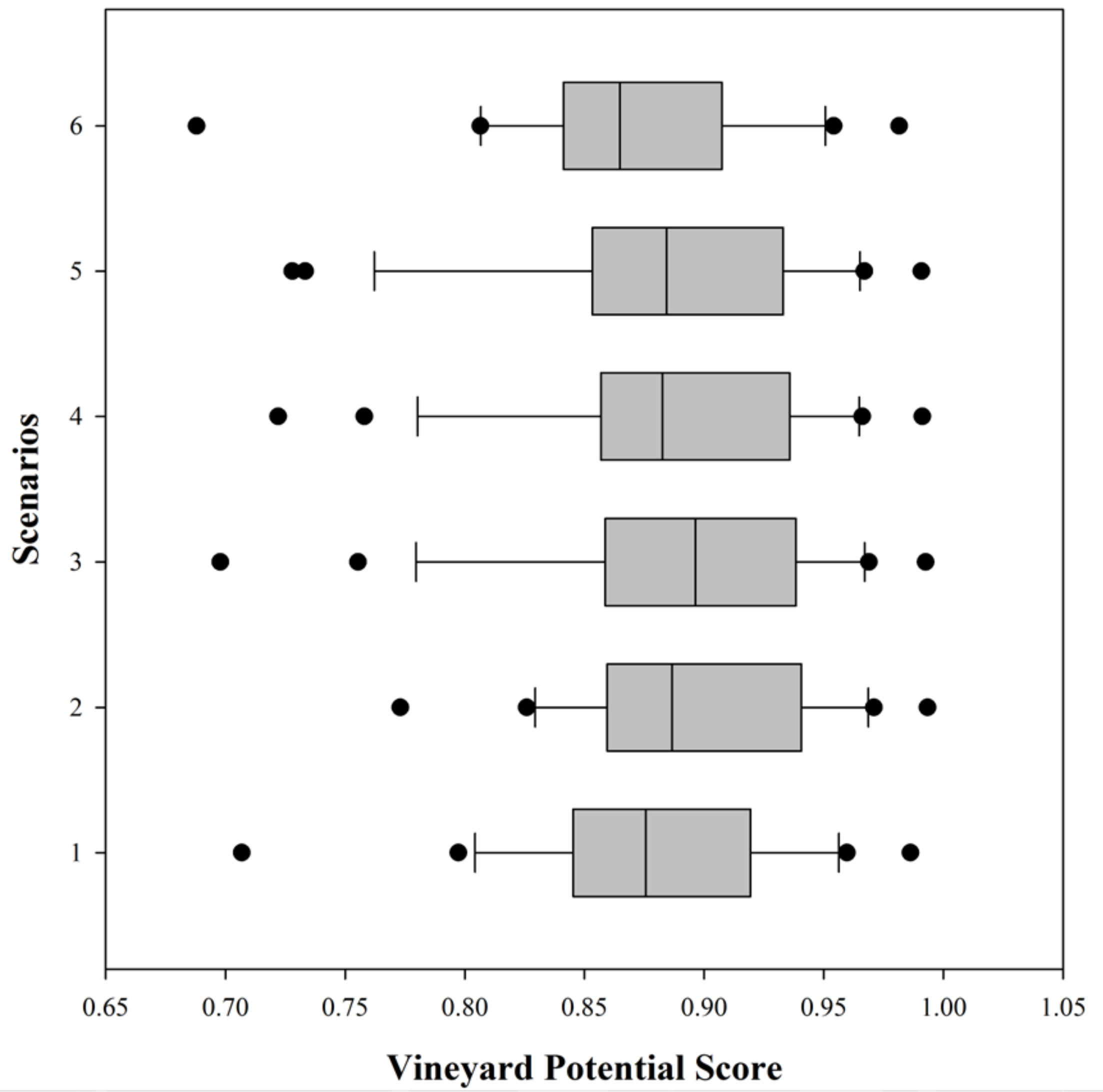

Figure 5. 5. Vineyard potential scores of the premium vineyards, separated for various scenarios (for a complete list of scenarios see Table 5.4.).

Ground truthing for non-ideal regions

The results of our non-ideal evaluation indicated that, as the number of restricting parameters increases, the probability of pixels having a high vineyard potential score decreases. Applying the restriction rules classified the region into six classes (Figure 5.6.); for regions where all five parameters did not meet the requirements, none of the pixels were classified as "high potential." In areas where only one of the restrictive parameters was outside of the desired range, an average of 13.7% of the pixels had a vineyard potential score above 0.8 (Table 5.12.). It should be noted that the usually combination of several biophysical factors leads to a low score for a pixel.

Table 5. 12. Vineyard potential classes based on non-ideal site evaluation.

One conditional restriction (% area)					
Scenario	Not applicable	No potential	Low potential	Moderate potential	High potential
1	71.3	0.5	2.5	8.8	16.9
2	71.4	1.5	6.5	14.4	6.2
3	71.5	0.2	1.6	7.8	18.8
4	71.5	0.1	2.5	10.2	15.7
5	71.3	0.9	4.2	10.7	12.9
6	71.5	0.6	4.4	11.8	11.6
Two conditional restrictions (% area)					
Scenario	Not applicable	No potential	Low potential	Moderate potential	High potential
1	82.7	0.6	3.8	8.2	4.8
2	82.8	0.2	5.8	6.4	2.9
3	82.9	0.2	2.4	7.8	6.6
4	82.9	0.4	3.7	9.1	3.9
5	82.8	2.6	5.7	6.8	2.1
6	83.0	1.4	6.5	7.4	1.7
Three conditional restrictions (% area)					
Scenario	Not applicable	No potential	Low potential	Moderate potential	High potential
1	91.8	1.6	3.4	2.8	0.3
2	92.8	3.8	2.7	0.6	0.1
3	94.2	0.2	1.5	3.2	0.9
4	94.2	0.3	2.0	3.2	0.2
5	92.6	4.3	2.3	0.8	0.0
6	94.3	1.1	3.7	0.9	0.0
Four conditional restrictions (% area)					
Scenario	Not applicable	No potential	Low potential	Moderate potential	High potential
1	94.1	2.5	2.5	0.9	0.0
2	96.1	3.2	0.8	0.0	0.0
3	97.8	0.1	0.7	1.2	0.1
4	97.9	0.2	0.9	1.0	0.0
5	95.7	3.7	0.6	0.0	0.0
6	97.9	0.6	1.4	0.1	0.0
Five conditional restrictions (% area)					

Scenario	Not applicable	No potential	Low potential	Moderate potential	High potential
1	96.8	1.7	1.2	0.3	0.0
2	98.1	1.5	0.3	0.0	0.0
3	99.0	0.0	0.4	0.5	0.0
4	99.3	0.6	0.1	0.0	0.0
5	98.0	1.8	0.2	0.0	0.0
6	99.1	0.7	0.2	0.0	0.0

Our results also indicated that when only one conditional restriction was present, scenario 2 had a lower percentage (6.2 %) of its area with vineyard potential scores higher than 0.8. This may have been due to the fact that scenario 2 was developed based on GDD and FFD (Yau et al., 2013); thus, the results may have been related to the fact that GDD and FFD were among the input layers used in applying the restrictions. However, when several restrictions exist, scenario 5 and scenario 6 have the smallest percentage of areas with vineyard potential scores above 0.8 (Table 5.12.), which can be due to several factors, such as the transformation scheme and the applied fuzzy rule set. It appears that the inclusion of certain bio-climatic indices for calculation of weather component results in a smaller percentage of areas with scores of “high potential.” Since air temperature was the key weather parameter used for our calculation of the bio-climatic indices, then other factors such as topography, time of day, time of season, solar radiation, wind speed, and relative humidity can potentially influence the air temperature and air movement in a region, which can indirectly impact the bio-climatic indices and resulting vineyard potential scores. It is highly recommended that users of vineyard potential scores always obtain additional information regarding underlying parameters contributing to the suitability of a particular region for growing grapevines. Some of these critical parameters such as elevation or FFD can potentially be transformed into a true-false dataset that enables the narrowing down of suitable areas for instance having a mask for elevations that are higher than 1200 m.

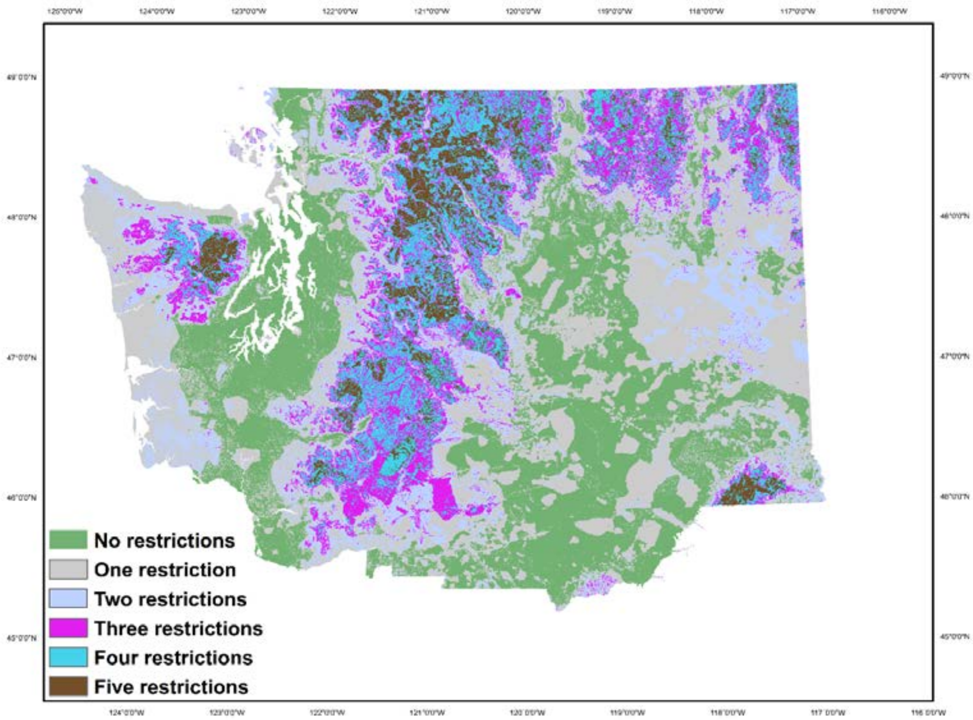

Figure 5. 6. The conditional restrictive map used to evaluate the performance of non-ideal locations.

Based on our evaluation results, non-ideal score pixels with low vineyard potential scores appear to have a variety of restricted environmental factors, and should be of concern to users. A location that has a restricting parameter may still be potentially suitable. With proper management and economic investment, a land parcel might be made into a successful vineyard. Yau (2011) reported soil and topographic suitability for individual AVAs located in inland PNW. The weather suitability component for that study was mainly focused on the classification of calculated GDD, FFD, and LTI in to high, medium, and low levels; however, their model was primarily concerned with edaphic and topographic parameters, and vineyard potential scores were not explicitly discussed.

Our assessment results indicated that the premium vineyards located in Western Washington have lower vineyard potential scores than those vineyards located in Eastern

Washington. This is mainly due to the fact that our transformation of the input data layers were primarily adjusted for the regions located in Eastern Washington; in addition the classification of GDD values can also contribute to lower scores associated with the western Washington regions. However, when the goal is to compare regions across a large-scale study area, then the homogeneity of the method used for development of the suitability analysis is imperative. The differences between the scores gathered from Western and Eastern Washington show that there are substantial differences between these two grape-growing regions due to their local environmental conditions which must be addressed.

No data layers representing the variability in management practices were used in our study; thus, in order to cluster the study areas based on various management strategies used in different regions, new databases are required. There is a need for local data collection and development of a statewide online database system that can be used by grape growers and vineyard managers. There is also a need for the development of a system that can record phenological events for each of the grape varieties grown in a specific region. Such a system could be used to update the formulation of relevant bio-climatic indices, as well as a stepping-stone to further the development of a comprehensive analytics platform based solely on the behavior of grape cultivars in a specific region.

In grape production, not only grape quantity is important, but also grape quality; therefore, the development of a land assessment system based on vineyard potential scores is more complicated than those used for other crops. Thus, there is great need for development of a site evaluation technique that can adjust vineyard potential scores based on the qualitative traits of grapes, including brix, total acid, and the anthocyanins of red cultivars. Coupling such a qualitative land assessment with a crowd sourcing system that reports consumer preferences for specific wines and vintages in a specific AVA is a potentially beneficial advancement for use in these types of land assessment systems. Although, it should be noted that wine quality is influenced by the winemaking techniques and also the wine might be made of grapes that come from regions other than the wine is produced in, this makes it even harder to track down the grapes quality based on the wine.

Future Work

Expert knowledge is an influential factor (Morlat and Lebon, 1992; Carey et al., 2007; Perrot et al., 2015) in vineyard management and strategy. The ability to fully acquire this expert knowledge is an integral part of land assessment systems; surveys can be developed and implemented to obtain the insight necessary for establishment of a relative weighting system. Weighting systems are used to express the importance or preference of each factor relative to other factors that may impact the overall performance of a grapevine. One method that can be used to apply the requisite expert knowledge on the fine-tuning of land assessment systems is the analysis hierarchy process (AHP) (Saaty, 1980; Saaty, 2008; Lee and Lee, 2010; Zhang, 2009; Wu, 1998; Reza, 2005). AHP is based on the prioritization of various contributing factors in a system, and the subsequent conduction of pairwise comparison between pairs of factors. It is an alternative method for determining the relative importance of various input layers and then calculating the weighting matrix based on the results. Another method that can be explored is the application of remote-sensing techniques for precision viticulture (Homayouni et al., 2008; Santesteban et al., 2013; Badr and Hoogenboom, 2013; Couleon-Leroy et al., 2013; Badr et al., 2015; Vaudour et al., 2015). The outcomes of remote-sensing techniques, such as time of phenological event, vine vigor, and vine stress status, can be further integrated into land assessment systems.

Finally, any decision regarding vineyard potential should be based on the tradeoffs between marketable grape production and sustainable management strategies, in order to guarantee sustainable productions that will also provide long-term economic benefits.

Conclusions

We conducted spatial land-assessment using biophysical models and fuzzy logic to develop vineyard potential scores for a study area located in the Pacific Northwest region of the U.S. Our results indicated that, on average, 11.4% of the study area had high vineyard potential score, with 97.3% of previously established vineyards located in high potential regions.

References

Abatzoglou, J. T. (2011). Development of gridded surface meteorological data for ecological applications and modelling. International Journal of Climatology, 33(1), 121–131.

Anderson, J. D., Jones, G. V., Andrew, T., Hall, A., and Throught, C. T. (2012). Analysis of viticulture region climate structure and suitability in New Zealand. Journal International des Sciences de la Vigne et du Vin, 46(3), 149–145.

Avellan, T., Zabel, F., and Mauser, W. (2012). The influence of input data quality in determining areas suitable for crop growth at the global scale–a comparative analysis of two soil and climate datasets. Soil Use and Management, 28(2), 249-265.

Badr, G., and Hoogenboom, G. (2013). Estimating the growing season length using remotely sensed based vegetation indices: a case study for Washington State vineyards. 2013 American Society of Agricultural and Biological Engineers International Meeting. http://doi.org/10.13031/aim.

Badr, G., Hoogenboom, G., Davenport, J., and Smithyman, J. (2015). Estimating growing season length using vegetation indices based on remote sensing: A case study for vineyards in Washington. Transactions of the ASABE, 58, 3, 551-564.

Boryan, C., Yang, Z., and Di, L. (2012). Deriving 2011 Cultivated Land Cover Data Sets Using USDA National Agricultural Statistics Service Historic Cropland Data Layers. Proc. IGARSS 2012 Conf., Munich, Germany, July 23-26, 2012.

Boryan, C., Yang, Z., Mueller, R., and Craig, M. (2011). Monitoring US Agriculture: The US Department of Agriculture, National Agricultural Statistics Service Cropland Data Layer Program" Geocarto International 26(5): pp. 341 –358.

Braimoh, A. K., Vlek, P. L. G., and Stein, A. (2004). Land evaluation for maize based on fuzzy set and interpolation. Environmental Management, 33(2), 226–238.

Carey, V., Archer, E., Barbeau, G., and Saayman, D. (2007). The use of local knowledge relating to vineyard performance to identify viticultural terroirs in Stellenbosch and surrounds. In: Nuzzo, V., Giorio, P., Giulivo, C. (Eds.), Proceedings of the International Workshop on Advances in Grapevine and Wine Research. International Society Horticultural Science, Leuven 1, pp. 385–391.

Chang, L., and Burrough, P. A. (1987). Fuzzy reasoning: A new quantitative aid for land evaluation. Soil Survey and Land Evaluation, *7*, 69–80.

Coulon-Leroy, C., Charnomordic, B., Rioux, D., Thiollet-Scholtus, M., and Guillaume, S. (2012). Prediction of vine vigor and percosity using data and knowledge-based fuzzy interface systems. J. Int. Sc. Vigne Vin., 46, 185-205.

Coulon-Leroy, C., Charnomordic, B., Thiollet-Scholtus, M., and Guillaume, S. (2013). Imperfect knowledge and data-based approach to model a complex agronomic feature—Application to vine vigor. Computers and Electronics in Agriculture, 99, 135–145.

Coulon-Leroy, C., Charnomordic, B., Thiollet-Scholtus, M., and Guillaume, S. (2014). Fuzzy Modeling of a Composite Agronomical Feature Using FisPro: The Case of Vine Vigor. In A. Laurent, O. Strauss, B. Bouchon-Meunier, & R. R. Yager (Eds.), Information Processing and Management of Uncertainty in Knowledge-Based Systems (pp. 127–137). Springer International Publishing.

Daly, C., Halbleib, M., Smith, J.L., Gibson, W.P., Doggett, M.K., Taylor, G.H., Curtis, J., and Pasteris, P.A. (2008). Physiographically-sensitive mapping of temperature and precipitation across the conterminous United States. International Journal of Climatology, 28, 2031–2064.

Das, P., and Sudhakar, S. (2014). Land Suitability Analysis for Orange and Pineapple: A Multi Criteria Decision Making Approach Using Geo Spatial Technology, Journal of Geographic Information System, 6 (1), 40-44.

Deloire, A., Prévost, P., and Kelly, M. (2008). Unravelling the terroir mystique—an agro-socio-economic perspective. In: CAB Reviews: Perspectives in Agriculture, Veterinary Science, Nutrition and Natural Resources, 3, No. 032.

Dougherty, P. H. (2012). The Geography of Wine: Regions, Terroir and Techniques. Springer.

Dry and Coombe (eds). (2004). Viticulture Volume 1 – Resources. 2nd ed. Winetitles. Adelaide, SA. 255p.

Dry, P.R. and Smart, R.E. (1988). Vineyard site selection: in Coombe, B.G. and Dry, P.R.(eds.), Viticulture; Winetitles, Adelaide, Australia.

ECY (Department of Ecology State of Washington Website).(2015). http://www.ecy.wa.gov/programs/wr/rights/water-right-home.html, last accessed March 3, 2016

ESRI. (2015). ArcGIS 10.2. Desktop. Redlands, CA: Environmental Systems Research Institute.

FAO. (1976). A Frame Work for Land Evaluation, Soils Bulletin No. 32. Rome: UNO-FAO.

Ferguson, J. C., Tarara, J. M., Mills, L. J., Grove, G. G., and Keller, M. (2011). Dynamic thermal time model of cold hardiness for dormant grapevine buds. Annals of Botany, 107(3), 389–396.

Ferguson, J. C., Moyer, M. M., Mills, L. J., Hoogenboom, G., and Keller, M. (2014). Modeling Dormant Bud Cold Hardiness and Budbreak in 23 Vitis Genotypes Reveals Variation by Region of Origin. American Journal of Enology and Viticulture, 32pp.

Fisher, P. (1996). Boolean and fuzzy regions, in: P.A. Burrough, A. Frank (EDs.), Geographic Objects with Indeterminate Boundaries, Taylor and Francis Publishing, London, UK, 87-94pp.

Fragoulis, G., Trevisan, M., Capri, E., Guardo, A., and Sorce, A.(2007). EIOVI: an indicator for the environmental impact of organic viticulture based on a fuzzy expert system. In Re, A. A. M. Del; Capri, E.; Fragoulis, G.; Trevisan, M. (Eds.) In 13th Symposium Pesticide Chemistry.

Environmental fate and ecological effects of pesticides (pp. 623-632), Pavia: La Goliardica Pavese s.r.l.

GDG (Geospatial Data Gateway). (2015). USDA. (Available online at https://gdg.sc.egov.usda.gov/ last accessed Feb25, 2016)

Gil Y., Sinfort C., Guillaume S., Brunet Y., and Palagos B. (2008). Influence of micrometeorological factors on pesticide loss to the air during vine spraying: Data analysis with statistical and fuzzy inference models. Biosystems Engineering. 100, 184–197.

Gladstones, J. (1992). Viticulture and Environment. Winetitles, Adelaide.

Gladstones, J. (2011). Wine, terroir and climate change. Kent Town, South Australia: Wakefield Press.

Grelier, M., Guillaume, S., Tisseyre, B., and Scholasch, T. (2007). Precision viticulture data analysis using fuzzy inference systems. Journal International des Sciences de la Vigne et du Vin, 41, 19–31.

Han, W., Yang, Z., Di, L., and Mueller, R.(2012). Crops cape: A Web service based application for exploring and disseminating US conterminous geospatial cropland data products for decision Support. Computers and Electronics in Agriculture Vol. 84, June, pp. 111–123.

Hidalgo, L. (2002). Tratado de viticultura general. Ediciones Mundi-Prensa, Madrid.

Homayouni, S., Germain, C., Lavialle, O., Grenier, G., Goutouly, J. P., Van Leeuwen, C., and Da Costa, J.P. (2008). Abundance weighting for improved vegetation mapping in row crops: application to vineyard vigor monitoring. Can. J. Remote Sens. 34, 228-239.

Huglin, P. (1978). Nouveau mode d'e´valuation des possibilite´s he´liothermiques d'un milieu viticole, Comptes Rendus de l'Acade´mie d'Agriculture, 117–126.

Jackson, R. S. (2008). Wine science principles and applications. 3rd ed. Academic Press, Burlington, MA.

Jackson, D.I., and Cherry, N.J. (1988). Prediction of a district's grape-ripening capacity using a Latitude-Temperature Index (LTI), American Journal of Enology and Viticulture, 39(1), 19–28.

Jones, A. J., Mielke, L.N., Bartles, C.A., and Miller, C.A. (1989). Relationship of landscape position and properties to crop production. Journal of Soil and Water Conservation, 44, 328–332.

Jones, G.V., Snead, N., and Nelson, P. (2004). Geology and wine 8 – modeling viticultural landscapes: A GIS analysis of the terroir potential in the Umpqua valley of Oregon. Geoscience Canada, 31, 167–178.

Jones, G. V. (2005a). Climate and terroir: Impacts of climate variability and change on wine. GeoScience Canada, Terroir Series, 1–14.

Jones, G.V. (2005b). Climate change in the western United States grape growing regions. Acta Horticulturae (ISHS), 689, 41–60.

Jones, G.V., White, M.A., Cooper, O.R., and Storchmann, K. (2005). Climate Change and Global Wine Quality. Climatic Change, 73(3), 319–343.

Jones, G.V. (2006). Climate and Terroir: Impacts of Climate Variability and Change on Wine. In Fine Wine and Terroir - The Geoscience Perspective. Macqueen, R.W., and Meinert, L.D., (eds.), Geoscience Canada Reprint Series Number 9, Geological Association of Canada, St. John's, Newfoundland, 247 pages.

Jones, G. V., Duff, A. A., Hall, A., and Myers, J. W. (2010). Spatial Analysis of Climate in Winegrape Growing Regions in the Western United States. American Journal of Enology and Viticulture, 61(3), 313–326.

Jones, G.V, Duff, A.A., Hall, A., and Myers, J. (2010). Spatial analysis of climate in winegrape growing regions in the western United States. American Journal of Enology and Viticulture, 61, 313–326.

Joss, B. N., Hall, R. J., Sidders, D. M., and Keddy, T. J. (2007). Fuzzy-logic modeling of land suitability for hybrid poplar across the Prairie Provinces of Canada. Environmental Monitoring and Assessment, 141(1-3), 79–96.

Kurtural, S.K., Dami, I.E. and Taylor, B.H. (2006). Utilizing GIS technologies in selection of suitable vineyard sites. International Journal of Fruit Science 6, 87–107.

Kurtural, S.K. (2007). Vineyard Site Selection. University of Kentucky Cooperative Extension Service.

Kravchenko, A., and Bullock, D. G. (2000). Correlation of corn and soybean grain yield with topography and soil properties. Agronomy Journal, 92, 75–83.

Lanyon, D.M., Cass, A., and Hansen, D. (2004). The Effect of Soil Properties on Wine Performance. CSIRO, Land and Water Technical Report No. 34/4, 54 p.

Lee, S. I., and Lee, S. S. (2010). Development of site suitability analysis system for riverbank filtration. Water Science and Engineering, 3(1), 85–94.

Liu, W., Gopal, S., and Woodcock, C.E. (2004). Uncertainty and confidence in land cover classification using a hybrid classifier approach, Photogrammetric Engineering and Remote Sensing, 70(8):963-971.

MacQueen, R.W., and Meinert, L. D. eds. (2006). Fine wines and terroir: The geoscience prespective. Geological Association of Canada.

Magarey, R., Seem, R. C. and DeGloria, S. D. (1998). Prediction of vineyard site suitability. Grape Research News 9: 1–2.

Malheiro, A.C., Santos, J.A., Fraga, H., and Pinto, J.G. (2010). Climate change scenarios applied to viticultural zoning in Europe. Climate Research, 43, 163–177.

McBratney, A. B., and Odeh, O. A. (1997). Application of fuzzy sets in soil science: Fuzzy logic, fuzzy measurements and fuzzy decisions. Geoderma, 77, 85–113.

McKinion, J. M., Willers, J. L., and Jenkins, J. N. (2010a). Spatial analyses to evaluate multi-crop yield stability for a field. Computers and Electronics in Agriculture, 70, 187–198.

McKinion, J. M., Willers, J. L., and Jenkins, J. N. (2010b). Comparing high density LIDAR and medium resolution GPS generated elevation data for predicting yield stability. Computers and Electronics in Agriculture, 74(2), 244–249.

Meinert, L., and Curtin, T. (2005). Terroir of the Finger Lakes of New York. In: Bettison-Varga L, et al., editors. 18th Keck Symposium. The Colorado College, Colorado Springs. Keck Geology Consortium, 34–40.

Mitchell, K.E., Lohmann, D., Houser, P.R., Wood, E.F., Schaake, J.C., Robock, A., Cosgrove, B.A., Sheffield, J., Duan, Q., Luo, L., Higgins, R.W., Pinker, R.T., Tarpley, J.D., Lettenmaier, D.P., Marshall, C.H., Entin, J.K., Pan, M., Shi, W., Koren, V., Meng, J., Ramsay, B.H., and Bailey, A.A. (2004). The multi-institution North American Land Data Assimilation System (NLDAS): Utilizing multiple GCIP products and partners in a continental distributed hydrological modeling system. Journal of Geophysical Research 109, D07S90.

Morari F, Castrignano A., and Pagliarin C. (2009). Application of multivariate geostatistics in delineating management zones within a gravelly vineyard using geo-electrical sensors. Computers and Electronics in Agriculture. 68, 97–107.

Morlat, R., and Lebon, E. (1992). Experience of multisite trials for the study of vineyards. Prog. Agric. Vitic. 109, 55-58.

Mullins, M.G., Bouquet, A., and Williams, L.E. (1992). Biology of the grapevine. Cambridge University Press, Cambridge, New York.

NASS. National Agricultural Statistics Service. (2015). CropScape and Cropland Data Layer. Available online at; http://www.nass.usda.gov/Research_and_Science/Cropland/Release/ last visit Jan 20, 2016.

Nisar Ahamed, T. R., Gopal Rao, K., and Murthy, J. S. R. (2000). GIS-based fuzzy membership model for crop-land suitability analysis. Agricultural Systems, 63(2), 75–95.

NRCS. Natural Resources Conservation Service.(2015). Description of Gridded Soil Survey Geographic (gSSURGO) Database Available online http://www.nrcs.usda.gov/wps/portal/nrcs/detail/soils/survey/geo/?cid=nrcs142p2_053627 last visit Jan 20, 2016.

Oberthur, T., Dobermann, A., and Aylward, M. (2000). Using auxillary information to adjust fuzzy membership functions for improved mapping of soil qualities. International Journal of Geographical Information Science, 14(5), 431–454.

Pan, Z., Ru, Y., Gao, H., and Yang, S. (2011). The suitability evaluation of field selection in cropland improvement project. In 2011 IEEE 18Th International Conference on Industrial Engineering and Engineering Management (IE EM) (Vol. Part 1, pp. 272–276).

Paoli, J. N., Tisseyre, B., Zebic, O., and Guillaume, S. (2005). Determination and mapping of vineyard potentials: an expert approach/De´termination et cartographie des potentialite´s viticoles: une approche experte. Progre`s Agricole et Viticole, 122, 508–511.

Perrot, N., Baudrit, C., Brousset, J. M., Abbal, P., Guillemin, H., Perret, B., Picque, D. (2015). A Decision Support System Coupling Fuzzy Logic and Probabilistic Graphical Approaches for the Agri-Food Industry: Prediction of Grape Berry Maturity. PLOS ONE, 10(7), e0134373.

Quezada, C., Soriano, M., Díaz, J., Merino, R., Chandía, A., Campos, J., and Sandoval, M. (2014). Influence of Soil Physical Properties on Grapevine Yield and Maturity Components in an Ultic Palexeralf Soils, Central-Southern, Chile. Open Journal of Soil Science, **4**, 127-135.

Ramos, M. C., Jones, G. V., and Martínez-Casasnovas, J. A. (2008). Structure and trends in climate parameters affecting winegrape production in northeast Spain. Climate Research, 38, 1–15.

Reshmidevi, T. V., Eldho, T. I., and Jana, R. (2009). A GIS-integrated fuzzy rule-based inference system for land suitability evaluation in agricultural watersheds. Agricultural Systems, 101, 101-109. http://dx.doi.org/10.1016/j.agsy.2009.04.001

Reza, B. K. (2005). A new method for site suitability analysis: The analytic hierarchy process. Environmental Management, 13(6), 685–693.

Robinson, V., and Frank, A. (1985). About different kinds of uncertainty in geographic information systems, in: Proceedings AUTOCARTO 7 Conference, American Society for Photogrammetry and Remote Sensing, Falls Church, VA, 1985, pp. 440–449.

Rosenzweig, C., and Hillel, D. (2008). Climate Variability and the Global Harvest: Impacts of El Niño and Other Oscillations on Agro-Ecosystems. Oxford University Press: New York, USA.

Saaty, T. L. (1980). The Analytic Hierarchy Process. New York: McGraw-Hill.

Saaty, T.L. (2008). Decision making with the analytic hierarchy process. International Journal of Services Sciences, 1(1), 83–98.

Sanga-Ngoie, K., Kumara, K. J. C. and Kobayashi, S. (2010). Potential Grape - Growing Sites in the Tropics: Exploration and Zoning using a GIS Multi-Criteria Evaluation Approach. In proceedings of Asian Association on Remote Sensing. PP. 6.

Santesteban, L. G., Guillaume, S., Royo, J. B., and Tisseyre, B. (2013). Are precision agriculture tools and methods relevant at the whole-vineyard scale? Precision Agriculture, 14(1), 2–17.

Santos, J.A., Grätsch, S.D., Karremann, M.K., Jones, G.V., and Pinto, J.G. (2012a) Ensemble projections for wine production in the Douro Valley of Portugal. Clim. Chang.

Santos, J. A., Malheiro, A. C., Pinto, J. G., and Jones, G. V. (2012b). Macroclimate and viticultural zoning in Europe: observed trends and atmospheric forcing. Climate Research. 51: 89-103.

Seguin, G. (1984). Les terroirs viticoles des grands crus du Bordelais. Cours DEA polycopié.

Sicat, R.S., Carranza, E. J.M., and Nidumolu, U. B. (2005). Fuzzy Modeling of Farmers' Knowledge for Land Suitability Classification. Agricultural Systems 83(1): 49–75.

Soil Survey Staff. (2015). The Gridded Soil Survey Geographic (gSSURGO) Database for Washington and Oregon. United States Department of Agriculture, Natural Resources Conservation Service. Available online at https://gdg.sc.egov.usda.gov/. Jan 10, 2014 (FY2014 official release).

Spomer, R. G., and Piest, R.F. (1982). Soil productivity and erosion of Iowa loess soils. Transactions of the American Society of Agricultural Engineers, 25, 1295–1299.

Stone, J. R., Gilliam, J.W., Cassel, D.K., Daniels, R.B., Nelson, L.A., and Kleiss, H.J. (1985). Effect of erosion and landscape position on the productivity of Piedmont soils Soil Science Society of America Journal, 49, 987–991.

Tagarakis, A., Koundouras, S., Papageorgiou, E. I., Dikopoulou, Z., Fountas, S., and Gemtos, T. A. (2014). A fuzzy inference system to model grape quality in vineyards. *Precision Agriculture, 15*(5), 555-578.

Tavana, M., Liu, W., Elmore, P., Petry, F. E., and Bourgeois, B. S. (2016). A practical taxonomy of methods and literature for managing uncertain spatial data in geographic information systems. Measurement, 81, 123–162.

UI GSM. (2015).The University of Idaho Gridded Surface Meteorological Dataset. Visited February 20, 2015.

Urretavizcaya I., Santesteban L. G., Tisseyre B., Guillaume S., Miranda C., and Royo J. B. (2014). Oenological significance of vineyard management zones delineated using early grape sampling. Precision Agric. 14, 18–39.

Van Leeuwen C., Friant Ph., Choné X., Trégoat O., Koundouras S., and Dubourdieu D. (2004). The influence of climate, soil and cultivar on terroir. American Journal of Enology and Viticulture, 55, 207–217.

Van Leeuwen C., and Seguin G. (2006). The concept of terroir in viticulture. Journal of Wine Research, 17, 1–10.

Van Ranst, E., Tang, H., Groenemans, R., and Sinthurahat, S. (1996). Application of fuzzy logic to land suitability for rubber production in peninsular Thailand. Geoderma, 70, 1–19.

Vaudour, E., Costantini, E., Jones, G. V., and Mocali, S. (2015). An overview of the recent approaches to terroir functional modelling, footprinting and zoning. SOIL, 1(1), 287–312.

Watkins, R. L. (1997).Vineyard Site Suitability in Eastern California. GeoJournal 43(3): 229–239.

White, R.E. (2009). Understanding Vineyard Soils. Oxford University Press. New York, NY. 230 p.

Wilson, J. E. (1998). Terroir: The role of geology, climate, and culture in making of French wines. Berkeley: University of California Press.

Winkler, A.J., Cook, J.A., Kliewer, W.M., and Lider, L.A. (1974). General Viticulture. 4th ed. University of California Press, Berkeley.

WRD (Water Resource Department of Oregon). (2015). Water resources maps. Available at http://www.oregon.gov/owrd/Pages/maps/index.aspx#Water_Right_Data/GIS_Themes last visit Jan 21, 2016.

Wu, F. (1998). SimLand: A prototype to simulate land conversion through the integrated GIS and CA with AHP-derived transition rules. International Journal of Geographical Information Science, 12(1), 63–82.

Zabel, F., Putzenlechner, B., and Mauser, W. (2014). Global Agricultural Land Resources – A High Resolution Suitability Evaluation and Its Perspectives until 2100 under Climate Change Conditions. PLoS ONE, 9(9), e107522.

Zadeh, L., Fu, K., Tanaka, K., and Shimura, M. (Eds.).(1975). *Fuzzy sets and their applications to cognitive and decision processes*. New York: Academic.

Zhang, H. (2009). The Analysis of the Reasonable Structure of Water Conservancy Investment of Capital Construction in China by AHP Method. Water Resources Management, 23(1), 1–18. http://doi.org/10.1007/s11269-008-9261-9

Yau, I.H., and Washington State University. Dept. of Crop and Soil Sciences. (2011). Developing a grape site selection GIS for the Inland Pacific Northwest. Retrieved February 18, 2013, from http://www.dissertations.wsu.edu/Thesis/Fall2011/i_yau_092211.pdf

Yau, I.H., Davenport, J.R., and Rupp, R.A. (2013) Characterizing Inland Pacific Northwest American Viticultural Areas with Geospatial Data. PLoS ONE 8(4): e61

Yau, I.H., Davenport, J. R., and Moyer, M. M. (2014). Developing a Wine Grape Site Evaluation Decision Support System for the Inland Pacific Northwestern United States. HortTechnology, 24(1), 88–98.

CHAPTER SIX

SUMMARY AND CONCLUSIONS

Background

Land assessment for the suitability analysis of vineyards is the process of selecting potential regions for grape production based on their environmental factors. Previous work has either concentrated on geographical regions outside of the Pacific Northwest (U.S.) or on main parameters such as weather. The aim of our research was to develop a spatial land assessment system for the site selection of vineyards in the Pacific Northwest (PNW). During the first phase of this project, several potential methods were investigated as means of obtaining the requisite input data based on satellite remote-sensing technologies. The next phase primarily focused on the compilation of long-term weather data for determining various bio-climatic indices. These indices transform weather parameters into different categories based on grapevine response, and so can be used to better understand the underlying dynamics of American Viticultural Areas in the PNW. The final phase of our study involved choosing the biophysical parameters most suited for use in the development of a potential vineyard scoring system, which could then be evaluated using vineyards that have already been established in the study area (Figure 6.1.).

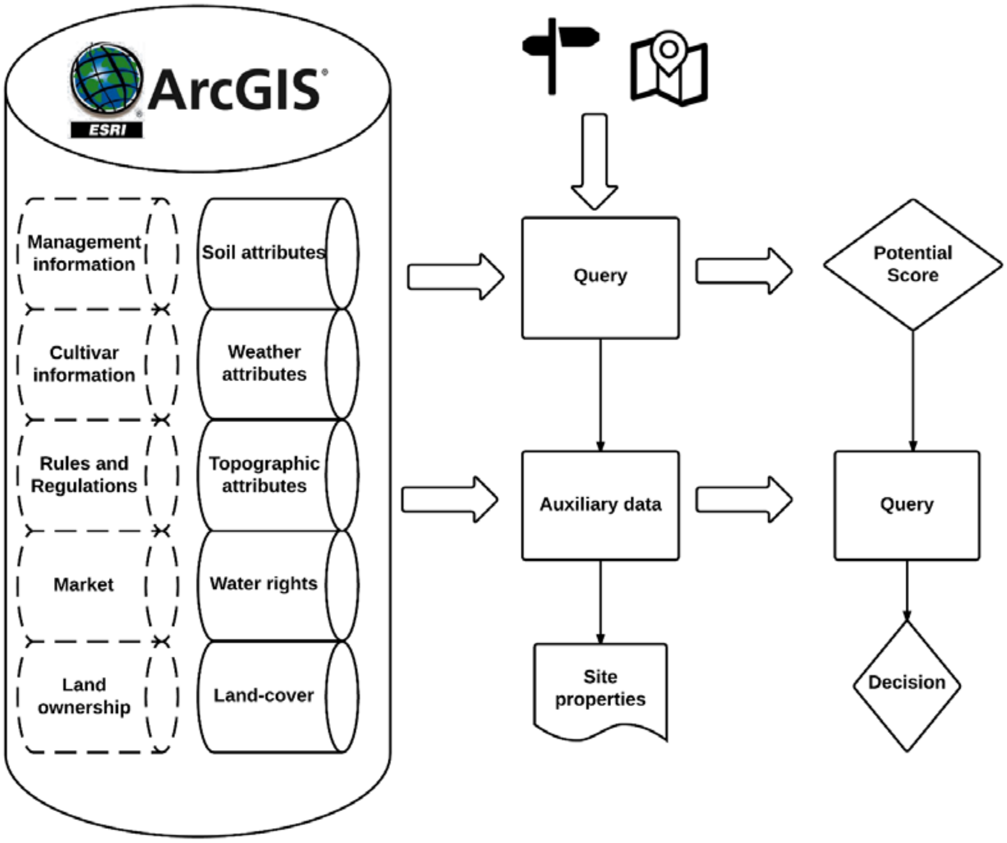

Figure 6. 1. Spatial database used in this study and the linkages between the different types of data.

The results of our study could potentially be combined with other auxiliary information, such as management strategies, data from other sensors, phenological data, soil and water test results, this information could then be stored in a cloud-based geospatial platform for the benefit of growers, decision-makers, scientists and others interested in the assessment of land potential for grape production (Figure 6.2.). This approach was beyond the scope of our study, and may require extensive socio-economic information obtained from surveys and other sources to fully understand the true impact of such land assessment on the grape and wine industry, but is worth consideration. Comprehensive studies on potential user perception and expectations of such a system should also be conducted. Although land assessment systems can be used as provisional tools for supporting onsite land evaluation for vineyard establishment, it may have some unforeseen impact on the economy or marketing which needs to be fully determined prior to giving the public access.

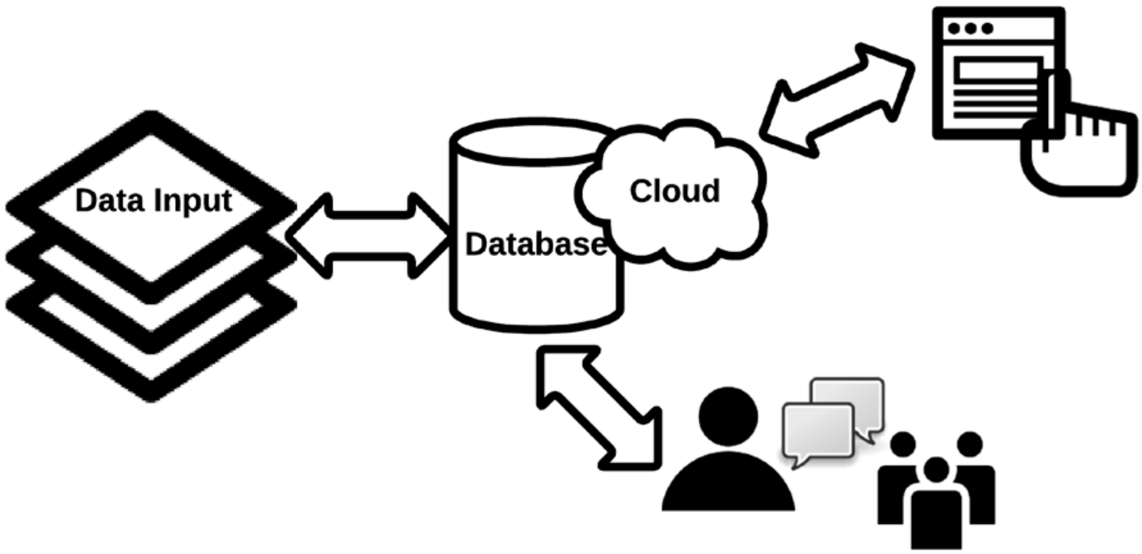

Figure 6. 2. Potential data access pathways.

The land assessment developed in our study primarily focused on the environmental status of a region. However, vineyard management decisions such as which grape variety to plant are usually based on many socio-economic factors, and are mainly driven by the potential to increase economic profits. Therefore, the land assessment system developed in this study and similar tools require further evaluation to determine its potential for success or failure; hence, utilizing this technology as an information support system for extension educators may be a more viable option. If extension educators had access to an accurate land assessment system they could provide support to potential growers and others interested in land assessment and suitability analysis (Figure 6.2.). This is a complex problem and requires input from multiple sectors involved in the grape production industry in order to be solved.

Overview

This chapter summarizes the results reported in our previous chapters (2-5) and discusses the findings in relation to the original objectives, which were defined as follows:

- Evaluation of available options for the selection of input data for use in development of a new land assessment system.
- Usage of bio-climatic indices to improve the classification of viticultural areas in the Pacific Northwest.
- Design of a state-of-the-art methodology for development of a new land assessment system.
- Formation of a land assessment system based on high spatial and temporal resolution biophysical data for the Pacific Northwest.

Phenology Metrics and Satellite Data

The first objective of our study pertained to the evaluation of available input data for development of a new land assessment system. This objective consisted of two sub-studies: a) the application of satellite data for obtaining the key phenological metrics of the study area; and b) the estimation of air temperature using satellite remote-sensing products. In Chapter 2, several crucial phenological metrics for grapevine production in Washington's Columbia Valley were computed using MODIS NDVI data. Utilizing MODIS NDVI, our hypothesis involved a fixed grape growing season from the beginning of April until the end of October in the chosen study area. Knowledge of growing season length and key phenological events are essential for adjustment of the management practices used in a region; the calculation of multiple bio-climatic indices also depends on the length of the growing season. We were interested in identifying whether these assumptions could be updated based on the geographic region, and so determined the growing season length, onset of greenness, end of greenness, and time of maximum NDVI for vineyards. Our results confirmed that this method could be successfully implemented in regions with a lack of access to historical phenological data, and also found that the average duration of a growing season is 216 days, beginning April 2nd and ending November 4th.

Estimation of air temperature using satellite remote sensing products

The second part of the first objective of this dissertation pertains to the employment of a vegetation-temperature index method for estimating air temperature. Unfortunately, the estimated values were not accurate enough to substitute for the ground measurement of air temperature. The method was used on various land cover types in the Yakima Valley, and the impact of each land cover type on the estimated air temperature was determined. This method is especially useful in regions with a lack of historical weather data due to sparse weather stations coverage.

Bio-climatic Indices and Their Role in Land Assessment

The second objective of this study was to obtain a better understanding of weather variability. Several bio-climatic indices were calculated for a 30-year period (1983 to 2012) (Chapter 4). The bio-climatic indices were then used to categorize the AVAs for grape production based on their underlying weather performance. The results showed that the general climatic phenomena of a region and its topographic complexity provide moderate control of the weather dynamics. The bio-climatic indices were further categorized into four major groups: 1) indices that mainly deal with heat unit accumulation; 2) indices that deal with low daily air temperature; 3) indices that use air temperature as a threshold for determining the number of days a certain condition will hold for a specific growing season; and 4) indices that use daily precipitation. These categories take into account various aspects of the climatic response of a region as they are based on long-term data. To successfully grow grapes in a region, one should initially evaluate the range of bio-climatic indices to make sure that the proposed region has values exceeding the lower thresholds of each indice. However, by applying proper management strategies and appropriate investments, grape production can be adjusted to sub-optimal sites, depending on the factor involved.

Spatial Land Assessment for Potential Site Selection of Vineyards

For our final objective, presented in Chapter 5, key environmental factors were used to conduct a comprehensive spatial land assessment for the PNW. Viability of the potential scores was further evaluated using previously established vineyards in the PNW. The results indicated that, on average, 11.4% of the regions evaluated were classified as having "high vineyard potential." Scores for "non-ideal" sites in the region were also determined, and their scores corresponded with the presence of environmental conditions that can potentially restrict grapevine production.

The Way Forward

In general, the results from the land assessment analysis conducted in this study and those of previous studies are promising; nonetheless, there is much that still needs to be addressed and clarified to prove the viability of this type of analysis. As spatial data becomes more readily available at a higher spatial and temporal resolutions, the system's input data can be improved; thereby improving the accuracy of vineyard potential scores. This is encouraging for future research, as it makes access to required data and information more likely. Future research opportunities based on our current work include:

- Coupling of grape quality traits based on vintage across various locations, with the bio-climatic indice scores for those same locations furthering our understanding of the impact that the spatial variability of weather has on the quality of grapes. This can, for instance, even be addressed by developing new indices that indicate potential grape quality based on weather conditions in a specific region.
- Development of a dynamic data repository system with the ability to save the records of key phenological stages for each vineyard. Such a database, when coupled with historical phenological data obtained from various sources (including satellite and other remote-sensing techniques) would have the ability to provide decision support for growers, managers, consultants, and extension specialists. This system could thus improve the knowledge of users regarding their vineyards and locations, and also provide guidance for adjusting management tasks based on the timing of various events.
    - Management strategies should be specifically categorized for each region and be made available as an auxiliary support dataset. Certain management strategies can be good indicators of the underlying physical environment of a region, which may be imposing the need for corrective measures.
    - Coupling a land assessment system with crowd sourcing data, including consumer preference, the reputation of a specific brand, or any associated quality traits of the grapes produced in specific AVAs.

    - Additional information on land ownership, onsite soil tests, and water quality tests.
    - The potential impact of the land assessment tool on local and regional producers and its associated economic response should also be studied.
- The estimation of phenological stages based on available satellite remote-sensing technology relies heavily on various vegetation indices. In this study, we only used the NDVI; however, other vegetation indices, such as the leaf area index (LAI) obtained from satellite data, can also be used to improve the estimation of key phenological stages. In addition, different types of sensor technologies can be used to improve the capture of the canopy structures for different vineyards, and then assimilate this information to help adjust management decisions.
- Our study used a large number of bio-climatic indices, many showing a similar response. Still, there is need for the development of new bio-climatic indices that focus on combining the most useful indices (when appropriate). These "combined" indices could potentially aid in narrowing down available land in the PNW for specific uses, including grape production.
- The traditional calculation method of bio-climatic indices still needs to be updated based on recent advances in weather parameter technology. There have been many improvements in recording devices and associated sensors during recent years, such that some of these sensors are now able to record weather parameters in very fine temporal resolutions, even to 15 seconds. With the advancement of sensor technologies and the "internet of things," data records will become available for use in creating very fine spatial and temporal resolutions. Manipulating and analyzing these data via cloud

technology could accelerate access to updated information, and could also assist in improving the definition of some already established bio-climatic indices. Most of the previously developed indices take into account only the daily maximum and minimum temperatures when computing the average daily temperature, and hourly and sub-hourly daily fluctuations are not well-represented based on only two observations per day. Consequently, the developers of the bioclimatic indices had to introduce adjustment factors in order to correct for the effect of seasonal fluctuations on daily air temperature.

- The relative importance of environmental factors on grape production can be defined by applying new methods for ranking these factors based on their specific region. The analysis hierarchy process (AHP) is one such method that can be tested and utilized to adjust the relative importance of environmental parameters within a specific geographical region. AHP requires an advanced survey system based on the expert opinions as well as grower perception of the relative importance of various environmental and geophysical factors. Future studies focusing on land assessment in the PNW region should plan to implement AHP or similar techniques to adjust the potential score based on the growers and/or experts' perception of a region.

Outcomes

- Fuzzy logic was successfully implemented for developing a spatial land assessment system for grapes.

- Key bio-climatic indices were computed for a 30-year period, and the corresponding bioclimatic indices for the AVAs located in Washington and parts of Oregon were reported.

- A cold damage index was established based on the cold hardiness model previously developed and this new index was computed for the PNW.

- A dynamic minimum temperature Index was developed to account for variability in cold hardiness of grapes.

- A Wind speed index was developed to help locate regions where wind speed often exceeds given thresholds.

- Limiting factors such as water rights and land cover type were incorporated into the land assessment system to better match the current restrictions of the region.

- The majority of vineyards already established in Washington are located in "high vineyard potential" regions as determined in this study.

APPENDICES

Appendix A: Bio-climatic indices applied for climatic zoning.

Bioclimatic Index	Equation	Reference
Growing Season Temperature (GST)	$\frac{\sum_{Apr1}^{Oct\ 31}(Tmax+Tmin)/2}{n}$	Jones, 2005a
Winkler Index (WI) or Growing Degree Days (GDD)	$\sum_{Apr1}^{Oct31} \max[\left(\frac{[Tmax+Tmin]}{2}\right)-10{,}0]$	Winkler et al. 1974, Jones et al. 2010
Huglin Index (HI)	$\sum_{Apr1}^{Sep30} max\left(\left[\frac{[Tmean-10]+[Tmax-10]}{2}\right],0\right).k$ Where k is an adjustment for latitude /day length.	Huglin 1978
Biologically Effective Degree Days (BEDD)	$\sum_{Apr1}^{Oct31} \min\left[\left(\max\left[\left(\frac{[Tmax+Tmin]}{2}\right)-10{,}0\right]\right),9\right].DTRadj.k$ Where *DTR adj* = $\begin{cases} 0.25[DTR-13].[DTR]>13 \\ 0,10<[DTR]<13 \\ 0.25[DTR-10],[DTR]<10 \end{cases}$ Where k is an adjustment for latitude/day length.	Gladstones, 1992
Mean Thermal Amplitude (MTA)	$\frac{1}{n}\sum_{1}^{n}(Tmax-Tmin)$ For the month of September in the Northern Hemisphere.	Mullins et al., 1992; Ramos et al., 2008
Cool Night Index (CI)	Average daily *Tmin* for the month of September (Northern Hemisphere).	Tonietto and Carbonneau, 2004
Minimum Temperature (Min. Temp.)	Daily minimum value for each year.	Hidalgo, 2002
Latitude Temperature Index (LTI)	$LTI = MTWM.(60-latitude)$ *MTWM* is the mean temperature of the warmest month of the growing season.	Jackson and Cherry, 1988

Frost Free Days (FFD)	Number of days between the last frost in spring and the first frost in Autumn.	Magarey, 1998
Growing Season Precipitation (GSP)	$$\sum_{Apr}^{Sep}(P)$$ Where *P* is the daily precipitation (mm).	Blanco-Ward et al., 2007
Growing Season Suitability (GSS)	Fraction of days between April to September where *Tavg* >10°C.	Malheiro et al., 2010; Santos et al., 2012b
Length of Growing Season (LGS)	Number of days between April first to end of October where*Tavg* >10°C.	Jackson, 2008
Hydrothermic Index (HyI)	$$\sum_{April}^{Aug}(P.T)$$ Where P is the daily precipitation (mm).	Branas et al., 1974
Dryness Index (DI)	$$\sum_{April}^{Sept}(w_0 + P + T_v + E_s)$$ *W0* is the initial soil water content P is the precipitation (mm) *TV* is the potential vineyard transpiration (mm) *ES* is the direct soil evaporation (mm). $$T_v = ETP.K$$ *ETP* is the potential evapotranspiration *K* is a coefficient of radiation absorption by vineyard. $$E_s = \frac{ETP}{(1-N)}(1-k)JP_m$$ *N* is the number of days of the month JP_m is the number of days with effective soil evaporation (calculated dividing P by 5mm), which should be equal to or lower than *N*.	Riou et al., 1994, Tonietto and Carbonneau, 2004
Composite Index (CompI)	Ratio of the years simultaneously verifying 4 criteria: HI ≥ 1400°C, DI ≥ - 100 mm, HyI ≤ 5100°Cmm and Min. Temp. > -17°C.	Malheiro et al., 2010; Santos et al., 2012

Appendix B: American Viticultural Areas (AVAs) in Washington and Oregon and various key bio-climatic indices computed over a 30-year period (1983-2012).

Bio-climatic Indices	**Ancient Lakes of the Columbia Valley**					**Columbia Gorge**				
	Min.	**Max.**	**Mean**	**±SD**	**Group letter**	**Min.**	**Max.**	**Mean**	**±SD**	**Group letter**
Biologically Effective Degree Days (BEDD)	231	305	283	11.9	H	211	564	466	71.49	I
Cold Damage Index (Five-years)	3	17	11	2.9	D	2	40	13	7.04	C
Cold Damage Index (10-years)	3	21	13	3.6	E	3	61	23	12.66	B
Cold Damage Index (20-years)	7	40	23	6.9	F	9	104	43	20.38	C
Cold Damage Index (30-years)	9	58	30	11.1	G	10	140	56	29.07	C
Cool Night Index (CI)	8.0	10.3	9.3	0.5	D	5.7	8.9	7.4	0.58	H
Dynamic Minimum Temperature	23	38	31	3.4	C	9	30	18	5.20	I
Frost Free Days (FFD)	159	186	171	5.9	F	145	189	164	9.39	I
Growing Degree Days (GDD)	1379	1725	1525	61.5	D	858	1372	1089	109.62	J
Growing Season Precipitation (GSP)	47.0	80.4	59.0	5.5	FGH	138.4	387.5	262.0	63.52	B
Out of Growing Season Precipitation (Out-GSP)	69.5	90.6	77.9	4.7	H	123.2	288.0	195.4	37.28	B
Growing Season Suitability (GSS)	0.86	0.92	0.90	0.0	D	0.73	0.89	0.82	0.03	J
Growoing Season Temperature (GST)	15.4	17.2	16.2	0.3	D	12.6	15.6	14.0	0.63	J
Huglin Index (HI)	2089	2464	2248	61.6	F	1394	2098	1740	126.12	J
Hydrothermic Index (HyI)	756	1035	863	66.9	GH	992	1687	1305	146.02	C
Latitude Temperature Index (LTI)	289	315	299	4.8	I	262	313	285	10.09	J
Length of Growing Season (LGS)	171	188	179	2.8	E	145	182	165	7.58	I
Mean thermal amplitude (MTA)	15.1	17.4	16.2	0.5	HG	13.4	18.1	16.3	0.66	EF
Wind Speed Index (WS)	10	38	19	7.0	G	20	58	32	8.80	D

Appendix B: American Viticultural Areas (AVAs) in Washington and Oregon and various key bio-climatic indices computed over a 30-year period (1983-2012).

Bio-climatic Indices	Columbia Valley					Horse Heaven Hills				
	Min.	Max.	Mean	±SD	Group letter	Min.	Max.	Mean	±SD	Group letter
Biologically Effective Degree Days (BEDD)	79	609	331	94.6	G	282	549	437	63.1	E
Cold Damage Index (Five-years)	0	95	14	9.6	C	3	18	9	3.6	E
Cold Damage Index (10-years)	0	157	20	16.3	C	4	26	12	4.8	E
Cold Damage Index (20-years)	1	281	36	29.8	D	6	50	20	8.8	G
Cold Damage Index (30-years)	1	378	48	41.3	D	7	75	23	12.3	H
Cool Night Index (CI)	5.0	11.9	8.8	1.0	E	8.0	10.7	9.5	0.7	C
Dynamic Minimum Temperature	7	73	28	12.3	D	14	31	20	3.4	H
Frost Free Days (FFD)	116	212	168	14.2	G	159	196	178	7.0	E
Growing Degree Days (GDD)	740	1908	1414	198.0	F	1210	1705	1566	86.0	C
Growing Season Precipitation (GSP)	42.9	347.3	81.1	26.9	E	55.8	96.8	64.7	5.7	F
Out of Growing Season Precipitation (Out-GSP)	64.4	435.1	119.6	40.6	D	82.8	122.9	95.7	6.9	F
Growing Season Suitability (GSS)	0.66	0.95	0.87	0.0	F	0.82	0.93	0.90	0.0	C
Growing Season Temperature (GST)	11.5	18.1	15.6	1.1	F	14.5	17.2	16.4	0.5	C
Huglin Index (HI)	1263	2602	2124	227.8	G	1874	2431	2289	92.0	E
Hydrothermic Index (HyI)	680	3218	1209	382.5	D	876	1299	1003	62.6	E
Latitude Temperature Index (LTI)	229	353	304	24.3	G	302	341	328	7.5	B
Length of Growing Season (LGS)	128	195	175	11.3	G	164	190	183	4.5	D
Mean thermal amplitude (MTA)	9.9	19.2	16.3	1.1	EF	14.0	17.3	16.1	0.9	H
Wind Speed Index (WS)	6	92	32	16.6	D	18	72	39	12.3	B

Appendix B: American Viticultural Areas (AVAs) in Washington and Oregon and various key bio-climatic indices computed over a 30-year period (1983-2012).

Bio-climatic Indices	**Lake Chelan**					**Naches Heights**				
	Min.	**Max.**	**Mean**	**±SD**	**Group letter**	**Min.**	**Max.**	**Mean**	**±SD**	**Group letter**
Biologically Effective Degree Days (BEDD)	148	241	204	18.9	J	215	358	295	37.6	D
Cold Damage Index (Five-years)	6	20	13	2.4	C	21	41	30	5.5	A
Cold Damage Index (10-years)	7	31	16	4.6	D	34	61	47	7.6	A
Cold Damage Index (20-years)	11	62	30	8.6	E	58	113	86	15.1	A
Cold Damage Index (30-years)	12	77	38	11.5	E	84	154	119	18.4	A
Cool Night Index (CI)	7.7	10.1	8.5	0.6	F	6.3	7.6	6.8	0.3	I
Dynamic Minimum Temperature	24	53	39	5.5	B	37	53	45	3.6	A
Frost Free Days (FFD)	151	184	166	5.8	HI	141	151	146	2.6	K
Growing Degree Days (GDD)	1073	1497	1329	72.2	H	1012	1362	1189	79.7	I
Growing Season Precipitation (GSP)	71.3	102.4	83.4	8.1	E	74.7	130.7	96.3	11.0	D
Out of Growing Season Precipitation (Out-GSP)	100.6	125.9	107.8	5.3	E	94.2	132.1	112.1	6.5	E
Growing Season Suitability (GSS)	0.80	0.89	0.86	0.0	H	0.78	0.87	0.83	0.0	I
Growing Season Temperature (GST)	13.6	16.0	15.1	0.4	H	13.3	15.3	14.4	0.5	I
Huglin Index (HI)	1716	2180	2019	93.0	H	1687	2130	1931	98.2	I
Hydrothermic Index (HyI)	1108	1263	1176	34.1	D	987	1103	1044	29.4	E
Latitude Temperature Index (LTI)	249	283	269	5.8	L	266	296	281	7.0	K
Length of Growing Season (LGS)	154	178	169	3.9	H	152	174	164	4.8	J
Mean thermal amplitude (MTA)	13.3	17.6	15.7	1.0	I	16.5	17.8	17.4	0.2	B
Wind Speed Index (WS)	22	32	27	2.2	F	31	44	39	2.7	B

Appendix B: American Viticultural Areas (AVAs) in Washington and Oregon and various key bio-climatic indices computed over a 30-year period (1983-2012).

Bio-climatic Indices	**Puget Sound**					**Rattle Snake Hills**				
	Min.	**Max.**	**Mean**	**±SD**	**Group letter**	**Min.**	**Max.**	**Mean**	**±SD**	**Group letter**
Biologically Effective Degree Days (BEDD)	68	685	319	138.4	K	268	400	329	34.4	C
Cold Damage Index (Five-years)	0	9	0	1.0	I	9	27	15	4.2	B
Cold Damage Index (10-years)	0	12	1	1.3	I	13	42	23	6.1	B
Cold Damage Index (20-years)	0	33	1	2.7	J	26	81	47	12.2	H
Cold Damage Index (30-years)	0	44	1	3.6	J	35	126	72	18.2	B
Cool Night Index (CI)	7.2	11.5	9.4	0.7	D	7.5	8.7	8.2	0.3	G
Dynamic Minimum Temperature	0	20	3	2.2	L	25	40	31	3.5	C
Frost Free Days (FFD)	91	266	230	19.1	A	146	165	157	3.8	J
Growing Degree Days (GDD)	619	1187	948	99.8	K	1176	1575	1386	102.6	G
Growing Season Precipitation (GSP)	119.9	860.9	331.8	93.9	A	53.4	63.9	56.8	2.1	HI
Out of Growing Season Precipitation (Out-GSP)	164.0	1289.6	414.9	121.1	A	80.0	106.9	90.2	6.1	FG
Growing Season Suitability (GSS)	0.00	0.91	0.86	0.0	G	0.82	0.91	0.87	0.0	F
Growing Season Temperature (GST)	11.6	14.9	13.6	0.5	K	14.3	16.5	15.5	0.6	G
Huglin Index (HI)	985	1719	1452	124.4	K	1833	2366	2138	135.0	G
Hydrothermic Index (HyI)	1148	7010	3145	774.8	A	850	1031	936	33.4	F
Latitude Temperature Index (LTI)	183	253	223	18.2	M	285	318	302	8.3	H
Length of Growing Season (LGS)	0	190	176	7.5	F	162	184	174	5.6	G
Mean thermal amplitude (MTA)	7.8	14.4	11.4	1.2	J	14.9	17.9	17.1	0.7	D
Wind Speed Index (WS)	0	62	19	11.7	G	11	49	29	10.3	E

Appendix B: American Viticultural Areas (AVAs) in Washington and Oregon and various key bio-climatic indices computed over a 30-year period (1983-2012).

Bio-climatic Indices	Red Mountain					Rock District of Milton Free Water				
	Min.	**Max.**	**Mean**	**±SD**	**Group letter**	**Min.**	**Max.**	**Mean**	**±SD**	**Group letter**
Biologically Effective Degree Days (BEDD)	354	379	365	6.7	D	873	1075	1075	51.1	H
Cold Damage Index (Five-years)	4	4	4	0.0	H	3	7	5	1.1	H
Cold Damage Index (10-years)	5	6	5	0.4	H	3	7	5	1.1	H
Cold Damage Index (20-years)	12	14	13	0.7	H	3	8	5	1.4	I
Cold Damage Index (30-years)	14	16	15	0.7	I	13	33	22	6.3	H
Cool Night Index (CI)	9.5	9.6	9.5	0.0	C	9.7	10.5	10.2	0.2	A
Dynamic Minimum Temperature	18	19	18	0.3	I	11	12	12	0.3	K
Frost Free Days (FFD)	179	180	179	0.2	D	199	206	203	2.0	B
Growing Degree Days (GDD)	1597	1647	1622	13.8	B	1621	1660	1649	9.7	A
Growing Season Precipitation (GSP)	59.4	62.1	60.8	0.6	FGH	97.0	100.4	98.4	0.9	D
Out of Growing Season Precipitation (Out-GSP)	83.7	88.0	85.8	1.0	G	182.4	187.9	184.8	1.2	C
Growing Season Suitability (GSS)	0.91	0.92	0.92	0.0	B	0.92	0.93	0.92	0.0	A
Growing Season Temperature (GST)	16.6	16.9	16.7	0.1	B	16.8	16.9	16.9	0.0	A
Huglin Index (HI)	2332	2395	2362	17.7	C	2320	2353	2332	8.4	D
Hydrothermic Index (HyI)	901	937	916	7.5	FG	1998	2068	2040	17.0	B
Latitude Temperature Index (LTI)	323	327	325	1.0	C	334	338	337	1.0	A
Length of Growing Season (LGS)	185	187	186	0.6	B	188	190	189	0.4	A
Mean thermal amplitude (MTA)	16.2	16.5	16.4	0.1	E	15.1	16.1	15.6	0.3	I
Wind Speed Index (WS)	15	17	16	0.5	H	24	33	29	2.2	E

Appendix B: American Viticultural Areas (AVAs) in Washington and Oregon and various key bio-climatic indices computed over a 30-year period (1983-2012).

Bio-climatic Indices	Snipes Mountain					Wahluke Slope				
	Min.	Max.	Mean	±SD	Group letter	Min.	Max.	Mean	±SD	Group letter
Biologically Effective Degree Days (BEDD)	338	350	343	2.9	A	286	402	339	25.7	F
Cold Damage Index (Five-years)	6	8	7	0.5	F	1	17	6	4.5	G
Cold Damage Index (10-years)	10	13	12	0.7	E	1	22	7	5.7	G
Cold Damage Index (20-years)	20	27	25	1.6	F	1	40	13	10.8	H
Cold Damage Index (30-years)	28	38	33	2.7	F	1	58	18	14.4	I
Cool Night Index (CI)	8.5	8.9	8.7	0.1	E	8.5	11.9	10.0	0.9	B
Dynamic Minimum Temperature	23	25	24	0.4	F	14	35	22	5.3	G
Frost Free Days (FFD)	164	168	166	1.2	H	160	206	180	11.1	D
Growing Degree Days (GDD)	1609	1643	1624	9.0	B	1388	1908	1662	127.1	A
Growing Season Precipitation (GSP)	51.0	54.9	52.1	0.9	I	56.5	62.7	58.4	1.0	GH
Out of Growing Season Precipitation (Out-GSP)	77.4	79.3	78.1	0.6	H	65.5	85.0	73.3	4.8	H
Growing Season Suitability (GSS)	0.91	0.92	0.92	0.0	B	0.87	0.95	0.91	0.0	B
Growing Season Temperature (GST)	16.7	16.8	16.7	0.0	B	15.4	18.1	16.9	0.7	A
Huglin Index (HI)	2408	2453	2425	10.4	A	2109	2602	2397	122.3	B
Hydrothermic Index (HyI)	830	850	840	5.2	H	770	924	834	36.5	H
Latitude Temperature Index (LTI)	321	324	322	0.8	D	296	340	319	10.9	E
Length of Growing Season (LGS)	186	187	186	0.4	B	173	195	185	5.5	BC
Mean thermal amplitude (MTA)	17.8	18.4	18.1	0.2	A	14.8	17.1	16.2	0.5	EFG
Wind Speed Index (WS)	49	59	56	2.7	A	17	41	27	5.6	F

Appendix B: American Viticultural Areas (AVAs) in Washington and Oregon and various key bio-climatic indices computed over a 30-year period (1983-2012).

Bio-climatic Indices	Walla Walla					Yakima Valley				
	Min.	Max.	Mean	±SD	Group letter	Min.	Max.	Mean	±SD	Group letter
Biologically Effective Degree Days (BEDD)	183	510	346	73.0	FG	212	456	331	37.9	B
Cold Damage Index (Five-years)	1	40	7	3.8	F	2	36	11	5.6	D
Cold Damage Index (10-years)	1	65	9	5.3	F	3	60	17	8.8	D
Cold Damage Index (20-years)	1	105	13	8.4	B	7	110	33	16.2	D
Cold Damage Index (30-years)	2	140	16	10.4	I	8	152	46	25.0	D
Cool Night Index (CI)	6.6	11.2	9.5	0.8	C	6.5	10.3	8.6	0.7	F
Dynamic Minimum Temperature	10	49	15	3.1	J	16	44	26	5.2	E
Frost Free Days (FFD)	144	212	189	11.3	C	140	186	164	8.6	I
Growing Degree Days (GDD)	909	1703	1566	95.4	C	1025	1684	1488	136.1	E
Growing Season Precipitation (GSP)	74.0	288.5	111.5	27.9	C	50.2	155.6	63.1	11.9	FG
Out of Growing Season Precipitation (Out-GSP)	129.4	417.9	197.3	39.2	B	67.8	125.9	86.8	11.0	G
Growing Season Suitability (GSS)	0.73	0.93	0.91	0.0	C	0.78	0.93	0.89	0.0	E
Growing Season Temperature (GST)	12.7	17.1	16.5	0.5	C	13.4	17.1	16.0	0.7	E
Huglin Index (HI)	1506	2391	2274	109.9	E	1686	2480	2248	166.4	F
Hydrothermic Index (HyI)	1400	3185	2050	305.4	B	714	1158	916	81.1	FG
Latitude Temperature Index (LTI)	275	342	329	7.7	B	269	331	312	12.0	F
Length of Growing Season (LGS)	143	190	184	4.9	C	154	189	179	7.1	E
Mean thermal amplitude (MTA)	14.4	18.9	16.2	1.2	FHG	14.3	18.5	17.2	1.1	C
Wind Speed Index (WS)	14	61	33	13.8	D	11	68	37	15.6	C